

AD 639231

REPORT NUMBER 166

MARCH 1966

PHASE I - FLIGHT TEST RESULTS
VOLUME I



CLEARINGHOUSE
FOR FEDERAL SCIENTIFIC AND
TECHNICAL INFORMATION

Hardcopy

Microfiche

\$6.00

\$1.25

19 pp 21

1 ARCHIVE COPY

F

DDC AVAILABILITY NOTICES

1. Distribution of ~~some~~ document is unlimited.
2. This document is subject to special report controls and each transmittal to foreign governments or foreign nationals may be made only with prior approval of US Army Aviation Materiel Laboratories, Fort Eustis, Virginia 23604.
3. In addition to security requirements which must be met, this document is subject to special export controls and each transmittal to foreign governments or foreign nationals may be made only with prior approval of USAAVLABS, Fort Eustis, Virginia 23604.
4. Each transmittal of this document outside the agencies of the US Government must have prior approval of US Army Aviation Materiel Laboratories, Fort Eustis, Virginia 23604.
5. In addition to security requirements which apply to this document and must be met, each transmittal outside the agencies of the US Government must have prior approval of US Army Aviation Materiel Laboratories, Fort Eustis, Virginia.
6. Each transmittal of this document outside the Department of Defense must have prior approval of US Army Aviation Materiel Laboratories, Fort Eustis, Va.
7. In addition to security requirements which apply to this document and must be met, each transmittal outside the Department of Defense must have prior approval of US Army Aviation Materiel Laboratories, Fort Eustis, Virginia 23604.
8. This document may be further distributed by any holder only with specific prior approval of US Army Aviation Materiel Laboratories, Fort Eustis, Va. 23604.
9. In addition to security requirements which apply to this document and must be met, it may be further distributed by the holder only with specific prior approval of US Army Aviation Materiel Laboratories, Fort Eustis, Virginia 23604.

DISCLAIMER

10. The findings in this report are not to be construed as an official Department of the Army position unless so designated by other authorized documents.
11. When Government drawings, specifications, or other data are used for any purpose other than in connection with a definitely related Government procurement operation, the United States Government thereby incurs no responsibility nor any obligation whatsoever; and the fact that the Government may have formulated, furnished, or in any way supplied the said drawings, specifications, or other data is not to be regarded by implication or otherwise as in any manner licensing the holder or any other person or corporation, or conveying any rights or permission, to manufacture, use, or sell any patented invention that may in any way be related thereto.
12. Trade names cited in this report do not constitute an official endorsement or approval of the use of such commercial hardware or software.

DISPOSITION INSTRUCTIONS

13. Destroy this report when no longer needed. Do not return it to originator.

14. When this report is no longer needed, Department of the Army organizations will destroy it in accordance with the procedures given in AR 380-5. Navy and Air Force elements will destroy it in accordance with applicable directions. Department of Defense contractors will destroy the report according to the requirement of Section 14 of the Industrial Security Manual for Safeguarding Classified Information. All others will return the report to US Army Aviation Materiel Laboratories, Fort Eustis, Virginia 23604.

ACCESSION for		
CPSTI	WHITE SECTION	<input checked="" type="checkbox"/>
DDC	BUFF SECTION	<input type="checkbox"/>
UN ANNOUNCED		<input type="checkbox"/>
JULIICATION		
BY		
DISTRIBUTION/AVAILABILITY CODES		
DIST.	AVAIL.	and/or SPECIAL
1		

Report Number 166

PHASE I FLIGHT TEST RESULTS
VOLUME I

XV-5A Lift Fan
Flight Research Aircraft
Contract DA 44-177-TC-715

DDC
RECORDED
SEP 28 1966
RECEIVED
B

March, 1966

ADVANCED ENGINE & TECHNOLOGY DEPARTMENT
GENERAL ELECTRIC COMPANY
CINCINNATI, OHIO 45215

19 MAY 1966
MF
1966 MAY 6

FOREWORD

For the convenience of the reader, this report is divided into three volumes - Volumes I, II and III.

Volume I contains Sections 1.0 through 6.2.

Volume II contains Sections 6.3 through 11.0.

Volume III contains Section 12.0, which consists of parameter illustrations only.

Volume I includes a complete Table of Contents for all three Volumes. A partial Table of Contents is included in the other Volumes.

CONTENTS - VOLUME I

SECTION	PAGE
FOREWORD	iii
1.0 SUMMARY	1
2.0 INTRODUCTION	5
3.0 GLOSSARY	11
4.0 TEST SUMMARY	27
5.0 DATA ACQUISITION	37
5.1 Instrumentation Capability	37
5.2 Data Handling System	38
5.3 Ground Calibrations	38
6.0 FAN FLIGHT TEST RESULTS	53
6.1 Performance	53
6.2 Stability and Control	83

CONTENTS - VOLUME II

6.3 Thermodynamics	195
7.0 CONVENTIONAL FLIGHT TEST RESULTS	269
7.1 Performance	269
7.2 Stability and Control	273
7.3 Thermodynamics	327
8.0 AIRCRAFT SYSTEMS	335
8.1 Hydraulic	335
8.2 Electrical	337
8.3 Propulsion System History	343
8.4 XV-5A Landing Gear	349
8.5 Airspeed System	351
9.0 STRUCTURES AND LOADS	375
10.0 REFERENCES	385
11.0 CONCLUSIONS	395

CONTENTS - VOLUME III

This Volume consists of Appendix Figures exclusively. These are Figures A-1 through A-166.	399
--	-----

BLANK PAGE

LIST OF ILLUSTRATIONS
VOLUME I

FIGURE		PAGE
2.1	XV-5A Three-View Drawing	7
2.2	XV-5A No. 62-4506 Flight Time History	9
2.3	" " " " "	10
5.1	In-Flight Test Data System	40
5.2	Flight Test Calibration Test Setup	41
5.3	Typical Calibration Test Setup	42
6.1	Wing Fan Lift Performance	60
6.2	Pitch Fan Lift Performance	61
6.3	Wing Fan Speed vs Gas Generator Speed	62
6.4	Pitch Fan Speed vs Wing Fan Speed	63
6.5	Wing Fan Lift Thrust vs Corrected Wing Fan RPM	64
6.6	Installed Fan Lift vs Gas Generator Speed, S. L., Std Day	65
6.7	Louver Stagger Effectiveness in Hover	66
6.8	Static Wing Fan Exit Louver Vector Effectiveness	67
6.9	Static Pitch Fan Lift vs Thrust Reverser Door Position	68
6.10	Trimmed Transition Parameters	74
6.11	" " "	75
6.12	" " "	76
6.13	Angle of Attack Correction vs Fan Tip Speed Ratio	77
6.14	Fan Flight Envelope	78
6.15	" " "	79
6.16	Static Longitudinal Stability - Fan Flight $-\beta_v = 7^\circ$	95
6.17	" " " " " $-\beta_v = 11^\circ$	96
6.18	" " " " " $-\beta_v = 20^\circ$	97
6.19	" " " " " $-\beta_v = 23^\circ$	98
6.20	" " " " " $-\beta_v = 27^\circ$	99
6.21	" " " " " $-\beta_v = 35^\circ$	100
6.22	Lateral Directional Control - Steady State Sideslips - Gross Weight 10,000 Pounds with CG at FS 240.00	101
6.23	Variation of Stagger Effectiveness with Collective Stagger	102
6.24	Roll System Root Locus After Louver & Servo Modifications	103
6.25	Roll System Root Locus After Louver & Servo Modifications	104
6.26	Roll System Root Locus After Louver & Servo Modifications	105
6.27	Root Locus for Roll After System Modification	106
6.28	" " " " " " "	107
6.29	" " " " " " "	108

LIST OF ILLUSTRATIONS (Continued)
VOLUME I

FIGURE		PAGE
6.30	Dual System Response with Linear Transfer Function Fit	109
6.31	Single System Response with Linear Transfer Function Fit	110
6.32	Frequency Response of Louver Servo	111
6.33	Fan Mode Longitudinal Control Power vs Indicated Airspeed	124
6.34	Fan Mode Longitudinal Control Power vs Indicated Airspeed	125
6.35	Fan Mode Lateral Control Power vs Indicated Airspeed	126
6.36	Fan Mode Lateral Control Power vs Indicated Airspeed	127
6.37	Fan Mode Directional Control Power vs Indicated Airspeed	128
6.38	Fan Mode Directional Control Power vs Indicated Airspeed	129
6.39	VTOL Flight Control System Operation	130
6.40	Flight Control System Schematic	131
6.41	Static VTOL Control System Calibration	133
6.42	" " " " "	134
6.43	" " " " "	135
6.44	" " " " "	136
6.45	" " " " "	137
6.46	" " " " "	138
6.47	" " " " "	139
6.48	" " " " "	140
6.49	" " " " "	141
6.50	" " " " "	142
6.51	" " " " "	143
6.52	Pitch Control Door Position vs Thrust Vector Range	144
6.53	Static Wing Fan Louver Calibration - Lateral Stick Sweeps	145
6.54	Static Wing Fan Louver Calibration - Rudder Pedal Sweeps	146
6.55	Static Wing Fan Louver Calibration - Lateral Stick Sweeps	147
6.56	Static Wing Fan Louver Calibration - Rudder Pedal Sweeps	148

LIST OF ILLUSTRATIONS (Continued)
VOLUME I

FIGURE		PAGE
6.57	Static Wing Fan Louver Calibration - Lateral Stick Sweeps	149
6.58	Static Wing Fan Louver Calibration - Rudder Pedal Sweeps	150
6.59	Static Wing Fan Louver Calibration - Lateral Stick Sweeps	151
6.60	Static Wing Fan Louver Calibration - Rudder Pedal Sweeps	152
6.61	Static VTOL Control System Calibration	153
6.62	" " " " "	154
6.63	" " " " "	155
6.64	" " " " "	156
6.65	" " " " "	157
6.66	" " " " "	158
6.67	Location of Tail Angle of Attack Indicator	169
6.68	Estimated Effect of Upwash on Local Angle of Attack at Horizontal Tail Vane	170
6.69	Indicated Local Angle of Attack at Vane vs Estimated Horizontal Stabilizer Angle of Attack	171
6.70	Typical Airfoil Section Characteristics Showing Effect of Leading Edge Slat	172
6.71	Ground Effect on Horizontal Tail Downwash	173
6.72	Estimated Horizontal Tail Angle of Attack and Downwash Angle vs Indicated Angle of Attack for Fan Flight	174
6.73	Estimated Horizontal Tail Angle of Attack and Downwash Angle vs Indicated Angle of Attack for Fan Flight	175
6.74	Estimated Horizontal Tail Angle of Attack and Downwash Angle vs Indicated Angle of Attack for Fan Flight	176
6.75	Estimated Horizontal Tail Angle of Attack and Downwash Angle vs Indicated Angle of Attack for Fan Flight	177
6.76	Estimated Horizontal Tail Angle of Attack and Downwash Angle vs Indicated Angle of Attack for Fan Flight	178
6.77	Fan to Turbojet Conversion Envelope	179
6.78	Turbojet to Fan Conversion Envelope	180
6.79	Conversion Control Interlocks	181

LIST OF ILLUSTRATIONS (Continued)
VOLUME I

FIGURE		PAGE
6.80	Flight Conversion Time Histories	182
6.81	" " " "	183
6.82	" " " "	184
6.83	" " " "	185
6.84A	" " " "	186
6.84B	" " " "	187
6.85A	" " " "	188
6.85B	" " " "	189
6.86	Flight Mode Conversion Control System Block Diagram - Conventional to Fan	190
6.87	Flight Conversion Time Histories	191
6.88	" " " "	192
6.89	" " " "	193

1.0 SUMMARY

The U. S. Army XV-5A has satisfactorily completed an extensive flight test program consisting of investigations of the hovering, transition and conventional flight regimes. This report documents the many aspects of this program. A total of 45 flight hours were accomplished during which 53 vertical take-offs, 72 conventional take-offs, 17 fan flight mode take-offs at forward speed, and 74 conversions between fan and conventional flight modes were performed. Original flight test objectives were systematically accomplished in successfully demonstrating the feasibility of the lift fan concept of flight.

Specific conclusions resulting from the 8-month test program which ended 28 January, 1965 are categorized below according to flight regime.

HOVERING

1. Propulsion system hover lift performance for the "stall-free" engine configuration equaled predicted values based on original system specifications.
2. Flying qualities in steady hover and translations were appraised as satisfactory. Although yaw control power was less than predicted, control solely derived from the lift fan system provided satisfactory control characteristics.
3. The partial authority stability augmentation system functioned as predicted permitting hovering flight with ease. Investigations at reduced system gains showed the necessity for operation of pitch and roll channels, while use of yaw channel was considered optional.
4. Operation in proximity to the ground increased levels of disturbance and fan exhaust gas reingestion into engines and fans. Effects noticeable to the pilot diminished above 3 feet gear height and basically disappeared at 10 feet. Level of reingestion of exhaust gases into engine inlet at very low ground heights was largely dependent on control positions.
5. High levels of translation speed stability predominated in forward, sidewise translations; a characteristic regarded as highly desirable.

TRANSITION

1. Engine power and longitudinal trim requirements generally matched expectations. Excess power margin and fan overspeed limit climb, maximum speed, and acceleration capabilities of present configuration in EAFB hot-day operations.
2. Negative speed stability characteristic, occurring above speed for maximum nose down trim, was not considered detrimental to evaluations of the capabilities of the aircraft.
3. Positive dihedral effect existed at all forward speeds; directional static stability was negative at low speeds and became positive at indicated airspeeds above 35 knots.
4. Phasing of authority of fan controls as a function of vector angle appeared to be satisfactorily coordinated with flight speed and conventional aerodynamic control effectiveness, although vectoring at low speeds without increase in flight speed produced noticeable reduction in control effectiveness.
5. During a series of Army envelope expansion tests before the completion of the flight test program, steady state flight between approximately minus 5 and plus 8 degrees angle of attack over the transition speed regime was demonstrated.
6. Short period responses to disturbances were well damped for both longitudinal and lateral directional modes. Records indicate a period of approximately 3 seconds for the longitudinal mode. Approximately the same frequency is shown for the lateral - directional mode although some departure from this mean takes place below 60 knots where uncoupled roll and yaw motions occur.

CONVENTIONAL FLIGHT

1. Conventional flight performance closely matches predicted performance based on climb and level flight capability demonstrations. Engine static performance in the "stall-free" configurations exceeded predicted values based on the propulsion system specifications.
2. Flutter tests (not reported herein) were conducted to 406 knots calibrated airspeed ($M = .7$) and both aircraft were flown to this speed in acceptance demonstrations.

3. Nose wheel lift-off speeds were lower than predicted but still higher than those required to meet conventional flying qualities specifications. This characteristic for future versions may be corrected with more forward positioning of the main landing gear.
4. Stall with and without flaps was characterized by prestall buffet which was indicated one to 3 degrees angle of attack below the conditions for maximum lift coefficient.
5. Conventional roll control was considered to be quite sensitive and to have low lateral stick forces. Rudder control was effective in maintaining heading during taxi above 20 knots. Although elevator control power was high, stick force per g increased to moderately high levels at increasing speeds. Due to decreasing stability margins at higher angles of attack, only slight aft stick force was required to trim full 45 degrees flap conditions at more critical forward cg condition.
6. The dynamic longitudinal short period mode was heavily damped at all test conditions. Damping of the phugoid was neutral in cruise configuration. Typical of wind tunnel model indications, flap deflection produced reductions in longitudinal static stability at higher angles of attack as stall was approached.
7. Control induced dutch-roll oscillations were well damped at all speeds. Mild adverse yaw was encountered during bank-to-bank rolling maneuvers in cruise and preconversion configurations, while favorable yaw was shown in rolling maneuvers in landing configuration.

CONVERSION

1. Fan to turbojet mode conversions were conducted with ease over a range of calibrated airspeeds at 86 to 109 knots and required only slight pilot corrections.
2. Turbojet to fan mode conversions performed over a speed range from 90 to 115 knots CAS were somewhat more difficult requiring the development of a technique involving throttle advance coordinated with conversion initiation. Thrust spoilers were not used. Simulator derived diverter valve time delay following start of horizontal tail programming was determined detrimental to smoothly performing the maneuver.

Certain minor modifications were required to complete the planned flight test program, but none indicated any concept deficiency. The wing fan exit louver actuators required increased power to motivate the louvers in the high load areas of maximum stagger and the louvers themselves required structural strengthening to eliminate bending under load. A nose wheel shimmy problem encountered during initial high speed taxi tests required structural strengthening of the nose wheel fork and a revised shimmy dampener.

An engine compressor stall problem, brought about by reingested hot gases during hover operations in close proximity to the ground was eliminated by increasing engine "stall margin". This was effected by making both engine installation and engine control changes. Maximum J-85 engine speed was increased to 102 percent as a part of this stall alleviation program.

Various local minor structural heating problems, often created because of research mission test requirements, were solved by additional insulation in the appropriate areas.

In high speed conventional flights, a local aerodynamic flow separation of the empennage intersection causing "stick shake" and longitudinal trim changes was eliminated by the addition of a "bullet" fairing in the area. An aircraft directional oscillation remaining after "rudder-kick" maneuvers was eliminated by the addition of 3/8" T-section along the trailing edge of the rudder.

On the basis of tests completed during the contractor flight test program, the XV-5A is considered flightworthy for evaluation flight testing by the U. S. Army. While aircraft performance closely matches predictions, significant improvements can be gained through modification. It is recommended that a program for evaluation of possible improvement measures be initiated at the earliest possible date.

2.0 INTRODUCTION

The XV-5A is a two-place 10,000 pound flight research vehicle fabricated for the purpose of investigating the feasibility of the lift-fan concept of lift and propulsion for V/STOL aircraft. The aircraft was designed and constructed by the Ryan Aeronautical Company of San Diego under Sub-contract P. O. 203-00727 to the General Electric Company at Evendale, Ohio, who in turn had direct overall contract responsibility for total system (airframe and powerplant) to the United States Army Transportation Research Command, Fort Eustis, Virginia, under Contract No. DA 44-177-TC-715.

Design of the XV-5A was initiated in November of 1961, ending in December of 1963, with fabrication of two aircraft Serial Numbers 62-4505 and 62-4506 from June 1962 to March 1963.

Flight testing of the XV-5A was conducted at the United States Air Force Flight Test Center at Edwards AFB, California, during the period from March 1964 to January 1965. The flight testing was accomplished by the Ryan Aeronautical Company with the operational direction by Republic Aviation of Farmingdale, New York. Technical support was accomplished by Republic, Ryan, and General Electric. Test support included the General Electric Facility at Edwards, and employed ground support, data handling and reduction capability.

The purpose of the flight test program was to prove the feasibility of the concept through a Phase I 50 hour test, to include hovering, transition, conversion to turbojet mode, flight to 450 knots and reverse of sequence. The aircraft were instrumented to obtain that data necessary to attain the objectives of the flight test program. Sufficient instrumentation was installed in the aircraft to monitor safety of flight, systems functional characteristics and to perform the study of problem areas, should any arise. The collection of data for analyses to establish characteristics pertaining to specification compliance and/or future design was not an objective of the program. The test program involved development of an operating envelope for the aircraft which was expanded during the U. S. Army funded Program of 17 flights on aircraft 62-4506 between December 1 and December 31, 1964. The purpose of the tests was to expand the fan mode flight envelope sufficiently to permit flight by other than contractor engineer test pilots with reasonable safety margins for experimental aircraft. Particular emphasis was placed on the acceptable range of angle of attack and fan exit louver thrust vector angle at speeds of 30 to 80 knots in fan mode.

The data of these tests are reported herein along with Phase I test results.

The purpose of this report is to document the results of the Phase I test program as part of contract fulfillment. The basic flight test program is outlined in Reference 2-1. The results of 80 flights on Aircraft 62-4506 and 29 flights on Aircraft 62-4505 are also presented with 10.9 hours of fan mode and 34.7 hours of conventional mode tests completed. The scope of the test program and test operations priority often limited the amount and quality of the recorded data useable for analysis purposes. However, sufficient data were available to permit quantitative investigation of problem areas and the test data clearly defines concept feasibility in terms of test program accomplishments. When problem areas arose, additional instrumentation facilitated the solution of the specific problem and prevented major schedule slippage. In general, when a problem arose in fan mode, its nature was determined, and the fix accomplished while conventional mode tests were conducted and vice-versa. The results from in-flight excitation of the airframe in investigation of flutter characteristics are to be reported separately. A three-view drawing of the XV-5A and an abbreviated chronological history of the Phase I Flight Test Program are shown in Figures 2.1 through 2.3.

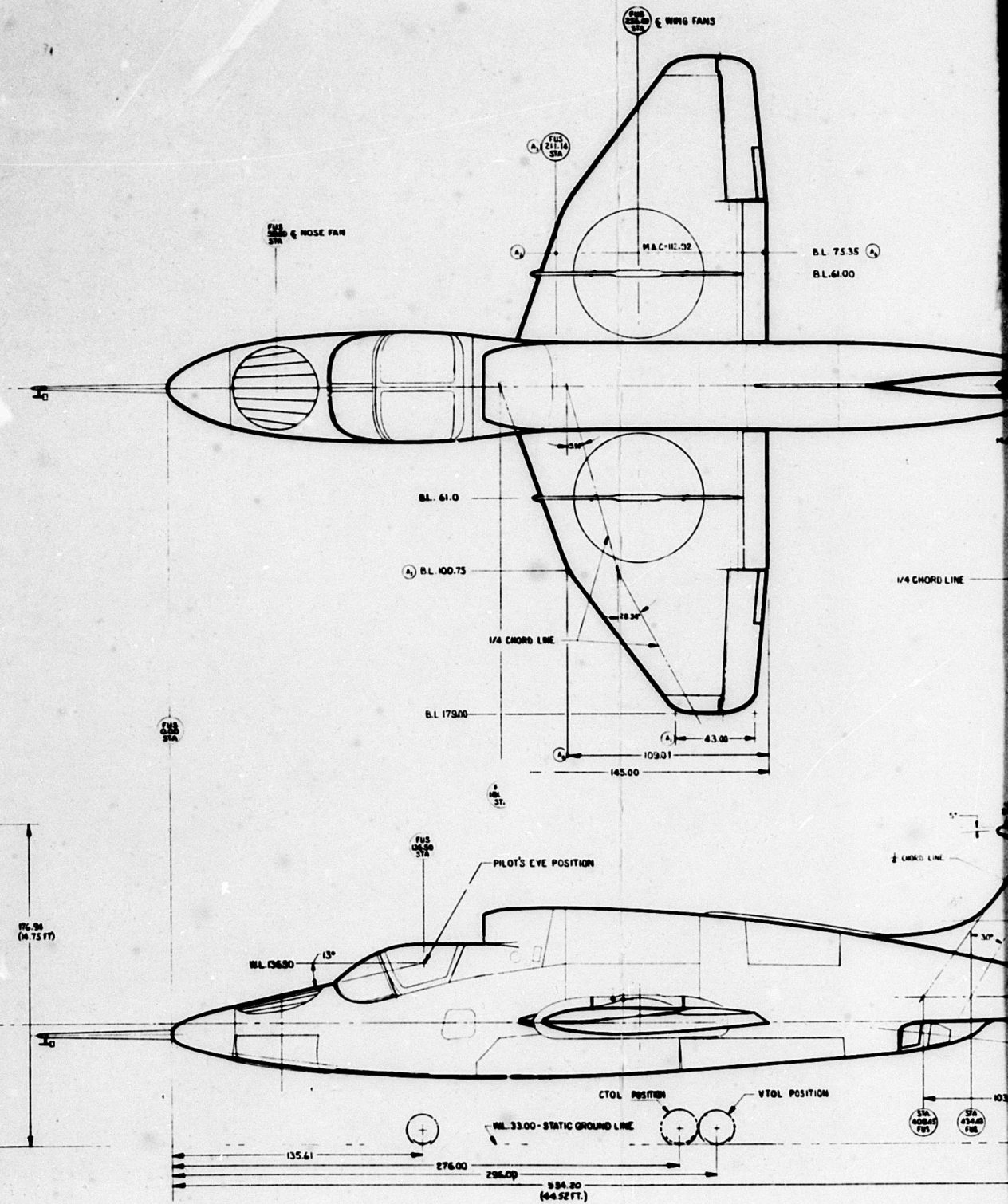


Figure 2.1 XV-5A Thr

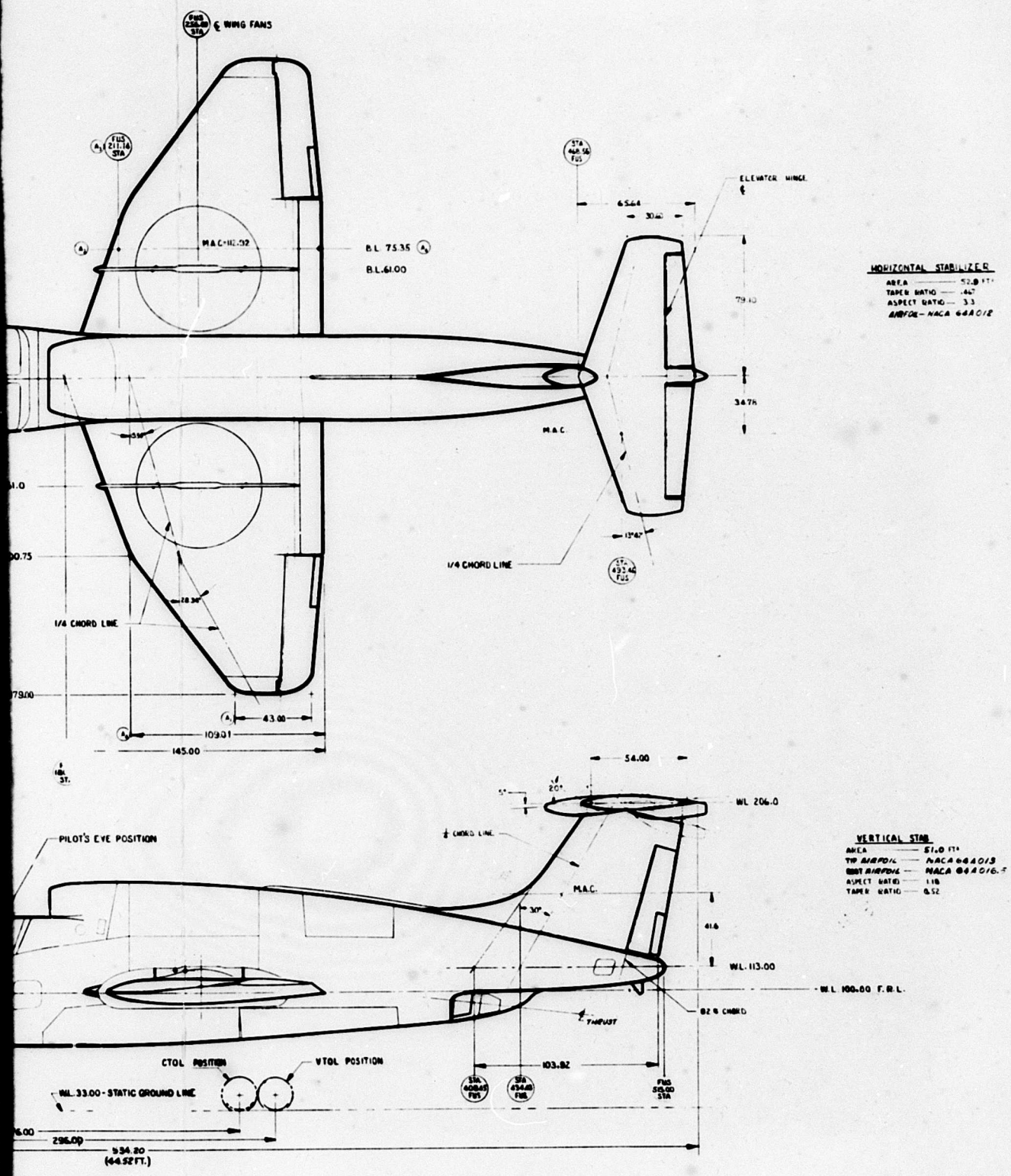


Figure 2.1 XV-5A Three-View Drawing

C

BLANK PAGE

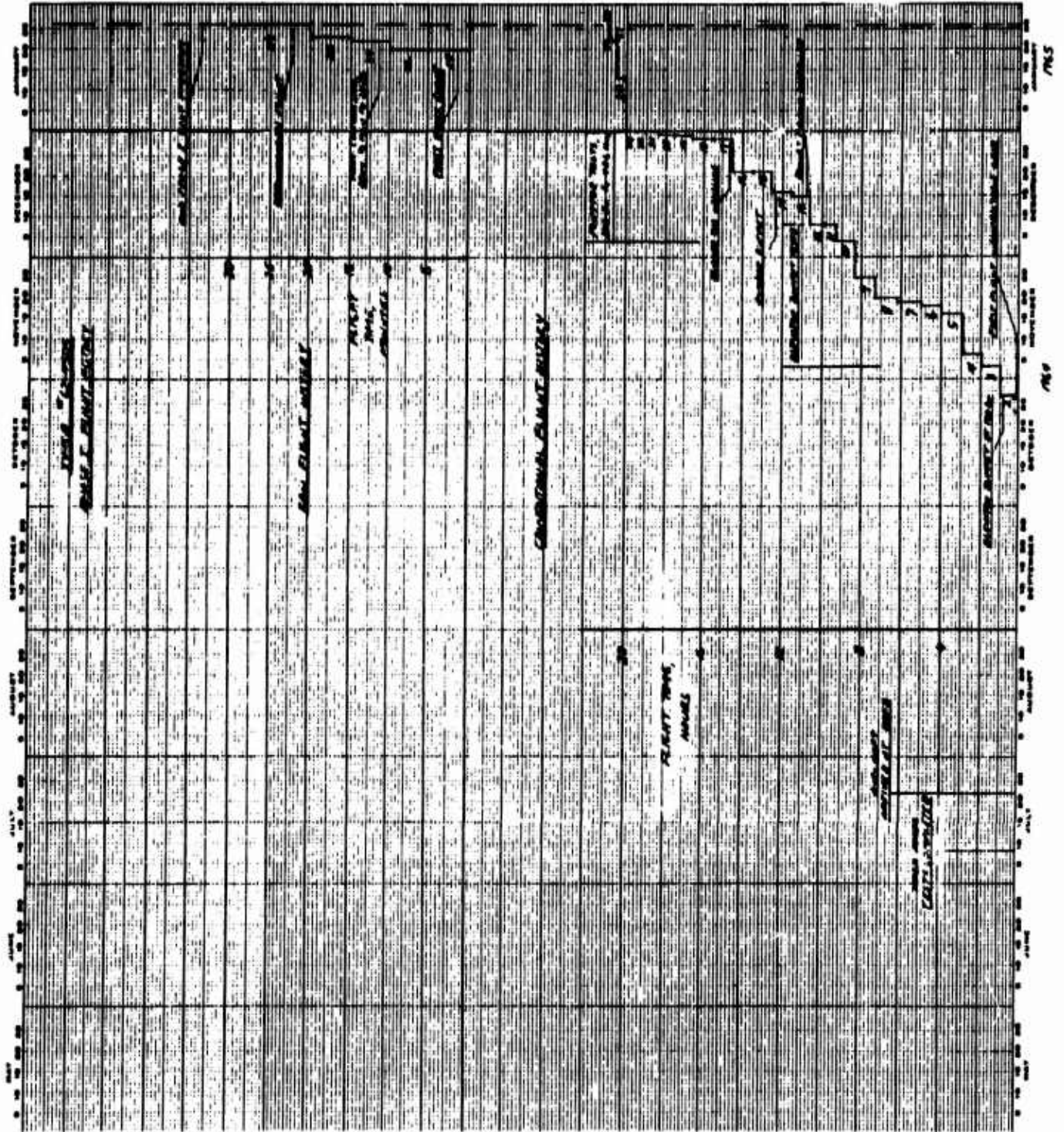


Figure 2.3 XV-5A No. 62-4505 Flight Time History

3.0 GLOSSARY

DEFINITIONS

Fan Mode	The aircraft configuration when deriving its lift and thrust from the wing fans.
Conventional Mode (also Jet Mode)	The aircraft configuration when deriving thrust from the tailpipe.
Transition	Condition of flight between hovering (2 - 5 kts) and conversion speed.
Hovering	Flight condition of zero or near zero flight speed including slight forward, side and aft speeds less than 5 kts.
Conversion	The act of changing between fan mode flight and conventional mode flight.
Preconversion	Conventional flight configuration just prior to conversion to fan mode. Exit louvers open 45° and pitch fan closures open.
Vectoring	Increasing wing fan exit louver thrust vector angle to increase speed.
Devectoring	Decreasing wing fan exit louver thrust vector angle to decrease speed.
Trim Transition	A transition when the vector angle and speed relationship follows a prescribed relationship, which results in minimum accelerations. A slow, almost steady state point-to-point transition, usually 2 minutes or more to conversion speed.
Thrust/Weight	Ratio of hovering takeoff maximum installed thrust (100% power, 100% collective stick), to hovering takeoff gross weight.

PCM	Pulse Code Modulation System; an airborne magnetic tape recording system.
Radio Log	Detailed record of test as monitored via radio by the flight test engineer.
T/M	Telemetry
Flight Card	Detailed listing of proposed flight plan prepared by the Flight Test Engineer for the pilot to follow at his discretion.
Flight Summary Report	Report prepared by the Flight Test Engineer for the Test Base Manager covering each test. Items covered are: <ol style="list-style-type: none"> 1. Flight number, aircraft serial number, pilot, takeoff time, time of flight, takeoff gross weight, c. g. location 2. Work accomplished prior to flight 3. Test configuration 4. Flight plan and actual flight 5. Flight discrepancies 6. Comments 7. Instrumentation
Pilot Report	Report on test prepared by the pilot. Items covered were: <ol style="list-style-type: none"> 1. Date, flight number, gross weight, c. g. location, configuration 2. Changes to aircraft since last flight 3. Discrepancies 4. Purpose of Flight 5. Summary of flight 6. Flight procedure 7. Flight results 8. Flight conclusions 9. Recommendations
STOL	Short takeoff and landing - applies to any aircraft take-off and/or landing operation performed in fan mode at forward speed.

CONFIGURATIONS

For the purposes of this report, the basic aircraft configurations shall be as described. Items of configuration not specified shall be in their normal settings for the particular configuration, except for standard deviations provided for under Subscripts, shown below.

CR: Cruise	Power for level flight at trim speed, flaps and gear up.
D: Dive	25 percent normal rated power or minimum operable power, whichever is greater, flaps and gear up.
G: Glide	Power off unless otherwise specified, flaps and gear up.
L: Landing	Power off, flaps 25° unless otherwise specified, gear down.
P: Power On Clean	Normal rated power, flaps and gear up.
PA: Power Approach	Power for level flight at 1.15 V_{SL} or normal approach speed, whichever is lower, flaps 25° unless otherwise specified, gear down.
PC: Preconver- sion Mode	Flaps 45°, gear up, wing fan doors unlocked, but closed. Wing fan exit louvers maximum aft, pitch fan doors and inlet vanes open.
WO: Wave Off	Takeoff power, flaps 25° unless otherwise specified, gear down.
TO: Takeoff	Takeoff power, flaps 25° unless otherwise specified, gear down.

SUBSCRIPTS

bf	Bullet fairing installed at intersection of horizontal and vertical tails.
fg	Fixed gear, in down position. Main landing gear doors removed, wheel well cover installed.
tr	T-section installed on trailing edge of rudder and rudder trim tab to alter rudder hinge moments.

SYMBOLS

A_F	Total fan area $\frac{2 \pi D^2}{4}$
C_D	Drag coefficient D/qS
C_D^S	Drag coefficient, $D/q^S A_F$
C_L	Lift coefficient, L/qS
C_L^S	Lift coefficient, $L/q^S A_F$
C_l	Rolling moment coefficient, L'/qSb
C_l^S	Rolling moment coefficient, $L'/q^S Sb$
C_m	Pitching moment coefficient, $M/qS\bar{c}$
C_m^S	Pitching moment coefficient, $M/q^S A_F D_F$
C_N^S	Normal force coefficient, NORMAL FORCE/ $q^S A_F$
C_n	Yawing moment coefficient, N/qSb
C_n^S	Yawing moment coefficient, $N/q^S Sb$
C_p^S	Fan power coefficient, $\frac{P \rho^{1/2}}{\left[\frac{T_{000}}{A_F} \right]^{3/2} A_F}$
C_Y	Sideforce coefficient, Y/qS

C_Y^s	Axial force coefficient, $X/q^s A_F$
\bar{c}	Mean aerodynamic chord. No subscript refers to wing. (feet)
D	Drag (pounds)
D	Fan diameter (feet)
d	Differential <p style="margin-left: 40px;">Example: dH_{ic} = differential indicated pressure altitude corrected for instrument error.</p>
G. W.	
G. W.	Gross weight (pounds)
g	Acceleration due to gravity, (feet/second ²)
H _g	Inches of mercury
H _i	Indicated pressure altitude (feet)
i	Horizontal stabilizer incidence angle, positive trailing edge down (degrees)
j	Complex multiplier, $\sqrt{-1}$
^o K	Degrees Kelvin
KW	Kilowatts
L	Lift force (pounds)
L'	Rolling moment (foot-pounds)

M	Pitching moment (foot-pounds)
N	Fan or gas generator RPM (percent)
N	Yawing moment (foot-pounds)
N. P.	Neutral point
n	Load factor (g's)
P	Power (foot-pounds/sec.)
P	The applied pressure at time t ($"H_g$, pounds/foot ²)
P _a	Atmospheric pressure corresponding to H _c ($"H_g$, pounds/foot ²)
P ^s _{SL}	Atmospheric pressure at standard sea level (29.92126 $"H_g$)
PSI	Pounds per square inch
p	Angular velocity about the airplane X axis (radians/second)
q	Angular velocity about the airplane Y axis (radians/second)
q	Free stream dynamic pressure, ($\rho/2 V_t^2$) ($"H_g$, pounds/foot ²)

q^s	Slipstream dynamic pressure, $q + T_{ooo}/A_F$ (H_g , pounds/foot ²)
q_c	Differential pressure or impact pressure, $P_t' - P_a$ (H_g , pounds/foot ²)
q_{cic}	Differential pressure corresponding to V_{ic} , $P_t' - P_s$ (H_g , pounds/foot ²)
R	Gas constant for dry air (5335 foot-pounds/pound/ ^o R)
o_R	Degrees Rankine
r	Angular velocity about the airplane Z axis (radians/second)
S	Reference area. Unsubscripted symbol refers to wing area. Control surface areas are aft of the hinge line. (feet ²)
T	Static fan thrust (pounds)
T_{ooo}	Wing fan static lift force with $\beta_v = 0^\circ$, $\beta_s = 0^\circ$ (pounds) and $V_T = 0$
T_a	Atmospheric temperatures (^o K)
T_{as}	Standard day atmospheric temperature corresponding to H_c (^o K)
T_{aSL}	Standard sea level atmospheric temperature (288.16 ^o K)

T_{at}	Test day atmospheric temperature ($^{\circ}$ K)
T_t	Total temperature ($^{\circ}$ K)
T_c^s	Fan thrust coefficient, $T_{000}/q^s A_F$ or $T_{NF}/q^s A_{NF}$
t	Time (seconds)
V	Velocity (feet/second)
V_c	Calibrated airspeed, $V_i + \Delta V_{ic} + \Delta V_{ic\ell} + \Delta V_{pc}$ (knots)
V_e	Equivalent airspeed, $V_c + \Delta V_t \sqrt{\sigma}$ (knots)
V_i	Indicated airspeed (knots)
V_{ic}	Indicated airspeed corrected for instrument error, $V_i + \Delta V_{ic}$ (knots)
ΔV_{ic}	Airspeed indicator instrument correction (knots)
$\Delta V_{ic\ell}$	Airspeed indicator lag correction (knots)
ΔV_{pc}	Airspeed indicator position error correction (knots)
V_{SL}	Stall speed in landing configuration - Power off.
V_t	True airspeed (knots)
v	Velocity along the airplane Y axis (feet/second)
W	Airplane gross weight (pounds)

W_f

Fuel flow (pounds/hour)

w

Velocity along the airplane Z axis (feet/second)

x

Distance from the airplane center of gravity along the airplane X axis (feet)

Y

Sideforce (pounds)

z

Distance from the airplane center of gravity along the airplane Z axis (feet)

GREEK SYMBOLS

α	Angle of attack (degrees)
β	Sideslip angle (degrees)
β	Wing fan exit louver angle, measured between louver aft surface tangent plane and a plane parallel to fan axis, positive trailing edge aft, (degrees)
β_1	Forward louver or odd numbered wing fan exit louver angle (degrees)
β_2	Aft louver or even numbered wing fan exit louver angle (degrees)
β_s	Wing fan exit louver stagger angle, $\beta_1 - \beta_2$ (degrees)
β_v	Wing fan exit louver vector angle, $\frac{\beta_1 + \beta_2}{2}$ (degrees)
δ	Flap or control surface deflection (degrees)
δ	Control input (inches or degrees)
δ	$P_a / P_{a_{SL}}$
δ_{ic}	$P_s / P_{s_{SL}}$
δ_{NF}	Nose fan thrust reverser door deflection measured from the closed position (degrees)
ϵ	Average downwash angle at horizontal tail (degrees)

η_t	Dynamic pressure ratio at the horizontal tail, q_t/q_o
θ	Pitch altitude (degrees)
θ	$T_a/T_{a_{SL}}$
μ	Wing fan blade tip advance ratio $\frac{V_t/\pi ND}{60}$
ρ	Air density (slugs/feet ³)
ρ_{SL}	Air density at standard sea level (0.0023769 slugs/feet ²)
σ	Sidewash angle at the vertical tail, $-\alpha_v - \beta$ (degrees)
σ	ρ/ρ_{SL}
ϕ	Roll attitude (degrees)
ψ	Yaw attitude (degrees)
ω_n	Undamped natural frequency of oscillation (radians/second)
ζ	Damping ratio

SUBSCRIPTS

0, 1, 2, etc.	Engine station designation
a	Aileron
ac	Aerodynamic center
d	Ailerons, drooped as flaps
e	Elevator
F	Wing fans
f	Wing inboard trailing edge flaps
L	Left hand
NF	Nose fan
NOM	Nominal
O	Zero velocity or free stream velocity
OL	Zero lift
O α	Zero angle of attack
P	Pedal
R	Right hand
r	Rudder
S	Wing stall
s	Longitudinal or lateral stick
TR	Trimmed flight ($C_m = 0$)
t	Horizontal tail
v	Vertical tail
V	Vector
w	Wing

ABBREVIATIONS

Avg.	Average
B. L.	Butt line
CAS	Calibrated airspeed
c. g.	Center of gravity
C. P. S.	Cycles per second
F. S.	Fuselage station
FWD	Forward
IP	Idle Power
KIAS	Knots indicated airspeed
MAC	Mean aerodynamic chord
Max.	Maximum
Min.	Minimum
MP	Maximum power
MRP	Military rated power
N. P.	Neutral Point
NRP	Normal rated power
OAT	Outside air temperature
PLF	Power for level flight
PTF	Power for constant turning flight
RPM	Revolutions per minute
SAS	Stability Augmentation System
S. L.	Sea Level
TEU	Trailing edge up
TOP	Takeoff power
W. L.	Waterline

SIGN CONVENTIONS

<u>PARAMETER</u>	<u>SIGN</u>	<u>CONVENTION</u>
El. Stick Pos.	+	Aft
Rud. Ped. Pos.	+	Rt. Fwd
Ail. Stick Pos.	+	Right
El. Stick Force	+	Pull
Pedal Force	+	Rt. Push
Ail. Stick Force	+	Right
Elev. Position	+	T. E. D.
Rudder Position	-	T. E. L.
Left Ail. Position	+	T. E. D.
Right Ail. Position	+	T. E. D.
Rudder Tab	-	T. E. L.
L. Ail. Tab Pos.	+	T. E. D.
R. Ail. Tab Pos.	+	T. E. D.
Horizontal Tail Pos.	+	T. E. D.
Ang. of Attack	+	Nose Up
Ang. of Sideslip	+	Nose Left
Pitch Attitude	+	Nose Up
Roll Attitude	+	R. W. D.
Pitch Rate	+	Nose Up
Yaw Rate	+	Nose Right
Roll Rate	+	R. W. D.

MISCELLANEOUS

PSID	Pounds per square inch differential
PSIG	Pounds per square inch gage
V	Volt
ma	Milliamperes
RMS	Root Mean Square
τ	Time constant
ω	Frequency, Rad/Sec
σ	Standard deviation of a normally disturbed random variable
e	Base of natural logarithm
DB	Decibels
K_H	Holding gain constant, Deg/Deg/Sec
K_M	Maneuvering gain constant, Deg/Deg/Sec
R	Ratio of high-frequency to low frequency gain of roll SAS lag-lead input network
S	Laplace transform operator
F	Thrust or force - pounds
θ	Relative absolute temperature, T/T_0 where θ and T have subscripts referring to static or total and to any particular station, $T_0 = 518.7^\circ R$.
δ	Relative absolute pressure, P/P_0 , where δ and P have subscripts referring to static or total and to any particular station, $P_0 = 29.92$ in. Hg.

BLANK PAGE

4.0 TEST SUMMARY

The Phase I test program development is shown in the following Tables 4.1 and 4.2. The tables show testing done in fan mode, jet mode, for stability performance, etc. Availability of and condition of recorded data concerning the subject tests are shown in Tables 5.1 through 5.5, which are explained in Section 5.0, Data Acquisition.

Additional tabular information concerning the development of Phase I test program with particular interest in thermodynamic investigation and information during ground test of Ship 2 A/C 62-4506 is presented in Table 6.1. A large percentage of these tests were conducted in the interest of engine and fan reingestion as related to installed lift losses and engine compression stall problems.

The following is a brief description of tests conducted during the Phase I program. All flight numbers are followed by an F. For example, 10F is the tenth time the wheels of the aircraft left the ground. All ground test numbers are followed by a G, (such as .06G) which is the sixth ground test following the previous flight. For example, "10.08G" would be the eighth ground test following the tenth flight.

Ship 2 A/C 62-4506 was delivered to EAFB in March 1964. The first three tests conducted were ground tests for purposes of functional checkout. Test .01G was an engine run with the aircraft in jet mode, while test .02G and .03G were engine runs with the aircraft in fan mode. Ground test .04G and .05G were low speed taxi tests in jet mode.

Test .06G was the first attempt at hovering flight. During this test, several attempts to hover the aircraft were unsuccessful due to inability to maintain wings level, while increasing power and collective lift to leave the ground (March 31). There was also an apparent lack of roll control power. Ground tests .07G to .10G determined that the wing fan exit louvers were not properly positioned with lateral stick displacement according to rigging specifications. Investigation of louver actuator position data and photographic data showed the louvers not staggering due to higher than estimated louver loads. These loads forced the actuator hydraulic cylinder to back-up, causing the louvers to deflect away from the fan airflow, (April 7).

During Tests 0.08G through 0.10G on Aircraft Serial Number 62-4506,

covering wing fan exit louver deflections, additional instrumentation was added to record the wing fan exit louver positions. Rectilinear potentiometers were installed and connected directly to the number 7 and 8 wing fan exit louvers to supplement the potentiometers already installed as part of the aircraft instrumentation which measured the wing fan exit louver actuator positions. In addition to the potentiometers to record wing fan exit louver position on the PCM, drill rod extensions were added to the louvers to facilitate photographic correlation of the louver positions. Adjustable load links were installed in place of the left wing fan exit louver actuators during Tests 0.12G through 0.14G on Aircraft Serial Number 62-4506. The load links were used to measure the loads transmitted by the wing fan exit louver to the forward and aft wing fan exit louver actuators.

While the data of the above tests were being studied and modifications being designed, the jet mode flight tests were accomplished. Initial attempts at jet mode high speed taxi tests indicated a nose wheel shimmy problem which caused a nose gear collapse during ground test .15G. This resulted in minor redesign and modification of the nose gear, successful high speed taxi was accomplished during ground test .16G. During test .17G, 3 to 5-foot "lift-offs" and "set-downs" were accomplished at approximately 96 knots indicated airspeed, (May 23).

Flight test 1. F through 8. F were qualitative evaluation tests of the low speed handling qualities, including static and dynamic longitudinal and lateral directional stability checks; power-on and power-off stall approaches, flaps-up and down. These tests were all conducted with landing gear fixed in the down position. Preconversion configuration investigations were included in tests 6F and 7F. Flight test 8F was an airspeed calibration test, (June 5, 1964).

Ground test 8.01G through 8.05G were fan mode tie-down tests for checkout of the modified wing fan exit louver actuation system and the structural stiffening of the louvers. Aircraft Serial Number 62-4506 was then installed on the Edwards AFB VTOL thrust stand for Tests 8.06G through 8.15G. During these tests, Gilmore recorders were used to record six-component force and moment data. Calibration checks were performed on the thrust stand by means of an electrical strain gage type load cell, and a potentiometer to read the load cell output. Prior to the tests, check calibrations of vertical force and pitching and rolling moments were made, aided by XV-5A test personnel. Subsequent to the tests, additional checks were conducted on axial force and yawing and pitching moments. The final calibration checks indicated that the pitching moment center was mislocated on the thrust stand. However, axial force and pitching moment data were

still suspect. Subsequent investigations indicated that the thrust stand vertical strut was binding against the pit cover used to protect instrumentation from the fan efflux. Temperature, control positions, and RPM data were recorded on the PCM system. A Brown recorder was used to monitor critical temperatures to prevent overheating and damage to the aircraft structure. Although these tests produced some questionable data concerning exit louver vectoring efficiency (which was later resolved on the jet mode thrust stand), they did produce the data which verified adequate hovering 3-axis control power. (July 10, 1964.) (Reference 4.1)

First hovering flight was accomplished in Flight 9. F. Hovering investigations were carried out through Flight 12. F, during which an engine stall terminated the test. During these flights, the ability to hover over a point and slight translational speed were investigated and SAS evaluations were conducted.

Tests 12.01G through 12.16G were conducted on Aircraft Serial Number 62-4506 to investigate compressor stall and reingestion of hot gases. A special air inlet screen was designed with 34 thermocouples to record the inlet air temperature on an oscillograph. An additional inlet temperature rake was installed in the right gas generator inlet duct at F. S. 201.88 comp and of 16 thermocouples and recorded on the PCM system. The left hand gas generator stub duct had 3 P_{t2} inlet pressure rakes installed and recorded on the PCM system. Instrumentation was also installed to monitor the compressor bleed valve position controlled by the T_{t2} sensor and compressor case temperature. Tests were conducted in the tie-down area to induce compressor stalls, which was done and the data studied. As a result several adjustments were made to improve engine stall margin such as modified compressor bleed valve schedule, additional cooling and tuning of the engines. During these tests, a check of the horizontal maximum thrust capability in fan mode, Test 12.03G, and in jet mode 12.15G using the EAFB conventional thrust stand was made.

Two static rigging checks on the lift fan control system were conducted on Aircraft Serial Number 62-4506 during this time, to obtain more information about the mechanical mixer mechanism and isolate any undesirable characteristics. A detailed control input schedule was outlined first. Data were recorded on the PCM system and final plots constructed and analyzed. Louver rigging was changed back to original gain configuration after Flight 21. First static rigging check was made September 11, 1964 prior to Test 22.0F. Additional checks were made in November.

Flights 13. F and 14. F were hovering tests to check out, in flight, the compressor stall alleviation modifications. (August 20, 1964)

Ground tests 14.01G and 14.02G were conducted for calibration of cockpit EGT and fuel flow indicators. Ground test 14.03G was a static check of the response characteristics of the SAS system.

The next 7 flights (15. F through 21. F) were conducted to evaluate the hovering flying qualities of the aircraft. The test included hovering in and out of ground effect at 3 - 5 feet and 7 - 30 feet, possible SAS switching transients, optimum SAS gain settings, low speed (2 - 8 knots) translational characteristics in all directions, altitude control both by recommended collective lift stick and with fixed collective and varying engine power setting. Flight 21. F was terminated by an inadvertent tip-over of the aircraft during a crosswind hover landing attempt, resulting in minor damage to the aircraft. (August 25, 1964)(Reference 4.2)

Ground tests 21.01G through 21.05G followed the repair of the aircraft, and consisted of functional checks of all systems and EGT calibrations and engine tuning (RPM and stall margin checks).

Flight tests 22. F, 23. F and 24. F were first attempts at forward transition to speeds of 20 knots or less and were conducted at an altitude of less than 30 feet. Qualitative evaluation of stability and control through pilot comment was made. (September 12, 1964)

Flight tests 25. F, 27. F and 28. F were conducted to further investigate handling qualities in the pre-conversion configuration in preparation for first conversion from fan mode to jet mode. Particular emphasis was placed on stall approaches and bank to bank turns.

Ground tests 24.01G, 24.02G and flight tests 26. F, 29. F, 30. F, 31. F and 32. F were conducted to evaluate the high speed (70 - 100 knots) fan mode flight characteristics in preparation for first conversion. Horizontal tail downwash data was collected during tests 24.01G and 24.02G for study of tail stall margins. All tests were conducted from the runway in STOL configuration including takeoff and landing and climbs and glides to and from altitudes in excess of 2000 feet terrain clearance. (October 1, 1964) The tests established that adequate power existed to climb on fans to 2000 foot terrain clearance for possible conversion from fan mode to jet mode and that tail stall margins were adequate. Flight 33. F was a last check on pre-conversion configuration characteristics and Flight 34. F was a runway takeoff in fan mode, climb to altitude, and the first conversion from fan mode to jet mode with "clean-up" to jet mode and conventional landing on runway. During flights 35. F, 36. F and 37. F, high speed fan mode flight handling characteristics were qualitatively evaluated in preparation for conversion from jet mode to fan mode. These

tests were conducted by runway takeoffs in fan mode, climb to altitude and tests of throttle advance and retard and 30 degree bank to bank turns and fan mode landing on the runway. During Flight 35. F, high wing fan inlet vane stresses were recorded by telemetry and the flight was terminated. A post-flight check showed that the telemetry indications were erroneous due to faulty instrumentation. In Flight 38. F, the first conversion from jet mode to fan mode and back was accomplished. This permitted further investigation into the fan mode transition speed range by jet mode takeoff with conversion to fan mode, and conversion to jet mode for conventional runway landing. (October 10, 1964)

Flight 39. F through 47. F optimized conversion techniques (fan mode to jet mode) and qualitatively evaluated fan mode handling characteristics at successively slower and slower speeds by de-vectoring. This test was conducted by jet mode takeoff, climb to test altitude, conversion to fan mode, slowing down to different speed-vector conditions by de-vectoring, ascertaining adequate trim and control at each new condition. At the completion of these tests, the aircraft was "vectored-up" to conversion speed and re-converted back to jet mode for a conventional runway landing. During these tests, close surveillance was maintained on horizontal tail angle of attack by means of an angle of attack indicator vane installed on a horizontal tail boom and recorded on PCM. Starting with 41.0F, horizontal tail angle of attack was monitored in real time V_{18} T/M during fan mode flight. Flights 48. F and 49. F were transition optimization flights with 48. F being a hover-off, transition out to 70 knots over the runway, climb out to altitude, conversion to jet mode and return to runway; and 49. F being jet mode takeoff, conversion to fan mode, let down from altitude and de-vector to hover landing on runway. Flight 50 was the first complete cycle of hover-off, transition, climb, convert to jet mode, re-convert to fan mode, descend, de-vector and hover land. (November 5, 1964)

Flight 51. F was aborted due to vibration of airframe and engine during climb-out.

Flights 52. F, 53. F, 55. F and 57. F were for further investigation into transition handling characteristics. Flights 54. F and 60. F checked hovering and ability to maintain hovering flight with separate channels of the SAS turned off. Flight 58. F was an investigation into the runway lift-off characteristics in fan mode at vector settings of 45° , 30° , 20° and 10° . Flight 59 was a check on the steel inlet guide vane stress levels.

Flights 61. F through 77. F were tests to expand the transition flight test envelope and to establish control power available over the transition speed range. During each test, a jet mode takeoff was effected, followed by a

climb to 3000-foot ground clearance altitude, where a conversion was made, a test conducted, a re-conversion to jet mode and a conventional runway landing made. Each test was limited to approximately 10 minutes duration due to fuel load and fuel consumption in fan mode. The transition trim speed attained and the vector angle of attack relationship was explored by increasing or decreasing vector and adjusting angle of attack in an effort to maintain speed and altitude. When the pilot became uncomfortable for any reason, such as attitude, control capability, aircraft disturbances, etc. the test was terminated. The test was also considered complete if changes in angle of attack or vector angle resulted in high rate of climb or sink (500 - 1000 fpm) or any "real-time" information such as tail angle of attack indicated a potential problem. (December 31, 1964)

Flights 78. F, 79. F, and 80. F on A/C 62-4506, were check flights and acceptance demonstration flights. (January 26, 1965)

Aircraft No. 1, Ship 62-4505, was used in the high speed jet mode development, coincident with structural flutter investigations in 29 flights from October 26, 1964 through January 26, 1965. The first two flights, 1. F and 2. F, checked out the landing gear retraction and dynamic low speed handling. Flight 1. F was terminated prematurely by a malfunctioning radio. Flight 2. F was terminated by elevator buffet (stick shake) at 180 knots indicated. Flight 3. F was flown with the aircraft "tufted" for flow studies including aerial photographs which showed the problem to be separated flow at the root intersection of the horizontal and vertical tails. (November 3, 1964) During flight 4. F, the stall characteristics for Ship 1 were investigated while solution to the buffet problem was being studied. Flights 5. F through 12. F were buffet investigation and static and dynamic stability checked with the exception of 10. F and 11. F which were terminated after takeoff because of malfunction of landing gear retraction and faulty instrumentation respectively. During these flights, the undisturbed (no elevator buffet) jet mode speed was raised from 180 knots to 220 knots by the use of vortex generator patterns on the horizontal and vertical tail. On Flight 13. F the final tail buffet fix (bullet fairing) was flight tested to 250 knots indicated. During flight 14. F, a residual undamped directional oscillation persisted, following rudder kick tests for structural flutter investigations. During Flights 15. F through 17. F, flutter investigations were continued out to 324 knots indicated at 20,000 feet altitude. During Flight 17.0F, the residual rudder oscillation mentioned above was eliminated by the addition of a "tee" angle added to the trailing edge of the rudder. Flight 19. F through 24. F were conducted to expand the high speed jet mode envelope through structural flutter checks at successively higher and higher speeds up to 406 knots indicated at 8000 feet altitude. Structural flutter testing is reported under separate cover. Some per-

formance testing and airspeed calibration work was also done during these flights. (January 13, 1965) (Reference 4.3)

Flights 27. F through 29. F were checkout flights of Ship 1's hover transition and conversion capability and acceptance demonstration flights. Fan mode operational capability with the retractable landing gear was briefly examined during Flight 28. F. (January 26, 1965)

TABLE 4.2 SUMMARY OF TESTS - A/C NO. 2 - SERIAL 62-4506

1. REPORT TO BE SUBMITTED
 2. BY DATE
 3. SERIAL NO. OF TEST
 RESULTS ONLY

TEST NUMBER	STABILITY		PERFORMANCE			
			PROPULSION		AERODYNAMICS	
	FALL	JET	FALL	JET	FALL	JET
1						
2						
3						
4						
5						
6						
7						
8						
9						
10						
11						
12						
13						
14						
15						
16						
17						
18						
19						
20						
21						
22						
23						
24						
25						
26						
27						
28						
29						
30						
31						
32						
33						
34						
35						
36						
37						
38						
39						
40						
41						
42						
43						
44						
45						
46						
47						
48						
49						
50						
51						
52						
53						
54						
55						
56						
57						
58						
59						
60						
61						
62						
63						
64						
65						
66						
67						
68						
69						
70						
71						
72						
73						
74						
75						
76						
77						
78						
79						
80						
81						
82						
83						
84						
85						
86						
87						
88						
89						
90						
91						
92						
93						
94						
95						
96						
97						
98						
99						
100						

BLANK PAGE

5.0 DATA ACQUISITION

The "Summary Test Results Available", Tables 5.1 through 5.5, list all of the aircraft test parameters or functions that were recorded on PCM (Pulse Code Modulation) equipment during the Phase I Flight Test Program. Considerably fewer aircraft test parameters were instrumented on aircraft serial number 62-4505, because development test flights using this aircraft were limited to conventional flight mode operations only.

During the VTOL Thrust Stand Test conducted with aircraft serial number 62-4506, Gilmore recorders were used to record six-component force and moment data. These force and moment data were then correlated with control inputs and power settings as recorded by the PCM system.

Safety of flight instrumentation telemetered to the ground station included fan and engine vibrations which were displayed on oscilloscopes during all flights. A Brown Recorder was used to monitor indicated aircraft angle of attack, indicated horizontal tail angle of attack, and longitudinal stick position during fan mode flight above hover velocities.

Aircraft serial number 62-4505 was used during Tests 10. F through 14. F primarily for in-flight flutter investigation. All data taken during these flights were transmitted via telemetry to a ground station and simultaneously recorded on magnetic tapes and Offner recorders which were monitored by the flight test engineer in charge of the flutter program.

5.1 INSTRUMENTATION CAPABILITY

The block diagram of Figure 5.1 shows how the in-flight test data system functioned. Because aircraft serial number 62-4506 was scheduled to be used primarily for fan mode flight testing, the instrumentation system was developed to provide the greater recording capacity of the two aircraft. Aircraft serial number 62-4506 had a maximum of 90 simultaneous PCM channels available. In order to increase the capability of the system still further, a commutated stepper mechanism was connected to four of the PCM channels. It has the capability of monitoring 150 thermocouples at the rate of three per second. It used three of the PCM channels for recording the data and the fourth channel for recording the stepper switch position. A photo panel and camera were also used on aircraft serial number 62-4506 during the first part of the flight test program. They were removed sub-

sequent to Test 21. F to reduce the overall weight of the aircraft's instrumentation system. The PCM system provided 16 minutes data recording time.

5.2 DATA HANDLING SYSTEM

Following a flight, the PCM data tape was removed from the in-flight recorder and was delivered to General Electric EDP (Engineering Data Processing). Complete one-per second digital data and Sanborn quick-look continuous data were processed from the flight tape by EDP on a priority basis. As a rule, this first-look test data were available to the flight test analysis group within two or three hours after a test flight.

The data were inspected by the data analysis group; the instrumentation engineer was informed as to the condition of the data. Often, additional requests were then submitted to EDP for digital data at a higher density and/or plotted data for specific flight intervals. The detailed data were then more fully analyzed.

5.3 GROUND CALIBRATIONS

Control surfaces and primary cockpit controls were calibrated with either inclinometers or protractors designed for the specific job. Pressure transducers were calibrated with either a standard water manometer or a calibrated pressure gage. Time slots or channels for recording temperature data were calibrated by use of a calibrated potentiometer to control the millivolt input to the PCM system. The output of the PCM system was read on an ASCRO unit, and recorded manually with the corresponding input by an instrumentation technician.

Because of the nature of the PCM recording system, the calibration method was somewhat unique. Figure 5.2 is a typical calibration form, and Figure 5.3 is a sketch of a typical calibration test setup. On this calibration form, there are five varying columns of figures. The first column was the value of pressure intended; the fourth column is the actual pressure achieved; the second column is the output of the PCM system that has been converted from binary to octal number base using an ASCRO unit. The third column is the output of the ASCRO unit converted into a decimal number base. The fifth column is the reading appearing on the cockpit pressure indicating gage. From this calibration form, two curves are plotted - oil pressure in PSIG versus PCM output in decimal counts, and oil pressure in PSIG versus cockpit indicated pressure.

Calibrations were generally conducted when a parameter was first connected to the instrumentation system, or if the data channel has been crabbed, i. e.,

data suspect. Periodically each data channel was checked to determine if it was within specified accuracies; however, often data were questionable due to recording tape noise, PCM noise, and/or induced cable pickup. These factors were either constant and affected the bias only, or the channel was erratic and could not be satisfactorily used for aircraft evaluation. When bias was distinguishable, adjustments were made as desired to the affected channels.

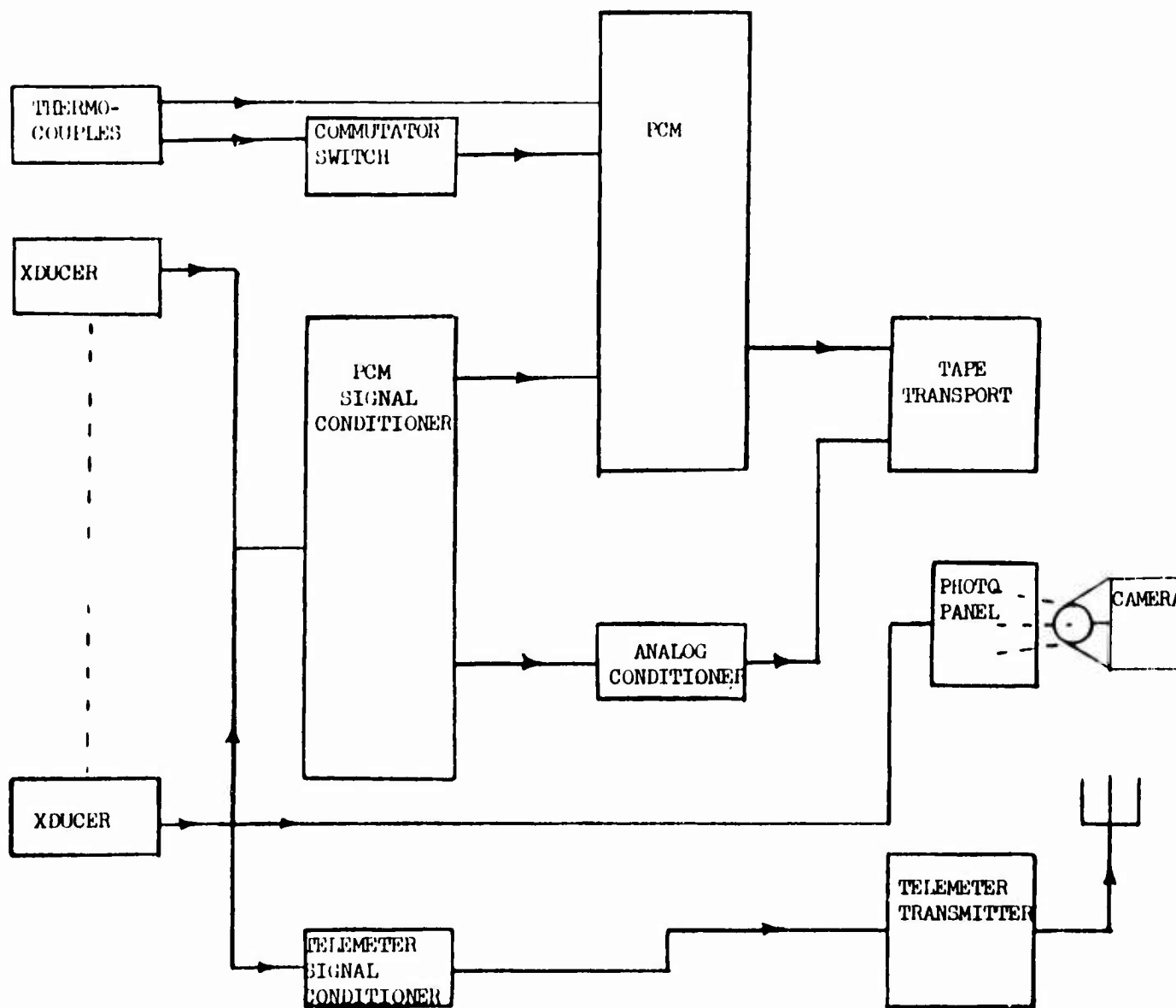


Figure 5.1 In-Flight Test Data System

PL-001-001-1

AIRCRAFT A-5A **CALIBRATION** DATE 6-16-54
 REF. FLT. 3 **GENERAL ELECTRIC** BY [Signature]
 ENG. N^o _____ **FLIGHT TEST**

PARAMETER PL1 L/H OIL PRESSURE RANGE _____
 CALIBRATION STANDARD Heise S/N^o H12214 RANGE _____
 PICKUP MFG. _____ MODEL _____ S/N^o _____ RANGE _____

TAPE S/N^o _____ TIME SLOT 38 CHANNEL N^o 49 CALIBRATION N^o _____ ON THIS TAPE
 OSCILLOGRAPH CHANNEL N^o _____ TYPE _____ CALIBRATION N^o _____ ON THIS ROLL
 PHOTO-RECORDER INDICATOR S/N^o _____ GALVO S/N^o _____
 COCKPIT INDICATOR S/N^o _____

CONDITIONS	START	FINISH	AIMS		PHOTO RECORDER	COCKPIT	GALVO POSITION	CONDITION COUNTER
			APPROX	ACTUAL				
PSIG			PSIG					
			0	314		0		
			10	320		9		
5 VOLT SUPPLY	4966	4967	20	354		17		
BAROMETER			30	616		28		
TEMPERATURE	81°	81°	40	1312		38		
TIME			50	1705		49		
			45	1524		44		
			40	1323		39		
REMARKS:			35	1074		34		
			30	630		29		
			20	354		19.5		
			10	320		10		
			0	316		0		

Figure 5.2 Flight Test Calibration Form

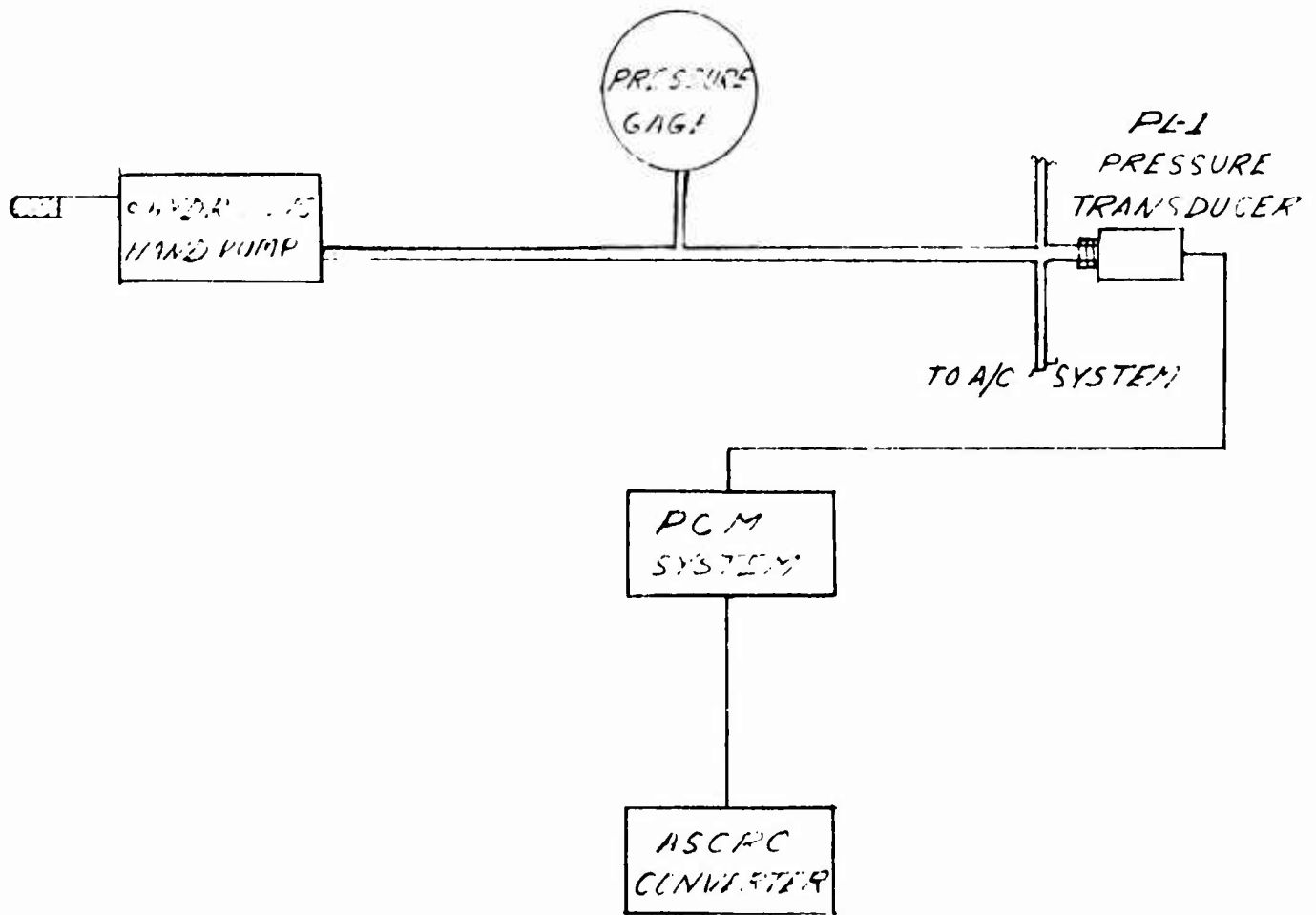


Figure 5.3 Typical Calibration Test Setup

NOTE: REFER TO FIGURE 6.96 FOR IDENTIFICATION OF LIQUID, AND STRUCTURAL TEMPERATURES

SUMMARY TEST RESULTS AVAILABLE, A

1	2	3	4
1	2	3	4
1	2	3	4
1	2	3	4
1	2	3	4

	PC-1	PC-2	PC-3	PC-4	PC-5	PC-6	PC-7	PC-8	PC-9	TC-17	CO-22	PC-32	PC-33	PC-34	PC-35	TC-2	TC-3	TC-5/11	TC-5/2	RPM-1	RPM-2	RPM-3	RPM-4	RPM-5	AR-1	AR-2	AR-3	AR-4	AR-5	F-1	F-2	F-3	PG-1	PG-2		
11																																				
21																																				
31																																				
41	X	X	X	X	X	X	X	X	X	X	X	X	X	X	X	X	X	X	X	X	X	X	X	X	X	X	X	X	X	X	X	X	X	X	X	
51	X	X	X	X	X	X	X	X	X	X	X	X	X	X	X	X	X	X	X	X	X	X	X	X	X	X	X	X	X	X	X	X	X	X	X	
61	X	X	X	X	X	X	X	X	X	X	X	X	X	X	X	X	X	X	X	X	X	X	X	X	X	X	X	X	X	X	X	X	X	X	X	
71	X	X	X	X	X	X	X	X	X	X	X	X	X	X	X	X	X	X	X	X	X	X	X	X	X	X	X	X	X	X	X	X	X	X	X	
81	X	X	X	X	X	X	X	X	X	X	X	X	X	X	X	X	X	X	X	X	X	X	X	X	X	X	X	X	X	X	X	X	X	X	X	
91	X	X	X	X	X	X	X	X	X	X	X	X	X	X	X	X	X	X	X	X	X	X	X	X	X	X	X	X	X	X	X	X	X	X	X	
101	X	X	X	X	X	X	X	X	X	X	X	X	X	X	X	X	X	X	X	X	X	X	X	X	X	X	X	X	X	X	X	X	X	X	X	
111	X	X	X	X	X	X	X	X	X	X	X	X	X	X	X	X	X	X	X	X	X	X	X	X	X	X	X	X	X	X	X	X	X	X	X	
121	X	X	X	X	X	X	X	X	X	X	X	X	X	X	X	X	X	X	X	X	X	X	X	X	X	X	X	X	X	X	X	X	X	X	X	
131	X	X	X	X	X	X	X	X	X	X	X	X	X	X	X	X	X	X	X	X	X	X	X	X	X	X	X	X	X	X	X	X	X	X	X	
141	X	X	X	X	X	X	X	X	X	X	X	X	X	X	X	X	X	X	X	X	X	X	X	X	X	X	X	X	X	X	X	X	X	X	X	
151	X	X	X	X	X	X	X	X	X	X	X	X	X	X	X	X	X	X	X	X	X	X	X	X	X	X	X	X	X	X	X	X	X	X	X	
161	X	X	X	X	X	X	X	X	X	X	X	X	X	X	X	X	X	X	X	X	X	X	X	X	X	X	X	X	X	X	X	X	X	X	X	
171	X	X	X	X	X	X	X	X	X	X	X	X	X	X	X	X	X	X	X	X	X	X	X	X	X	X	X	X	X	X	X	X	X	X	X	
181	X	X	X	X	X	X	X	X	X	X	X	X	X	X	X	X	X	X	X	X	X	X	X	X	X	X	X	X	X	X	X	X	X	X	X	
191	X	X	X	X	X	X	X	X	X	X	X	X	X	X	X	X	X	X	X	X	X	X	X	X	X	X	X	X	X	X	X	X	X	X	X	
201	X	X	X	X	X	X	X	X	X	X	X	X	X	X	X	X	X	X	X	X	X	X	X	X	X	X	X	X	X	X	X	X	X	X	X	

IDENTIFICATION OF GAS,
TEMPERATURES

TABLE, A/C 62-9505

1	□	⊕	◻
USABLE OR DATA TESTED ANALYSIS	NOT RECORDED IDENTIFY ONLY NO PLATS NO ANALYSIS	NON COMPUTA- TED TEMP RECORDED GOOD	N.G.

F-3	PG-1	PG-2	PG-3	S-504	S-506	S-509	S-510	S-522	AV-21	AV-22	AV-23	M-1	M-2	EVMX
														1-F
														2-F
														3-F
X	X	X	X	X	X	X	X	X	X	X	X	X	X	4-F
X	X	X	X	X	X	X	X	X	X	X	X	X	X	5-F
X	X	X	X	X	X	X	X	X	X	X	X	X	X	6-F
X	X	X	X	X	X	X	X	X	X	X	X	X	X	7-F
X	X	X	X	X	X	X	X	X	X	X	X	X	X	8-F
X	X	X	X	X	X	X	X	X	X	X	X	X	X	9-F
														10-F
														11-F
														12-F
														13-F
														14-F
X	X	X	X	X	X	X	X	X	X	X	X	X	X	15-F
X	X	X	X	X	X	X	X	X	X	X	X	X	X	16-F
X	X	X	X	X	X	X	X	X	X	X	X	X	X	17-F
X	X	X	X	X	X	X	X	X	X	X	X	X	X	18-F
X	X	X	X	X	X	X	X	X	X	X	X	X	X	19-F
X	X	X	X	X	X	X	X	X	X	X	X	X	X	20-F
X	X	X	X	X	X	X	X	X	X	X	X	X	X	21-F
														22-F
X	X	X	X	X	X	X	X	X	X	X	X	X	X	23-F
X	X	X	X	X	X	X	X	X	X	X	X	X	X	24-F
X	X	X	X	X	X	X	X	X	X	X	X	X	X	25-F
X	X	X	X	X	X	X	X	X	X	X	X	X	X	26-F
X	X	X	X	X	X	X	X	X	X	X	X	X	X	27-F
X	X	X	X	X	X	X	X	X	X	X	X	X	X	28-F
X	X	X	X	X	X	X	X	X	X	X	X	X	X	29-F

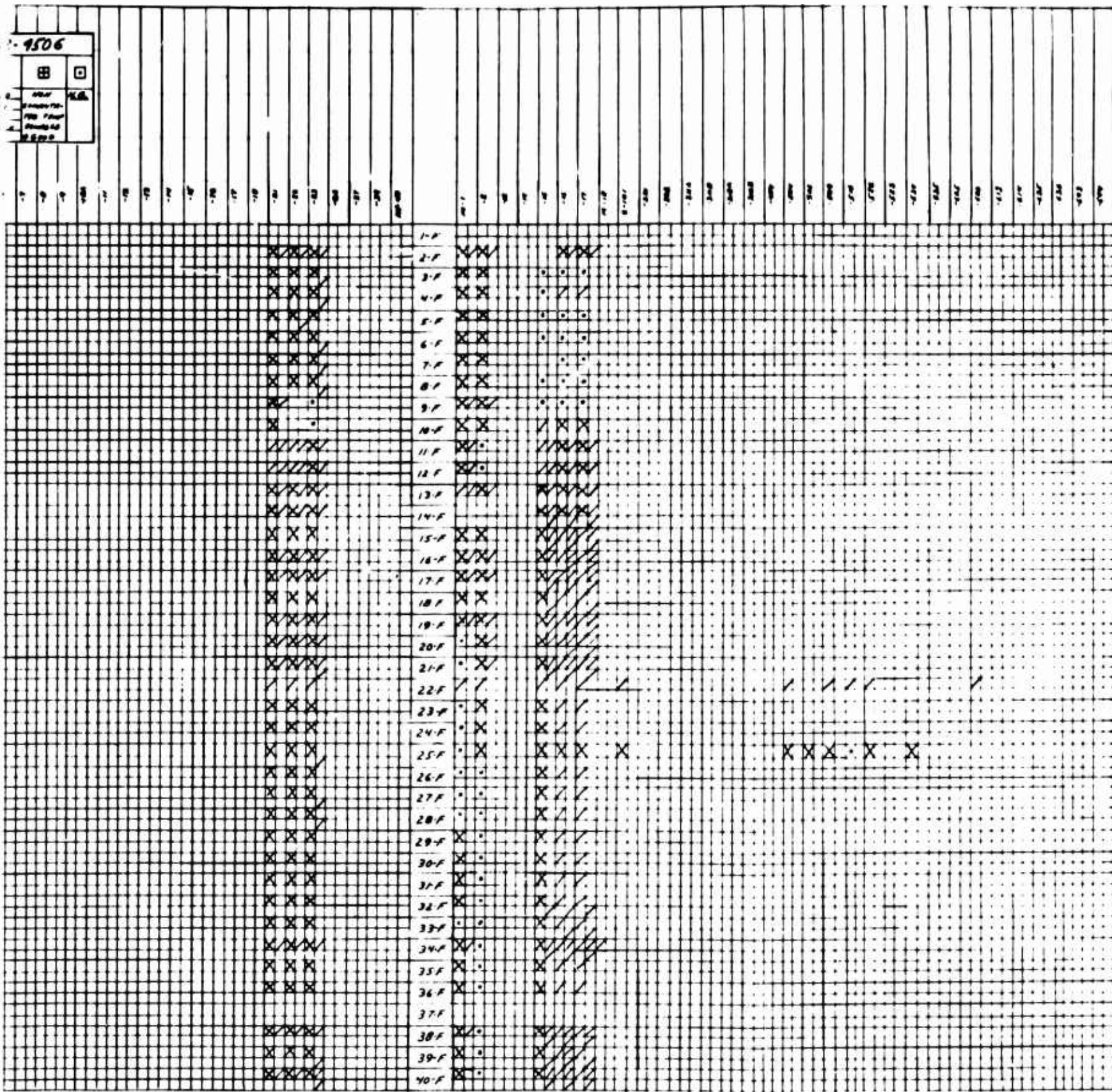
B

TABLE 5.1 SUMMARY TEST RESULTS AVAILABLE

<u>PARAMETER</u>	<u>CODE</u>	<u>PARAMETER</u>
Pitch Attitude	RPM-1	L/H Engine RPM
Roll Attitude	RPM-2	R/H Engine RPM
Pitch Rate	RPM-3	L/H Wing Fan RPM
Roll Rate	RPM-4	R/H Wing Fan RPM
Yaw Rate	RPM-5	Pitch Fan RPM
Lateral C. G. Acceleration	S-504	Stress, Space Frame Member 26-29
Longitudinal C. G. Acceleration	S-506	Space Frame Member Stresses SFM-2S-2B
Vertical C. G. Acceleration	S-509	Space Frame Member Stresses SFM- 8-13
	S-510	Stress, Space Frame Member 11-14
Lateral Stick Force	S-522	Stress, Space Frame Member 9-13
Longitudinal Stick Force		
Rudder Pedal Force	EVMK	Event Marker
L/H Fuel Flow Rate		
R/H Fuel Flow Rate		
Altitude		
Indicated High Airspeed		
Indicated Low Airspeed		
Angle of Attack, Nose Boom		
Angle of Sideslip, Nose Boom		
Elevator Position		
R/H Elevator Tip Position		
Rudder Position		
L/H Aileron Position		
R/H Aileron Position		
Flap Position		
Horizontal Stabilizer Position		
Vector Command		
Pitch Fan Exit Door Position		
Lateral Stick Position		
Longitudinal Stick Position		
Rudder Pedal Position		
Collective Control Position		

1506

☐	☐
☐	☐
☐	☐
☐	☐
☐	☐



C



CODE	PARAMETER
AR-1	Pitch Attitude
AR-2	Roll Attitude
AR-3	Pitch Rate
AR-4	Roll Rate
AR-5	Yaw Rate
AV-21	Lateral C. G. Acceleration
AV-22	Longitudinal C. G. Acceleration
AV-23	Vertical C. G. Acceleration
BVPL	Compressor Bleed Valve Position
BVPR	Compressor Bleed Valve Position
CDPL	Compressor Discharge Pressure
C DPR	Compressor Discharge Pressure
F-1	Lateral Stick Force
F-2	Longitudinal Stick Force
F-3	Rudder Pedal Force
M-1	L. H Fuel Flow Rate
M-2	R. H Fuel Flow Rate
M-15	Pitch Auto. Stab. Ampl. Output
M-16	Roll Auto. Stab. Ampl. Output
M-17	Yaw Auto. Stab. Ampl. Output
M-18	Power Strain Gages
PG-1	Altitude
PG-2	Indicated High Airspeed
PG-3	Indicated Low Airspeed
PG-8	Cockpit Static Pressure
PG-35	L. H Wing Fan Cooling Air Eject.
PG-37	L. H Wing Fan Fwd. Cooling Air
PG-40	L. H Engine Bleed Duct (LHSP)
PG-41	Compressor Discharge Pressure
PG-42	Compressor Discharge Pressure
PG-43	PT2 L H Engine Duct Ring
PG-50	PT2 L H Engine Duct Ring
PG-51	PT2 L H Engine Duct Ring
PG-52	PT2 L H Engine Duct Ring
PG-53	PT2 L H Engine Duct Ring
PG-54	PT2 L H Engine Duct Ring
PG-55	PT2 L H Engine Duct Ring

CODE PARAMETER

AR-1 Pitch Attitude
 AR-2 Roll Attitude
 AR-3 Pitch Rate
 AR-4 Roll Rate
 AR-5 Yaw Rate

AV-21 Lateral C. G. Acceleration
 AV-22 Longitudinal C. G. Acceleration
 AV-23 Vertical C. G. Acceleration

BVPL Compressor Bleed Valve Position, Left
 BVPR Compressor Bleed Valve Position Right

CDPL Compressor Discharge Pressure, Left
 CDPR Compressor Discharge Pressure, Right

F-1 Lateral Stick Force
 F-2 Longitudinal Stick Force
 F-3 Rudder Pedal Force

M-1 L. H Fuel Flow Rate
 M-2 R. H Fuel Flow Rate
 M-15 Pitch Auto. Stab. Ampl. Output
 M-16 Roll Auto. Stab. Ampl. Output
 M-17 Yaw Auto. Stab. Ampl. Output
 M-18 Power Strain Gages

PG-1 Altitude
 PG-2 Indicated High Airspeed
 PG-3 Indicated Low Airspeed
 PG-8 Cockpit Static Pressure
 PG-35 L. H Wing Fan Cooling Air Ejector - Alt
 PG-37 L. H Wing Fan Fwd. Cooling Air Ejector Pressure
 PG-40 L. H Engine Bleed Duct (LHSP)
 PG-41 Compressor Discharge Pressure Left
 PG-42 Compressor Discharge Pressure Right
 PG-43 PT2 L. H Engine Duct Ring
 PG-50 PT2 L. H Engine Duct Ring
 PG-51 PT2 L. H Engine Duct Ring
 PG-52 PT2 L. H Engine Duct Ring
 PG-53 PT2 L. H Engine Duct Ring
 PG-54 PT2 L. H Engine Duct Ring
 PG-55 PT2 L. H Engine Duct Ring

CODE PARAMETER

PG-56 PT5 Turbine Discharge
 PG-57 Dynamic Press. Horiz.

PL-1 L/H Engine Oil Pressure
 PL-2 R/H Engine Oil Pressure
 PL-7 L/H Hydraulic Accumulator
 PL-8 R/H Hydraulic Accumulator

PO-1 Angle of Attack, Nose Boom
 PO-2 Angle of Sideslip, Nose Boom
 PO-3 Elevator Position
 PO-4 R/H Elevator Tip Position
 PO-5 Rudder Position
 PO-6 L/H Aileron Position
 PO-7 R/H Aileron Position
 PO-8 Flap Position
 PO-9 Horizontal Stabilizer Position
 PO-11 L/H Elevator Tab Position
 PO-12 R/H Elevator Tab Position
 PO-13 L/H Odd Wing Fan Louver
 PO-14 L/H Even Wing Fan Louver
 PO-15 R/H Odd Wing Fan Louver
 PO-16 R/H Even Wing Fan Louver
 PO-17 Vector Command
 PO-18 +2.5 Inst. Power Supply
 PO-19 L/H Outboard Fan Door
 PO-20 -2.5 Inst. Power Supply
 PO-21 R/H Outboard Fan Door
 PO-22 Pitch Fan Exit Door Position
 PO-23 R/H Pitch Fan Door Position
 PO-25 L/H Diverter Valve Position
 PO-32 Lateral Stick Position
 PO-33 Longitudinal Stick Position
 PO-34 Rudder Pedal Position
 PO-35 Collective Control Position
 PO-36 L/H Elevator Tip Position
 PO-38 Compressor Bleed Valve
 PO-39 Compressor Bleed Valve
 PO-43 L/H Odd Louver Position
 PO-44 L/H Even Louver Position
 PO-45 R/H Odd Louver Position
 PO-46 R/H Even Louver Position
 PO-47 Angle of Attack, Tail Boom
 PO-48 Auto. Stab. Gain Switch



TABLE 5.2 SUMMARY TEST RESULTS AVAILABLE

<u>PARAMETER</u>	<u>CODE</u>	<u>PARAMETER</u>
PT5 Turbine Discharge Press.	RPM-1	L/H Engine RPM
Dynamic Press. Horiz. Tail Boom	RPM-2	R/H Engine RPM
L/H Engine Oil Pressure	RPM-3	L/H Wing Fan RPM
R/H Engine Oil Pressure	RPM-4	R/H Wing Fan RPM
L/H Hydraulic Accumulator Pressure	RPM-5	Pitch Fan RPM
R/H Hydraulic Accumulator Pressure	S-101	Axial, Actuator Load
Angle of Attack, Nose Boom	S-504	Stress, Space Frame Member 26-29
Angle of Sideslip, Nose Boom	S-506	Space Frame Member Stresses SFM-2S-2B
Elevator Position	S-509	Space Frame Member Stresses SFM-8-13
R/H Elevator Tip Position	S-510	Stress, Space Frame Member 11-14
Rudder Position	S-522	Stress, Space Frame Member 9-13
L/H Aileron Position	S-523	Stress, Space Frame Member 10-14
R/H Aileron Position	S-534	Space Frame Member Stresses SFM-1-3
Flap Position	S-606	Wing Spar Stresses of BL 40 L/H Fwd LC
Horizontal Stabilizer Position	S-643	Wing Spar Stresses at BL 40 R/H Fwd LC
L/H Elevator Tab Position	S-663	Fan Support Link Stresses Upper L/H Link
R/H Elevator Tab Position	S-664	Fan Support Link Stresses Upper R/H Link
L/H Odd Wing Fan Louver Actuator Position	S-656	L/H Leading Edge Stress
L/H Even Wing Fan Louver Actuator Position	SSP	Stepper Switch Position
R/H Odd Wing Fan Louver Actuator Position	LHSP	L/H Static Port Pressure
R/H Even Wing Fan Louver Actuator Position	EVMK	Event Marker
Vector Command		
+2.5 Inst. Power Supply Voltage		
L/H Outboard Fan Door Position		
-2.5 Inst. Power Supply Voltage		
R/H Outboard Fan Door Position		
Pitch Fan Exit Door Position		
R/H Pitch Fan Door Position		
L/H Diverter Valve Position		
Lateral Stick Position		
Longitudinal Stick Position		
Rudder Pedal Position		
Collective Control Position		
L/H Elevator Tip Position		
Compressor Bleed Valve Position, Right		
Compressor Bleed Valve Position, Left		
L/H Odd Louver Position		
L/H Even Louver Position		
R/H Odd Louver Position		
R/H Even Louver Position		
Angle of Attack, Tail Boom		
Auto. Stab. Gain Switch Position		

6.0 FAN FLIGHT TEST RESULTS

6.1 PERFORMANCE

6.1.1 Hover

6.1.1.1 Maximum Installed Lift

Within this report, the maximum installed hover lift for the aircraft will be defined as the maximum weight that may be supported in trimmed hover flight. With this definition, for a given atmospheric environment, maximum lift is of concern both in and out of ground effect; the difference between them being the accumulative effects of fan back pressuring, hot gas ingestion other than direct fan forces, and possible differences in required control settings.

The maximum installed hover lift for the propulsion system is the maximum lift that the system is capable of presenting to the aircraft regardless of the manner in which it may be used. In establishing this value from test results, accumulative effects of ground proximity, ambient conditions, control settings and ingestion factors are automatically included; and philosophical arguments regarding identification of aircraft and propulsion system contributions are automatically resolved. Any differences between maximum lift values for the propulsion system, and for the aircraft, should be accountable in terms of aircraft operational requirements (control degradations, ground effect, etc.).

The best values of installed lift obtainable during fan mode operation occur during hover conditions, where, based on fuel accountability, aircraft weights are quite accurately known. During the Phase I Flight Test Program, nearly 100 fan mode lift-off and touchdown maneuvers were conducted. Of the 100 conditions, eight were selected covering the nominal range of aircraft weight conditions during the time period following installation of aircraft and engine "stall-free-operation" modifications (see Section 7.3.1). The eight hover conditions together with the procedure and results are summarized in Table 6.1. Corrected installed wing fan lift performance, correlated in terms of zero louver stagger angle ($\beta_s = 0$), as

a function of corrected lift fan rpm is presented in Figure 6.1 where it is compared with other data. Stagger corrections were applied according to the test derived effectiveness curve of Figure 6.7 and the corrected fan lift is subject to any errors existing in the stagger effectiveness data. Using this curve, a maximum wing fan lift 1.5 percent higher than that shown in Figure 6.1 is available at 13° stagger angle. The comparison of lift fan performance data shows very good agreement with the X353-5B specification data. Account has been taken of wing fan inlet air temperature as the data reduction procedure of Table 6.1 shows. Wing fan lift was established by two methods; summation of vertical forces assuming wing fan and pitch fan lift equal aircraft hover weight, and summation of pitching moments taken about the pitch fan hub center. The rather close agreement of these two methods is shown in Table 6.1 (columns 26 and 27). The pitch fan performance used is shown in Figure 6.2 and was that derived by E. G. Smith from pitch fan performance tests at Evendale (Reference 6.1).

Actual pitch fan lift developed was obtained through the ratio of actual to maximum pitch fan lift as a function of pitch fan thrust reverser door position which is presented in Figure 6.9. The maximum installed lift is obtained using the stagger effectiveness curve of Figure 6.7 bearing in mind that the minimum louver stagger angle is 17° ($\beta_s = 17^\circ$) at full up collective as the XV-5A aircraft controls system is rigged.

Correlations of wing fan, pitch fan and gas generator rpm are presented in Figures 6.4 and 6.5. In spite of considerable scatter, the few data correlate reasonably well with estimates of E. G. Smith. The variation of maximum wing fan lift (or thrust) as a function of wing fan speed and referenced to the maximum corrected rpm, 95% at 102% engine speed, is presented in Figure 6.6. This data is used in subsequent calculations.

Based on the foregoing data, maximum installed pitch and wing fan lift for the aircraft as rigged for sea level standard day conditions are shown in Figure 6.6. Included are corrections for the stagger effectiveness at $\beta_s = 17^\circ$; and the following: nominal "out-of-ground-effect" temperature increments for hot gas ingestion: engine inlet air 15° F, wing fan inlet air 0° F, pitch fan inlet air 15° F. Combining these with the data of Figure 6.3 permits establishment of aircraft hovering control setting for out of ground effect operation.

		①	②	③	④	⑤	⑥
TEST 143-2	OP'N	OAT oF	Pamb "HG	$W_{A/C}$ lbs.	CG STA.	δ_{SC} "	$\beta_{V_{AVE}}$ D
21F	TO	77	27.61	9815	240.8	92.7	-2.9
	TO	77	27.61	9700	239.9	90.8	-2.4
	L	77	27.61	9560	240.0	93.5	-2.4
48F	TO	39	27.78	10100	240.1	38.3	-2.5
50F	TO	40	27.73	10300	240.3	24.3	-2.8
	L	40	27.73	9350	239.8	58.5	- .8
80F	TO	54	27.925	10660	—	48.3	-4.8
	L	54	27.925	9760	—	51.5	-3.7

- ① OAT — Outside Ambient Temperature.
- ② P_{amb} — Ambient or Barometric Pressure.
- ③ $W_{A/C}$ — Weight of Aircraft
- ④ CG — Center of Gravity of Aircraft.
- ⑤ δ_{SC} — Collective Stick Position .
- ⑥ $\beta_{V_{AVE}}$ — Average Fan Louver Vect. or Angle.
- ⑦ $\beta_{S_{AVE}}$ — Average Fan Louver Stagger Angle.
- ⑧ P_{022} — Pitch Fan Thrust Reverser Door Position Angle.
- ⑨ t_2 — Engine Inlet Air Temperature.

- ⑩ t_1
- ⑪ t_2
- ⑫ N
- ⑬ N
- ⑭ N
- ⑮ N

	⑥	⑦	⑧	⑨	⑩	⑪	⑫	⑬
	$\beta_{V_{AVE}}$ Deg.	$\beta_{S_{AVE}}$ Deg.	P022 Deg.	t_2 °F	t_{10} °F	t_{2D} °F	N_{PF} %	$N_{WF_{AVE}}$ %
	-2.945	15.5	75.5	93	127	86	98.69	90.08
	-2.417	15.7	81.6	96	127	86	98.58	89.93
	-2.408	15.1	73.8	98	127	86	100.88	90.63
	-2.221	28.6	73.0	55	49	77	99.39	94.58
	-2.825	29.7	72.2	57	40	50.5	100.69	96.01
	- .879	24.0	70.0	50	45	89.0	95.38	89.02
	-4.826	25.4	76.2	73	55.5	69.0	100.38	93.42
	-3.750	23.2	71.2	62	53	66.0	97.02	90.92

⑩ t_{10} — Wing Fan Inlet Air Temperature.

⑪ t_{20} — Pitch Fan Inlet Air Temperature.

⑫ N_{PF} — % RPM Pitch Fan.

⑬ $N_{WF_{AVE}}$ — Average % RPM of Left and Right Wing Fans.

⑭ $N_{E_{AVE}}$ — Average % RPM of Left and Right Engines.

⑮ $N_{PF} / \sqrt{\theta_{20}}$ — $N_{PF} [(t_{20} + 459.69) / 518.69]^{1/2}$

⑯ N_{WF}

⑰ N_E

⑱ LPI

⑲ LPI

⑳ W_A

㉑ L_W

(13)	(14)	(15)	(16)	(17)	(18)	(19)	(20)
$N_{WF\ AVE}$ %	$N_{E\ AVE}$ %	$\frac{N_{PF}}{\sqrt{\theta_{20}}}$ %	$\frac{N_{WE}}{\sqrt{\theta_{10}}}$ %	$\frac{N_E}{\sqrt{\theta_2}}$ %	$\frac{LPFD}{\delta}$ lbs.	$\frac{LPF}{LPFD}$	$\frac{W_{A/C}}{\delta}$ lbs.
90.08	102.06	96.18	84.72	98.90	1575	.468	10636
89.93	101.76	96.07	84.58	98.32	1575	.638	10512
90.63	102.15	98.31	85.24	98.51	1645	.406	10360
94.58	103.45	97.72	95.52	103.80	1625	.375	10878
96.01	103.12	101.50	97.82	103.32	1765	.308	11113
89.02	98.46	92.76	90.25	99.32	1460	.280	10089
93.42	102.28	99.46	93.74	100.92	1690	.490	11421
90.92	99.61	96.68	91.69	99.30	1590	.315	10457

$$(16) \frac{N_{WF}}{\sqrt{\theta_{10}}} = \frac{N_{WF\ AVE}}{\left[(t_{10} + 459.69) / 518.69 \right]^{1/2}}$$

$$(22) L_{WF}$$

$$(17) \frac{N_E}{\sqrt{\theta_2}} = \frac{N_{E\ AVE}}{\left[(t_2 + 459.69) / 518.69 \right]^{1/2}}$$

$$(23) \frac{L_{WF}}{\delta}$$

$$(18) LPFO/\delta = \text{Maximum Installed Pitch Fan Lift at } (15)$$

$$(24) \frac{L_{WF}}{2\delta}$$

$$(19) LPF/LPFO = \text{Ratio Actual to Maximum Pitch Fan Lift at } (8)$$

$$(25) \frac{Total}{A}$$

$$(20) \frac{W_{A/C}}{\delta} = (3) / \delta \text{ where } = Pamb/29.92. \text{ The Engine Air Inlet Pressure Recovery was Assumed } = 1.0.$$

$$(26) L_{WF}$$

$$(21) \frac{L_{WFOO}}{\delta} = (20) - (18) \times (19) = \text{Total Wing Fan Lift at } \beta_{S\ AVE}$$

$$(27) L_{WF}$$

δ

TABLE 6.1
XV-5A FLIGHT TEST DATA

(20)	(21)	(22)	(23)	(24)	(25)	(26)	(27)
$\frac{W_{A/C}}{\delta}$ lbs.	$\frac{L_{WF00}\beta_s}{\delta}$ lbs.	$\frac{L_{WF}\beta_s}{L_{WF}\beta_s = 0}$	$\frac{L_{WF000}}{\delta}$ lbs.	$\frac{L_{WF000}}{2\delta}$ lbs.	$\frac{T_{000}}{AF}$ lbs./ft. ²	L_{WFL} lbs.	L_{WFM} lbs.
9636	9900	1.005	9850	4925	231	9135	9058
9512	9505	1.004	9467	4733	222	8773	8907
9360	9690	1.006	9632	4816	226	8944	8783
10878	10269	.855	12010	6005	282	9535	9285
1113	10569	.827	12780	6390	300	9796	9479
10089	9679	.930	10408	5204	244	8971	8581
10421	10593	.910	11640	5820	273	9887	9800
10457	9957	.945	10537	5268	247	9293	8933

(2) $\frac{L_{WF}\beta_s}{L_{WF}\beta_s = 0}$ = Wing Fan Lift Stagger Effectiveness Factor from Figure 6.7 at $\beta_{S_{AVE}}$.

(3) $\frac{L_{WF000}}{\delta}$ = (21) / (22) = Maximum Connected Wing Fan Lift at $\beta_s = 0$

(4) $\frac{L_{WF000}}{2\delta}$ = (23) / 2 = Lift per Fan.

(5) $\frac{T_{000}}{A}$ = (23) / 42.61 ft.² = Lift Per Unit Area of Fan.

(6) L_{WFL} = Uncorrected Lift of Aircraft $W_{A/C}$ - (18) + (19) + δ

(7) L_{WFM} = Uncorrected Lift of Aircraft = [(4) - 59] + (3) / 197

(Based on Moment Balance about Pitch Fan Center.)

BLANK PAGE

6.1.1.2 Louver Stagger Effectiveness

6.1.1.2.1 Actuator Stall Problems and Louver System Modifications

A deficiency in roll control effectiveness was noted by the pilot during the first hover attempts. Flight test data showed that less than commanded louver deflections were obtained during the test. Subsequent louver actuation load tests indicated that the louver loads were much higher than predicted, verifying that stalling of the actuators at moderately high stagger angles and high power settings had occurred. Tests were also conducted which showed that large improvements in stagger effectiveness could be obtained from stiffening the louver system. Work was initiated to stiffen the entire fan louver system and actuation linkage, and to procure new louver servo actuators capable of producing the required 4800 pound louver actuation force using a single hydraulic system. In addition, a change was made in the mechanical mixer system which was designed to provide increased differential stagger for increased roll control power.

6.1.1.2.2 Measurement of Stiffened Fan System Louver Stagger Effectiveness

Following the fan system modifications described above, the aircraft was installed on the EAFB Vertical Thrust Stand to determine hover control effectiveness. During Test 8.14G a series of full control sweeps were conducted at minimum, mid, and maximum collective lift settings with 95 percent gas generator RPM and zero axial thrust. The pure lift data and the rolling moment data were then normalized to obtain the louver stagger effectiveness of the fan system. As a result of this test, the louver stagger effectiveness for the stiffened fan system was found to be considerably changed from the data used on the simulator. Figure 6.7 presents both the old and new louver stagger effectiveness curves for hover.

It is seen that although the two curves cross at $\beta_s = 30^\circ$, they grossly differ at all other stagger settings. In particular, the test data show that stagger settings below 13° produce some slight negative fan thrust modulation.

As discussed in Section 6.2.5, the slopes of the new stagger effectiveness curve has been to some degree verified over the 20° to 40° stagger range based on roll SA system gain settings determined to produce system instability.

6.1.1.3 Collective Vector Effectiveness

Edwards AFB VTOL Thrust Stand tests were conducted to obtain static wing fan exit louver vector effectiveness. These data indicated a reduction in vector effectiveness for wing fan louver vector angles greater than 20° . The data was questioned and a second check was made on the CTOL thrust stand in the fan mode with approximately 45° vector angle. This second check indicated that the wing fan exit louver vector effectiveness was only slightly less than previously developed for the unstiffened louver system. Part of the loss may be due to the increased thickness ratio of the louvers required to stiffen them. Subsequent checks on the VTOL thrust stand uncovered an interference problem between the vertical lift post of the thrust stand and the pit cover which resulted in the erroneous data.

Figure 6.8 presents normalized horizontal thrust data as a function of the measured lift at $\beta_v = 0^\circ$ and $\beta_s = 0^\circ$ for test 8.15G. However, since the CTOL thrust stand only measured horizontal force, it was necessary to use the data of Figure 6.1 to normalize the horizontal thrust data of test 12.03G.

An attempt was made to expand the wing fan exit louver vector effectiveness curve using pure yaw control data from the VTOL thrust stand test. Correlation proved unsatisfactory and therefore is not included. As covered in Section 6.2.6.3, directional control power at hover is only 40 percent of the estimated control power based upon the estimated wing fan exit louver vector effectiveness curve from wind tunnel test data.

6.1.1.4 Pitch Fan Thrust Reverser Door Effectiveness

The pitch fan thrust reverser door effectiveness as presented in Figure 6.9 was obtained from the NASA Ames Ramp Test conducted with aircraft S/N 05. The lift of the pitch fan was obtained from the summation of forces in the vertical plane subsequent to solving for the lift of the wing fans from moments taken around the centerline of the pitch fan. The pitch fan thrust reverser door effectiveness parameter;

$$\left(\frac{\frac{L_{PF/\delta}}{T_{PFO}}}{A_{PF}} \right) \times 7.07$$

was then obtained by normalizing the corrected pitch fan lift with the calculated net thrust of the pitch fan. The net thrust of the pitch fan was based upon G. E. performance data and the corrected recorded pitch fan

RPM, $\left(\frac{RPM_{PF}}{\sqrt{\theta}} \right)$. The data shown here differs from that given in Figure

13, reference 6.2 due to a revision in the net thrust upon which the ratio is based.

Data from the Edwards vertical thrust stand tests could not be used to verify the pitch fan thrust reverser door effectiveness curve because of the erroneous pitching moment data recorded as discussed in other sections of this report.

WING FAN LIFT PERFORMANCE

$$\beta_s = 0$$

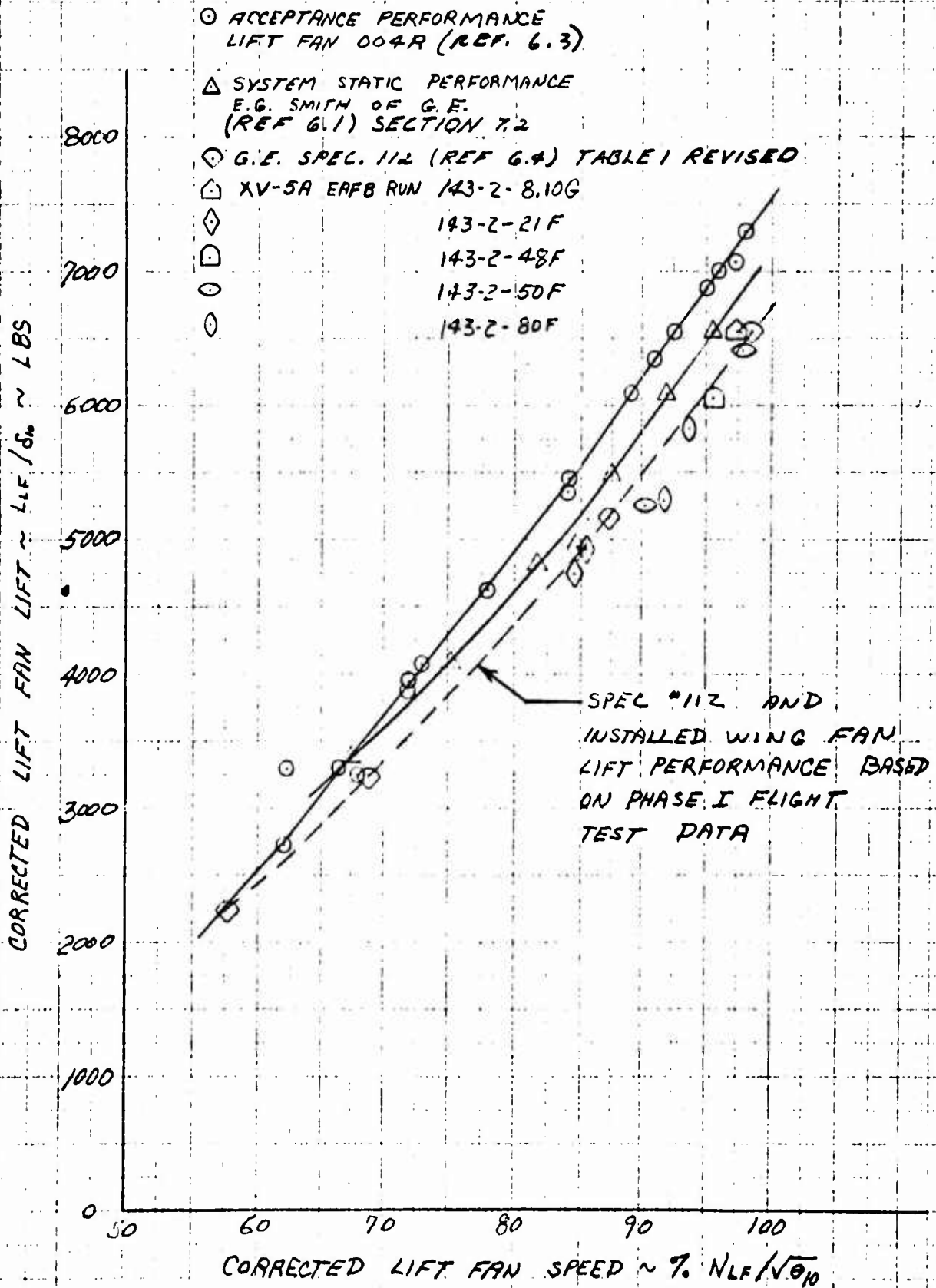


Figure 6.1 Wing Fan Lift Performance

PITCH FAN LIFT PERFORMANCE

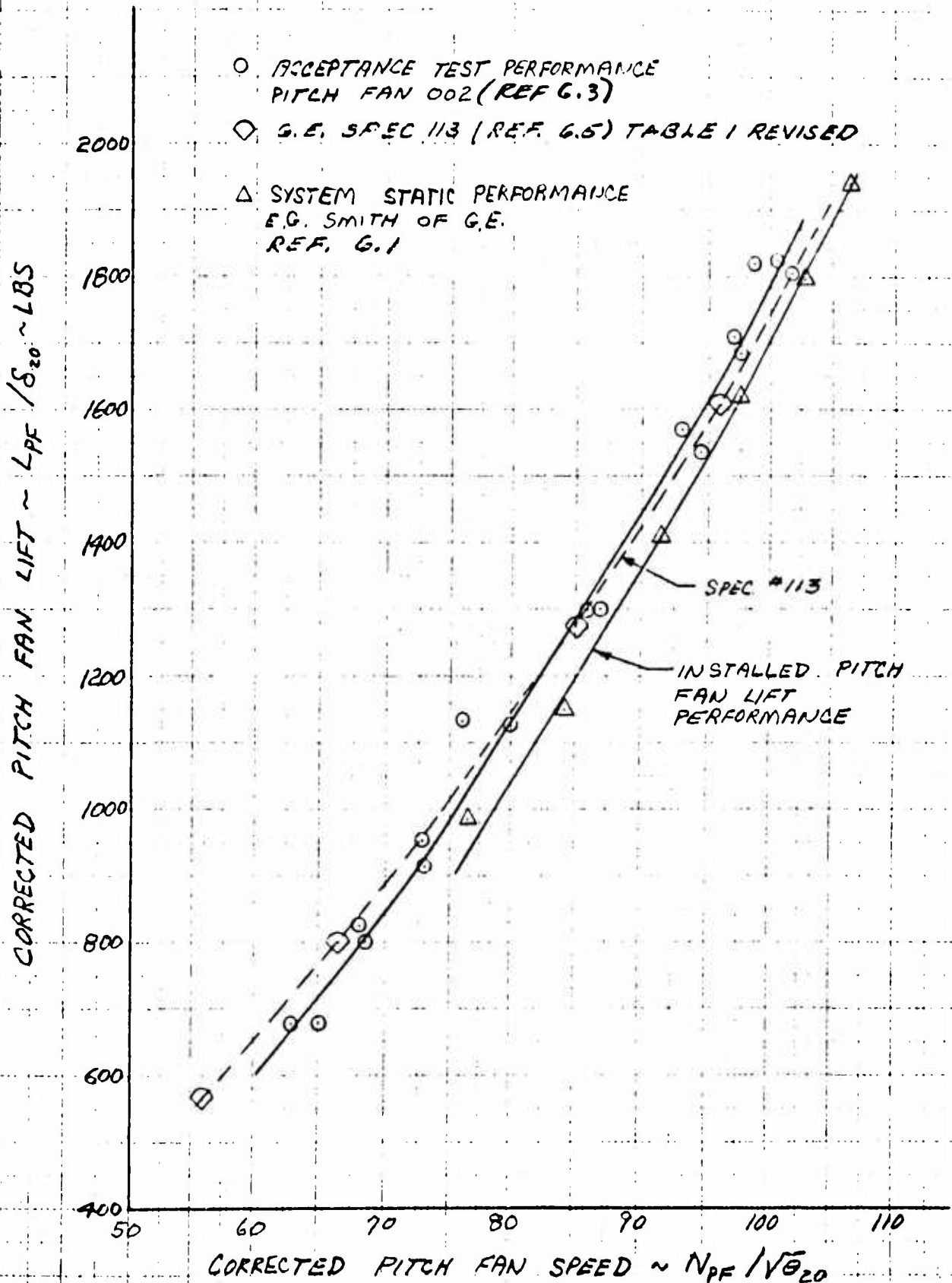


Figure 6.2 Pitch Fan Lift Performance

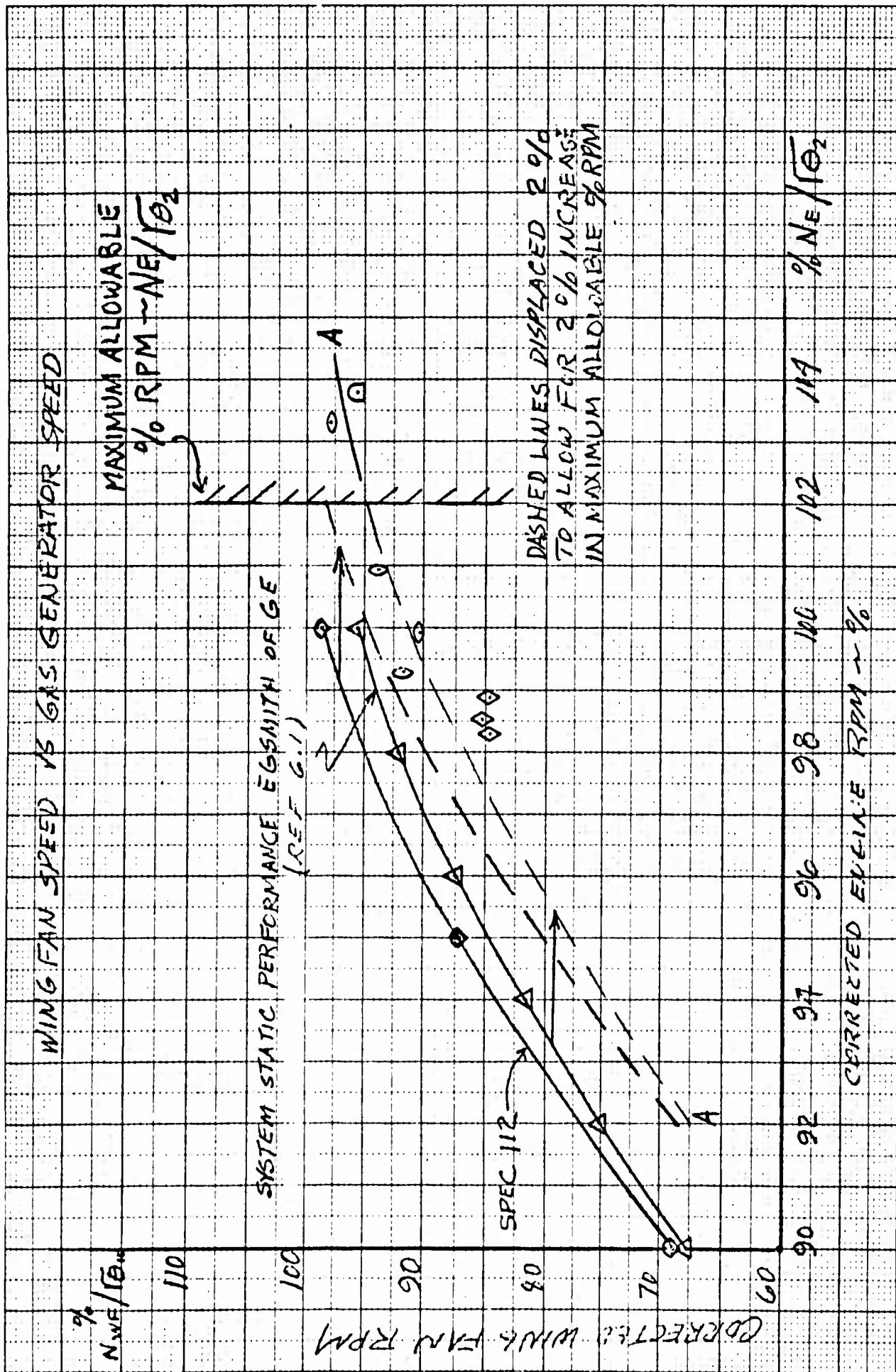


Figure 6.3 Wing Fan Speed vs Gas Generator Speed

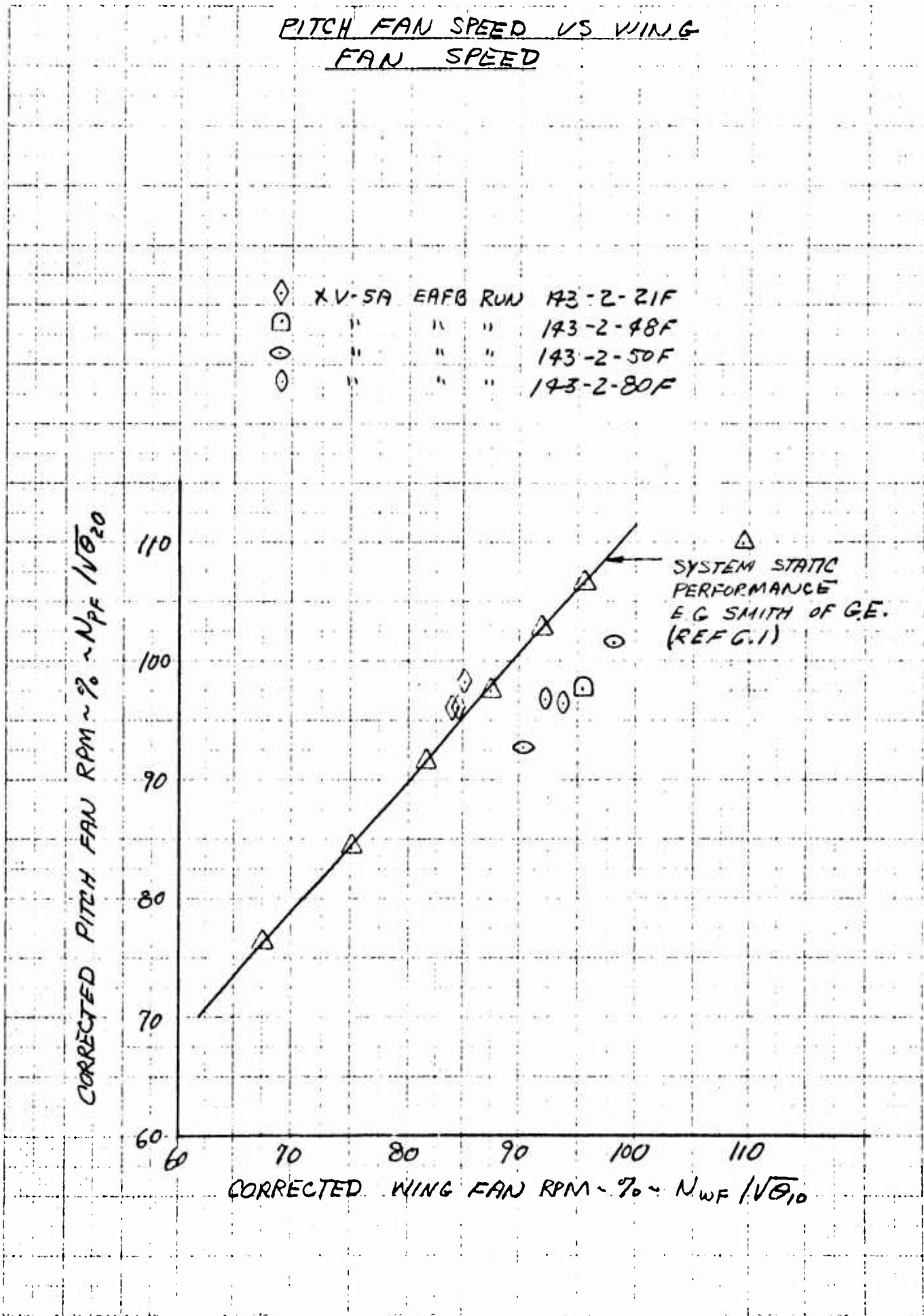


Figure 6.4 Pitch Fan Speed vs Wing Fan Speed

WING FAN LIFT (THRUST) REFERENCED TO 95% RPM VS FAN SPEED

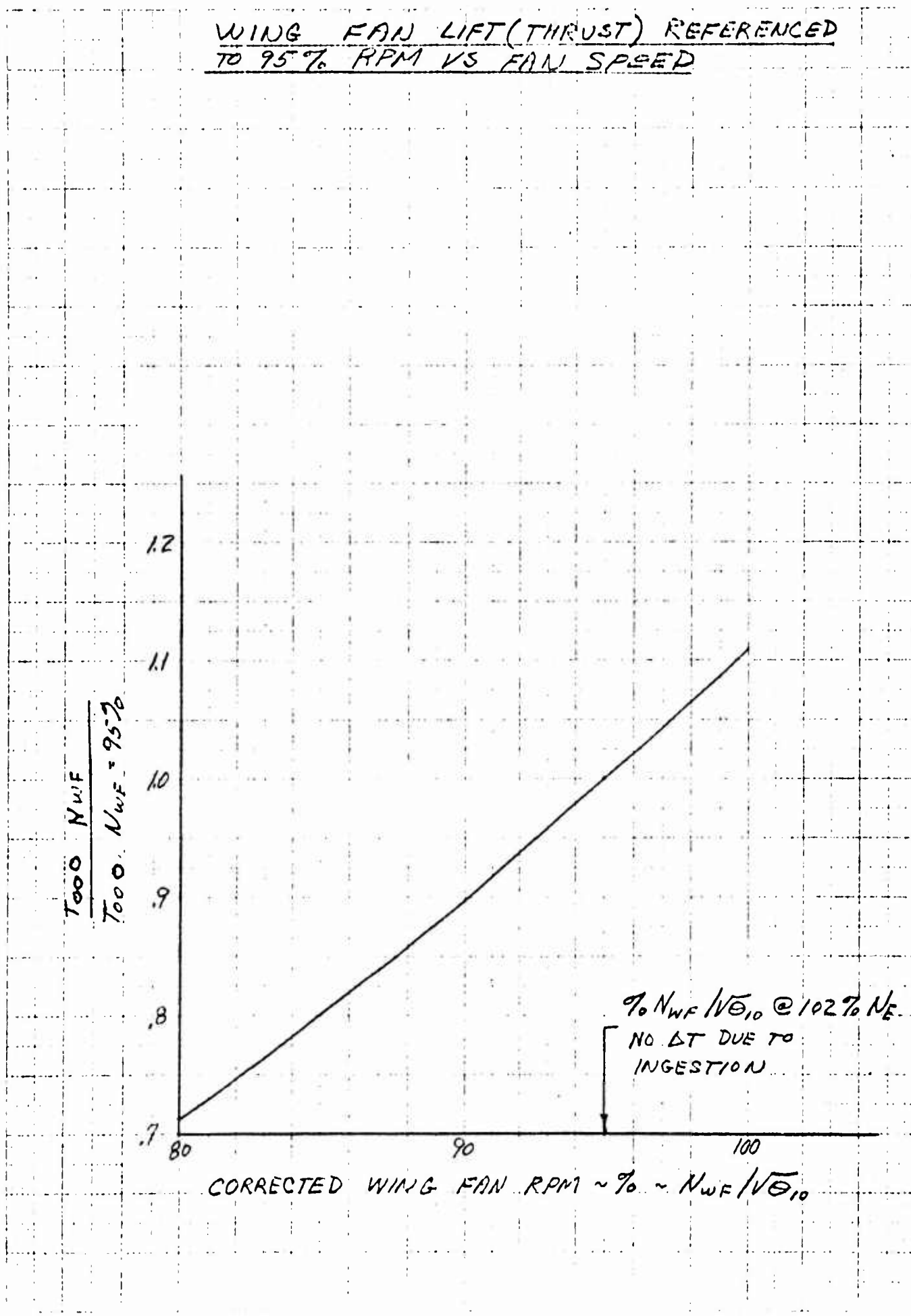


Figure 6.5 Wing Fan Lift Thrust vs Corrected Wing Fan RPM

AIRCRAFT INSTALLED FAN LIFT VS GAS GENERATOR SPEED FOR SEA LEVEL
STANDARD DAY FULL UP COLLECTIVE $\beta_s = 17^\circ$

ALLOWANCES FOR HOT GAS INGESTION:
 ENGINE INLET $15^\circ F$
 WING FAN INLET 0°
 PITCH FAN INLET $15^\circ F$

$T_{00\beta_s=17} = L_{00\beta_s=17} = 11,540 \text{ LBS}$

$\left(\frac{T_{00\beta_s=17}}{A}\right)_{102\% N_E} = 270.8$

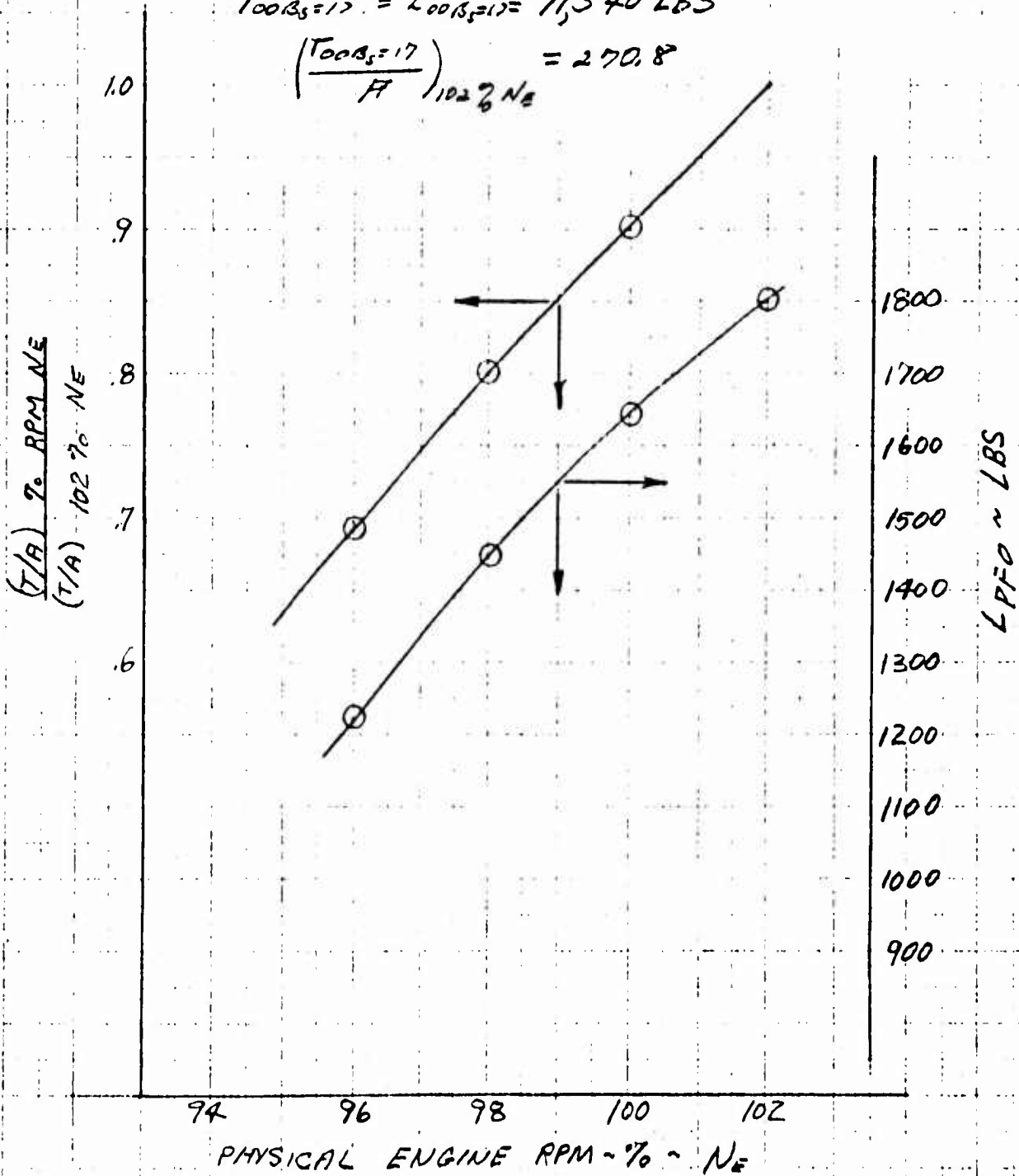


Figure 6.6 Installed Fan Lift vs Gas Generator Speed, S. L., Std Day

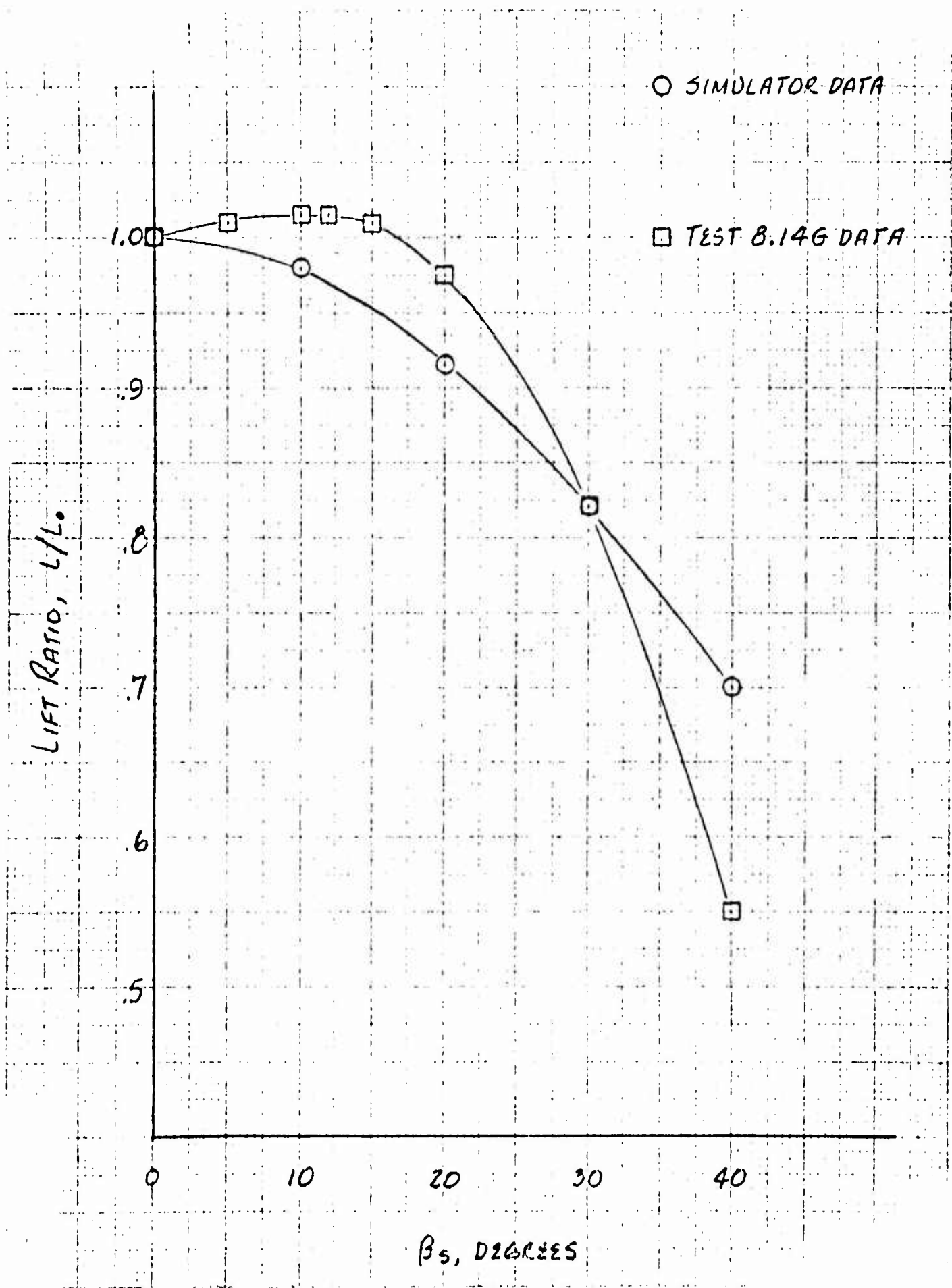
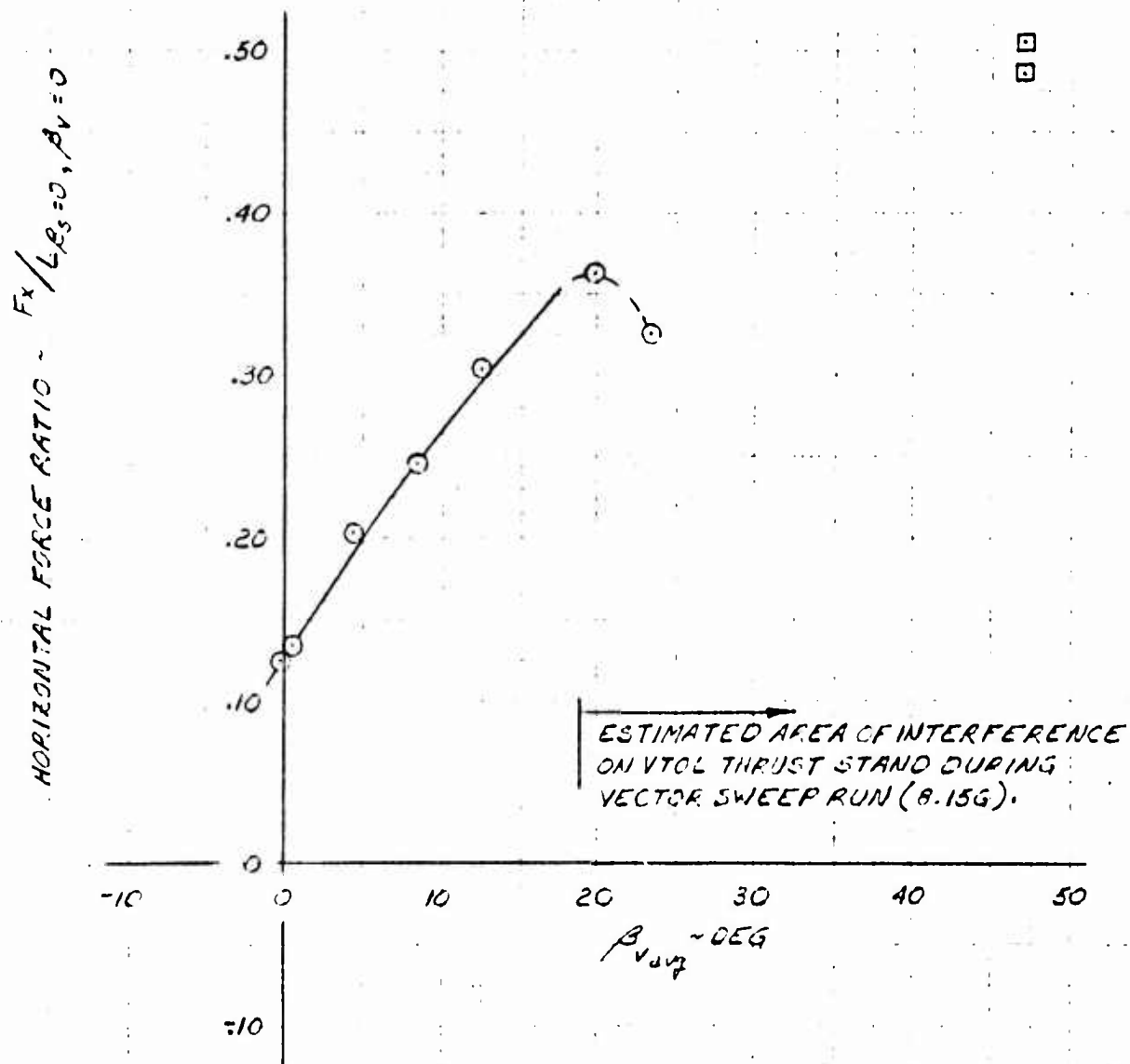


Figure 6.7 Louver Stagger Effectiveness in Hover

XV-5A
 STATIC WING FAN EXIT LOUVER VECTOR
 EFFECTIVENESS DATA



SYM TEST REMARKS

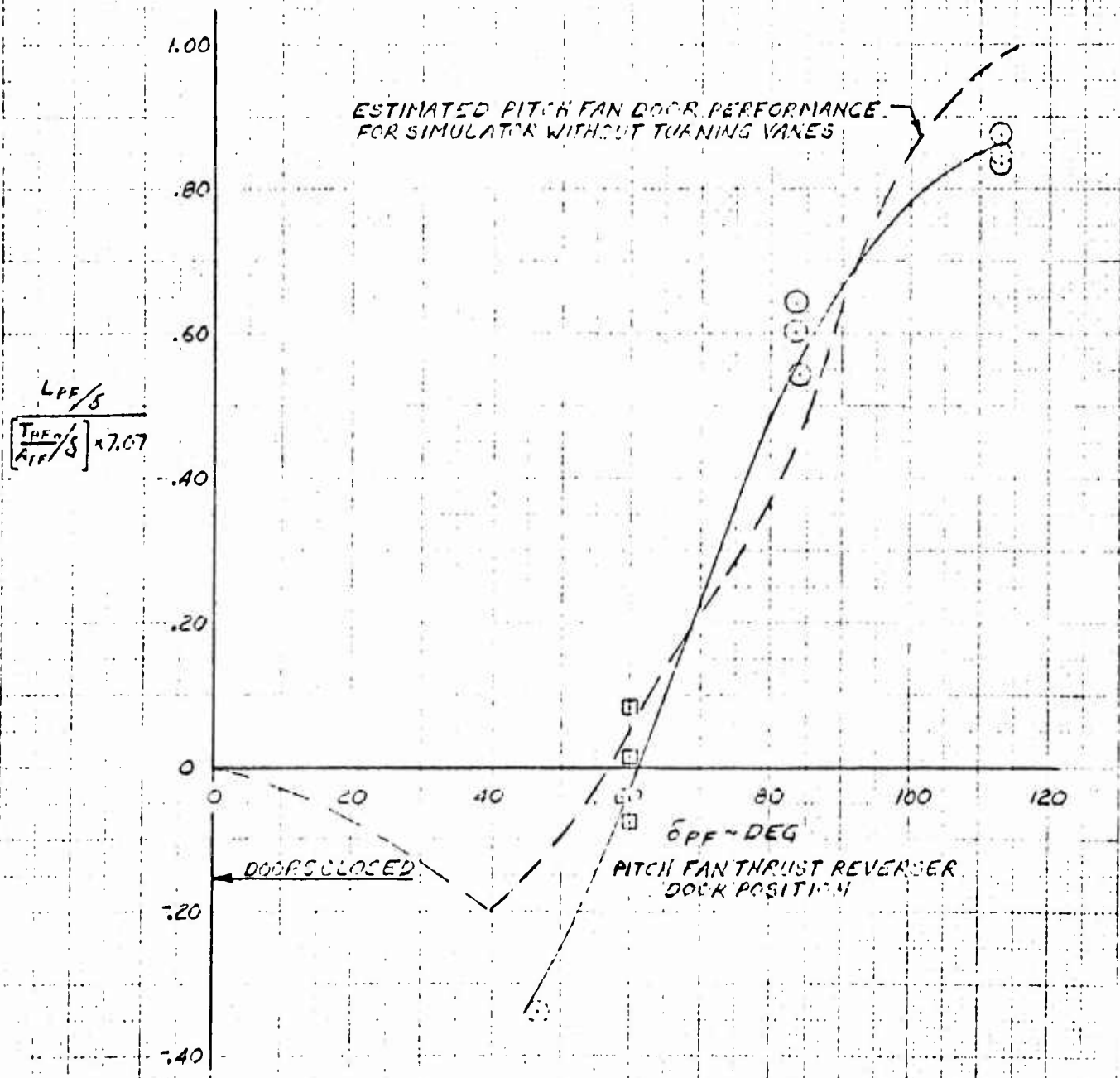
- 8.15G EAFB VTOL THRUST STAND DATA (REF 4.1)
- 12.03G EAFB CTOL THRUST STAND DATA

NOTE: ABOVE DATA WITH STIFFENED WING FAN EXIT LOUVERS INSTALLED.

8-2-65 JLS

Figure 6.8 Static Wing Fan Exit Louver Vector Effectiveness

STATIC PITCH FAN LIFT VS THRUST REVERSER DOOR POSITION
AUXILIARY VANE INSTALLED



NOTE: $\left[\frac{LPF/S}{APF/S} \right] \div \left[\frac{7.2 RPM \times 10^{-2}}{\sqrt{g}} \right]^2 = \frac{2.11.2 \text{ LBS/FT}^2 \text{ (BASED ON GE. DATA, 12.3% BLEED)}}{(100.7 RPM \times 10^{-2})^2}$

8-11-68. DCS

Figure 6.9 Static Pitch Fan Lift vs Thrust Reverser Door Position

6.1.2 Transition

6.1.2.1 Trim Transition

Original estimates of transition performance as a function of angle of attack indicated the best approach to the transition to be by increasing vector angle, holding an angle of attack of zero. Any increases in total lift as a result of increased alpha at intermediate speeds could not be utilized because the speed in fan mode necessary for conversion could only be developed at zero or negative angle of attack.

Therefore, early Phase I transition flight tests were conducted at or near zero angle of attack. As stated in the test description (Section 4.2.1) early transitions were conducted from the high speed end of fan mode flight and at altitude for safety of flight reasons. Aircraft performance in high speed fan mode flight was first ascertained by runway takeoffs and climb-outs in fan mode at high vector angles and as reported in Paragraph 6.1.3. Having ascertained that the aircraft could sustain fan mode flight at altitude, the transition was pursued from a conventional flight base where conversion to fan mode was performed at altitude and the aircraft was operated at successively lower speeds.

During initial high speed fan mode operations from the runway, a full span leading edge slat was installed on the horizontal tail with an angle of attack and dynamic pressure boom to monitor tail performance. Tail stall had been indicated as a definite problem area from the Ames wind tunnel test of the aircraft. Fan mode flight was approached with caution until an adequate tail stall margin was assured by flight test. (See Paragraph 6.2.8 for the tail downwash study during transition.) As a result of confidence gained from data collected in this manner and the unfavorable predicted conventional negative angle of attack stall characteristics of the slatted tail (as obtained during flaps down operation), it was removed. Fan mode operations involving transition investigations at altitude were then continued down to 35 knots. Earlier hovering and translational flights had resulted in a forward speed of 25 knots in ground proximity. These investigations were the building blocks to the complete transitions to follow which involved vertical takeoffs and landings.

The variation of the more important parameters during transition are compared with estimates in Figures 6.10 through 6.12 for a zero angle of attack trim transition. To determine the fan flight characteristics in such a way as to be able to compare the data from the two sources, it was necessary to adjust the conditions prevalent at the test point to standard day conditions. Wing fan thrust, or lift, was calculated using Figures

6.1 to 6.6 after having chosen test points at which $\alpha_{CORR} \approx 0^\circ$. This wing fan lift was then used to determine the nose fan lift adjusted to standard conditions. From these results, various parameters were determined for comparison with estimated data. Data points were taken from Flights 39F, 40F, 44F, 50F, 65F, and 71F, all on A/C 62-4506. A sample calculation for Flight 44F is presented in Table 6.2.

The development of the basic maximum installed performance steady hovering flight conditions is covered in Paragraph 6.1.1.1. It can be seen that the flight test data agrees well with estimates. The difference in vector angle at high speed end of transition shown in Figure 6.10 is probably due to the fact that the estimate was worked out using louver effectiveness of the unstiffened louvers. The stiffened louvers may have more effective camber, hence not as much louver angle is required. The lower value of elevator required to trim in the 50 knot region is probably due to the increased nose fan lift over estimate (see Paragraph 6.1.1.1) and increased turning capability of the nose fan thrust reverser doors. The nose fan thrust required for trim is approximately the same as estimated but the elevator position and longitudinal stick position result in a nose fan thrust reverser door position required that is less than estimated for the original system.

Figure 6.11 presents the slipstream trimmed lift coefficient (C_L^S) versus thrust coefficient (T_c^S) and fan cross flow ratio (μ) and (T_c^S).

The data show that there is generally good agreement with estimates.

A check of fan mode flight angle of attack as compared to pitch attitude during steady state conditions indicates some position error is induced in the angle of attack possibly due to flow conditions through the fans. This change in flow field conditions is considered to be a function of the wing fan blade tip advance ratio, μ . Several flights in the fan mode have been investigated near zero pitch attitude for various vector angles and speed conditions with adjustments made due to rate of climb when these data were available. The increment needed to correct the angle of attack was determined by assuming the pitch attitude data was correct. This increment as a function of the fan tip speed parameter is presented as Figure 6.13. These data indicate the largest negative increment occurs in the vicinity of 60 knots airspeed, the speed regime where the maximum down load due to nose fan for trim occurs.

These data were not considered conclusive and were not used to correct flight test data, except in this transition comparison.

6.1.2.2 Fan Flight Envelope

During Flights 60 to 78, or Phase I-A flight tests, the fan mode transition flight envelope was broadened somewhat. During these flights, the trim transition tests described above were expanded on by first establishing a trim condition of velocity, vector angle and zero angle of attack, and then varying vector angle and angle of attack attempting to maintain power and speed. All flights were conducted at a constant conversion gross weight and discontinued on the basis of pilot comfort and/or real time telemetered data indicating a questionable area of safety being entered. This approach was taken in an effort to gain the maximum of data in a minimum time. It was not intended to evaluate the maximum fan mode envelope but to merely expand it. Figures 6.14 and 6.15 present the angle of attack-vector relationship established during these tests. These data show fan flight to have been conducted from zero speed to 88 knots and angles of attack from -6.2 to +9.0 degrees.

Some data are also presented from Flights 30.0F, 31.0F, 32.0F, which were reduced power descents in fan mode. The data presented as a function of T_c^s and μ were developed as in Paragraph 6.1.2.1.

TABLE 6.2

Sample Calculation Transition

Data:	Flight No. 44F	OAT 8.08° C
	A/C No. 506	H_i 7720 Ft.
	PCM C/N 1273.09	q_{oi} .0730 psi
	Test Point 11	N_{GG} 102.2%
	i_H 18.2 deg.	N_F 98.15%
	δ_e 5.2 deg.	
	β_v 22.6 deg.	N_{NF} 102.1%
	β_s 12.9 deg.	α_i 2.3 deg.
	δ_e 100.1%	θ .117 deg.
	$\delta_{PF} = 57.75$ deg	

Calculation:

- (1) Find static thrust corresponding to test point conditions, of fan speed, zero vector angle and zero stagger using basic fan lift curve and correcting for temp. and pressure:

$$OAT' \text{ } ^\circ F = ^\circ C \times 1.8 + 32 = 8.08 \times 1.8 + 32 = \underline{46.58^\circ}$$

$$^\circ R = ^\circ F + 459.7 = \underline{506.24^\circ}$$

$$\sqrt{\theta} = \sqrt{\frac{506.24}{518.7}} = \underline{.9879}$$

$$N_F / \sqrt{\theta} = 98.15 / .988 = 99.35\%$$

$$L/\delta = 2 = \underline{13,360} \text{ Lb. Figure 6.1}$$

$$\delta = .7508 \text{ from ICAO at } H_1 \text{ 7720}$$

$$L = .7508 \times 13,360 = 10,031 \text{ Lb.}$$

$$\therefore T_{\text{OOO}}/A = 10,031/42.4 = \underline{236.58} \text{ PSF}$$

- (2) Find static thrust corresponding test point conditions of power setting, zero vector and zero stagger:

$$N_{CG} / \sqrt{\theta} = 102.2 / .9879 = \underline{103.5\%}$$

$$N_F / \sqrt{\theta} \text{ Static} = 96.8\% \text{ Figure 6.3}$$

$$\left(\frac{N_F}{N_{F_0}} \right)^2 = \left(\frac{99.35}{96.8} \right)^2 = (1.026)^2 = \underline{1.053}$$

- (3) Calculate Airspeed

$$q_{o_c} = q_{o_i} + \Delta q_E = .0730 + .00036 = .07336$$

$$q_{o_c} = q_{o_e} \text{ assuming no compressibility}$$

$$V_e = 56.76 \text{ knots}$$

$$V_T = V_e / \sigma^{1/2} = 56.76 / .890 = \underline{\underline{63.78 \text{ kts.}}}$$

(4) Trim lift coefficient

$$C_{L_{\text{TRIM}}}^s = \frac{GW}{q_s A_F} = \frac{9750}{(236.58 + 10.51) \times 42.4} = \underline{\underline{.9306}}$$

where $q_s = T_{\text{ooo}}/A + q_o$

$$(5) \quad \mu = \frac{1.69 V_T}{7.2 N_F} = \frac{1.69 \times 63.7}{7.2 \times 98.1} = \underline{\underline{.152}}$$

$$T_c^s = \frac{T_{\text{ooo}}/A}{T_{\text{ooo}}/A + q_o} = \frac{236.6}{236.6 + 10.5} = \underline{\underline{.957}}$$

(6) Nose fan lift

$$\left(\frac{L_{\text{NF}}}{L_{\text{WF}}} \right)_{\text{SLSD}} = \text{Const.} = \frac{1800}{11500} = .1565$$

$$L_{\text{NF}_{\text{Test}}} = .1565 \times 10.03 \phi = 1570 \text{ Lb.}$$

Correcting for thrust reverser door position from

$$\delta_{\text{PF}} = 57.75, \quad L_{\text{PF}}/L_{\text{PF}_{\text{max}}} = \underline{\underline{-.115}}$$

$$L_{\text{PF}} = -.115 \times 1570 = -181 \text{ Lb.}$$

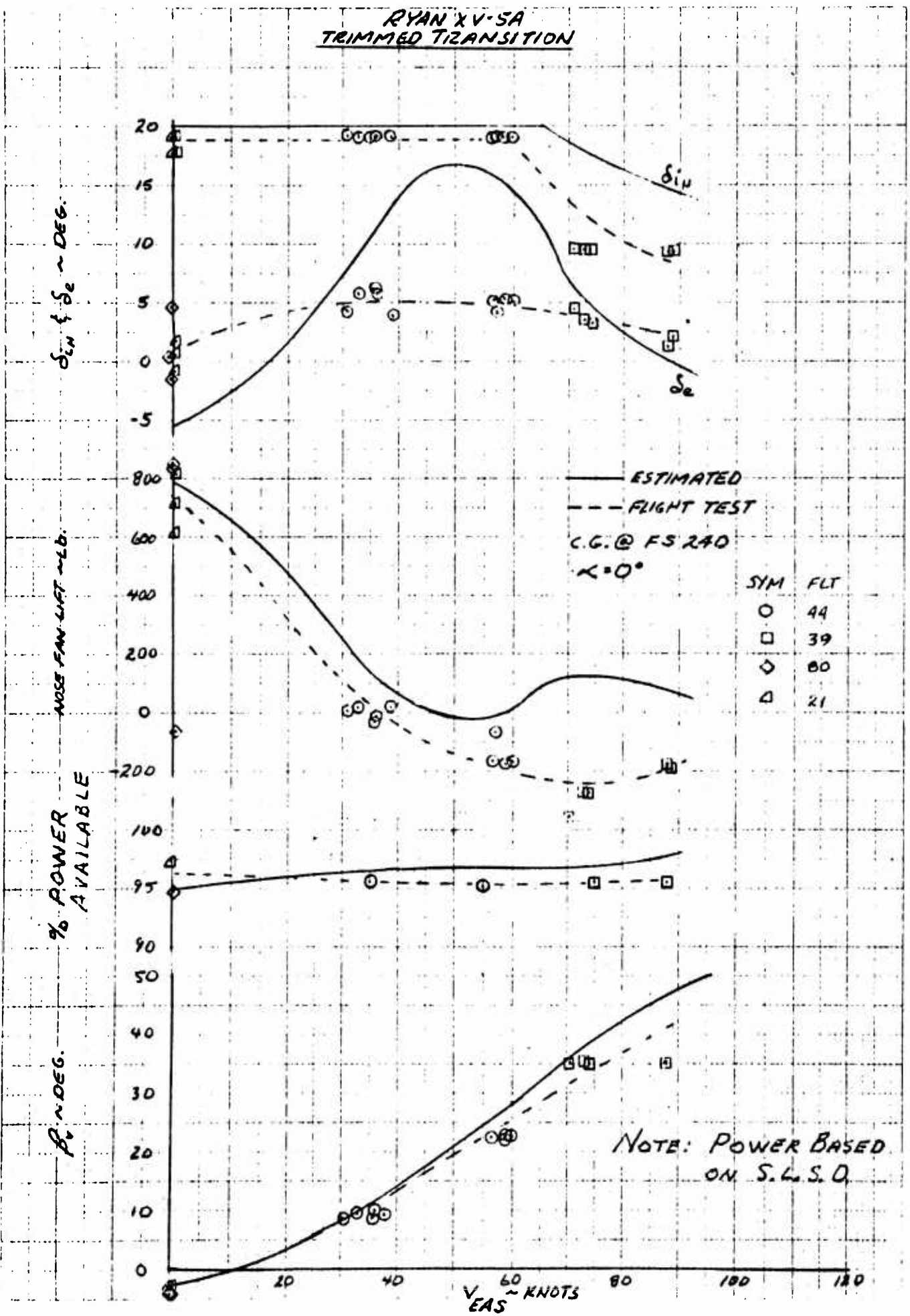


Figure 6.10 Trimmed Transition Parameters

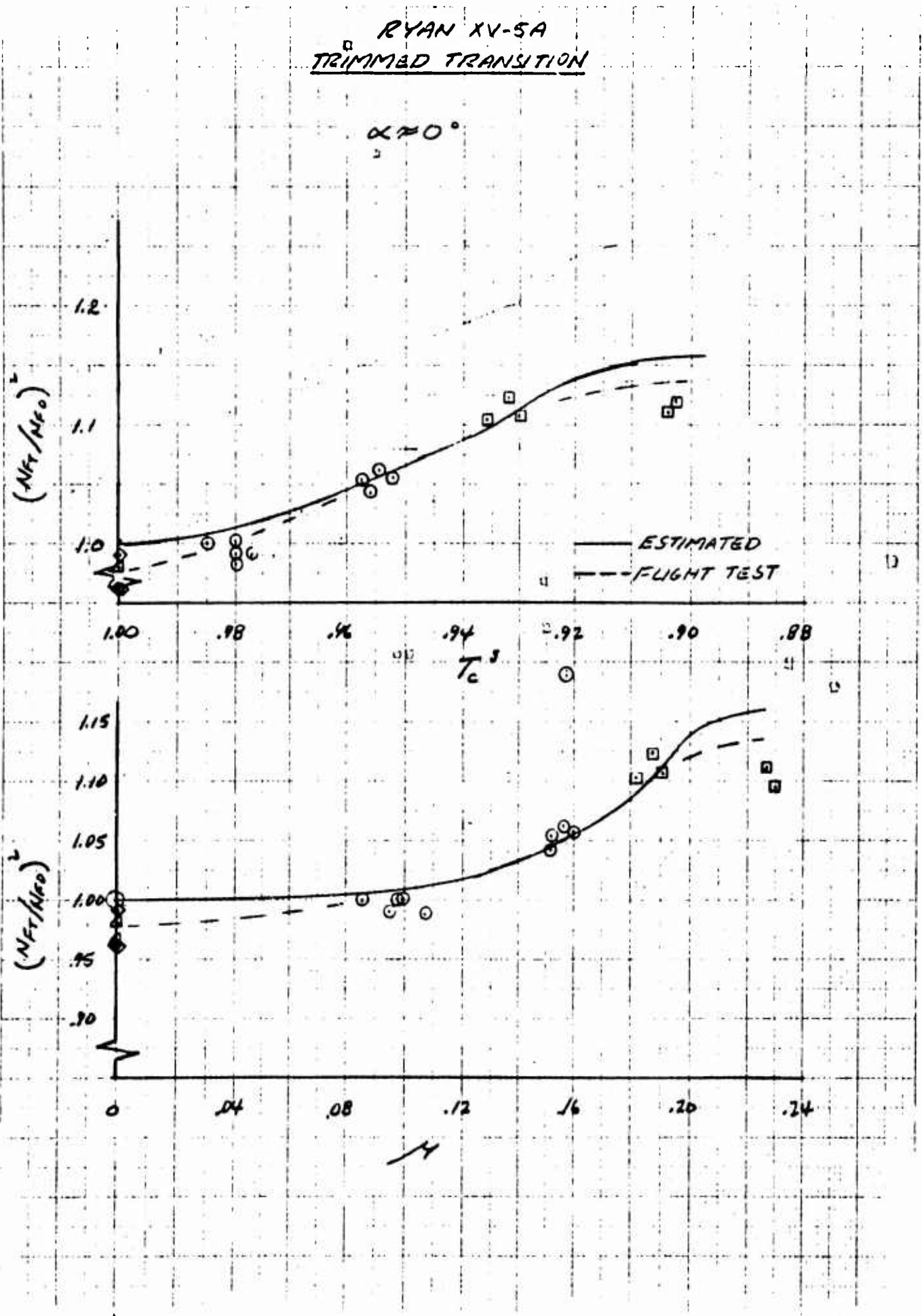
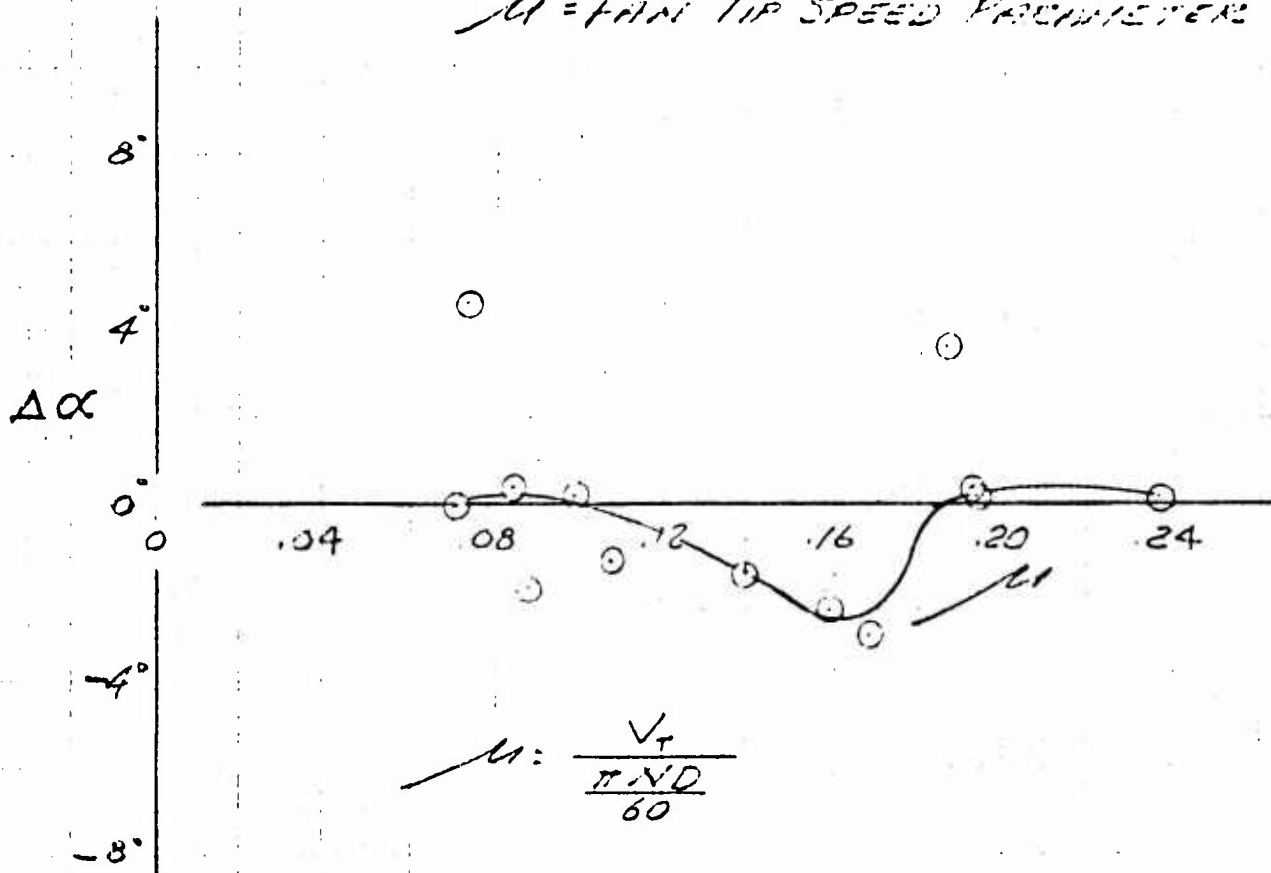


Figure 6.12 Trimmed Transition Parameters

$$\alpha_{CORR} = \alpha_{PCM} + \Delta\alpha$$

α_{CORR} = CORRECTED ANGLE OF ATTACK
 α_{PCM} = PCM ANGLE OF ATTACK
 $\Delta\alpha$ = ANGLE OF ATTACK CORRECTION
 U = FAN TIP SPEED FEET/MINUTE



VARIATION IN ANGLE OF ATTACK CORRECTION
 WITH FAN TIP SPEED RATIO -

Figure 6.13 Angle of Attack Correction vs Fan Tip Speed Ratio

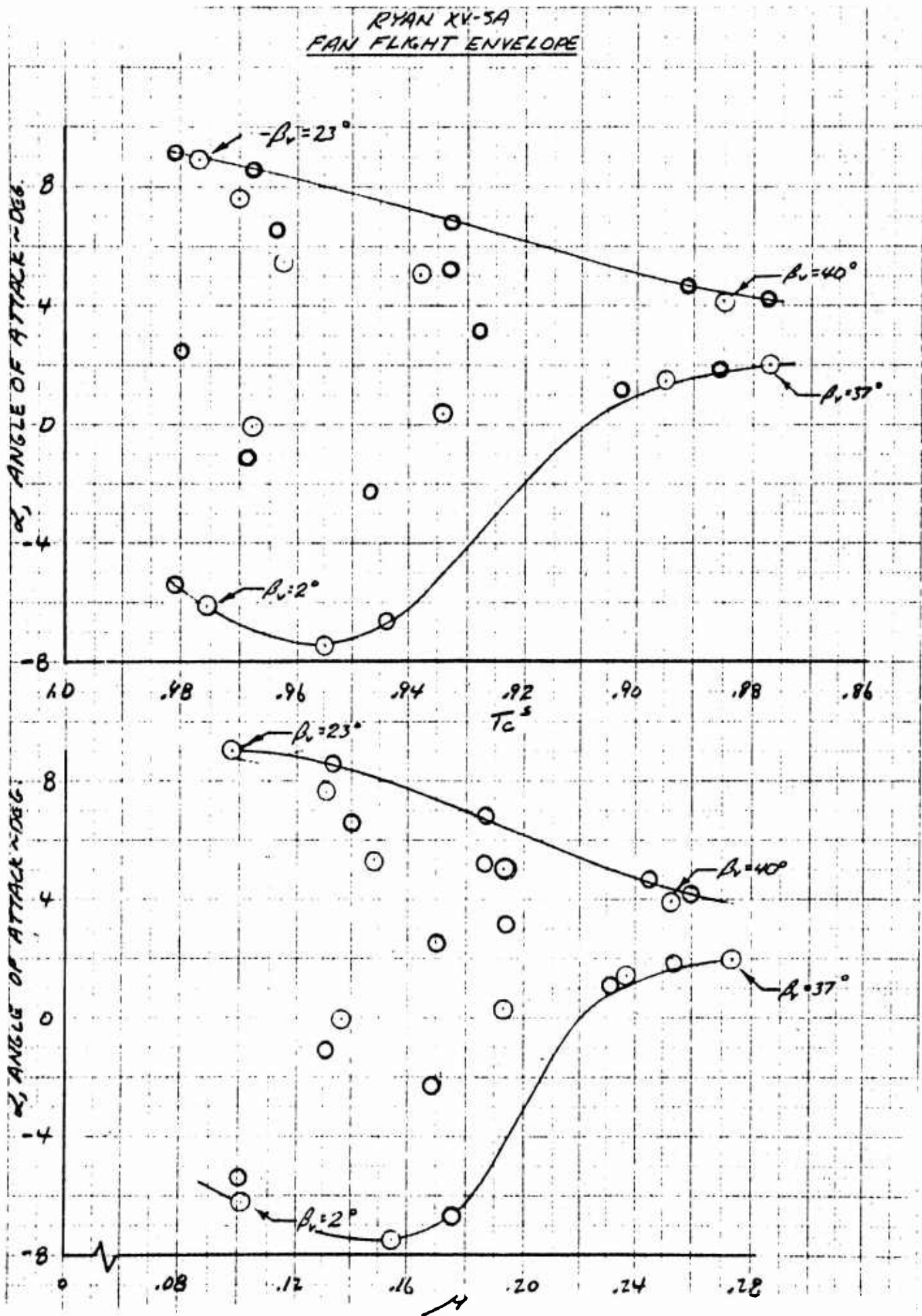


Figure 6.14 Fan Flight Envelope

6.1.3 STOL Operation

Fan mode takeoffs and landings from the runway at forward speed were used in several aircraft test operations. The procedure was first followed to gain familiarity with the operational characteristics of the aircraft at near conventional flight speeds, as the feasibility of performing the first conversion from fan mode operation to conventional flight, following a high speed takeoff, was explored. The procedure also permitted the early monitoring of stresses at critical locations at high speed in the wing fan inlet vane system, a structure in which problems had been encountered during wind tunnel test of the aircraft. During 58F, aircraft S/N 06, a number of fan mode takeoffs and landings were performed at various flight speeds and vector angles in exploration of the effects of ground proximity on the operational characteristics of the aircraft. None of the STOL operations were conducted for the purpose of determining maximum STOL performance capabilities; however, data derived from the STOL operations and associated climb studies provide valuable information applicable to this portion of the flight regime. This information is summarized below or in other referenced sections.

6.1.3.1 Takeoff and Landing

The first high speed fan mode operations on the runway were performed during ground test 24.01G and 24.02G using S/N 506. These tests involved flight at altitudes not exceeding 5 feet and were conducted with the horizontal tail slat installed. As described in Paragraph 6.2.8, downwash data gathered during these investigations enabled the removal of the slat for subsequent tests. Louver vectoring capability (45 degrees actual vector angle was provided corresponding to an indicated 50 degrees) was considered to be excessive as a result of these and subsequent flight tests (beginning with 26F) due to the reduced level flight performance capability of the aircraft at the high vector angles. Some of the performance loss was attributed to restrictions in maximum useable power while observing the 100 percent wing fan speed limitation, the remainder from excessive flow turning associated with the lift fan exit louver system and loss in direct lift (vertical thrust component).

During Flight 26, an indicated liftoff speed of 92 knots was demonstrated which was maximum for this and subsequent flights and was achieved using 48 degrees indicated vector angle at approximately 10,000 lb. gross weight. Improved climb performance was obtained during Flight 26 using 46 degrees indicated vector angle and lift off was accomplished at 85 knots IAS. Improvements in takeoff and climb performance were also obtained by increasing tail incidence from the original 12 to 15 degrees. Using this

procedure both tail lift and nose fan lift were increased sufficiently to increase climb rate. Subsequently, takeoffs were accomplished between 82 and 90 knots IAS using an indicated vector angle of 46 degrees (approximately 41 degrees actual) and a horizontal tail incidence of 15 degrees. Average gross weight at takeoff corresponding to the conditions was approximately 9900 lbs.

During Test 58.0F, aircraft S/N 506, a number of STOL takeoffs were performed at various indicated vector angles. Indicated vector angles of 40, 30, 20, and 10 degrees produced liftoff speeds of 69, 57, 50, and 40 knots IAS, respectively. Gross weight varied from 10,050 to 9700 pounds. Downwash data derived from these and other STOL flights is presented in Paragraph 6.2.8. In general, liftoffs were accomplished by increasing indicated angle of attack to 3 or 4 degrees.

The first STOL landings were performed at an indicated vector angle of 46 degrees and an angle of attack of 3 degrees. Sink rate was regulated using power adjustment. In Test 58.0F landings were performed 3 to 6 knots IAS slower than liftoff speeds as a result of devectoring following liftoff. Some hot gas reingestion was noticed by the test pilot while landing with an indicated vector angle of 10 degrees. This is discussed more fully in Paragraph 6.3.3.

6.1.3.2 Climb

Adequate terrain clearance was primary to the execution of a plan for a least risk approach to demonstration of the first complete VTOL operation, which was actually accomplished during Flight 50 (S/N 506). Both rate of climb and conditions for best rate of climb, within a rather restrictive speed range, were of concern because the plan involved the attainment of 1,000 to 2,000 feet terrain clearance following vertical and short takeoffs.

Attempts were made during the period of testing beginning with Test 24,01G and extending to 50F to determine the conditions for best rate of climb. In general, it was determined that flight speeds below which wing fan speed produced a power limitation provided the higher climb rates. During Flight 48, having selected 40 degrees indicated vector angle (approximately 36 degrees actual) from previous flights, it was concluded that climb rates were maximum at 75 knots IAS rather than 70 knots IAS as had previously been determined. As mentioned previously, the use of some excess in tail incidence above that required for trim also proved beneficial. For this particular flight (48F) the pilot quoted a rate of climb of nearly 1500 ft./min. at a pressure altitude of 2900 ft. and a

gross weight of 9750 lb. An average wing fan speed of 98.5 percent on PCM at 102 percent engine speed was recorded.

Estimates of climb rates were developed using NASA Ames wind tunnel data from test of S/N 505 (reference Datum Numbers 10a, 31, and 33). A cursory comparison of flight test results with those estimates which were developed from a force analysis of the climb conditions shows reasonable agreement. The calculated performance data indicates increased climb rates are achievable at airspeeds less than those previously discussed. Extrapolation of Ames wind tunnel data shows highest climb rates to be obtainable at airspeeds less than 60 knots at higher than trim (for zero angle of attack) vector angles and at negative angles of attack. This type of operation was not explored during the test program. The lower speeds quoted for maximum rate of climb do however coincide with the speeds for minimum power indicated in Figure 6.10.

6.2 STABILITY AND CONTROL

6.2.1 Static Longitudinal Stability

No specific tests were conducted to evaluate quantitatively the static longitudinal stability during fan-mode flight. Most of the data presented in Figures 6.16 through 6.21, illustrating speed stability characteristics, were obtained from small variations in angle of attack, with vector angle and gas generator power held constant for the particular maneuver. Since speeds were not usually permitted to stabilize completely at each longitudinal stick position, some dynamic effects may be present in the data.

Based upon pilot comment and data available, it appears that the longitudinal static speed stability of the aircraft progresses from slightly positive to neutral, to negatively stable, going from low-speed to high-speed fan flight. The static longitudinal stick-fixed angle of attack or attitude stability of the aircraft is positive at speeds of 30 knots and above, based on pilot comment and test data. This characteristic is illustrated in Figures A-9 through A-11, (see Appendix) in that an oscillatory response was derived from longitudinal disturbances. Pilots did, however, note that although the initial response to stick hit was oscillatory (and well damped), a gradual divergence in the direction of the disturbance occurred over the speed range of 30 to 75 knots investigated. Pilot comments indicate the longitudinal static stability to be satisfactory for an experimental test aircraft.

6.2.2 Static Lateral-Directional Stability

The static lateral-directional stability characteristics of the aircraft are illustrated in Figure 6.22 as ratios of sideslip angle to rudder pedal displacement, lateral stick to pedal displacement, and roll to sideslip angles. The data were developed from test results recorded during steady sideslip investigations and are presented in Figures A-1 through A-8.

The data indicate that the aircraft possesses high levels of lateral and directional stability at speeds above 50 knots IAS. At speeds below 50 knots the directional stability weakens. In terms of lateral stick-to-pedal displacement, this produces an apparent increase in the lateral stability (dihedral effect) of the aircraft as shown in Figure 6.22. Based on pilot comment, the aircraft, at forward translational speeds of 35 knots IAS and below, possesses a mild directional instability in

and around zero sideslip angle. Pilots stated that above 15 knots, if allowed to rotate in yaw, the aircraft would assume a balance condition in sideslip. At 20 knots, the balance condition was quoted as 15 degrees. At airspeeds of 15 knots and below, it was felt the aircraft would rotate through 90 degrees sideslip if permitted.

The low-speed directional instability has been attributed to ram drag of the nose fan. The aircraft evidently seeks a balance condition where the yawing moment due to nose fan is balanced by the yawing moment due to the vertical tail. The phenomenon is considered to be interesting, but not of a particularly troublesome nature.

During sideward translation from hovering flight the aircraft exhibited a positive speed stability or dihedral effect, requiring an increase in lateral control for trim, with increase in sideward velocity to keep the leading wing down. Based on flight test data, approximately 0.7 inch of lateral stick and 0.2 inch rudder pedal was required in trim of a sideward translational velocity of an estimated 10 knots. The aircraft possesses a mild static directional instability at low sideward translational speeds as well, and therefore directional control is used to oppose a tendency for the nose to turn downwind. The maximum comfortable sideward velocity was considered to be 15 knots.

Rudder pedal and sideslip data of Figure A-1 illustrate the magnitude of the directional instability encountered during low-speed forward translational sideslip investigations of flight 23.0F.

6.2.3 Longitudinal Dynamic Stability

In the speed range between 35 and 75 knots in the fan mode, the pilot reported the longitudinal dynamic response of the aircraft short-period mode to be very well damped. Long-period oscillatory modes were not investigated due to the rapidity at which conditions change during fan flight. The response of the aircraft to longitudinal disturbance is illustrated in Figures A-9 through A-11. The flight test data indicate that the stick-fixed pitching motion following a stick hit damped within one cycle over the recorded speed range of 40 to 75 knots IAS. Virtually a constant period of 3.0 seconds is shown. Variations in airspeed and the associated vector angle do not appear to have a significant effect on the damping characteristics at near-zero angle-of-attack trim conditions.

The dynamic stability characteristics of the aircraft in hover flight are discussed in Paragraph 6.2.5.

6.2.4 Lateral-Directional Dynamic Stability

Representative time histories of aircraft response to lateral and directional control inputs in transition flight with SAS on are shown in Figures A-12 through A-28 . At the higher airspeeds, the pilot reported very high damping of the aircraft following release from steady sideslip, with lower damping at the slower speeds investigated (30-35 knots).

The test data indicates that below approximately 60 knots IAS, the aircraft has an uncoupled roll and yaw response to disturbance, with oscillatory motions at different frequencies, while above 60 knots the motion is coupled. The introduction of coupling can be attributed to the growing significance of conventional aerodynamic terms as speeds increase. At 90 knots, the lateral directional stick-fixed oscillation appears to damp in less than one cycle, and a period of approximately 2.5 seconds is displayed. A period of approximately 3.0 seconds is recorded at 75 knots, and cycle to damp has increased slightly. Between 40 and 60 knots IAS, the directional oscillation from rudder disturbance displays a period of approximately 3.0 seconds, while damping of the disturbance occurs in one to one and one-half cycles. As speed decreases below 60 knots, the disturbance in roll displays a frequency of 1.5 seconds with approximately 2.0 cycles to damp.

Pilot comments regarding adverse yaw obtained in bank-to-bank rolls with pedal fixed are somewhat in conflict. The data shown in Figures A-12 through A-23 generally indicate favorable yaw as an immediate result of roll control at speeds of 50 knots IAS and below. At 60 knots IAS and above, the behavior of the aircraft in yaw and sideslip as a direct result of roll control application is difficult to discern from inspection of the data. At speeds of 60 knots and below, the aircraft appears to develop an adverse sideslip angle as a result of the bank angle attained, as if the top rudder were being held in the banked turn. This is probably due to a sliding off of the aircraft in the banked condition. This sideslip angle, large at low speed, diminishes with time.

The dynamic stability characteristics of the aircraft in hover are discussed in Paragraph 6. 2. . .

6.2.5 Stability Augmentation System

6.2.5.1 Roll Axis

Hover

Most of the flight test SAS evaluations have concerned the roll axis in hovering and low-speed translation. Attention was called to the roll axis during the first hover attempts with the original louver servos, and again when the landing tipover occurred.

The redesign of the louver servos and the stiffening of the louver system resulted in invalidation of the previous roll hover root locus analysis. Further, the inclusion of the notch network in the roll axis and the method for discharging the holding capacitor while in the maneuvering mode, coupled with the lowered response of the reworked louver servos, resulted in a 1.5-cps limit cycle oscillation during Flight 14F. Knowing the gain through the SAS and the frequency of oscillation of the system, root locus plots were made to determine the system characteristics which would give the observed results.

At about the same time, stagger effectiveness data for the stiffened louvers at hover were obtained from ground test 8.14G. This data is plotted in Figure 6.7. The slope of this curve is utilized to obtain the rolling moment per degree (each wing) stagger plotted in Figure 6.23 versus collective stagger setting.

Figures 6.24 through 6.26 show the results of a study of the limit-cycle oscillation of Flight 14F.

The SAS parameters used in the roll axis for Flight 14F were as follows:

Ratio Pos. 5	(R = .05)	SAS numerator $\tau = .5$ sec
Holding	.12V = 8 ma	22.5 deg stagger (each wing) per deg/sec roll rate
Maneuver.	4V = 8 ma	.68 deg stagger (each wing) per deg/sec roll rate

Figure 6.25 is a root locus plot using a louver servo first-order lag of .1 sec, and a second-order lag with a natural frequency of 188

rad/sec, critically damped. In addition, a .013-second time delay is included.

The locus crosses the $j\omega$ axis at a gain of 37 deg/deg/sec using a roll control effectiveness of 880 ft lbs per degree of β_S (each wing). Since the vehicle became unstable at a gain of 22.5 deg/deg/sec, the roll control effectiveness must have been 1450 ft lbs/degree β_S , which is within the range of Figure 6.23. A similar result holds true for the maneuver mode.

In order to return the vehicle closed loop to the point picked as "best" during the simulator program, the roll notch network was removed and the holding capacitor discharge resistor was changed from 470 Ω to 47 Ω . This resulted in the regaining of considerable phase margin and a system comparable to the simulator configuration.

Figures 6.27 through 6.29 show the resulting root locus for roll after the system modifications were incorporated. Use of an $R = .1$ (ratio position 6) results in a locus similar to that obtained on the simulator with $R = .05$ (ratio position 5).

These loci were verified on Flight 16F when double roll holding gain was investigated. The normal roll gains were modified subsequent to Flight 14F to those shown below

Ratio pos.	6 ($R = .1$)	SAS numerator $\tau = 1.0$ sec
Holding	.36 V = 8 ma	7.55 deg stagger (each wing) per deg/sec
Maneuvering	4V = 8 ma	.68 deg/deg/sec

Figure 6.27 shows that the roll holding mode will be unstable at a gain of 22.8 deg/deg/sec for a roll control effectiveness of 880 ft lbs/deg.

On Flight 16F, a roll holding gain of 15 deg/deg/sec was used, and a 2.5-cps oscillation ensued. For this gain, a roll control effectiveness of 1340 ft lbs/deg is required, which again is well within the range shown in Figure 6.23.

Subsequent to Flight 16F, "hot" frequency-response measurements were made during a ground tie-down run at EAFB, using both dual and single hydraulic systems.

The data for the dual-system response are plotted in Figure 6.30, along with a linear transfer function fit.

The data for the single hydraulic system response are plotted in Figure 6.31.

There is almost no difference between the two sets of data, but it is noted that the resulting transfer function differs from that used in the root locus plots previously discussed. Figure 6.32 is a frequency response of the servo used in the root locus plots. It is seen that the two servos are almost identical over the frequency range of 10-20 rad/sec, which is the important region as far as stability is concerned.

The roll system gains chosen for subsequent flights afford a 2:1 gain margin at the minimum collective lift setting and have proven to be very satisfactory.

Transition

Roll SAS has proven to be required only below an airspeed of 40 knots. As a matter of interest, there have been no roll transients noted during conversion.

6.2.5.2 Pitch Axis

Hover

The pitch axis SAS channel was flown through most of the flight test program in the configuration determined to be optimum during the flight simulation. The inclusion of the "holding" mode was tested on Flight 16F and demonstrated a deterioration in handling qualities. Rate damping alone proved to be highly satisfactory.

During two portions of Flight 54F the pitch SAS was turned off, and in both cases a diverging .4-cps pilot-in-the-loop oscillation resulted. The bare aircraft in the pitch mode is theoretically barely flyable, and it is felt that the criteria used to determine this have been validated.

The pitch axis during hover was essentially unaffected by ground effect and offered no control problems.

Transition

As in the roll axis, SAS was found to be required only at 40 knots air-

speed and below.

Conversion

Conversions were made during Flight 56F both with and without pitch SAS, and the pilots indicated a smoother conversion resulted when using SAS.

6.2.5.3 Yaw Axis

Hover

The yaw axis has proven to be as uncritical during actual flight as it was during the simulator program. The yaw SAS was turned off during flight 54F with no apparent variation in vehicle handling qualities.

6.2.5.4 RMS Control Parameter Evaluation

Pertinent instrumentation data were reviewed on several test flights of interest to attempt to measure the effectiveness of the SAS as well as interaxis coupling and lift control parameters. Table 6.3 comprises a tabulation of the RMS values of the control parameters for the flights listed. RMS values were obtained by the following method:

1. Assume that for each maneuver the control inputs are normally distributed about some mean.
2. Measure the peak-to-peak parameter variations during a given maneuver. This value is equivalent to six standard deviations ($\pm 3\sigma$).
3. Calculate σ . The RMS value for a normally distributed variable is equal to the standard deviation.

The validity of this method was substantiated during previous analog simulation hover studies, where the mean square deviations were actually calculated. These calculated values agreed closely with the approximation $\sigma = \frac{\text{peak-to-peak deviation}}{6}$. The method has the further

advantage that much data can be scanned rapidly. To determine the maximum value of any parameter during a flight, multiply the RMS value (σ) by 3, remembering that the variable will go between lines of $\pm 3\sigma$.

Interaxis Coupling

Reference to Table 6.3 shows that the yaw axis parameters were basically unaffected by roll and pitch. Comparison of the yaw SAS output for Flight 12F with that of Flight 14F shows similar results. During Flight 14F the first roll oscillation occurred. A roll oscillation also occurred during the double gain portion of Flight 19F, and at this time the yaw SAS output was the least measured on the flights listed in the table.

Roll and pitch are also isolated from each other, as Table 6.3 shows. The longitudinal stick and pitch rates during Flights 14F and 19F were comparable to flights with normal roll operation.

Flight 54F portions without pitch SAS showed no increase in roll control over flights with normal pitch axis operation.

Lift Control

Lift control, using power variations instead of collective stagger, was evaluated on Flights 18F and 19F in hover, and on Flights 46F and 48F during transition.

Lift control using power variations was unsatisfactory at speeds below 45 knots due to the slow response rates. Above 45 knots, vehicle attitude and power provide effective altitude control.

Mixer Changes

Due to the lack of roll control power evident on the first hover attempts, in addition to servo redesign and installation of stiffened louvers, the mechanical mixer was modified to provide decreased lift stick authority and increased roll power. Flights 8.01G through 21F were conducted using the revised mixer. This mixer configuration resulted in a $+ .15$ L/w variation over the collective range, and a roll stick sensitivity varying between $.25$ and $.96$ rad/sec²/inch with $.62$ rad/sec²/inch at mid-collective. Subsequent to Flight 21F, the old mixer configuration was re-installed. This resulted in a $+ .15 - .28$ L/w lift control and a roll stick sensitivity varying between $.22$ and $.8$ rad/sec²/inch, with $.47$ rad/sec²/inch at mid-collective.

Six of the tests listed in Table 6.3 involved hovering in the nominal SAS state on Flight 21F and preceding flights. Four of the tests involved hovering in the nominal SAS state subsequent to Flight 21F. The RMS

values were averaged, and these averages are shown as "Case A" and "Case B." Case A is an average of the parameter RMS values for normal hover flights before Flight 22F, and Case B is an average for similar flights including Flight 22F and those performed subsequently. It is concluded that the replacement of the old mixer configuration reduced the lateral vehicle disturbances, but increased pilot stick inputs.

SAS Gains

Given below is a summary of the nominal SA System gains applicable to the Phase I test program.

Pitch

The pitch system, using rate alone, had gains during the Phase I Flight Test Program of about 1.4 deg nose door per deg/sec. Using a nominal nose-fan thrust reverser door effectiveness of 30 lbs/deg, the pitch damping was 40,000 ft lbs/rad/sec.

Roll

The roll system used the leaky integrator for the holding mode, and the value chosen for this system after test 16F, was 7.55 deg stagger (each wing) per deg/sec roll rate. The compensation network had a numerator time constant of 1 second and a denominator time constant of 10 seconds. This is equivalent to 381,000 ft lbs/rad/sec, using a nominal stagger roll effectiveness of 880 ft lbs/deg stagger (each wing).

The roll maneuver mode had a gain of .68 deg stagger (each wing) per deg/sec of roll rate, or 34,000 ft lbs/rad/sec.

Yaw

The yaw SAS used the same system as pitch, but in this case the holding and maneuvering gains were not the same. The holding gain was .26 deg vector (each wing) per deg/sec yaw rate. The maneuvering gain was .17 deg/deg/sec. This corresponds to 13,000 ft lbs/rad/sec in holding and 8500 ft lbs/rad/sec in maneuver, using 870 ft lbs/deg vector (each wing).

6.2.5 Explanation of Tests in Table 6.3

Test No.	Flight No.	Description and Comments
1	12F	Two minutes of steady hovering. 1 cps pilot-induced oscillation present. Roll SAS gain 15 deg stagger per deg/sec roll rate. Notch network in roll SAS
2	14F	Hover flight similar to 12F, but with oscillation in roll axis. Limit-cycle with frequency of 1.5 cps. Roll gain 15°/deg/sec.
3	16F	Roll gain reduced to 7.5%/sec. Notch network removed. 1 cps pilot-induced oscillation in roll. Normal pitch system
4	16F	Same as test 3, but holding condenser operative in pitch axis, giving quasi-attitude SAS
5	16F	Identical to test 3. Used to check normal variation of control parameters
6	18F	Flight with 1/2 nominal roll gain
7	18F	Flight with all gains nominal. Equivalent to test 3
8	19F	Double roll gain. 2.5 cps oscillation resulted
9	19F	Nominal gains. Equivalent to test 3
10	20F	Normal hovering. Nominal gains
11	21F	Nominal gains. Tipover on landing in crosswind
12	21F	Hover flight with nominal gains and old mixer configuration. (All subsequent flights same mixer configuration)
13	46F	Hover at nominal gains

14	46F	Transition at 20 kts IAS
15	46F	Transition at 30 kts IAS
16	46F	Hover at nominal gains
17	54F	Hover with nominal gains
18	54F	Hover with nominal gains but pitch SAS turned off. This resulted in a diverging .4-cps oscillation. This was tried twice.

TABLE 6.3 RMS VALUES OF VARIABLES ON SELECTED FLIGHTS

(RMS Derived as P-P-9)

VARIABLE	FLIGHT HOUR	COLLECTIVE STICK PERCENT	ROLL SAS MILLIAMPS (5 MA MAX.)	ROLL ANGLE DEGREES	ROLL RATE DEG SEC	LATERAL STICK INCHES (4 IN. MAX.)	PITCH ANGLE DEG.	PITCH RATE DEG SEC	PITCH SAS MILLIAMPS (5 MA MAX.)	LONG. STICK INCHES (5 IN. MAX.)	RUDDER PEDAL INCHES (3.25 IN. MAX.)	YAW SAS MILLIAMPS (5 MA. MAX.)
1	11F	5.9	1.54	4.26	—	.174	1.31	—	3.6	.13	.36	1.6
2	14F	3.35	—	—	—	—	—	.5	1.05	.13	—	1.95
3	16F	5.9	1.5	—	—	.145	—	.53	1.	.26	.37	.43
4	16F	11.4	1.5	—	—	.290	—	1.06	1.5	.26	.37	.43
5	16F	5.35	1.5	—	—	.455	—	.52	1.	.26	.37	.43
6	1*F	5.9	1.4	2.5	—	.290	1.7	.47	1.	.13	.36	.43
7	1*F	2.7	1.4	3.5	1.1	.145	1.5	.32	.5	.13	.07	.22
8	19F	5.3	1.5	2.4	1.3	.290	3.7	.27	5	.13	.18	.22
9	19F	4.0	1.5	2.4	2.0	.290	1.7	.34	1.	.13	.37	.44
10	20F	2.3	2.1	3.0	2.1	.145	3.7	.27	1.	.12	.37	.44
11	21F	5.3	1.2	3.0	1.07	.290	.92	1.07	1.	.26	.19	.30
12	22F	4.9	1.7	1.3	1.6	.56	1.5	1.07	2.2	.26	.37	.30
13	46F	3.5	1.52	1.2	.33	.36	1.2	.53	.75	.12	.10	.43
14	46F	3.9	1.6	2.4	1.07	.77	1.2	2.2	.75	.12	.40	.63
15	46F	3.5	2.0	3.7	2.7	1.04	1.2	2.2	.75	.12	.37	1.3
16	46F	4.7	1.52	2.4	2.2	1.04	1.2	2.2	.75	.12	.37	.90
17	54F	7.0	1.2	—	2.2	3	—	.55	1.0	.12	—	—
18	54F	4.7	1.52	—	2.2	.3	—	3.3 (oscillation)	(OFF) 0.0	1.4 (osc.)	—	—
Nominal Hover	3 16F	5.0	2.5	—	—	.145	—	.33	1.	.26	.37	.43
Flights Before 21F	5 16F	5.33	1.5	—	—	.435	—	.53	1.	.26	.37	.43
With Nominal Gains	7 19F	2.7	1.4	3.0	1.0	.145	1.7	.32	.5	.13	.18	.22
	9 19F	4.	1.53	2.7	1.0	.29	1.7	.54	1.0	.13	.37	.44
	10 20F	5.3	2.1	3.0	2.1	.145	3.7	.27	1.0	.12	.37	.44
	11 21F	5.3	1.2	3.0	1.07	.29	.92	1.07	1.0	.26	.19	.30
Average of Above	Case A	5.1	1.7	2.97	2.05	.24	2.06	.515	.92	.193	.306	.46
Nominal Hover After	12 21F	5.0	1.7	1.5	1.6	.36	1.9	1.07	2.2	.26	.37	.30
21F with Nominal Gains	13 46F	1.5	1.52	1.2	.33	.30	1.2	.53	.75	.12	.10	.43
	15 46F	4.7	1.52	2.4	2.2	1.04	1.2	2.2	.75	.12	.37	.90
	17 54F	7.0	1.2	—	2.2	.3	—	.55	1.0	.12	—	—
Average of Above	Case B	5.40	1.14	1.7	1.63	.57	1.40	1.08	1.18	.16	.347	.743

RYAN XV-5A
STATIC LONGITUDINAL STABILITY

FAN FLIGHT

$\beta_V = 7^\circ$

INT. 18.5

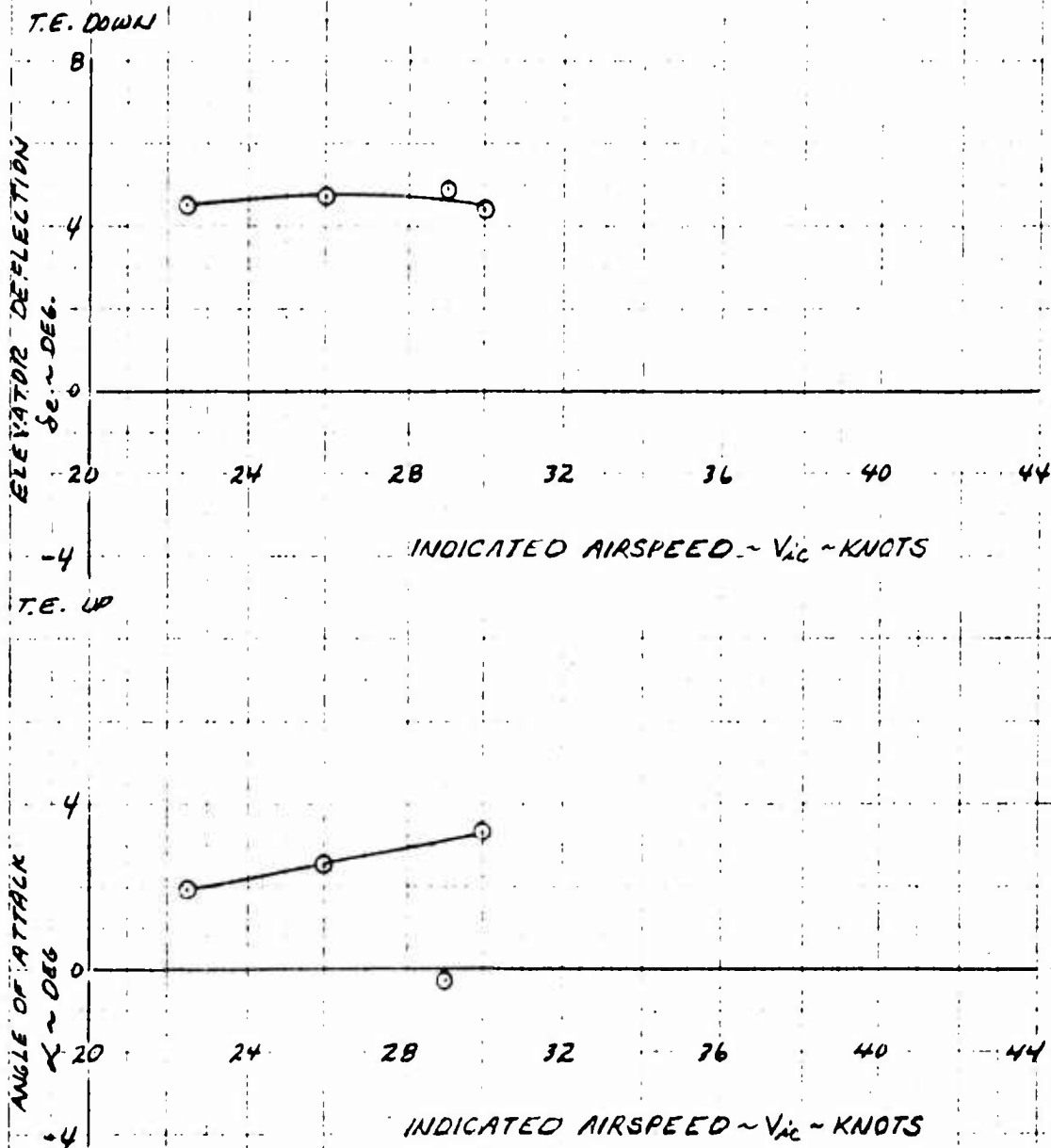


Figure 6.16 Static Longitudinal Stability - Fan Flight - $\beta_V = 7^\circ$

RYAN XV-5A
STATIC LONGITUDINAL STABILITY
FAN FLIGHT
 $\beta_V = 11^\circ$

$\lambda_{HT} = 18.3^\circ$

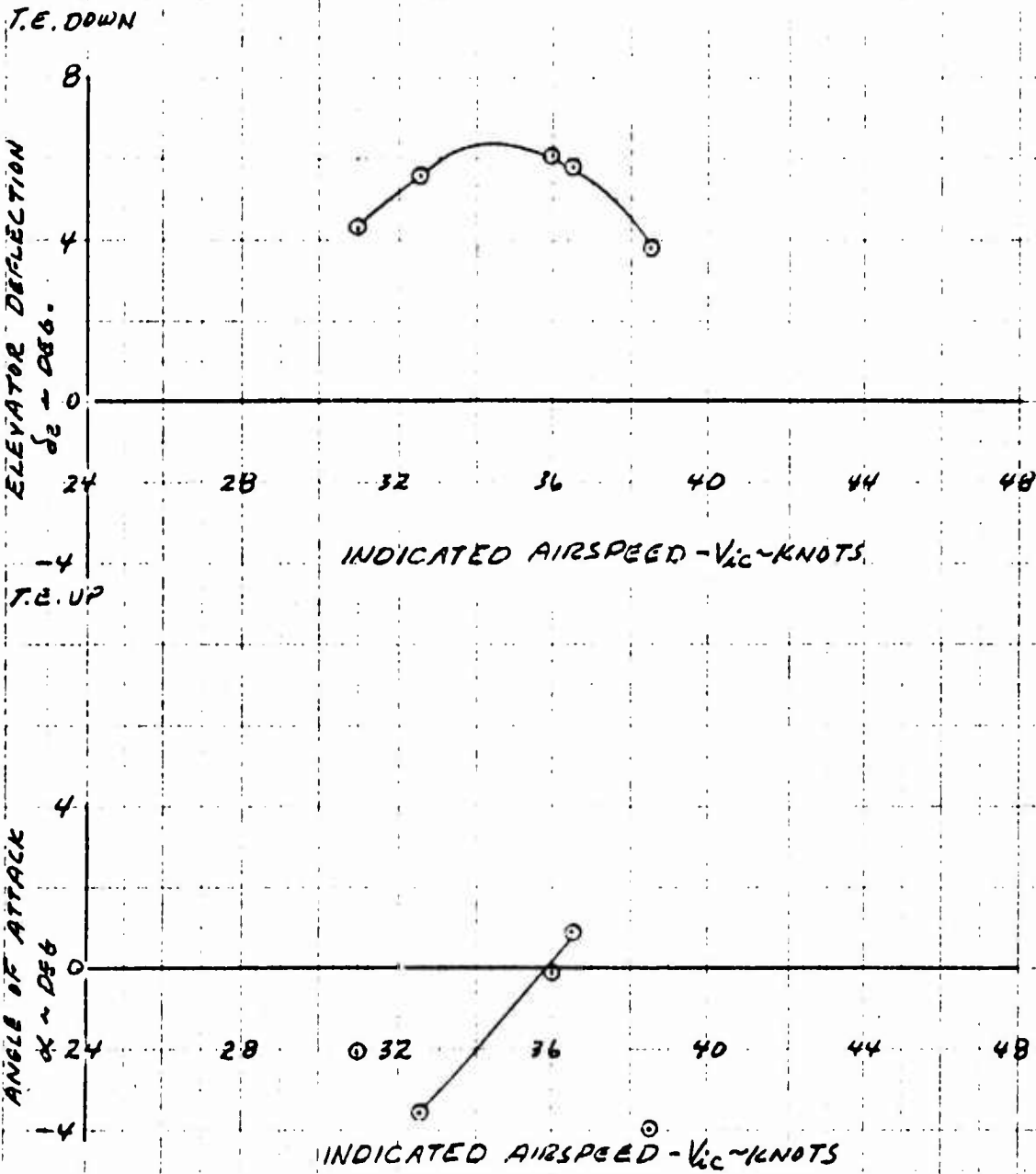


Figure 6.17 Static Longitudinal Stability - Fan Flight - $\beta_V = 11^\circ$

RYAN XV-5A
STATIC LONGITUDINAL STABILITY

FAN FLIGHT

$\beta_v = 20^\circ$

$\lambda_{HT} = 18.3^\circ$

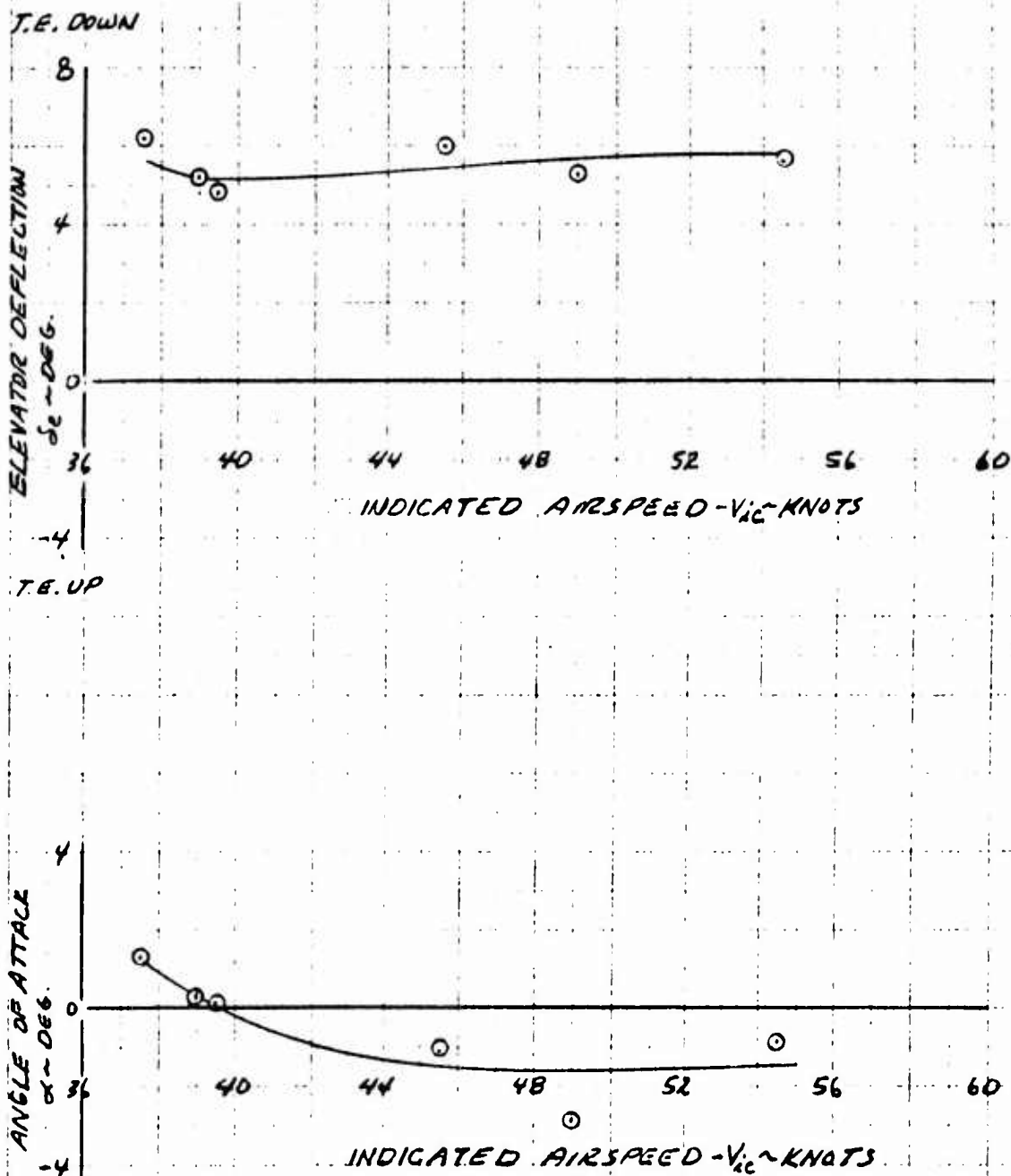


Figure 6.18 Static Longitudinal Stability - Fan Flight - $\beta_v = 20^\circ$

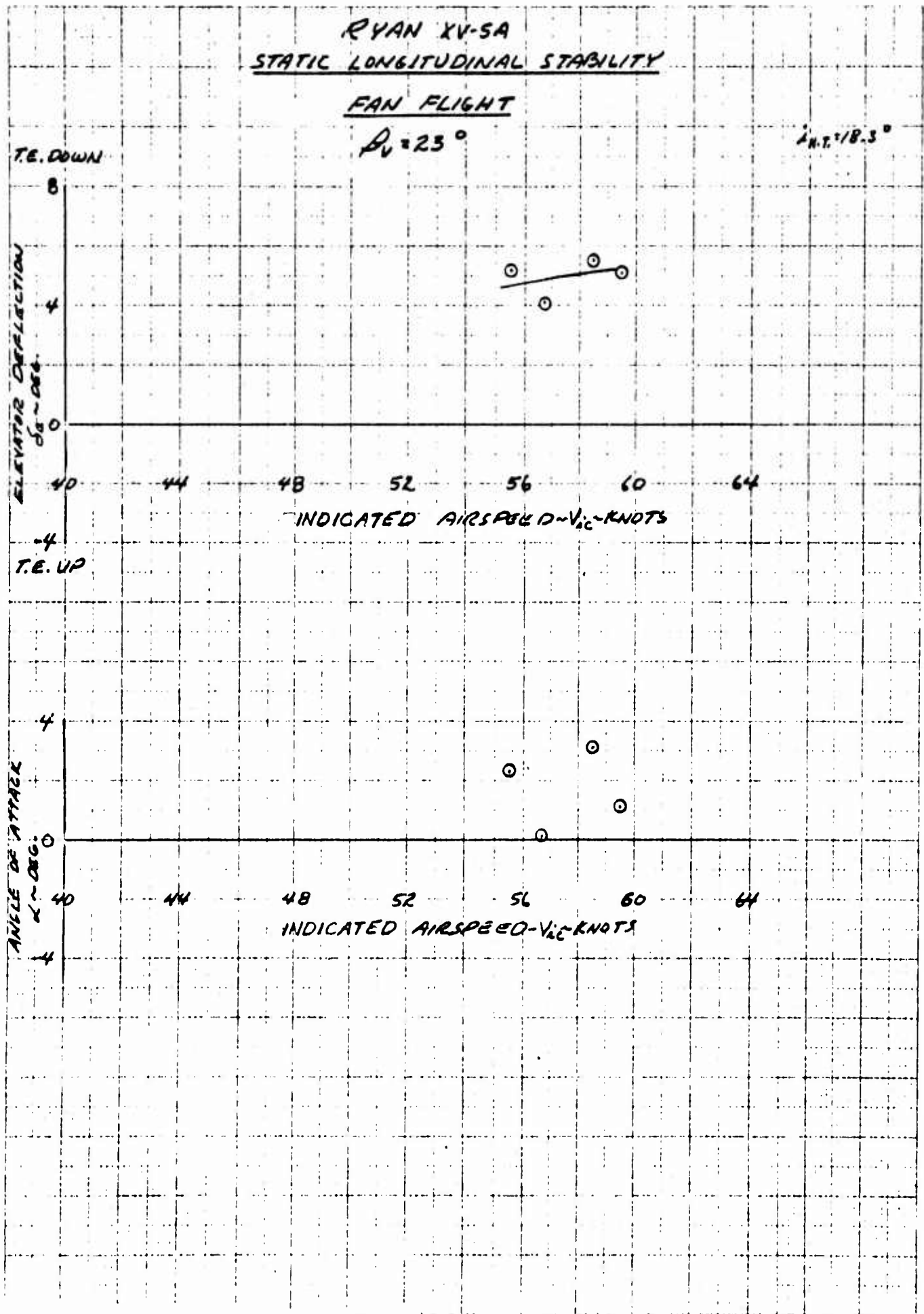


Figure 6.19 Static Longitudinal Stability - Fan Flight - $\beta_v = 23^\circ$

RYAN X1-5A
STATIC LONGITUDINAL STABILITY

FAN FLIGHT
 $\beta_v = 27^\circ$

$i_{NT} = 13.6^\circ$

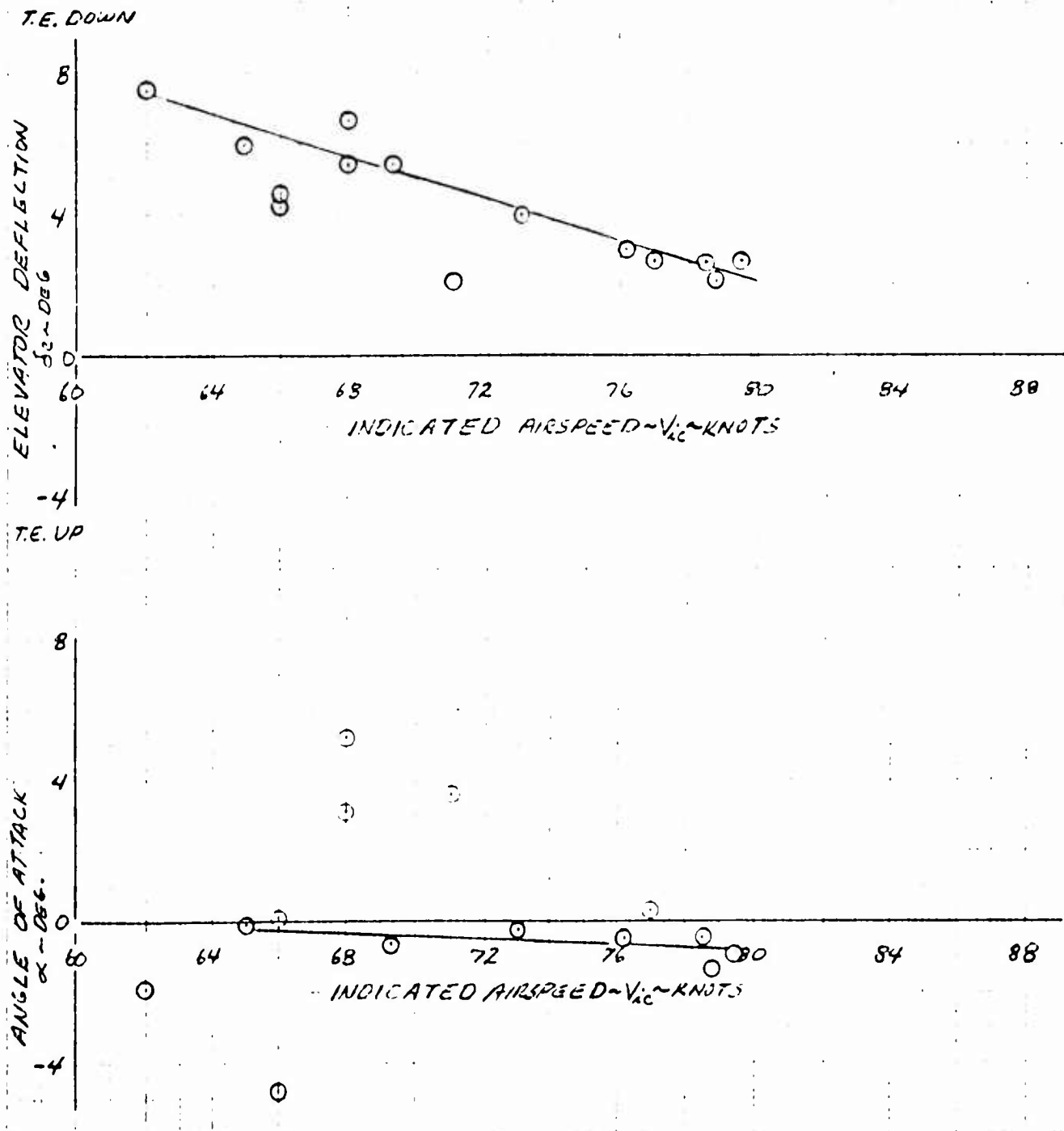


Figure 6.20 Static Longitudinal Stability - Fan Flight - $\beta_v = 27^\circ$

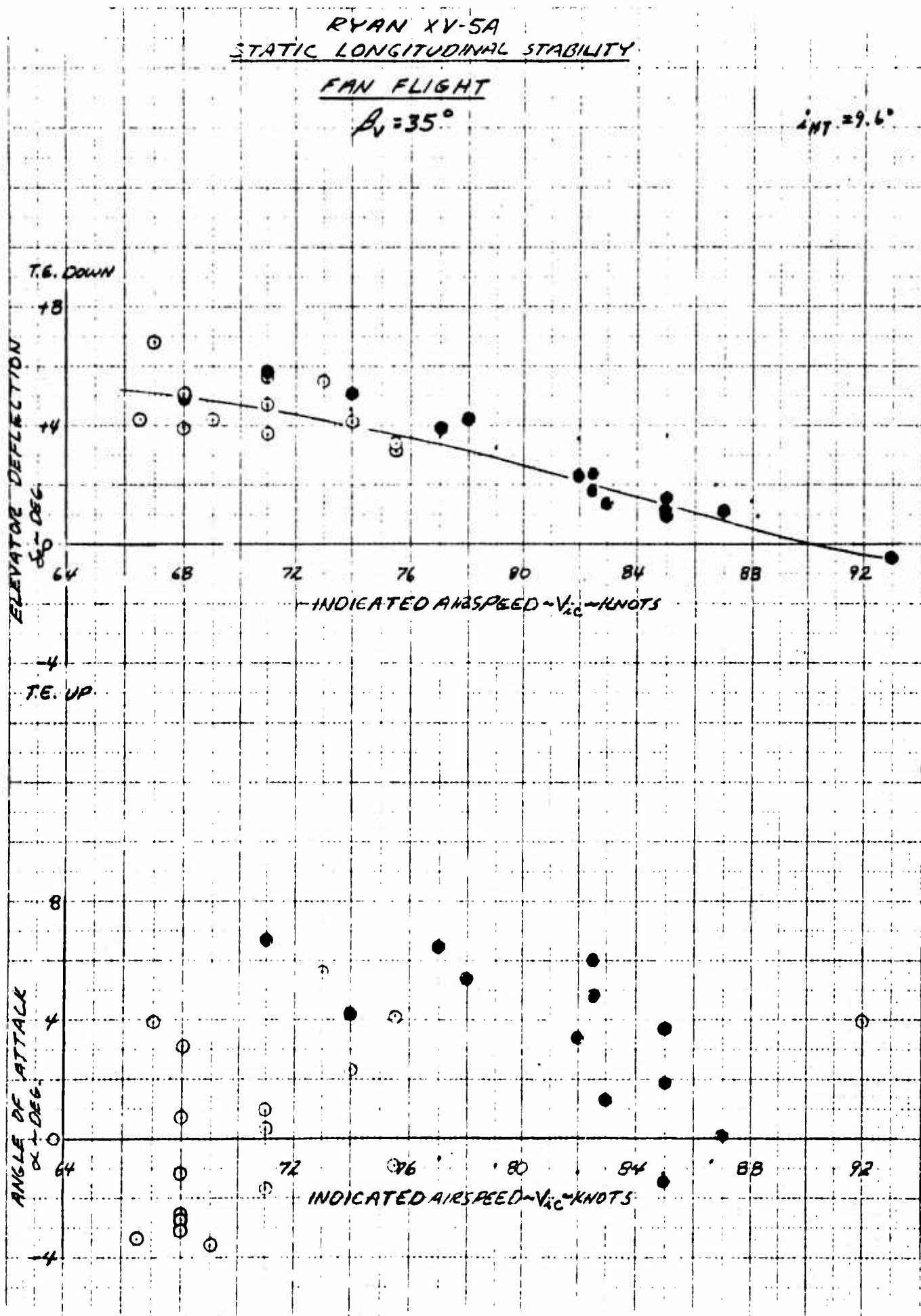


Figure 6.21 Static Longitudinal Stability - Fan Flight - $\beta_V = 35^\circ$

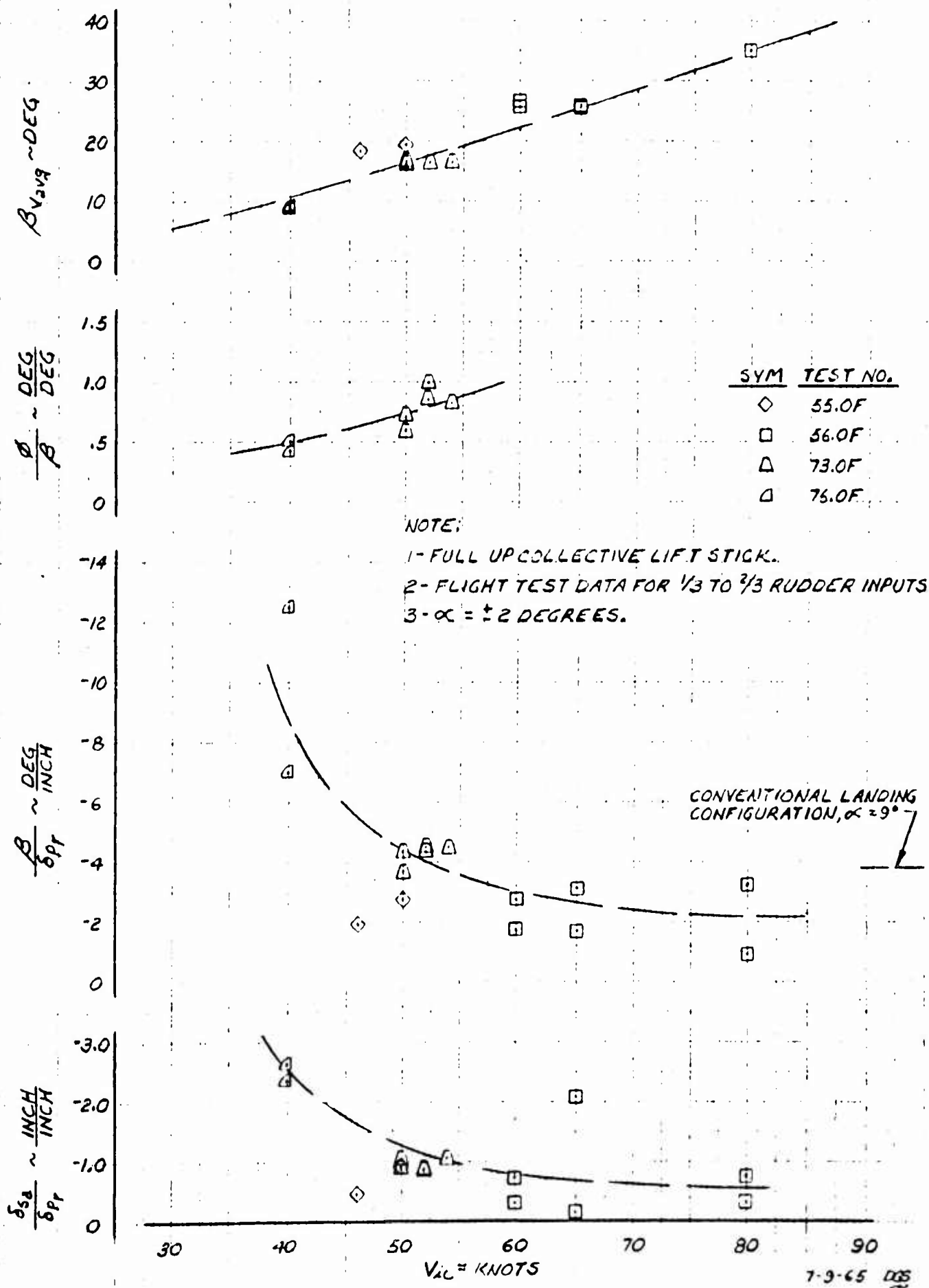


Figure 6.22 Lateral Directional Control - Steady State Sidelips - Gross Weight 10,000 Pounds with CG at FS 240.00

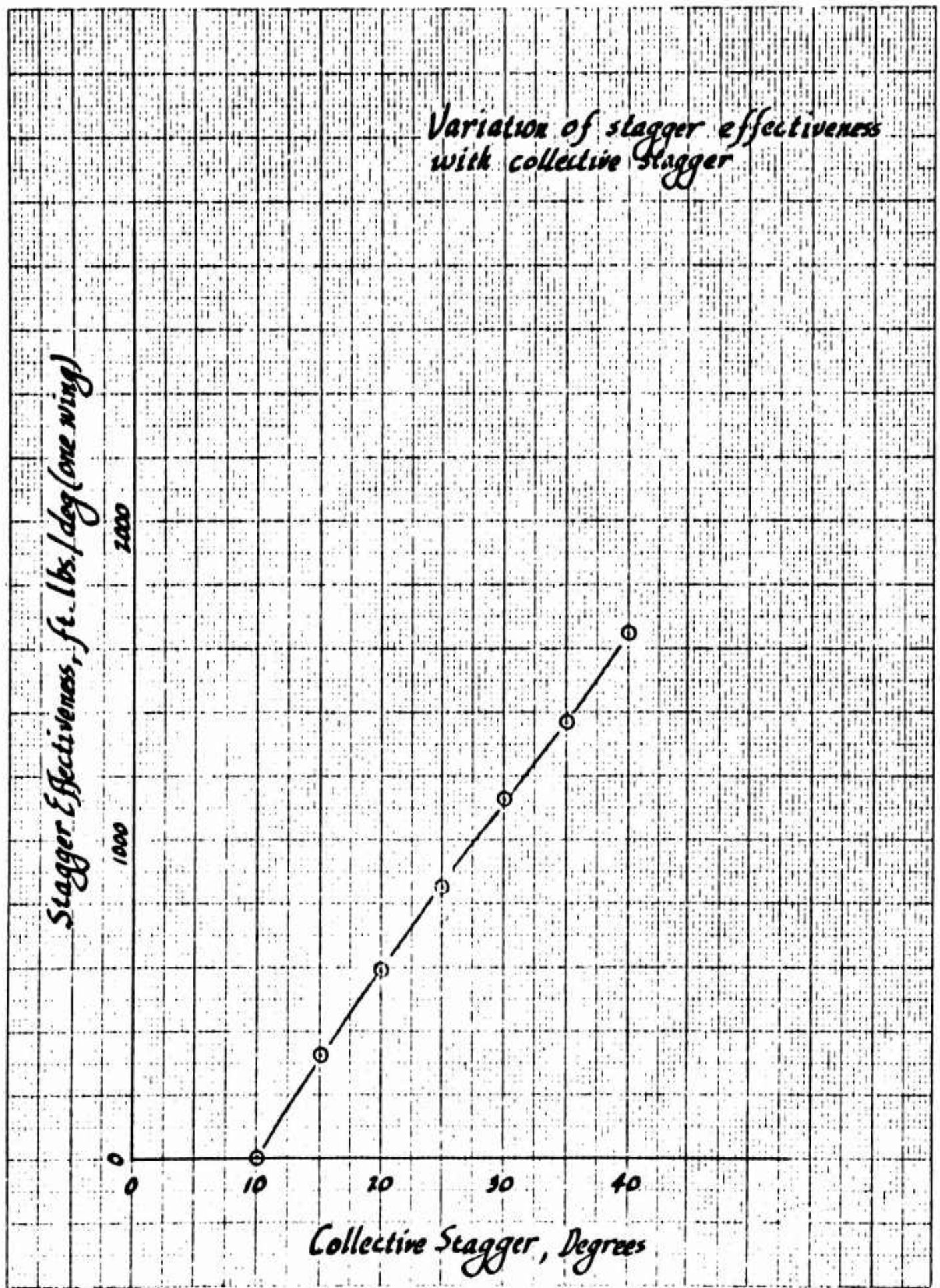


Figure 6.23 Variation of Stagger Effectiveness with Collective Stagger

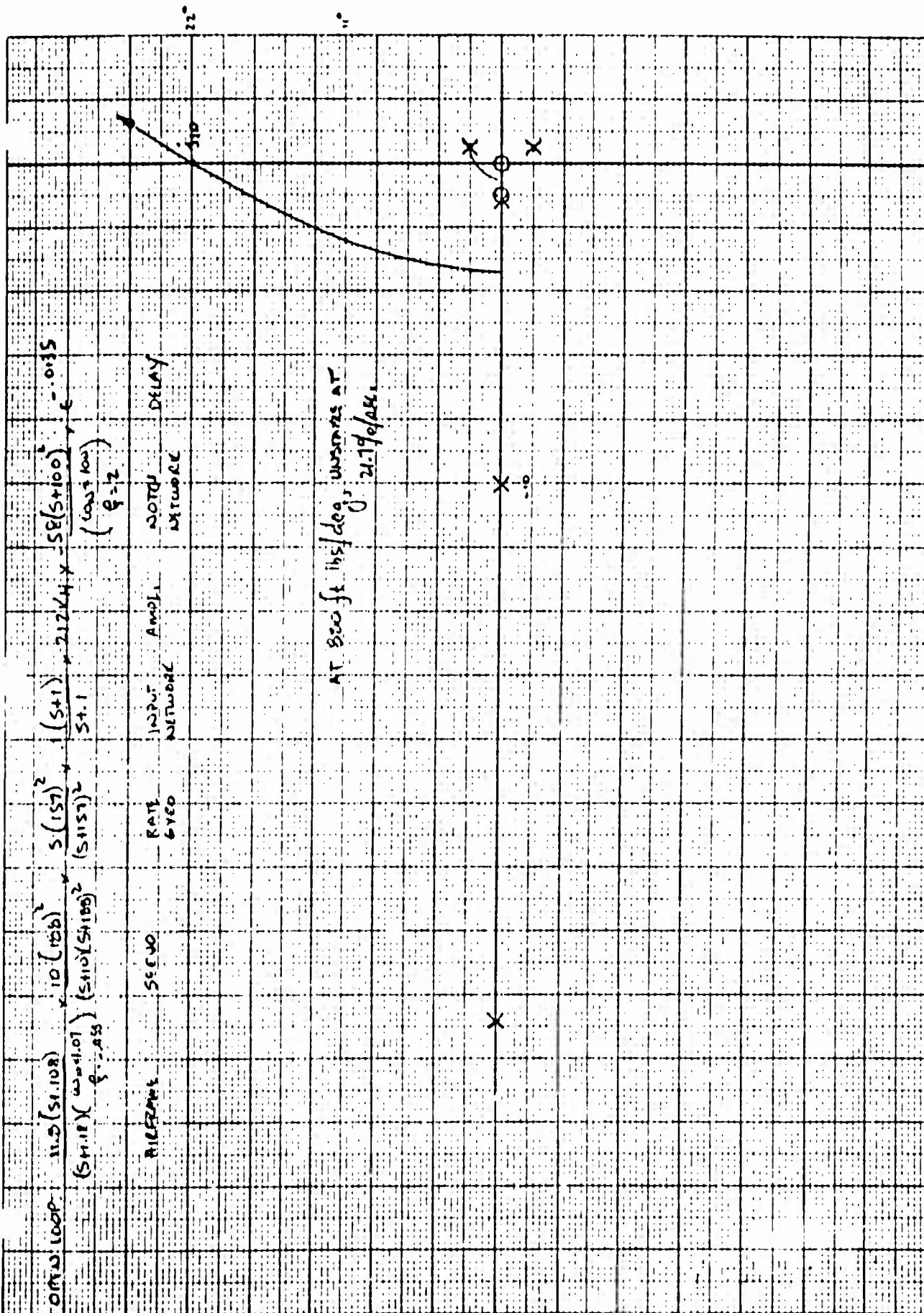


Figure 6.24 Roll System Root Locus After Louver & Servo Modification

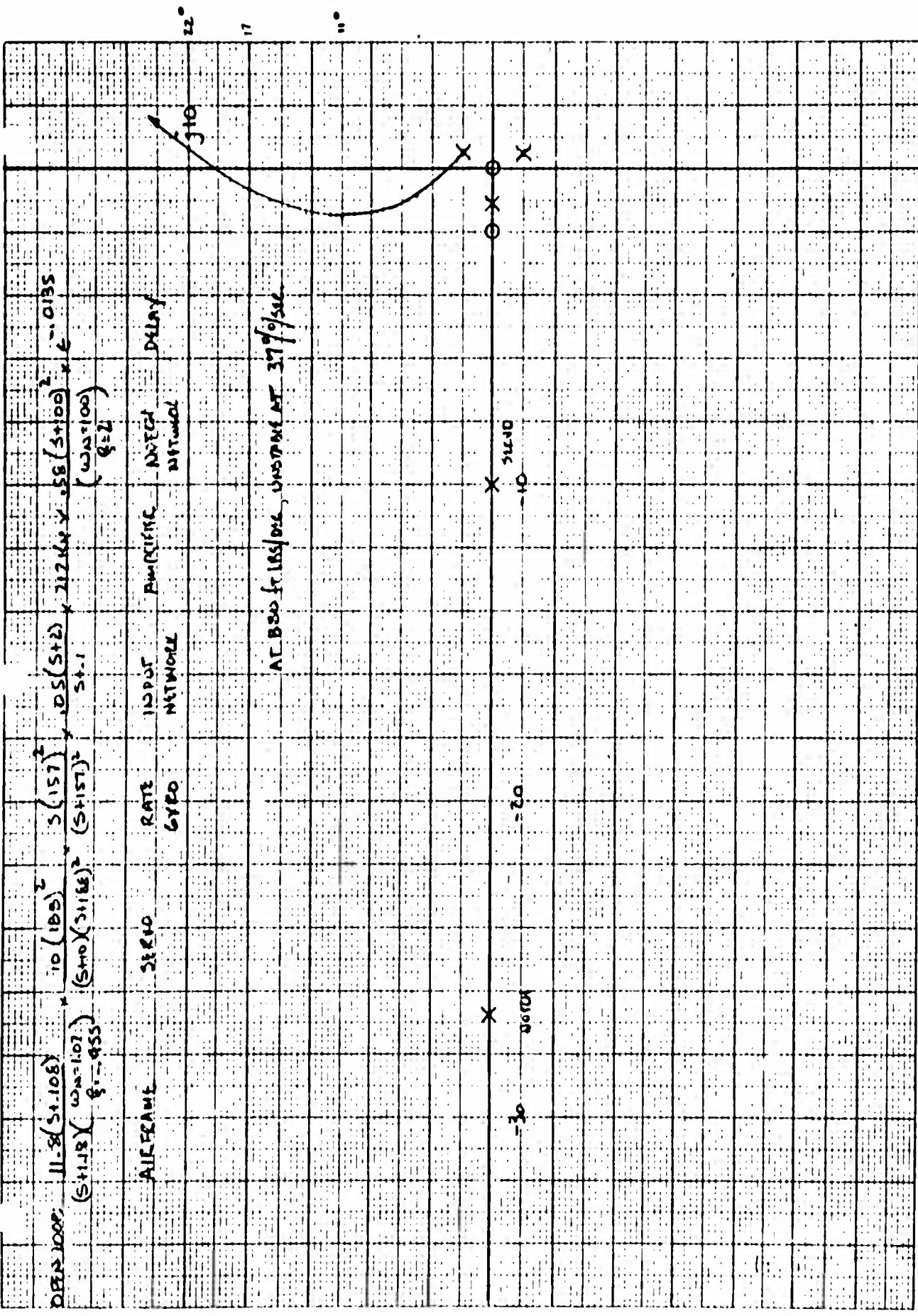


Figure 6.25 Roll System Root Locus After Louver & Servo Modifications

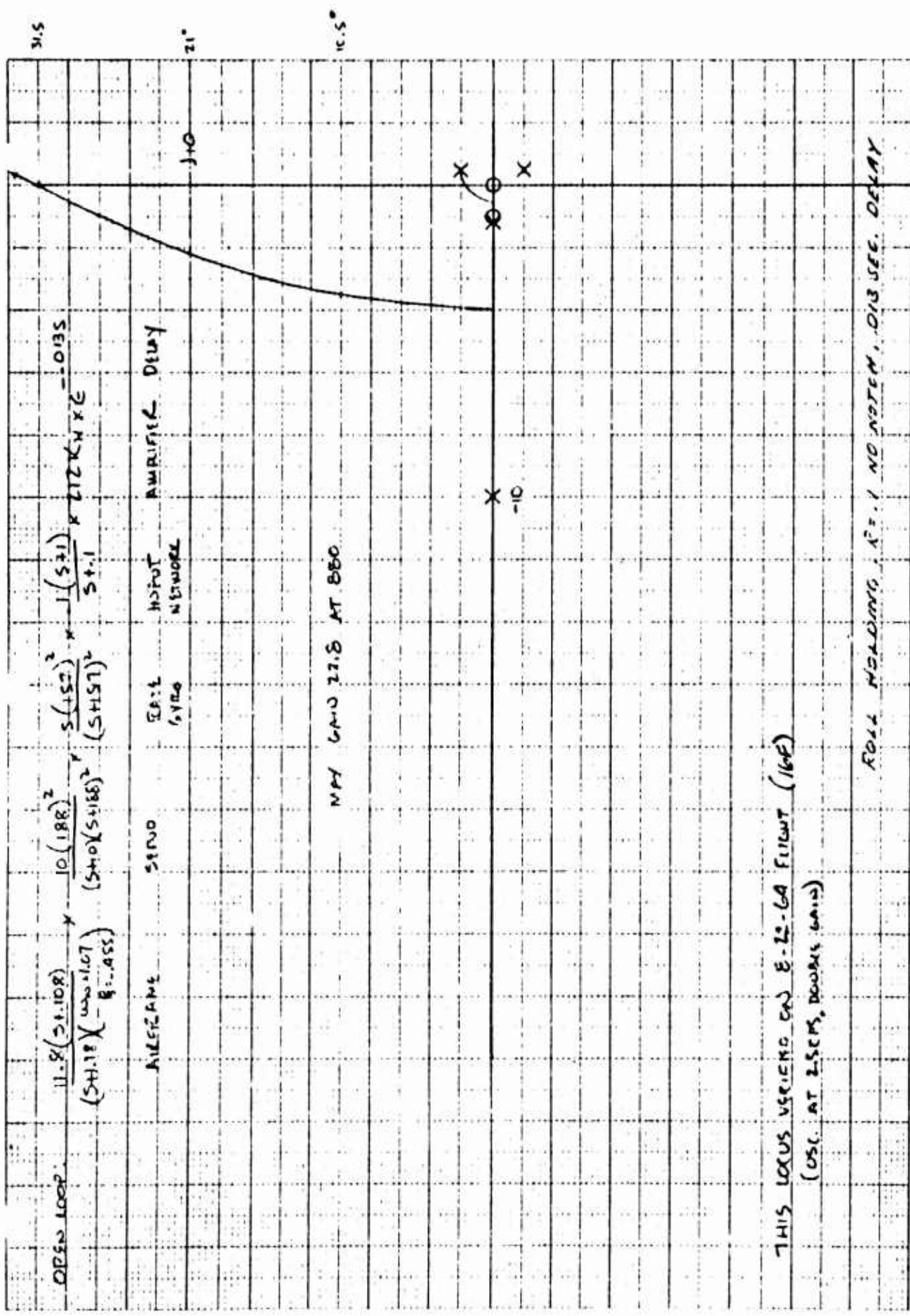


Figure 6.27 Root Locus for Roll After System Modification

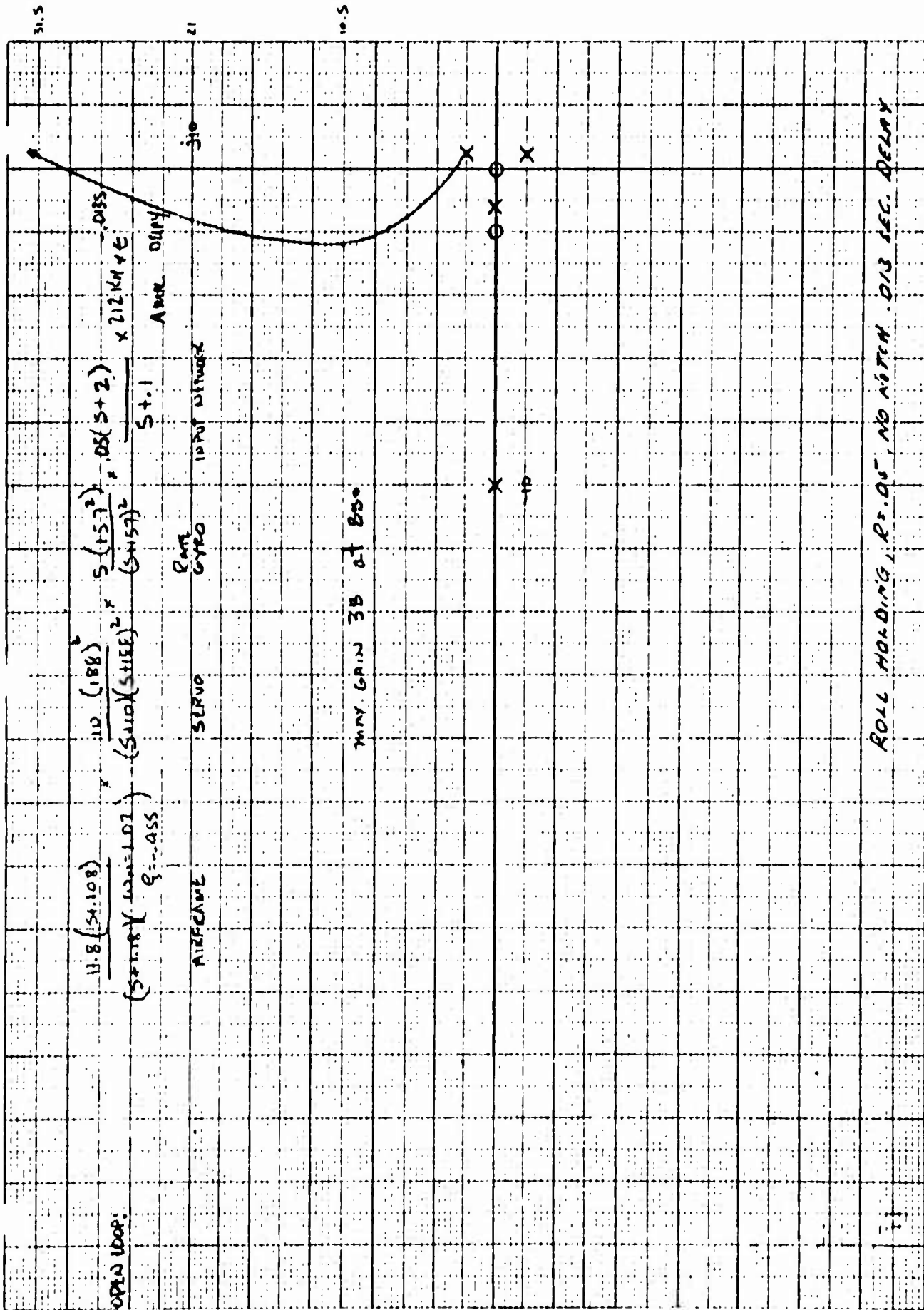


Figure 6.28 Root Locus for Roll After System Modification

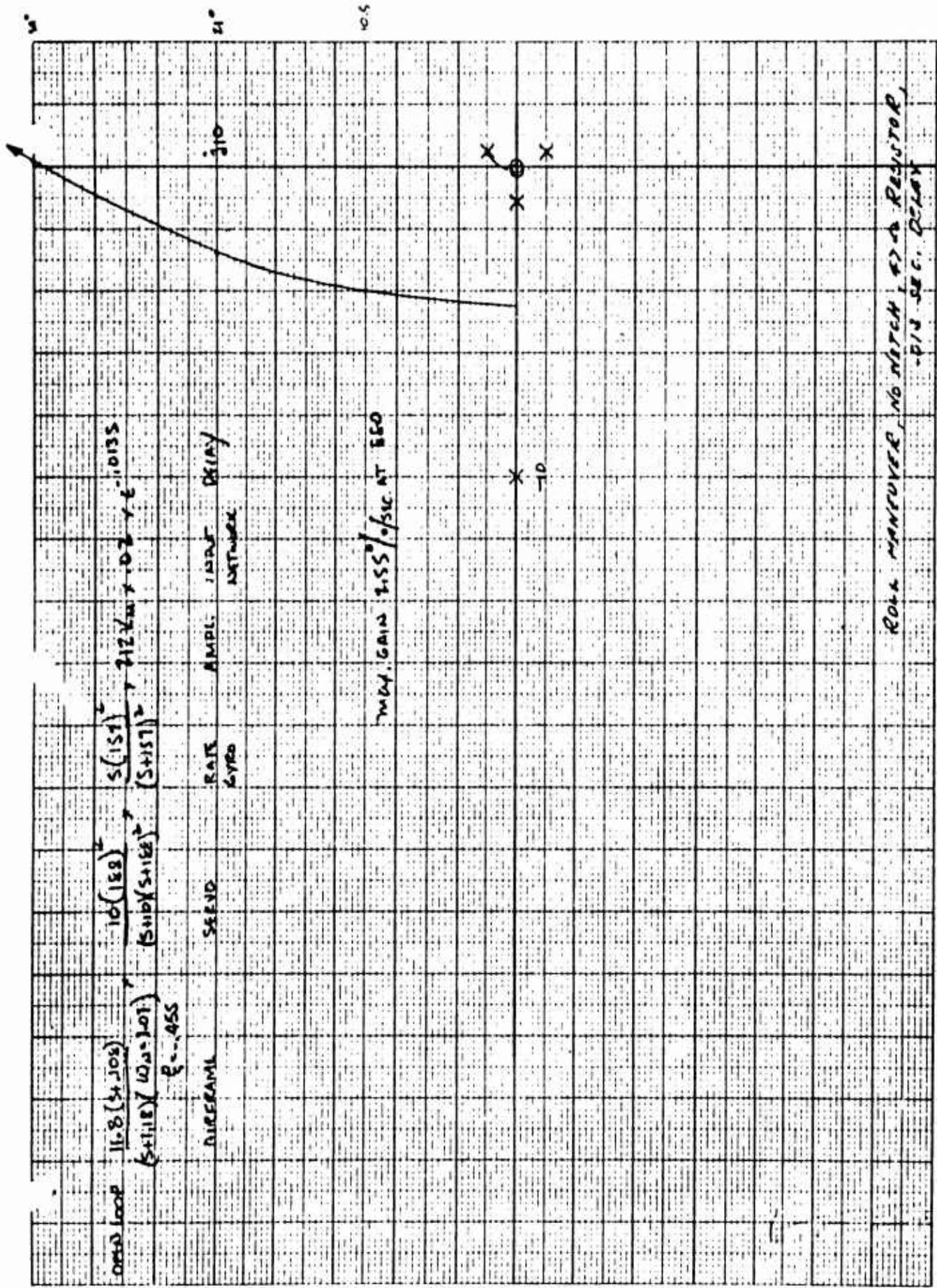


Figure 6.29 Root Locus for Roll After System Modification

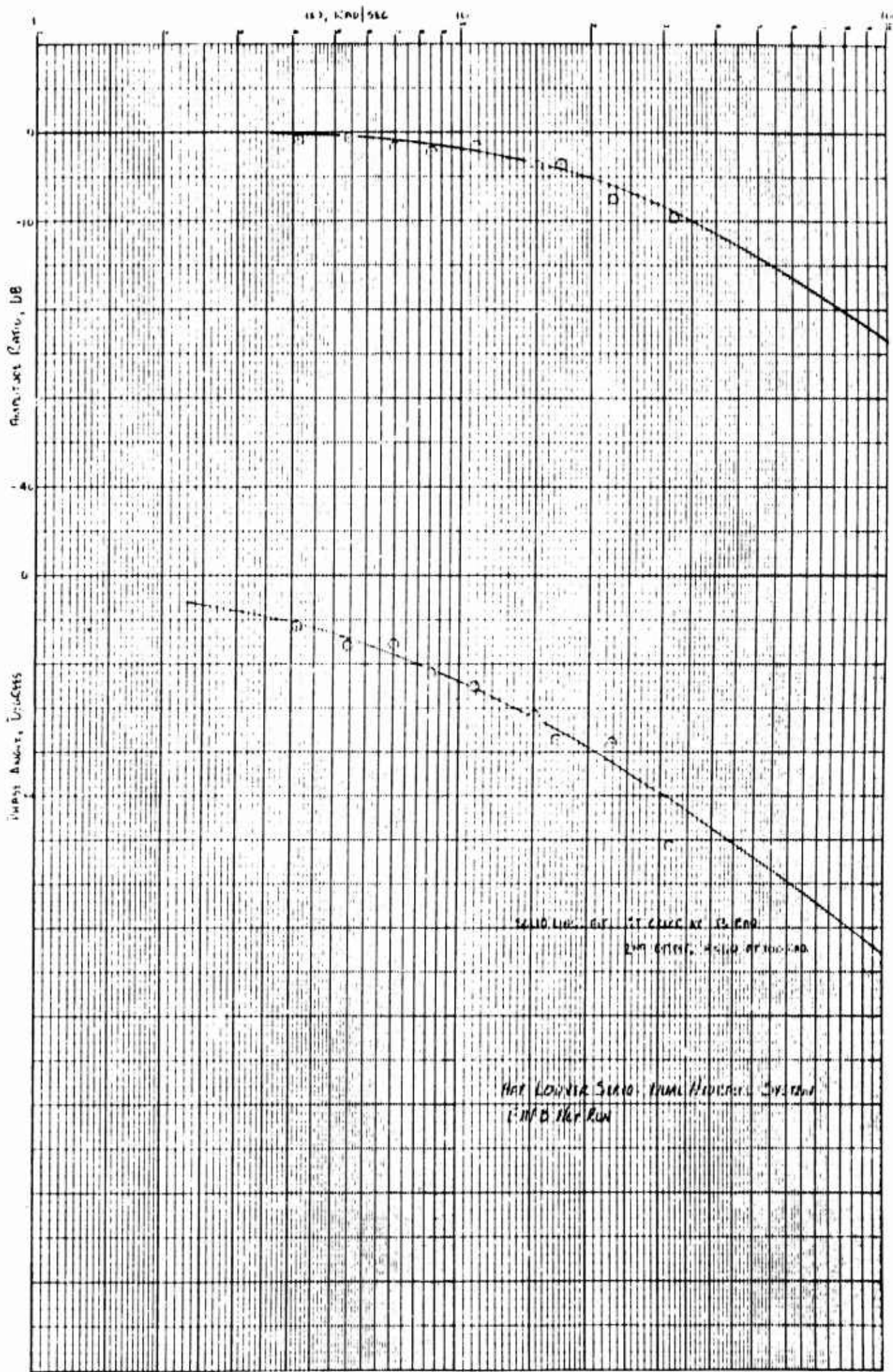


Figure 6.30 Dual System Response with Linear Transfer Function Fit

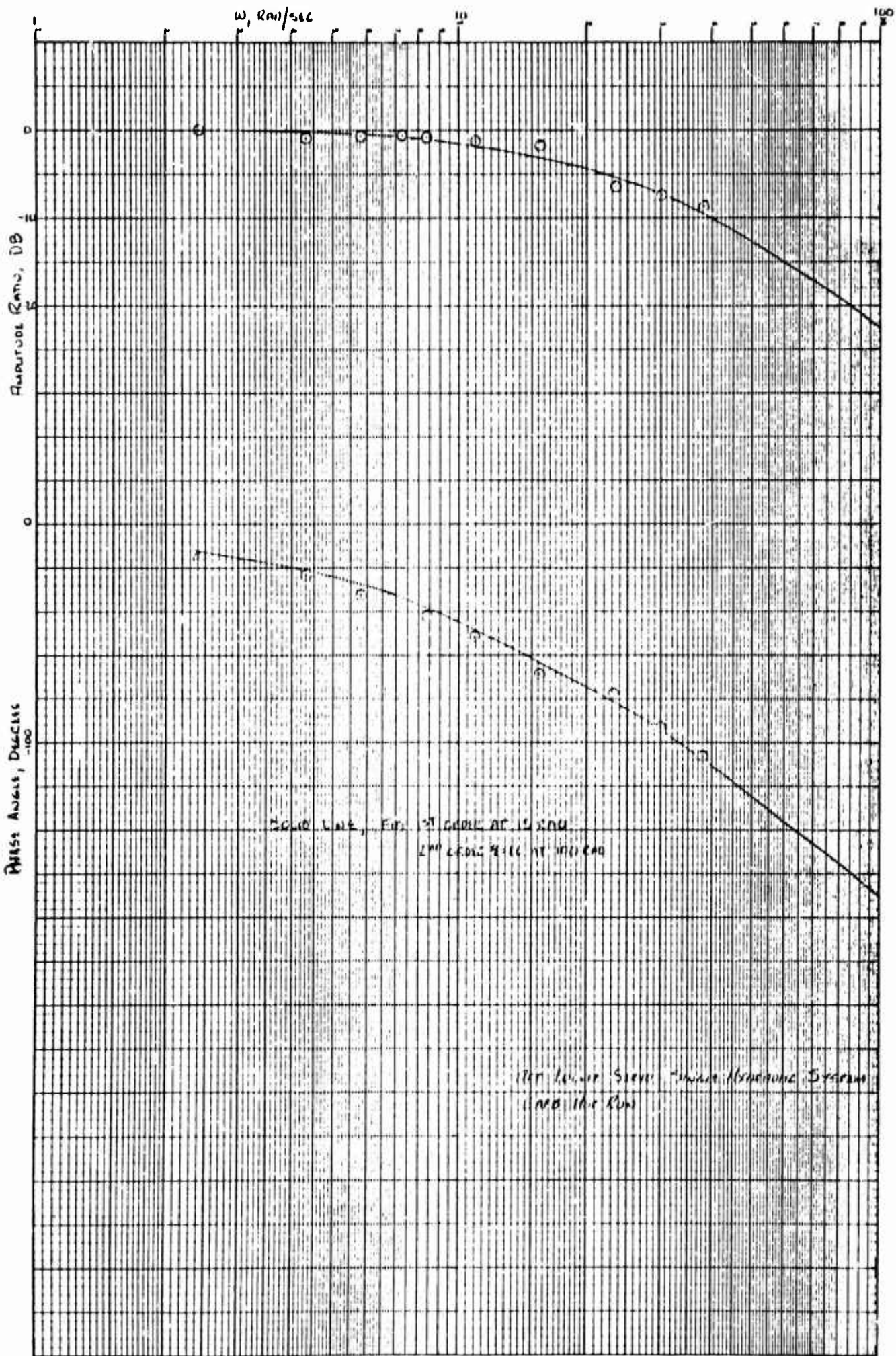


Figure 6.31 Single System Response with Linear Transfer Function Fit

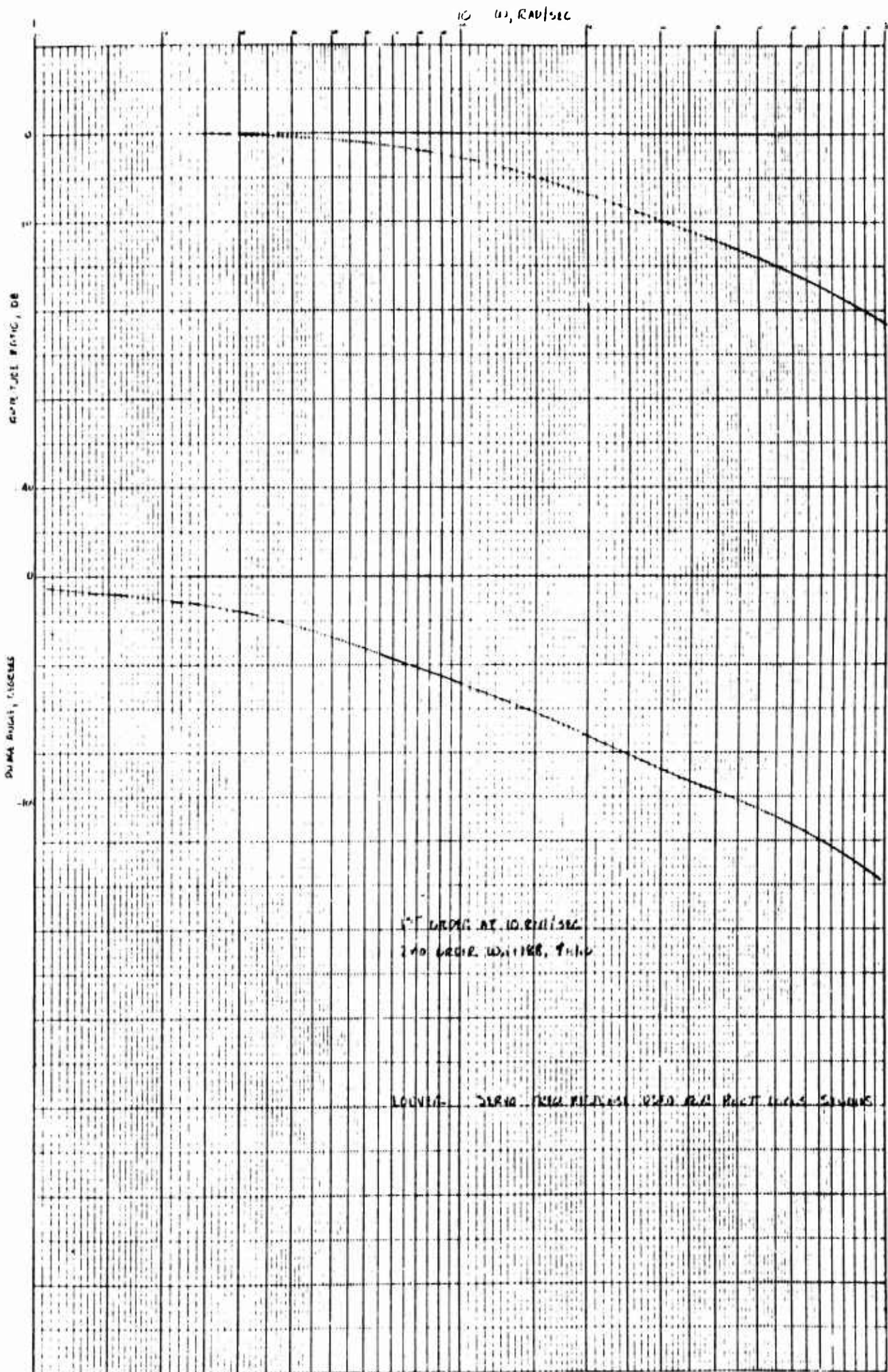


Figure 6.32 Frequency Response of Louver Servo

6.2.6 Control Power

The lift fan system provides all of the control capability during hover flight. During transition flight, conventional aerodynamic control capability increases with forward speed, permitting the gradual phase-out of the lift fan controls by the mechanical mixer mechanism. (Reference Paragraph 6.2.7, Control Rigging.)

During initial envelope penetration tests, evaluations of fan flight control power were almost exclusively based upon the pilot's comments. Basic procedure was for the pilot to feel out the controls about all three axes as the envelope was expanded. The Edwards AFB VTOL thrust stand provided some hover control power data. Toward the end of the program a definite effort was made to obtain reliable control power data in the 40-to-80-knot speed range, and this work provides the basis for the data presented in subsequent sections. Control power data is still lacking in the zero-to-40-knot speed range. Cockpit control force data obtained during fan mode flight was either not available or suspect and therefore will not be included.

6.2.6.1 Longitudinal Control Power

Figures 6.33 and 6.34 present longitudinal control power as a function of indicated airspeed. Control inputs were measured from trimmed flight conditions and varied between half and maximum control deflection. Maximum pitch accelerations are based upon linear extrapolation of measured control inputs to full control input from the trimmed flight position. Hover longitudinal control power was estimated from the VTOL thrust stand data (see Figure 6.9 for this data) and hovering flight lift conditions. Throughout the transition speed range at least 10 percent of the maximum attainable pitching acceleration at hover is retained, as required by Reference No. 6.6. At hover, maximum pitch accelerations are calculated as $+0.60 \text{ rad/sec}^2$ and -1.23 rad/sec^2 . The most critical speed range for longitudinal control power during transition is between 50 and 60 knots, during which minimum pitch accelerations of $+1.00$ and -0.64 rad/sec^2 were measured.

Pilot comments indicate that satisfactory levels of longitudinal control power were available during all phases of fan mode flight. Minimum longitudinal control inputs were required during hover flight. A slight increase in longitudinal control power was noted at 40 knots over the speed range of 50 to 60 knots. An estimated 5 pounds forward stick

pressure was required in level flight at 50 knots when trimmed at 60 knots. The pilot felt that longitudinal control power during conversion from jet to fan mode was sufficient to arrest the pitchover at any desired point.

Appendix Figures A-9 through A-11 and A-29 through A-37 present time histories of longitudinal control inputs recorded during dynamic response and control power evaluation tests with the SA system on.

6.2.6.2 Lateral Control Power

Lateral control power is presented in Figures 6.35 and 6.36 as a function of indicated airspeed. Control inputs were measured from either neutral or trimmed flight condition, using the lesser of the two, and varied between 1/3 and 2/3 maximum control deflection. Maximum roll accelerations are based upon linear extrapolation of measured control inputs to full throw. Hover lateral control power was established from the VTOL thrust stand data. Maximum lateral control power at hover is calculated to $\pm 2.38 \text{ rad/sec}^2$. This reduces to approximately $\pm 1.55 \text{ rad/sec}^2$ above 40 knots, based on flight test results.

First hover attempts indicated a definite lack of lateral control power. Investigation revealed insufficient wing fan exit louver actuator capability and wing fan exit louver bending. Prior to the first actual hover flight, the above problem areas were corrected. In addition, the mechanical mixer mechanism was modified to increase lateral control power (reference Paragraph 6.2.7, Control Rigging). After the pilot once became familiar with the aircraft in hover flight he reported that the lateral stick sensitivity was higher than optimum (approximately $\pm 3.0 \text{ rad/sec}^2$ for full control input). Prior to test 22.0F on Aircraft S/N 62-4506, the mechanical mixer mechanism was modified again, returning it to the originally designed lateral control sensitivity.

During investigation of the use of rapid vectoring and devectoring in study of transition technique, the pilot noted a significant reduction in roll control effectiveness where continuous vectoring was used between 10 and 20 degrees vector angle. Inasmuch as the fan roll control authority is phased out with vector angle, this effect may be attributed to the reduction in fan control effectiveness where the conventional control effectiveness is low.

Lateral control characteristics of the aircraft, as determined from

investigation of bank-to-bank rolling maneuvers at transition flight speeds, are discussed in Paragraph 6.2.4.

Appendix Figures A-12 through A-23, as well as Figures A-38 and A-39 present time histories of lateral control inputs obtained during maneuvering response and control power investigations with the SA system on.

6.2.6.3 Directional Control Power

Directional control power is presented in Figures 6.37 and 6.38 as a function of indicated airspeed. Control inputs were measured from either neutral or trimmed flight condition, using the lesser of the two, and varied from approximately one-third to maximum control deflection. Maximum yaw accelerations are based upon linear extrapolation of measured control inputs to full throw. Maximum directional control power at hover is only $\pm 0.32 \text{ rad/sec}^2$. This is about 40 percent of the estimated directional control power, based upon collective vector louver effectiveness full-scale test data. At present, this reduction of directional control power is unexplainable and should be further investigated. Flight test data indicate a gradual increase in directional control power with forward velocity.

Pilot noted that in hover flight the yaw control power seemed weak compared to longitudinal and lateral control power. However, yaw control power was considered adequate.

Figures A-40 through A-43 present time histories of directional control inputs recorded during maneuvering and dynamic response investigations with SA system on.

Directional control power in terms of sideslip angle attainable may be estimated using the data of Figure 6.22. While a control capability in excess of that required to produce 13 degrees sideslip is estimated for the landing configuration, the maximum trimmed sideslip capability in high-speed fan mode operation appears to be approximately 8 degrees. This increases to 15 degrees at 50 knots.

6.2.7 Control Rigging

6.2.7.1 Wing Fan Exit Louver and Nose Fan Thrust Reverser Door Control System

The lift fan system provides the necessary control forces and moments for altitude and attitude control in hovering flight. During transition flight, the fan control is phased out as conventional aerodynamic control power increases. Control power is obtained from the lift fan system by means of the wing fan exit louvers and the nose fan thrust reverser doors. These control surfaces are connected to the primary cockpit controls through a mechanical mixer mechanism and hydraulic actuators. The mechanical mixer mechanism provides for the phasing out of the fan control power as a function of the average wing fan exit louver vector angle, i. e., forward speed.

The control forces or moments produced by the wing fans become a function of the wing fan exit louver angle β , which is measured between the louver aft surface tangent plane and a plane parallel to the fan axis, positive when measured trailing edge aft. The inboard wing fan exit louvers are numbered 1 through 14, starting with the most forward louver. For purposes of relating control power to the wing fan exit louver position, β_1 is defined as the forward or odd-numbered wing fan exit louver and measured on number 7 louver. β_2 is defined as the aft or even-numbered wing fan exit louver and measured on number 8 louver. The wing fan exit louvers, operating basically in pairs, provide louver stagger and louver vector control. Wing fan exit louver stagger angle β_s is equal to $\beta_1 - \beta_2$. Wing fan exit louver vector angle β_v is equal to $1/2 (\beta_1 + \beta_2)$. Lateral control power (roll) is obtained by use of differential stagger between the right and left wing fans. Differential stagger $\Delta \beta_s$ is equal to $\beta_{sR} - \beta_{sL}$. A positive value indicates a right or positive rolling moment. Directional/control power (yaw) is obtained by differential vector between the left and right wing fans. Differential vector $\Delta \beta_v$ is equal to $\beta_{vL} - \beta_{vR}$. A positive value indicates a nose-right or positive yawing moment. Forward or aft thrust is obtained from the wing fans by vectoring the wing fan exit louvers aft (positive) or forward (negative) respectively.

Longitudinal control forces or moments are a function of the nose fan thrust-reverser doors position δ_{NF} , which is measured from the full-closed position.

Altitude control becomes a function of the wing fan exit louver stagger angle and the nose fan thrust reverser doors position. Collective lift control determines the wing fan exit louver stagger angle and the position of the pitch fan thrust-reverser doors required to trim the aircraft along the pitch axis. Figure 6.39 illustrates the operation of the lift fan control system. Louver effectiveness and control power are discussed in other sections of this report.

6.2.7.2 Lift Fan System Mechanical Mixer Mechanism

The mechanical mixer mechanism is the tie-in between the primary cockpit controls, the wing fan exit louver hydraulic actuators, and the hydraulic actuator for nose fan thrust-reverser doors. It determines the amount of differential wing fan exit louver stagger or vector provided by a given lateral stick or rudder pedal input based on the average wing fan exit louver vector angle, i.e., forward speed of the aircraft. It also determines the position of the nose fan thrust reverser doors for a given longitudinal stick input, based on the average wing fan exit louver stagger and vector angle. In addition, it provides for the phasing out of the fan system control as forward speed increases and conventional aerodynamic control becomes adequate, so that in conventional flight the fan control system is disengaged at the mechanical mixer mechanism. Figure 6.40 is a schematic diagram of the flight control system, illustrating the tie-in of the mechanical mixer mechanism with the primary cockpit controls and lift fan control system actuators.

6.2.7.3 Design of the Lift Fan System Mechanical Mixer Mechanism

In order to design the lift fan system mechanical mixer mechanism, it was necessary first to determine the effectiveness of the wing fan exit louvers and the nose fan thrust-reverser doors both for hovering flight and transitional speeds. This information was obtained from test data of a 1/6-scale, powered, wind-tunnel model (Reference Number 6.7), and from unpublished full-scale test results from full scale model tests at the NASA Ames Research Center's 40 x 80-foot wind tunnel. The stability and control requirements of the lift fan system were derived with consideration of the XV-5A flying-qualities criteria given in Reference Number 6.6.

6.2.7.4 Modifications to the Lift Fan System Mechanical Mixer Mechanism, Aircraft Serial Number 62-4506

Unsatisfactory lateral control power during hovering flight resulted in

incorporation of several minor changes in the mechanical mixer mechanism. The original configuration provided the following louver stagger control at $\beta_v = 0^\circ$;

<u>Collective Lift</u>	<u>Lateral Stick</u>	β_{sL}	β_{sR}	$\Delta\beta_s$	β_s/δ_{sa}
		Deg	Deg	Deg	
Stick Position	Position	Deg	Deg	Deg	
Max. Lift	Neutral	13	13		
Nom. Lift	Neutral	27	27		
Min. Lift	Neutral	37	37		
Max. Lift	Full Right	0	29	29	3.87
Nom. Lift	Full Right	12	38	25	3.34
Min. Lift	Full Right	25	40	15	2.00

The first attempt to hover indicated a lack of lateral control power, which was further investigated during the NASA Ames Ramp Test with aircraft Serial Number 62-4505. Based on the results of this test, a number of modifications were incorporated into the lift fan system, including provisions for increased lateral control power by increasing the amount of wing fan exit louver differential stagger available for a given lateral stick input. The following louver stagger control at $\beta_v = 0^\circ$ was incorporated in the mechanical mixer mechanism:

<u>Collective Lift</u>	<u>Lateral Stick</u>	β_{sL}	β_{sR}	$\Delta\beta_s$	β_s/δ_{sa}
		Deg	Deg	Deg	
Stick Position	Position	Deg	Deg	Deg	
Max. Lift	Neutral	15.5	15.5		
Nom. Lift	Neutral	27	27		
Min. Lift	Neutral	33	33		
Max. Lift	Full Right	0	33	33	4.4

Nom. Lift	Full Right	7	40	33	4.4
Min. Lift	Full Right	15.5	40	24.5	3.27

This modification was effective during the Edwards AFB VTOL thrust Stand Test and through test 21F, 31 August 1964. Prior to test 22.OF, the mechanical mixer was again modified, returning it to a configuration similar to that used originally except for an increase in the minimum collective stagger at maximum lift. The following louver stagger control at $\beta_v = 0^\circ$ was obtained:

<u>Collective Lift</u>	<u>Lateral Stick</u>	β_{sL}	β_{sR}	$\Delta\beta_s$	β_s/δ_{sa}
		_____	_____	_____	_____
Stick Position	Position	Deg	Deg	Deg	
Max. Lift	Neutral	17	17		
Nom. Lift	Neutral	27	27		
Min. Lift	Neutral	37	37		
Max. Lift	Full Right	0	33	33	4.4
Nom. Lift	Full Right	12	38	26	3.47
Min. Lift	Full Right	25	40	15	2.0

Other minor modifications incorporated in the mechanical mixer mechanism during the test program included changing the limit on the maximum aft vector angle obtainable and adjustments as to the vector angle at which conversion to the jet mode may be initiated..

Modifications to the mechanical mixer mechanism in aircraft Serial Number 62-4505 were carried out in several steps, all being incorporated prior to the first hover flight.

6.2.7.5 VTOL Static Check on the Lift Fan Control System Rigging, Aircraft Serial Number 62-4506

Subsequent to the modifications to the mechanical mixer mechanism prior to test 22.OF, an extensive rigging check was conducted on the lift fan control system in an attempt to obtain a better understanding of

the mechanical mixer mechanism and isolate any undesirable characteristics. Figures 6.41 through 6.60 are included to illustrate some of the functions of the mechanical mixer mechanism.

Figures 6.41 and 6.42 illustrate the phase-out of altitude control or wing fan exit louver stagger angle as a function of the average wing fan exit louver vector angle with both lateral stick and rudder pedals neutral for maximum and nominal collective lift stick position. The small amount of differential stagger shown is due principally to differences between the left and right wing destaggering cams within the mixer box. Figure 6.43 presents the stagger angle of the right and left wing fan exit louvers for three collective lift stick positions as a function of the average louver vector angle with neutral rudder and full right lateral stick control inputs. The difference between the right wing fan and left wing fan exit louver stagger angles for the same collective lift stick position and average louver vector angle indicates the amount of louver lateral control available. The results of multiple control inputs are presented in Figures 6.44 and 6.45 as a function of the wing fan exit louver differential stagger angle and average vector angle. In Figure 6.45, note the reduction of the left lateral control with right rudder input. Part of this reduction is due to incorrect rigging of the mechanical mixer mechanism and has subsequently been corrected. Proper rigging should produce approximately zero differential stagger for full right rudder and neutral lateral stick inputs at an average louver vector angle of -2.5 degrees of nominal collective lift stick position.

Figure 6.46 presents the vector angle of the right and left wing fan exit louvers as a function of the average louver vector angle. Collective lift stick position has very little effect on the exit louver vector angle. The difference between the left and right wing fan exit louver vector angle for the same basic condition indicates the amount of louver directional control available. Figures 6.47 and 6.48 illustrate the results of multiple control inputs on fan-induced directional control power. Lateral stick has much less effect on fan directional control power than the rudder has on lateral control power, due to the roll compensation feature of the mechanical mixer.

By the time an average wing fan exit louver vector angle of 40 degrees is reached, the mechanical mixer mechanism has phased out both lateral and directional fan induced control power.

Figures 6.49 through 6.51 present the effects of various control inputs on the nose fan thrust reverser doors. Figure 6.49 presents the nose fan thrust reverser doors position as a function of longitudinal

stick position for three collective lift stick positions and an average wing fan exit louver vector angle of 12 degrees. Some misrigging is evident here, because full-forward longitudinal stick should not close the nose fan thrust reverser doors less than 40 degrees.

Based on test data, maximum nose fan thrust reversal was obtained at the 40-degree open position. Figure 6.50 presents the positions of the nose fan thrust reverser doors for full-forward and full-aft longitudinal stick positions as a function of the collective lift stick position for an average wing fan exit louver vector angle of 12 degrees. Figure 6.51 completes the picture of the nose fan thrust reverser doors by presenting them as a function of the average wing fan exit louver vector angle. The phase-out was based on the nose fan thrust reverser door position required to trim the aircraft during transition and the longitudinal control power required of the nose fan to meet the requirements established in the XV-5A Flying Qualities Report.

Table 6.4 and Figure 6.52 are taken from the XV-5A Control Systems Rigging Procedures and are used to correlate final stick or pedal to control surface rigging adjustments, (Reference 6.8).

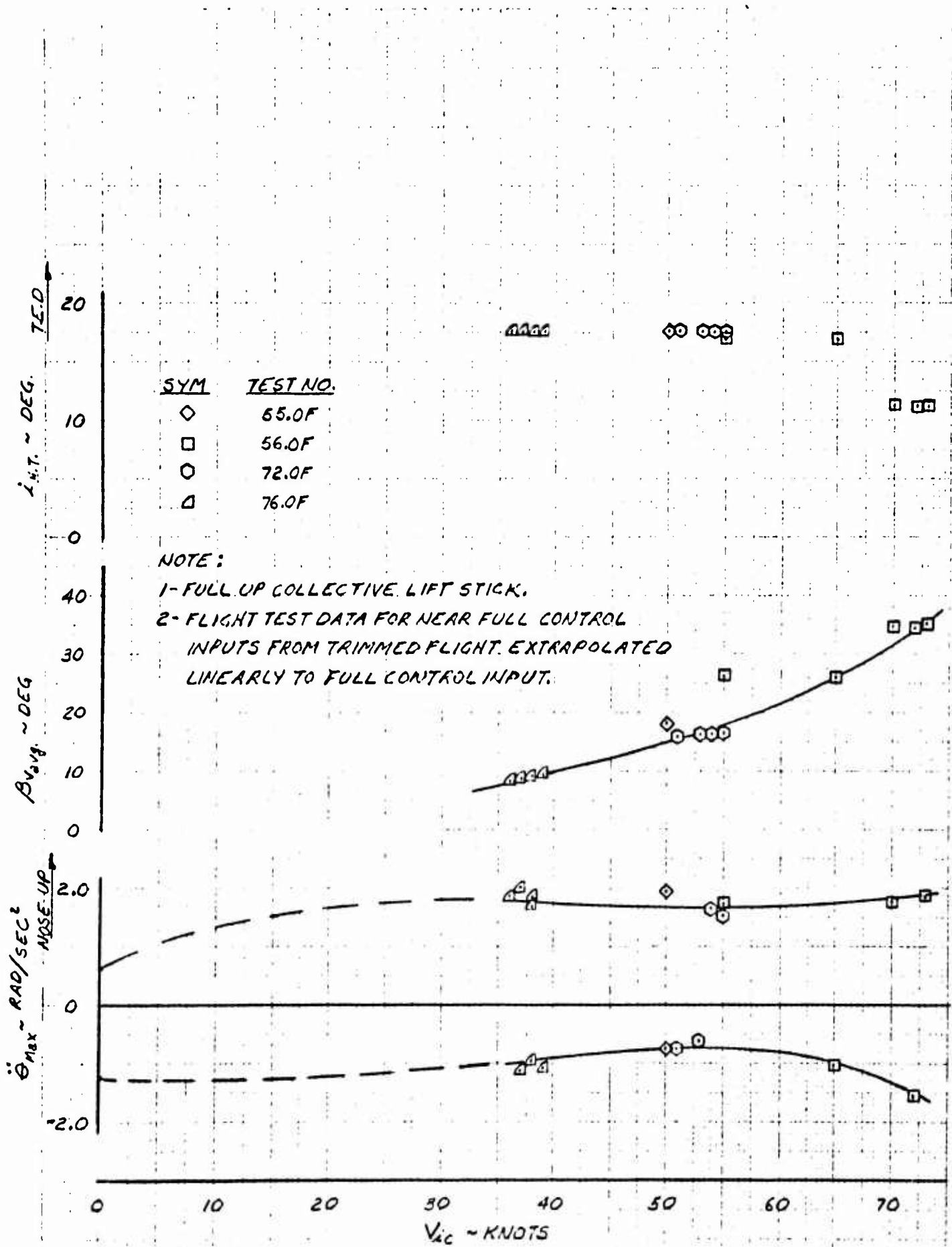
Figures 6.53 through 6.58 present lateral stick and rudder pedal sweeps for maximum, nominal, and minimum collective lift stick positions for an average wing fan exit louver vector angle of zero degrees. Figures 6.59 and 6.60 present lateral stick and rudder sweeps for nominal collective lift stick position and an average wing fan exit louver vector angle of 12 degrees. Special attention should be paid to control inputs which cause one or more of the louver actuators to reach a maximum travel limit and introduce severe nonlinearities in the wing fan exit louver schedule. An example of this condition can be seen in Figure 6.56, where the left even-number wing fan exit louver β_{2L} has reached its maximum travel limit from a full-left lateral stick and approximately two inches of left rudder pedal.

6.2.7.6 Hysteresis of the Mechanical Mixer Mechanism

A certain amount of hysteresis was recorded within the mechanical mixer mechanism due to the backlash and friction within the system. The most severe conditions were shown to occur when one of the wing fan exit louver actuators reached a maximum-travel limit. Figures 6.61 through 6.66 illustrate this hysteresis and were obtained from data taken during several static hangar rigging checks on the lift fan control system.

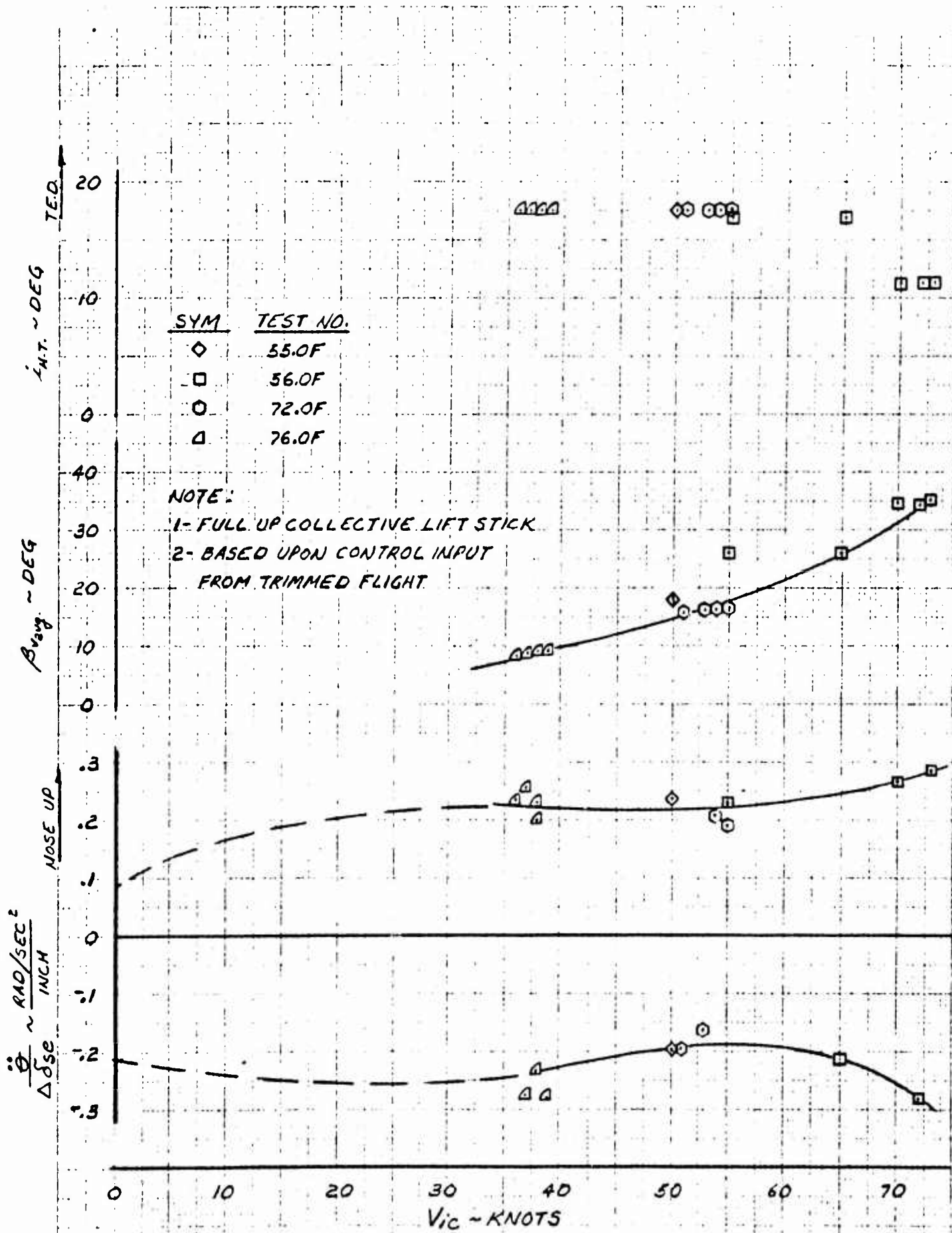
No detrimental effects were noted by the test pilots due to this hysteresis. The lack of discernible effects is not surprising, however, for several reasons: the characteristic lies outside of the normal operating envelope for the control system, vibration due to engine operation may reduce the effect significantly, and the operation of the louver system on the opposite wing without hysteresis would tend to mask the undesirable effects.

BLANK PAGE



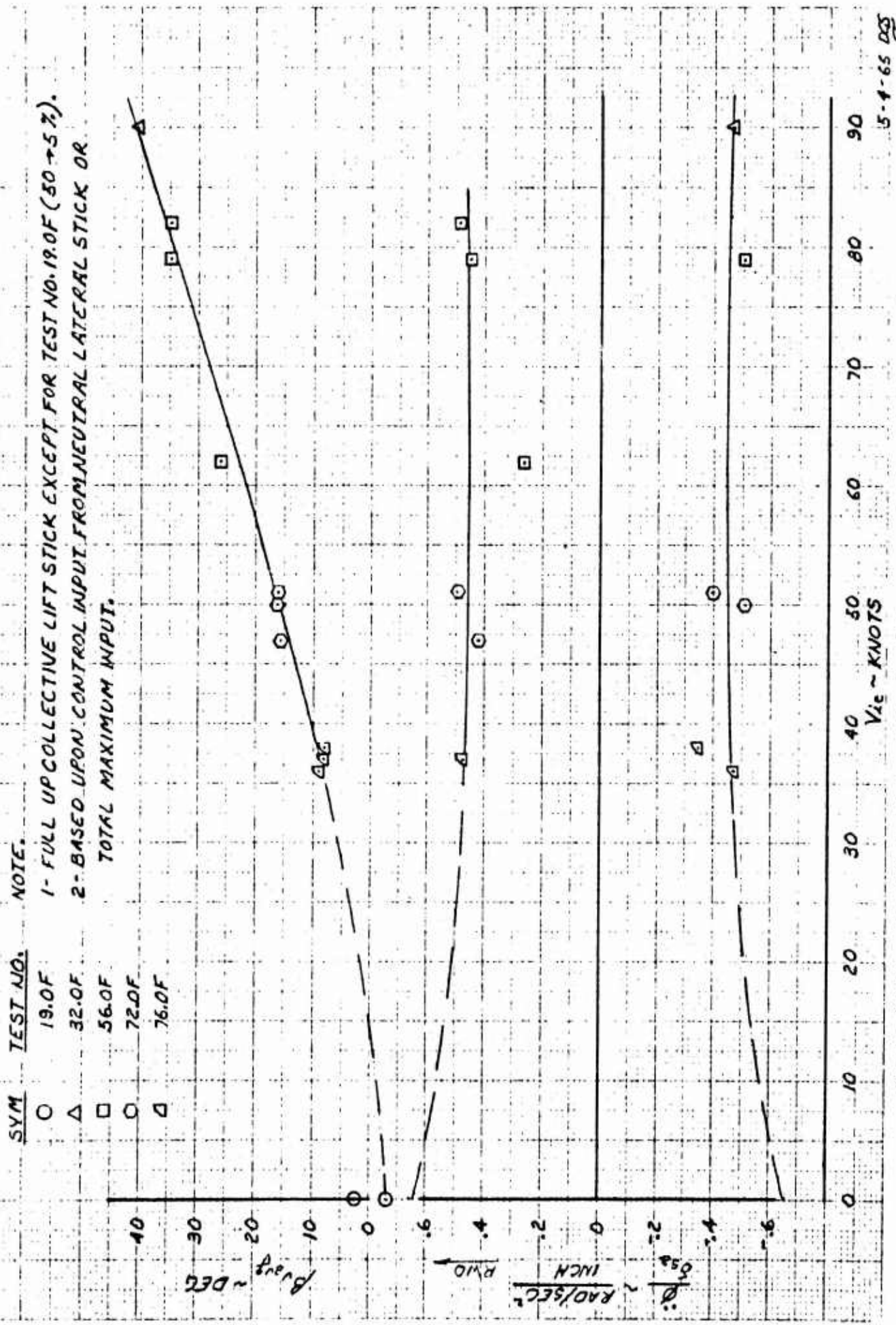
5-1-65 DJS

Figure 6.33 Fan Mode Longitudinal Control Power vs Indicated Airspeed



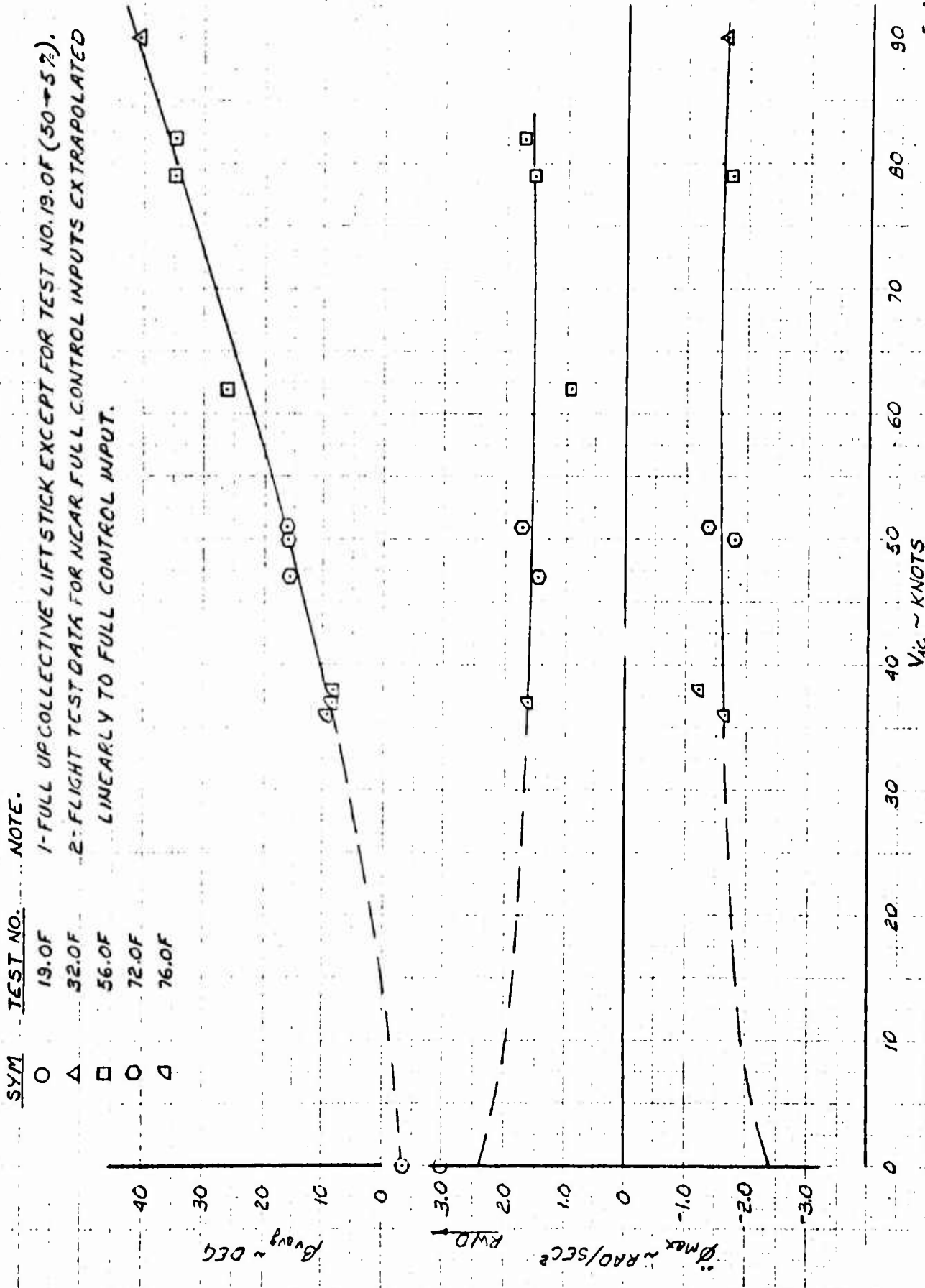
5-1-65 RJS

Figure 6.34 Fan Mode Longitudinal Control Power vs Indicated Airspeed



5-4-65 DCS

Figure 6.35 Fan Mode Lateral Control Power vs Indicated Airspeed



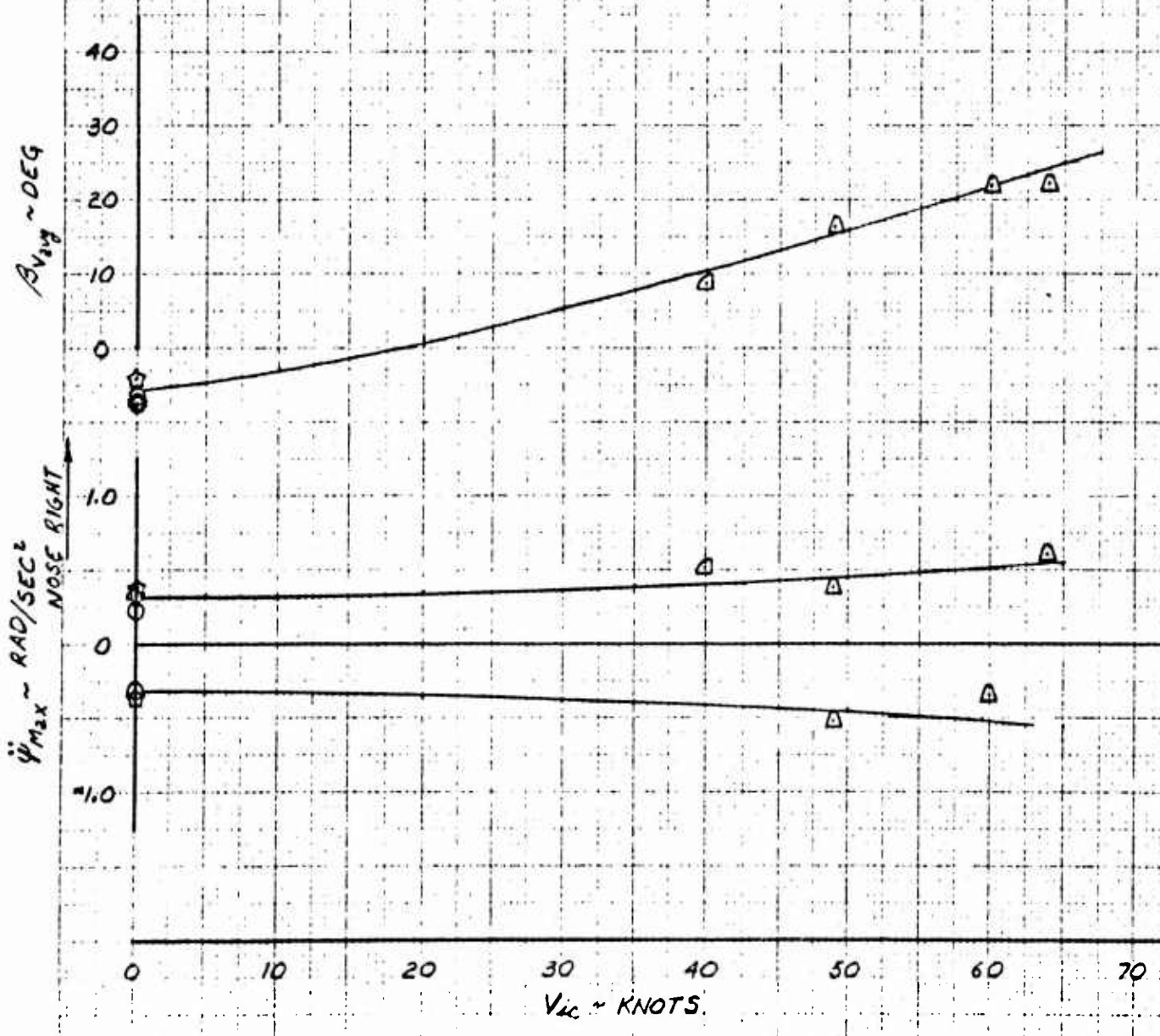
5-1-65 DS

Figure 6.36 Fan Mode Lateral Control Power vs Indicated Airspeed

<u>SYM</u>	<u>TEST NO.</u>
☆	16.0F
⊛	29.0F
○	54.0F
△	73.0F
◻	76.0F

NOTE:

- 1-FULL UP COLLECTIVE LIFT STICK EXCEPT DURING HOVERING FLIGHT.
- 2-FLIGHT TEST DATA FOR NEAR FULL CONTROL INPUTS EXTRAPOLATED LINEARLY TO FULL CONTROL INPUT.



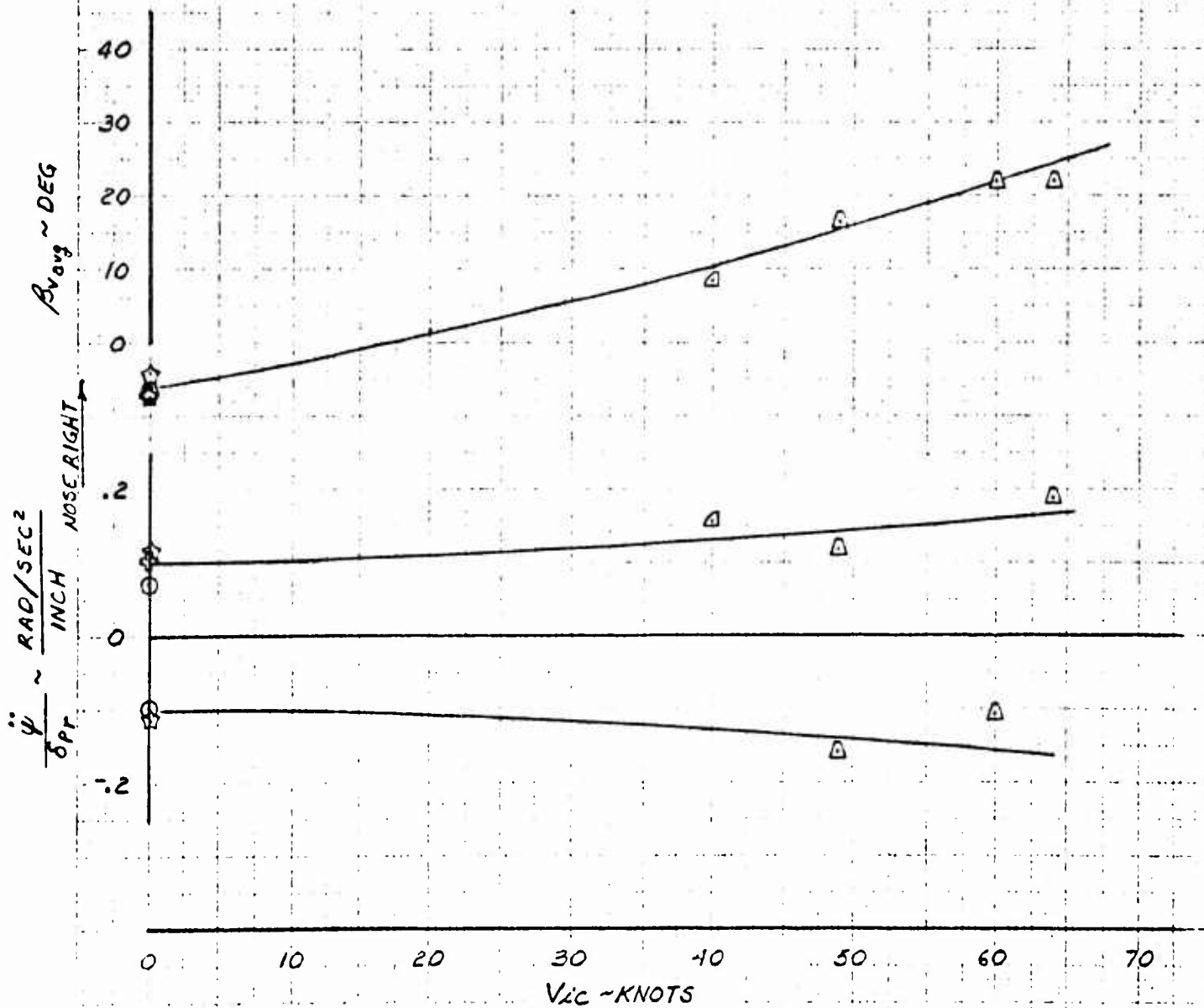
5-5-65 DJS

Figure 6.37 Fan Mode Directional Control Power vs Indicated Airspeed

SYM	TEST NO.
☆	16.OF
◇	23.OF
○	54.OF
△	73.OF
◻	76.OF

NOTE.

- 1- FULL UP COLLECTIVE LIFT STICK EXCEPT DURING HOVERING FLIGHT.
- 2- BASED UPON CONTROL INPUT FROM NEUTRAL RUDDER POSITION OR TOTAL MAXIMUM INPUT.



5-5-65 DJS

Figure 6.38 Fan Mode Directional Control Power vs Indicated Airspeed

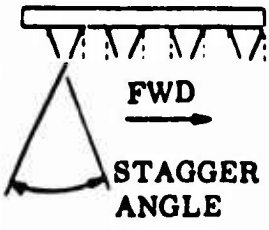
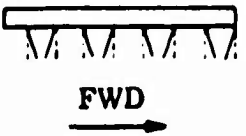
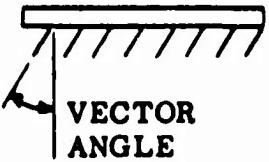
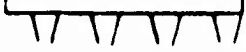
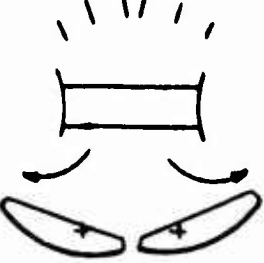
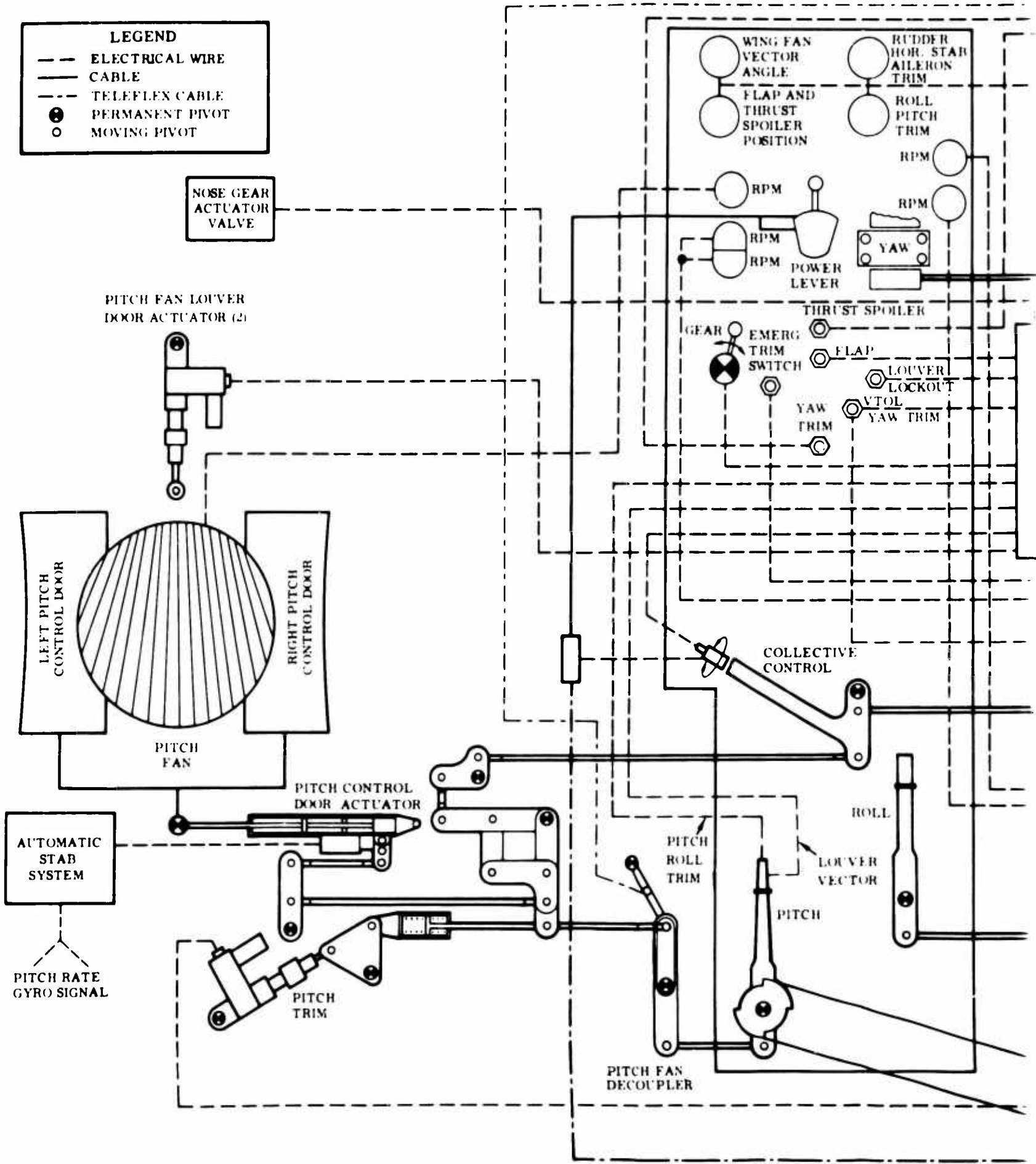
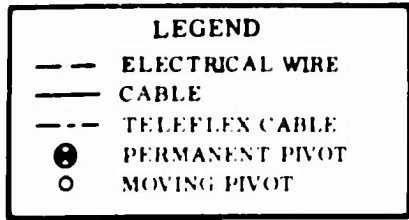
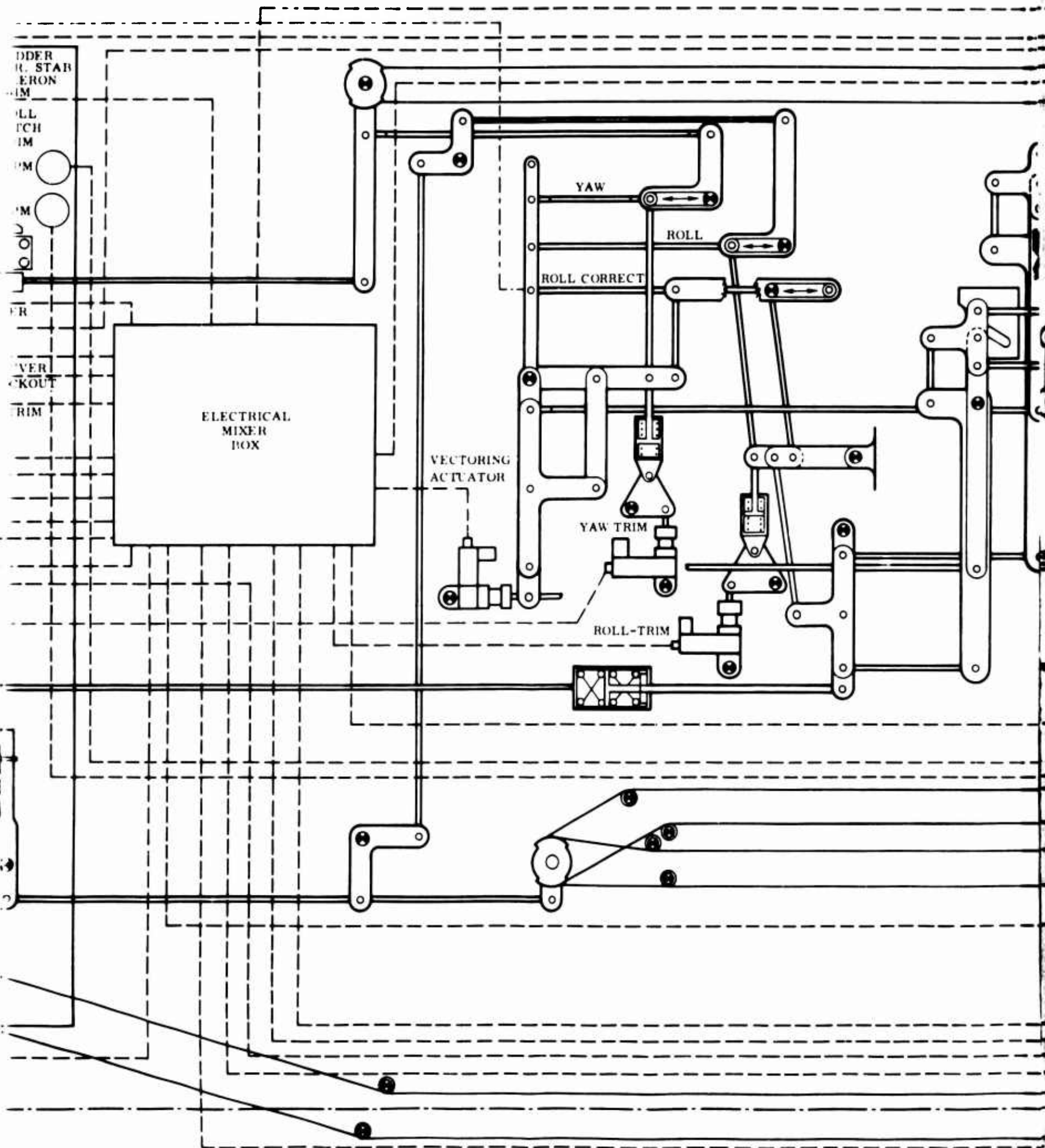
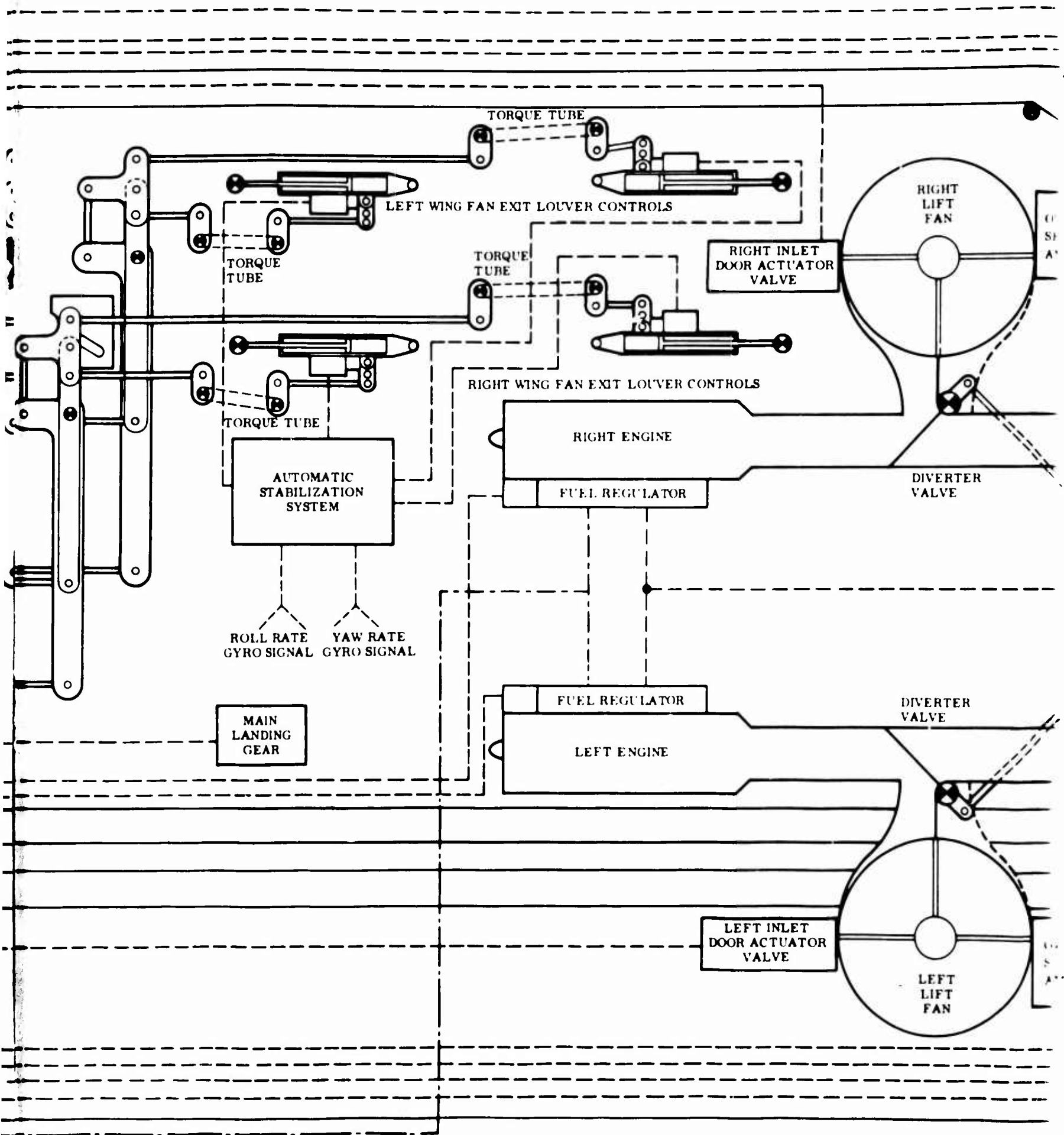
RIGHT FAN	LEFT FAN	NOSE FAN	FUNCTION
 <p>FWD STAGGER ANGLE</p>	 <p>FWD</p>		LIFT - COLLECTIVE STAGGER
 <p>VECTOR ANGLE</p>			ACCELERATION CONTROL - COLLECTIVE VECTOR
			DIRECTIONAL TRIM & CONTROL - DIFFERENTIAL VECTORING
			LATERAL TRIM AND CONTROL - DIFFERENTIAL STAGGER
			PITCH TRIM AND CONTROL (NOSE UP)
			PITCH TRIM AND CONTROL (NOSE DOWN)

Figure 6.39 VTOL Flight Control System Operation







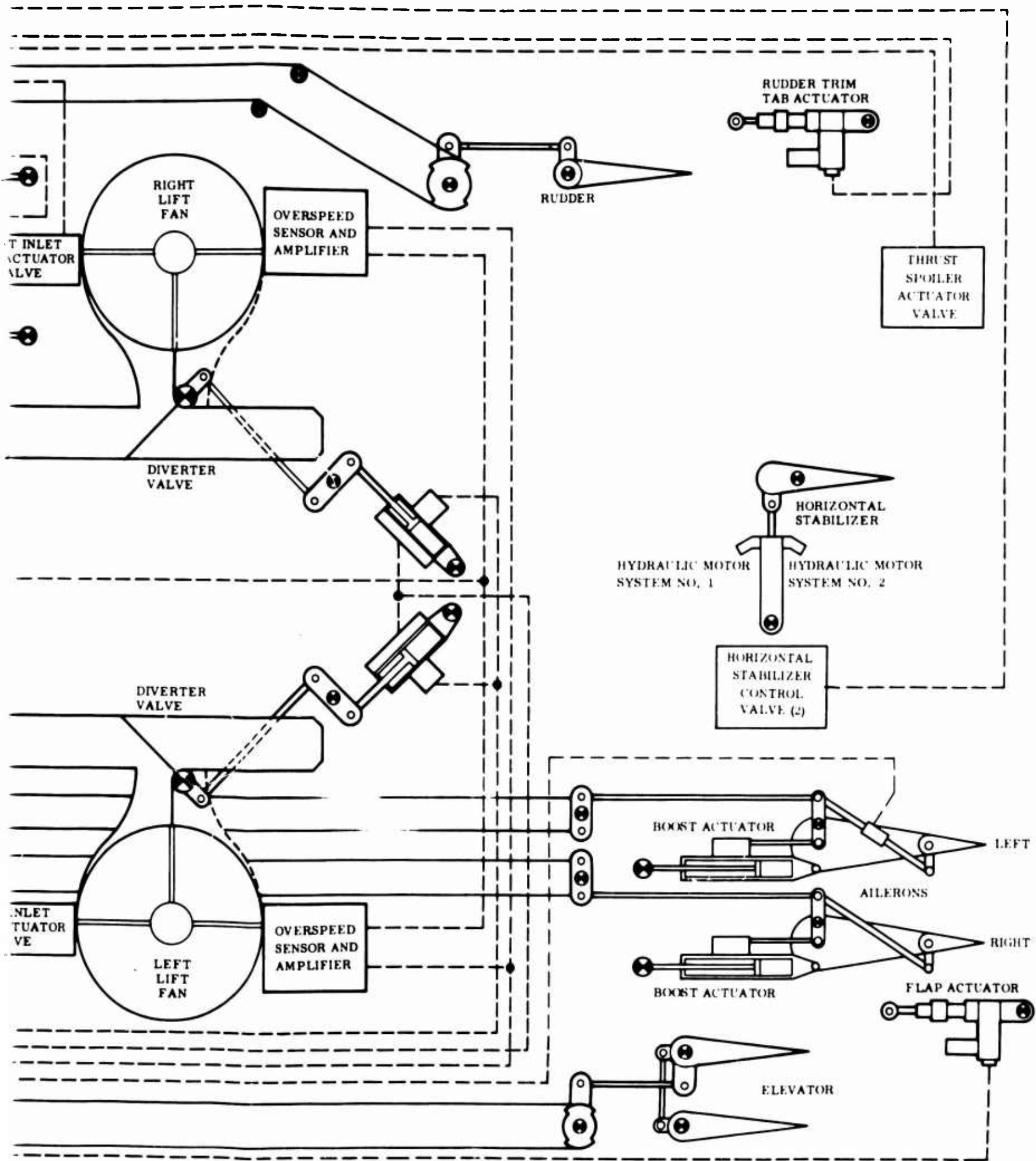


Figure 6.10 Flight Control System Schematic Diagram

A/C No. 62-4506

Run 1-1

Variable Collective Vector
Neutral Stick
Neutral Rudder
Max-Collective

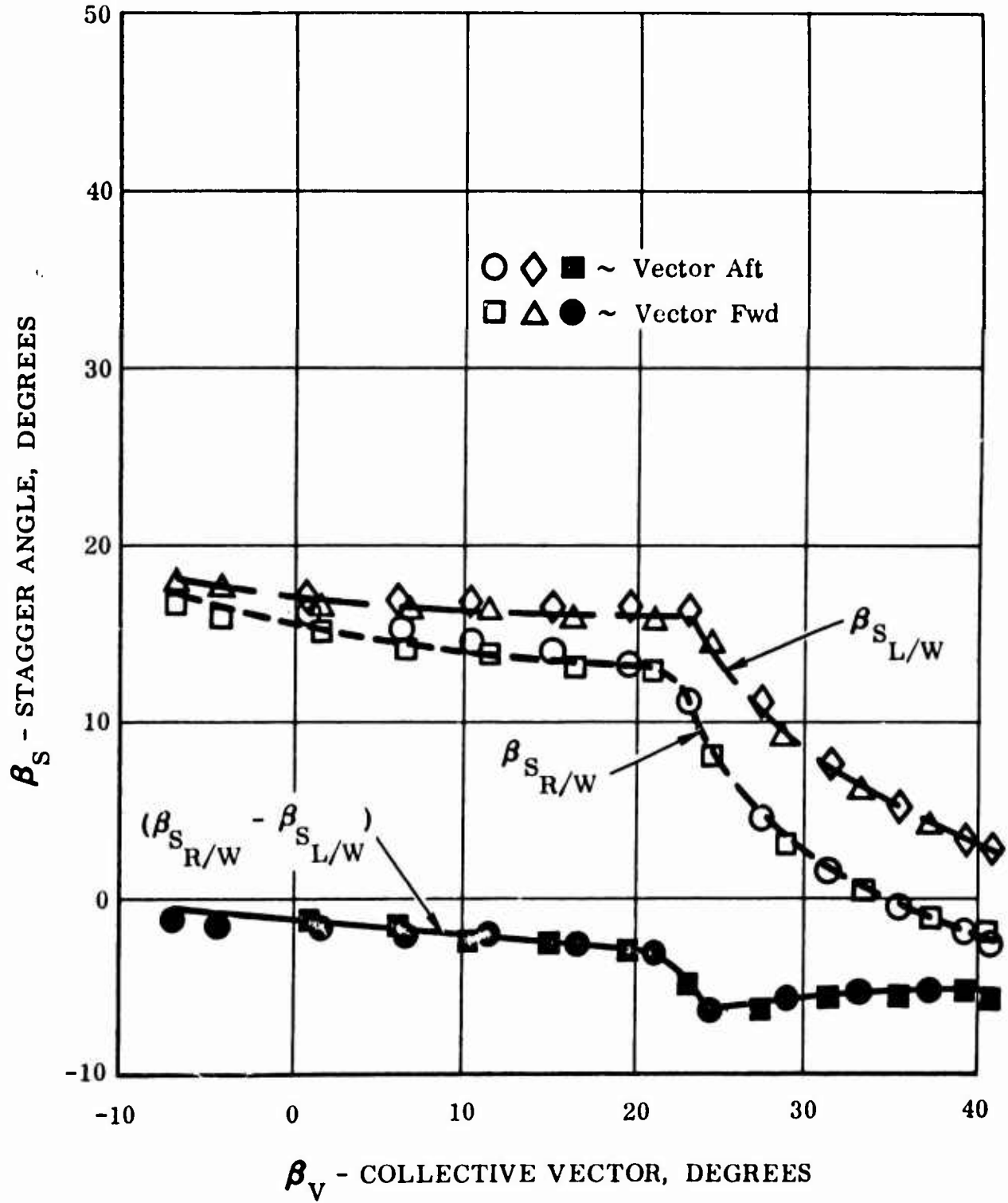


Figure 6.41 Static VTOL Control System Calibration

A/C No. 62-4506

Run 1-10

Variable Collective Vector

Neutral Stick

Neutral Rudder

Mid-Collective

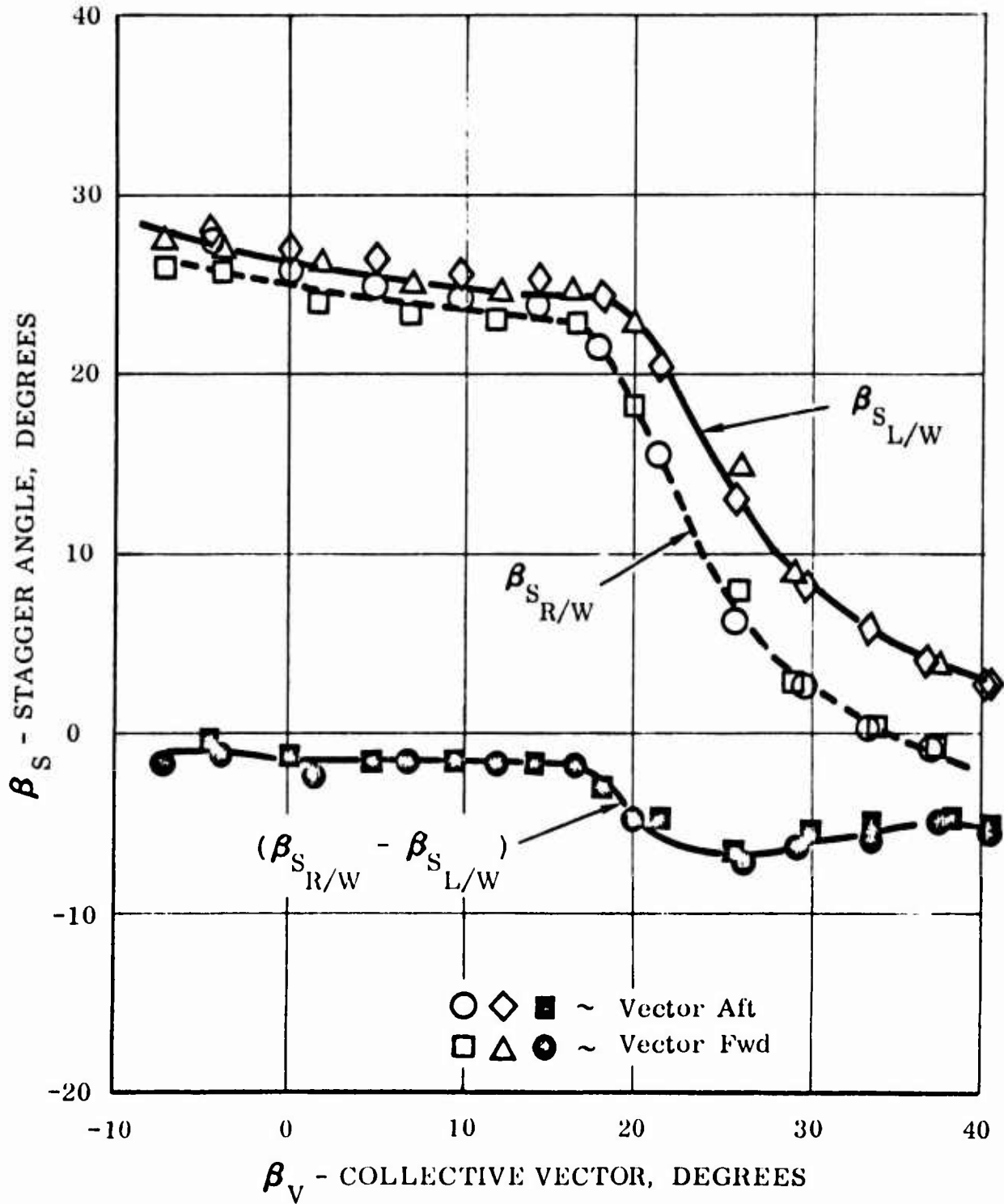


Figure 6.42 Static VTOL Control System Calibration

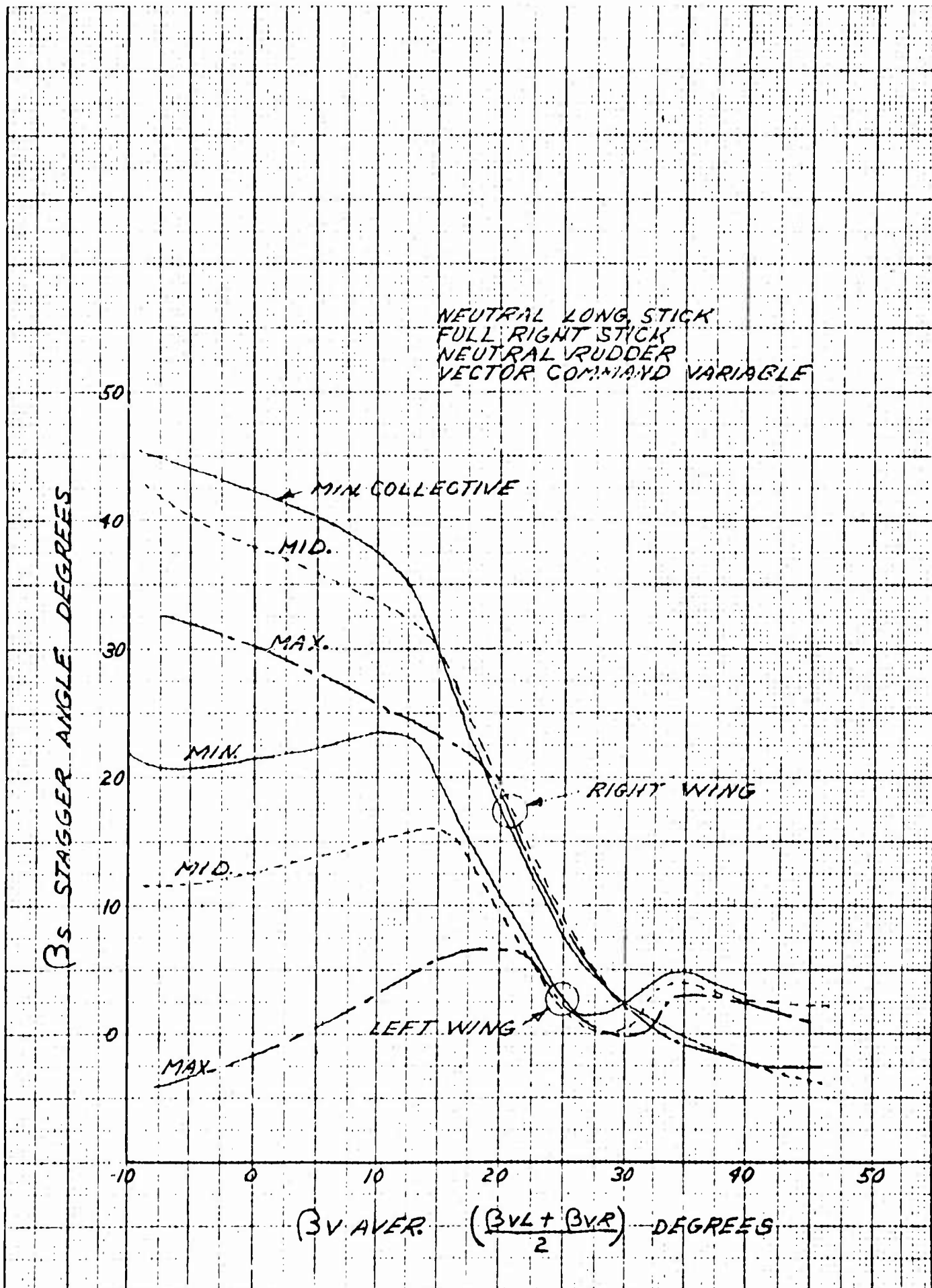


Figure 6.43 Static VTOL Control System Calibration

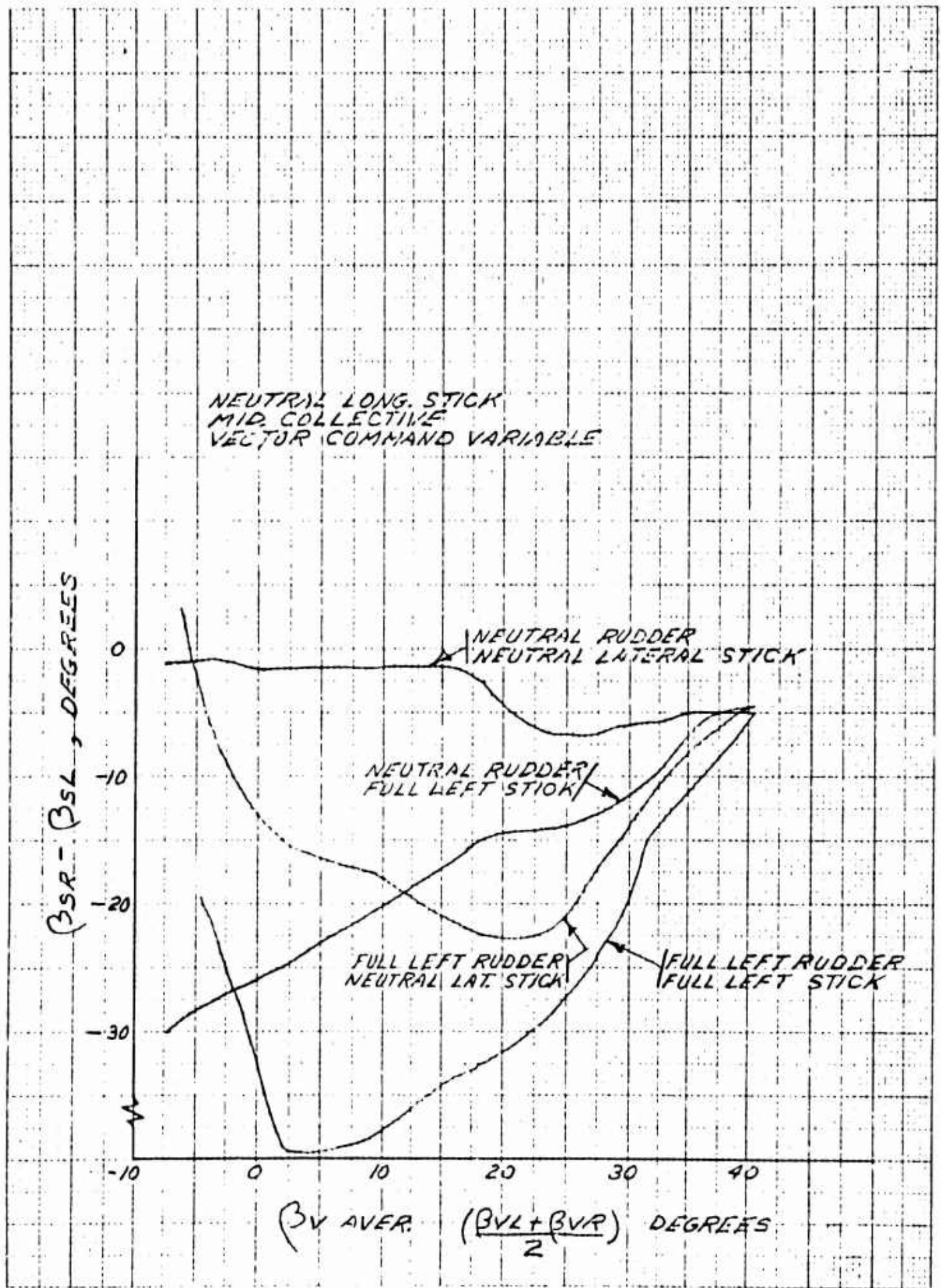


Figure 6.44 Static VTOL Control System Calibration

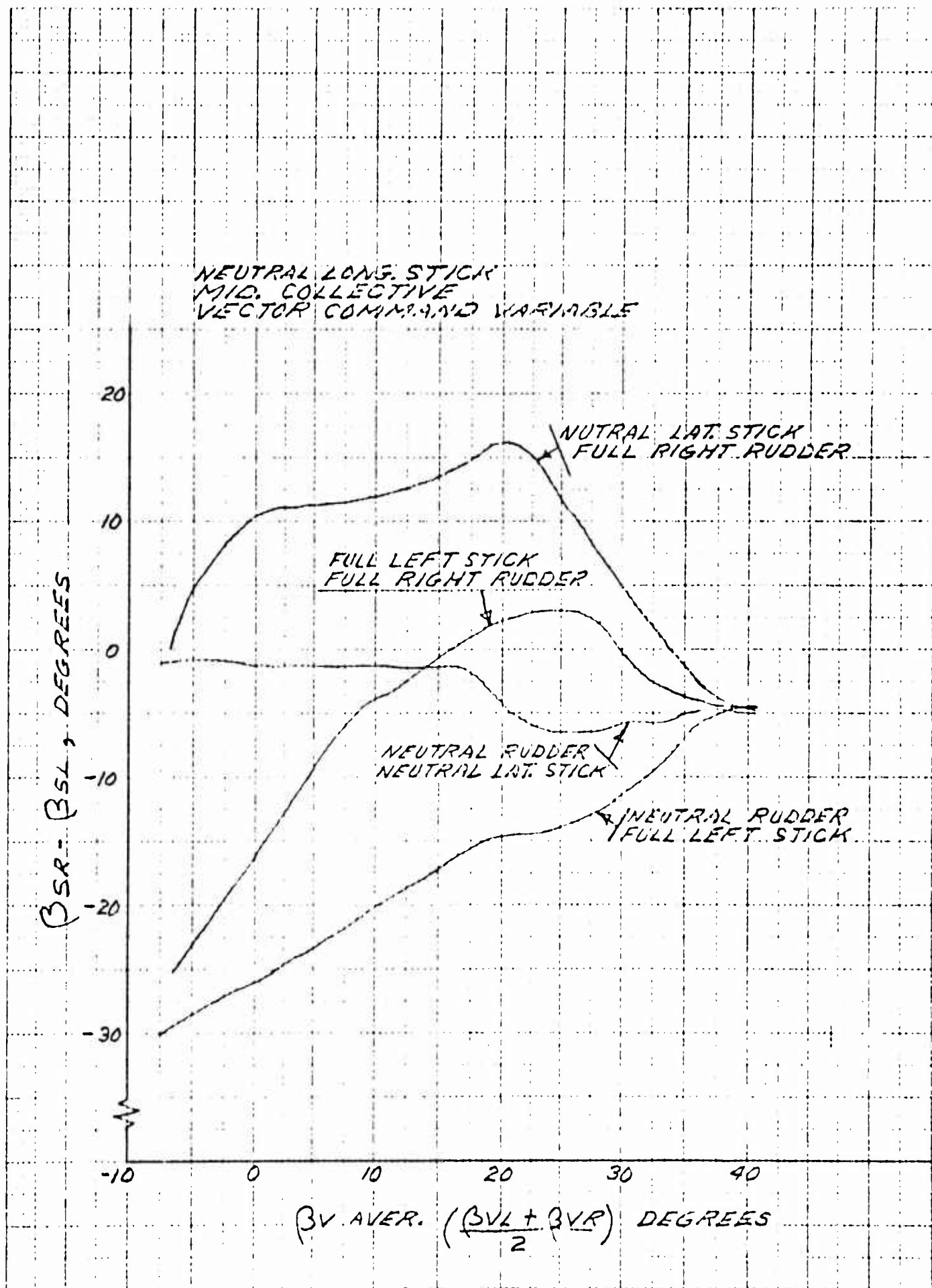


Figure 6.45 Static VTOL Control System Calibration

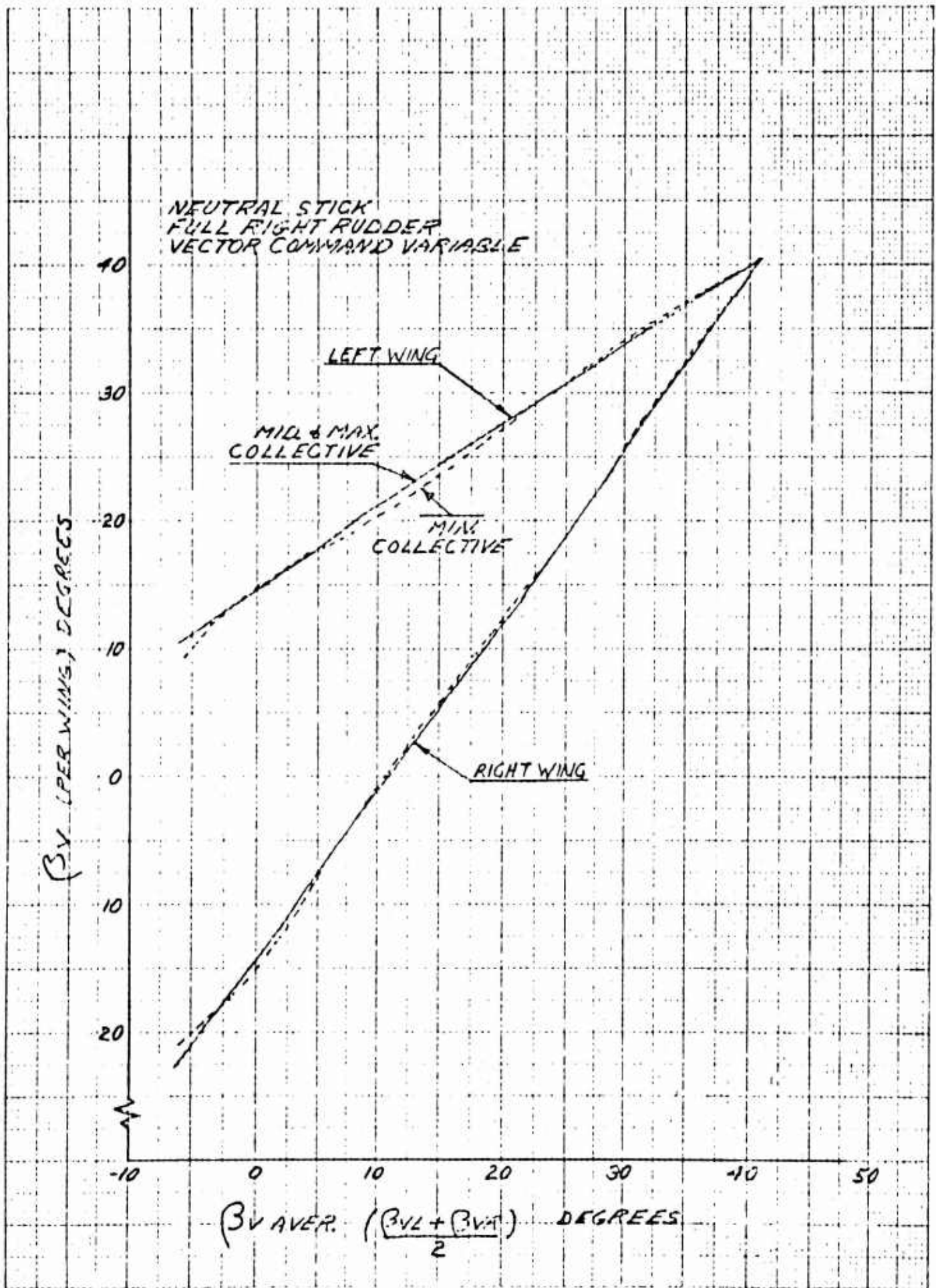


Figure 6.46 Static VTOL Control System Calibration

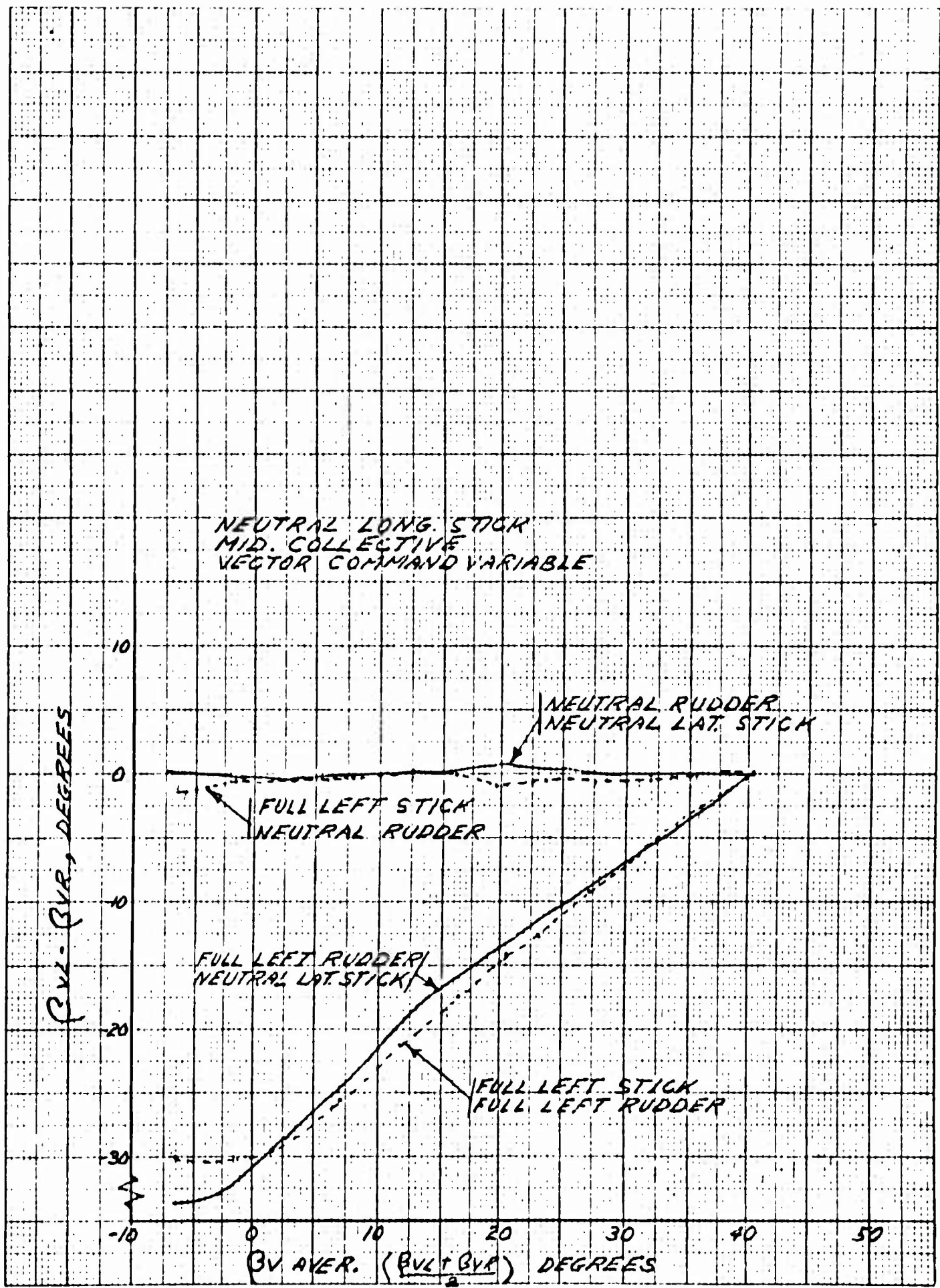


Figure 6.47 Static VTOL Control System Calibration

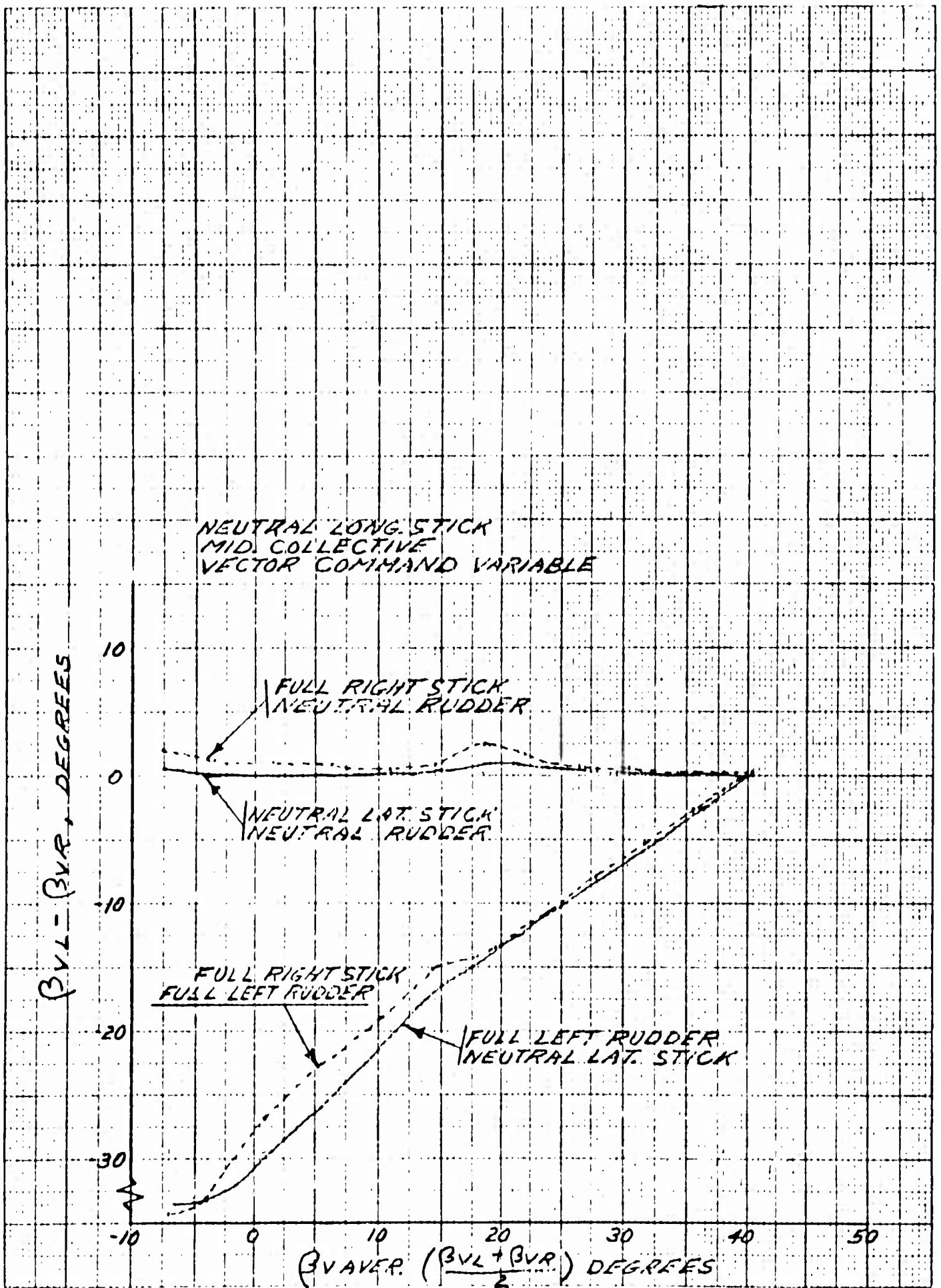


Figure 6.48 Static VTOL Control System Calibration

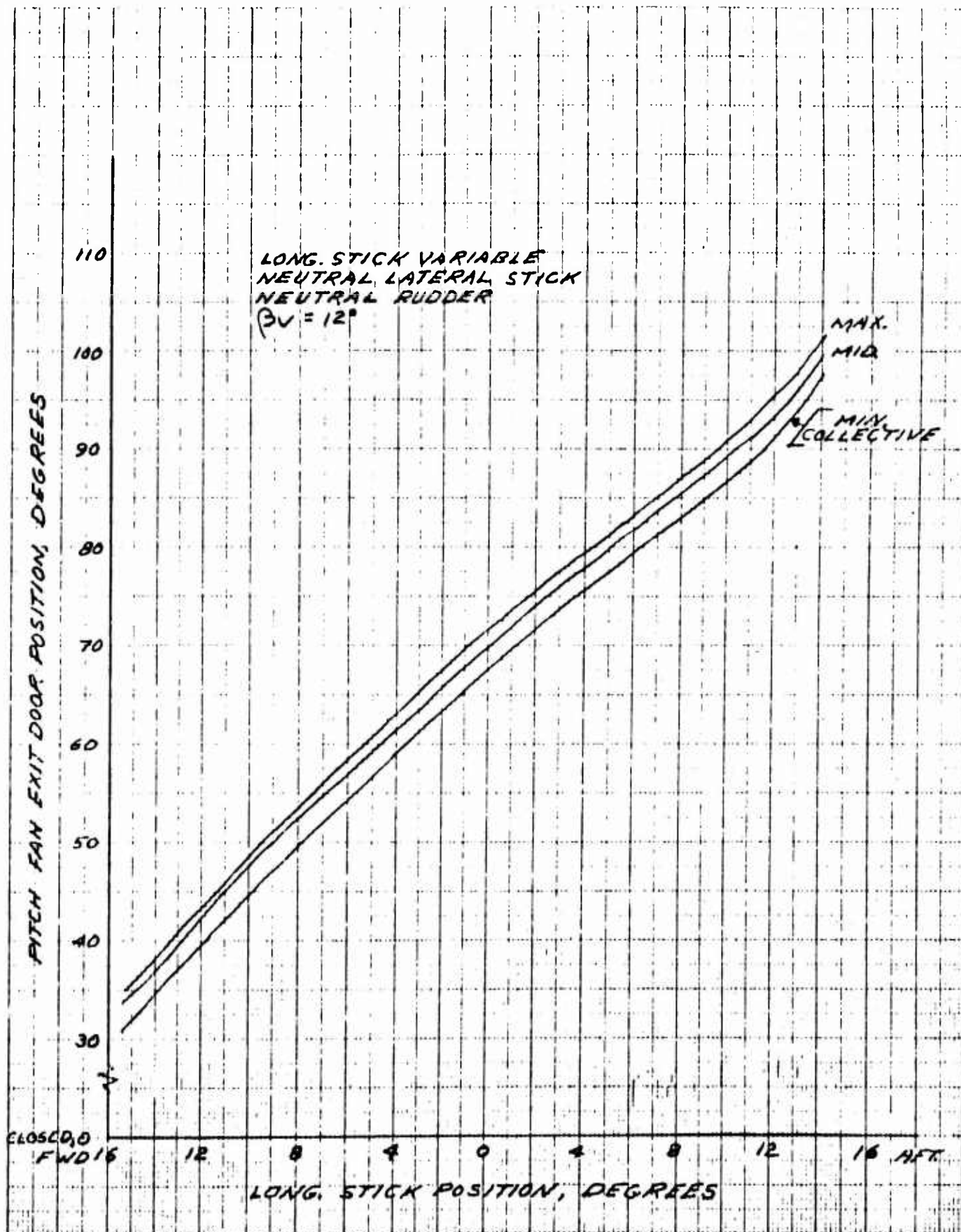


Figure 6.49 Static VTOL Control System Calibration

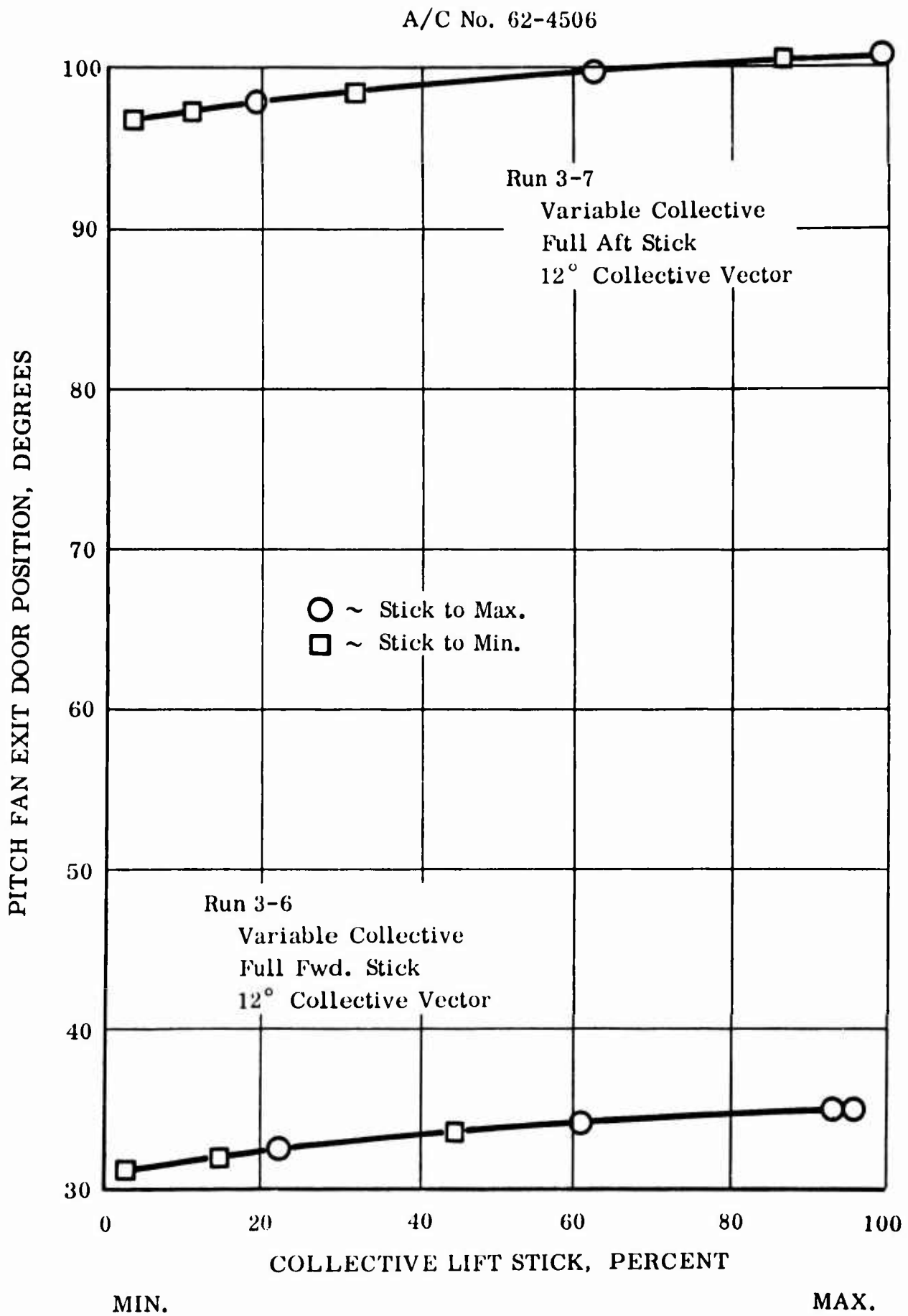


Figure 6.50 Static VTOL Control System Calibration

A/C No. 62-4506

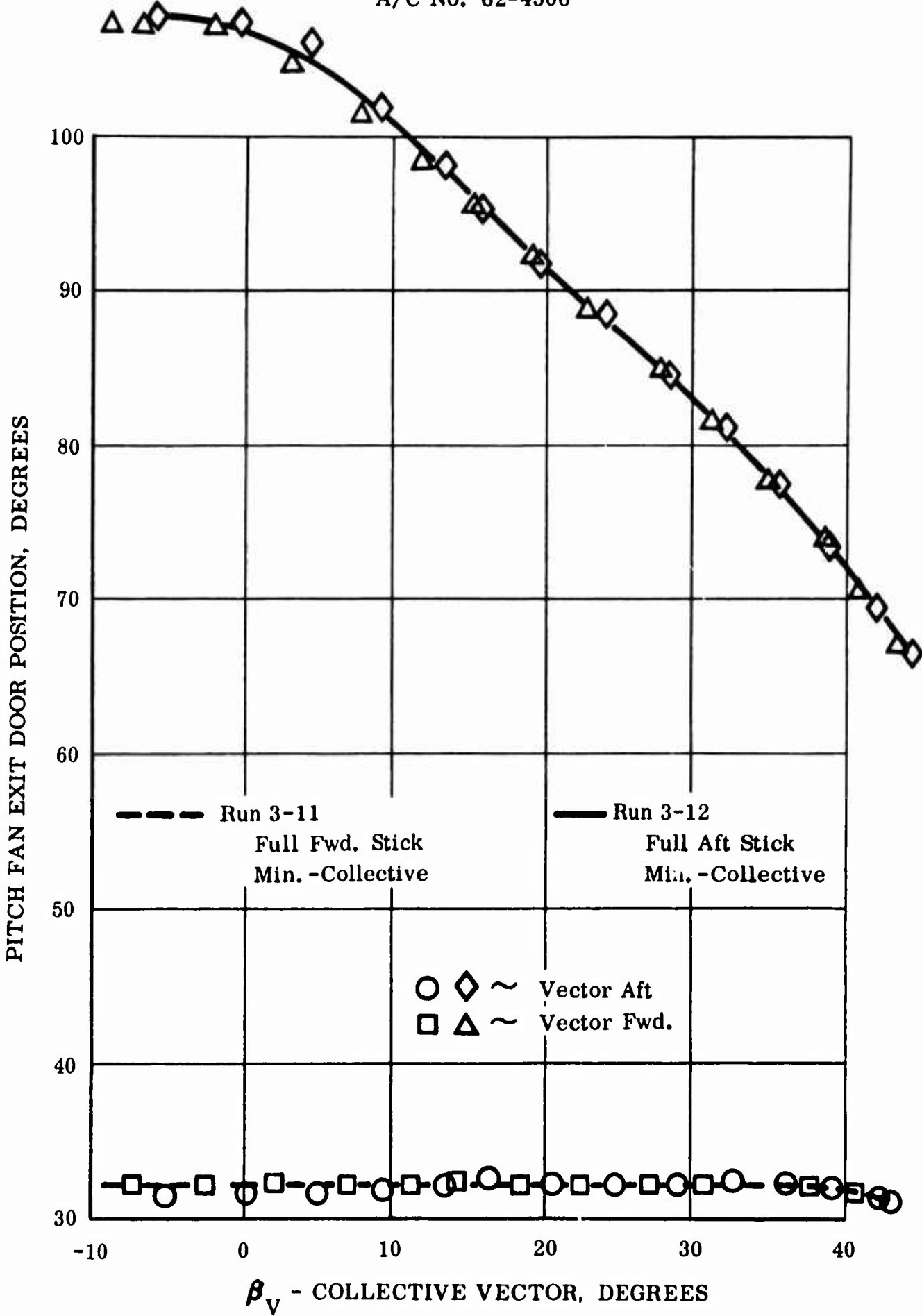


Figure 6.51 Static VTOL Control System Calibration

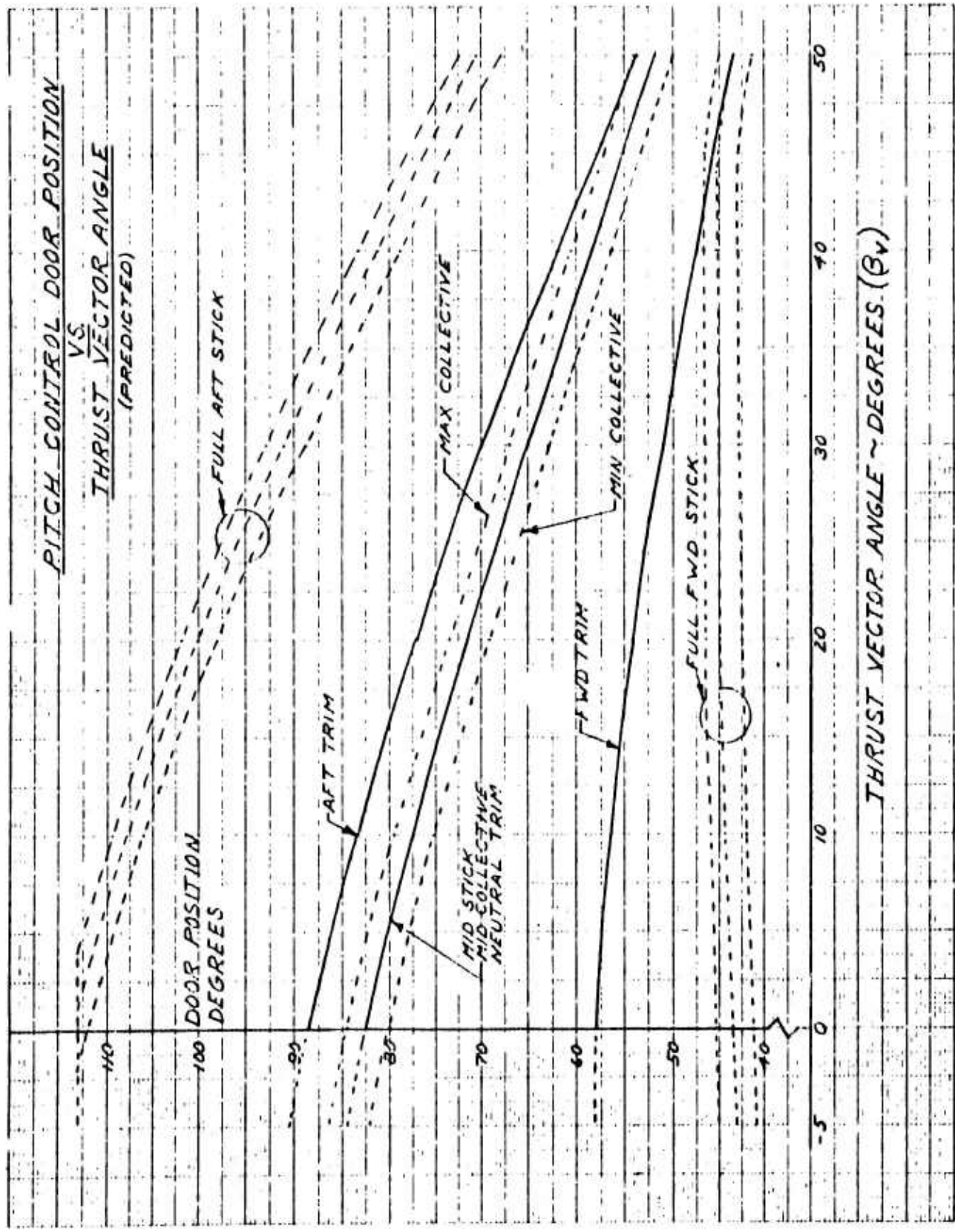


Figure 6.52 Pitch Control Door Position vs Thrust Vector Range

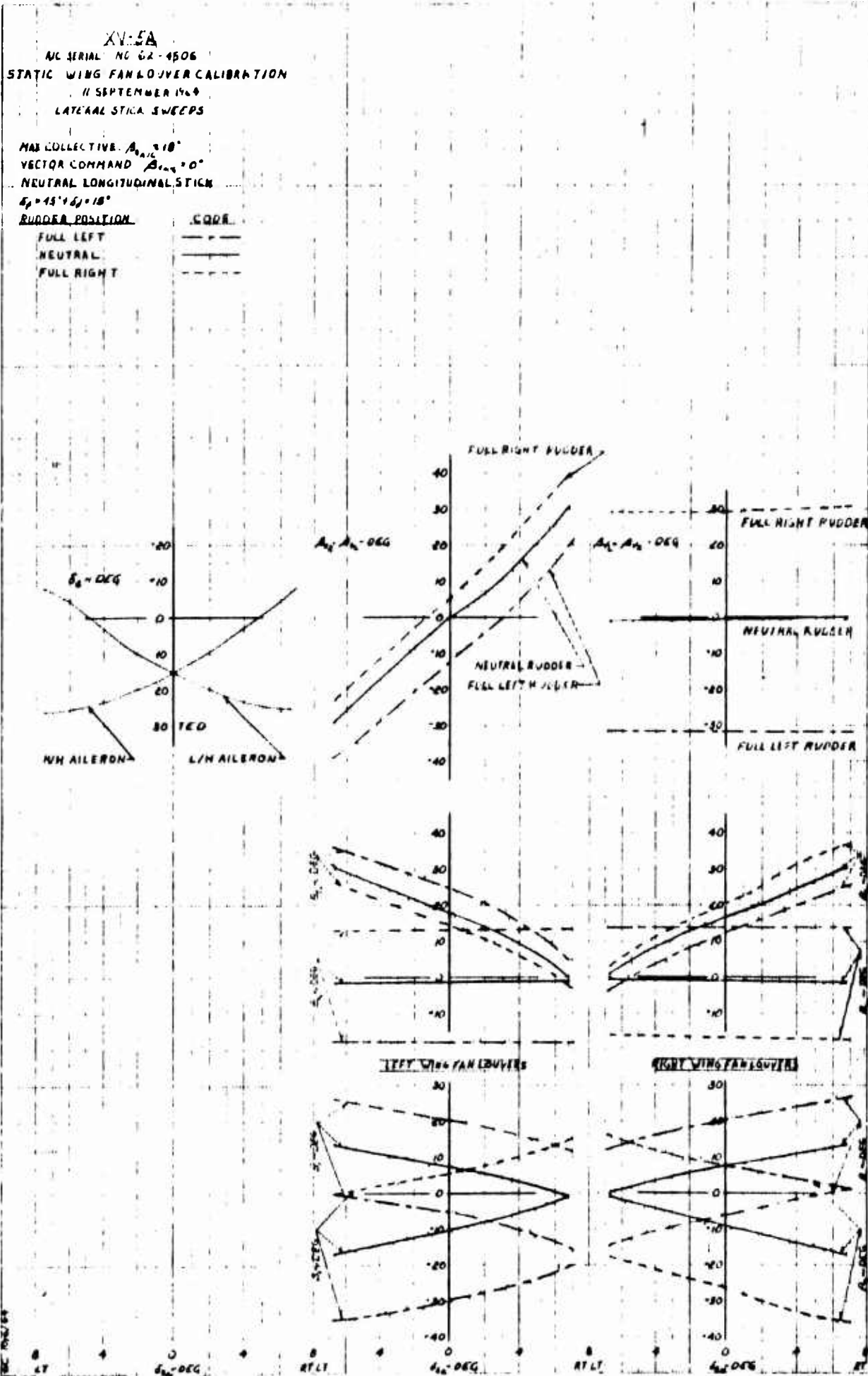


Figure 6.53 Static Wing Fan Louver Calibration - Lateral Stick Sweeps

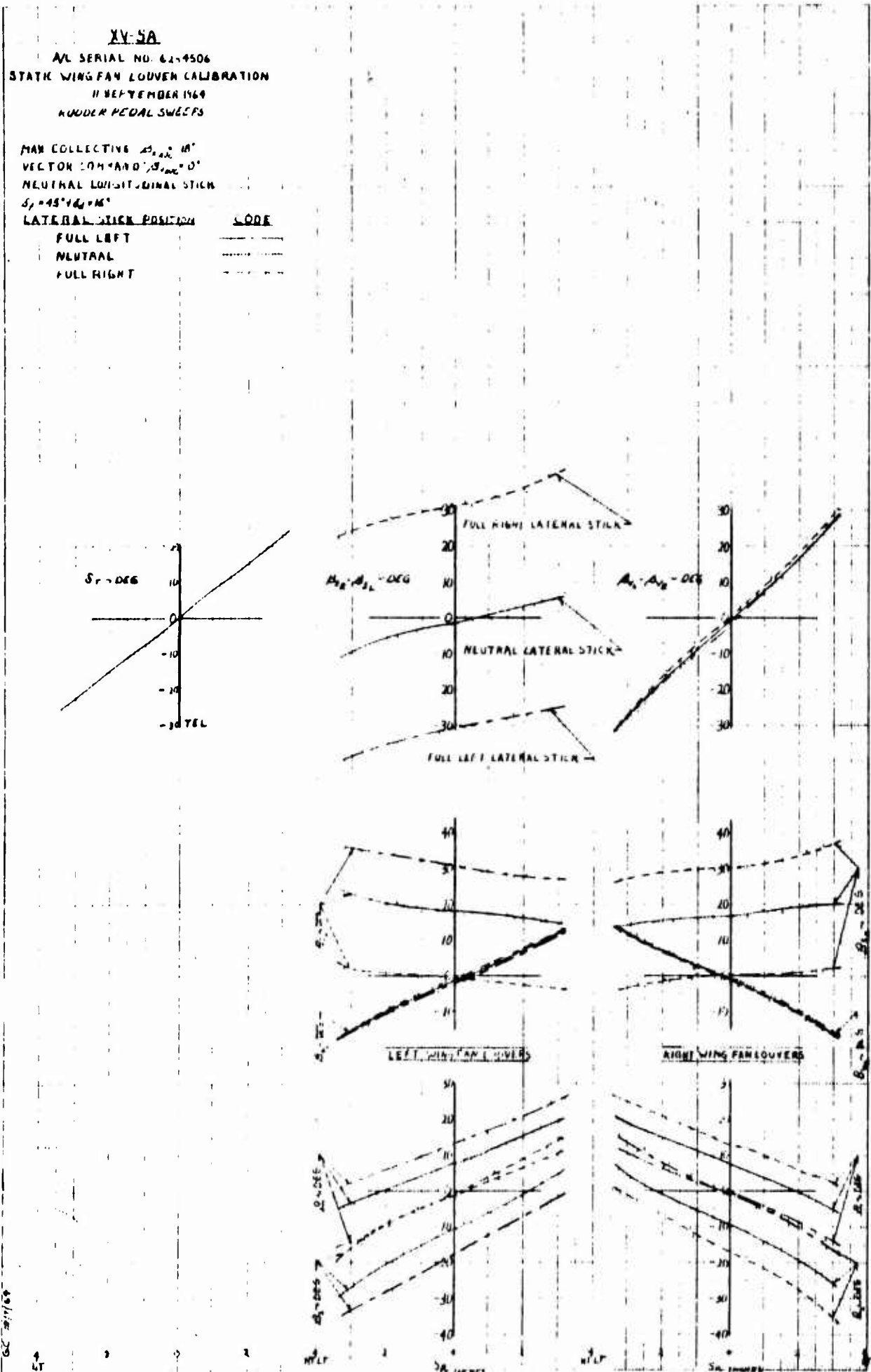


Figure 6. 54 Static Wing Fan Louver Calibration - Rudder Pedal Sweeps

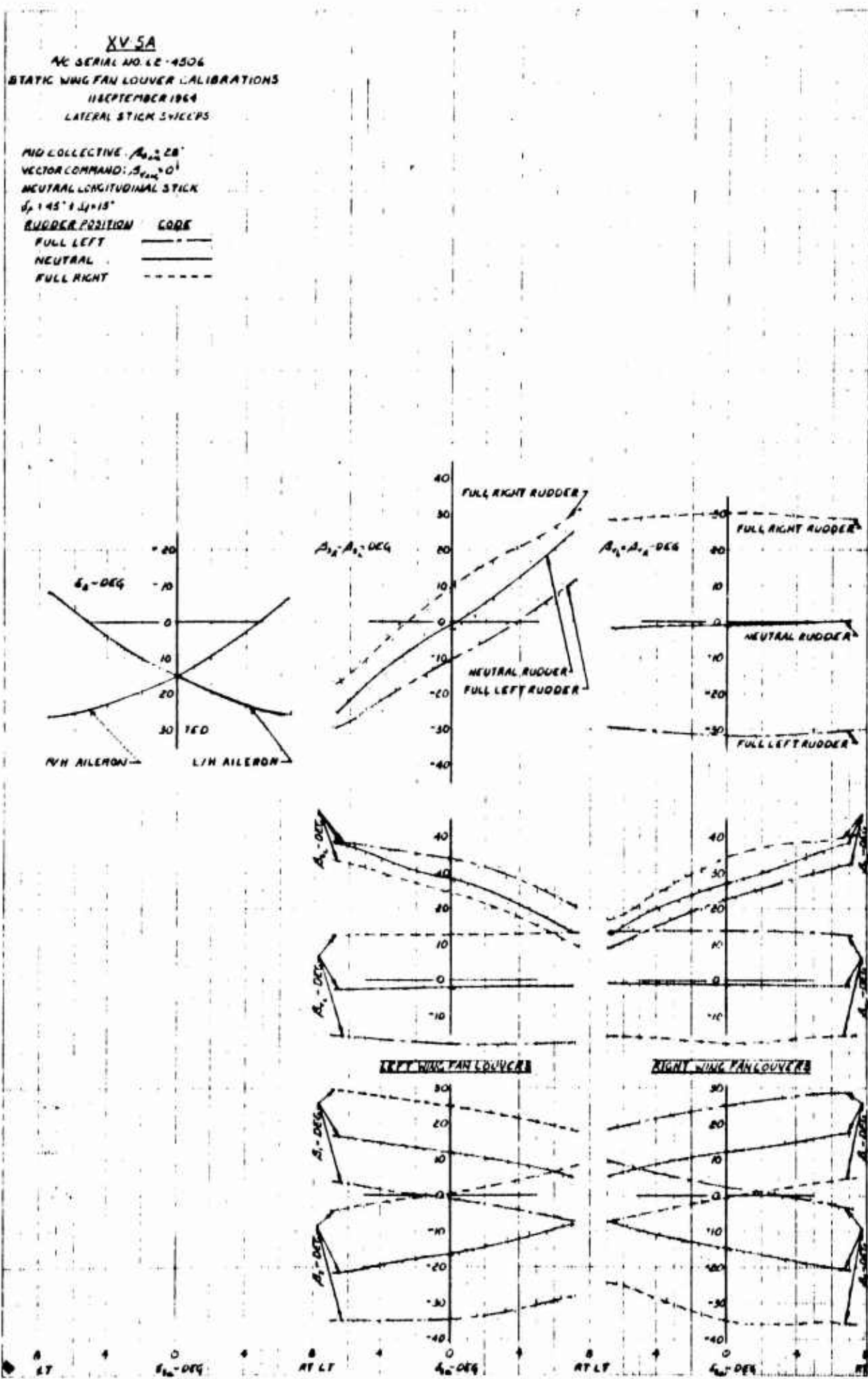


Figure 6.55 Static Wing Fan Louver Calibration - Lateral Stick Sweeps

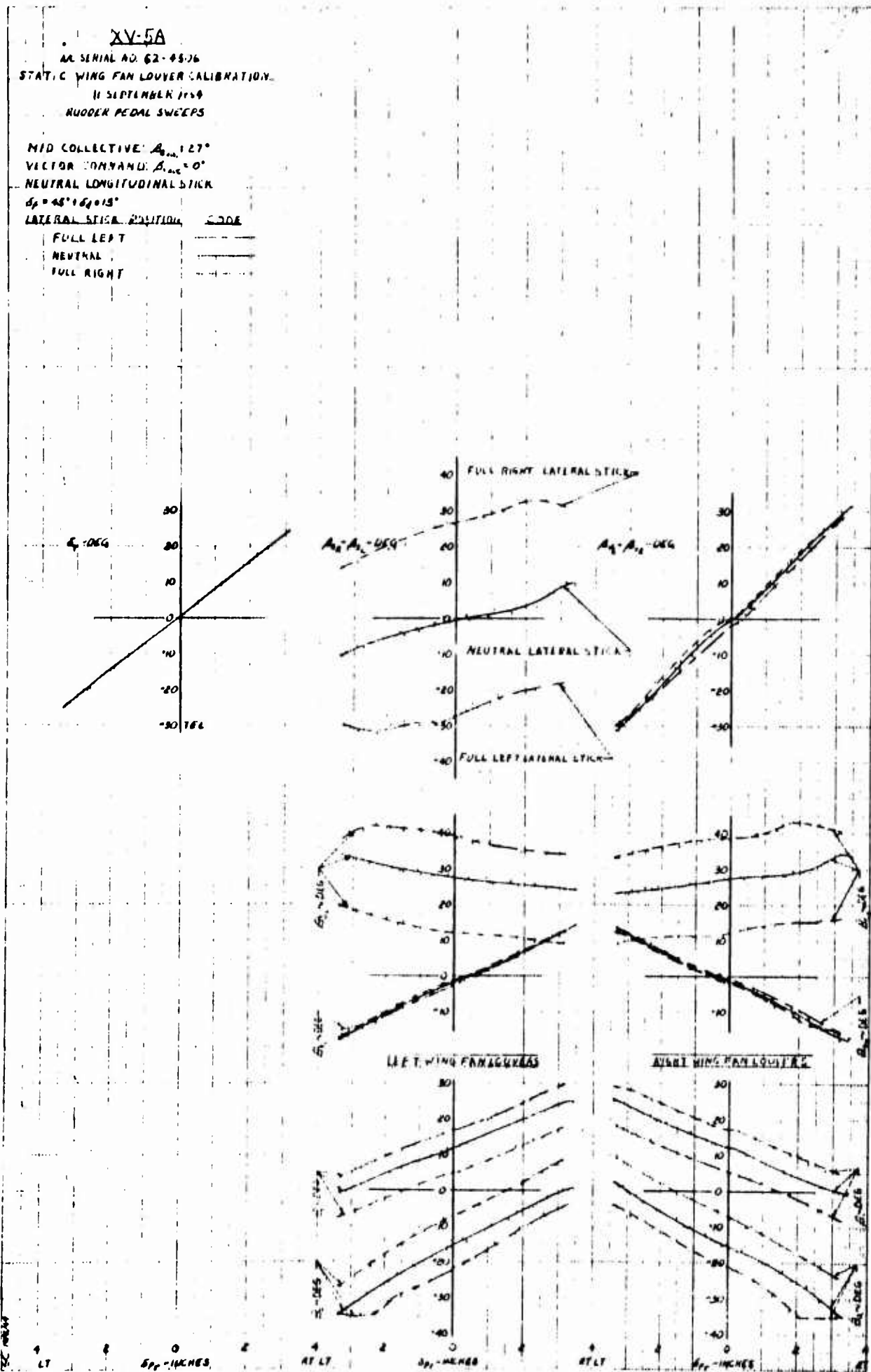


Figure 6.56 Static Wing Fan Louver Calibration - Rudder Pedal Sweeps

XV-5A

AIC SERIAL NO 62-4506
 STATIC WING FAN LOUVER CALIBRATION
 SEPTEMBER 11 1969
 LATERAL STICK SWEEPS

MIN COLLECTIVE $A_{32} = 25'$
 VECTOR COMMAND $A_{31} = 0'$
 NEUTRAL LONGITUDINAL STICK
 $S_2 = 45^\circ / 10^\circ = 15'$

RUDDER POSITION
 FULL RIGHT
 NEUTRAL
 FULL LEFT

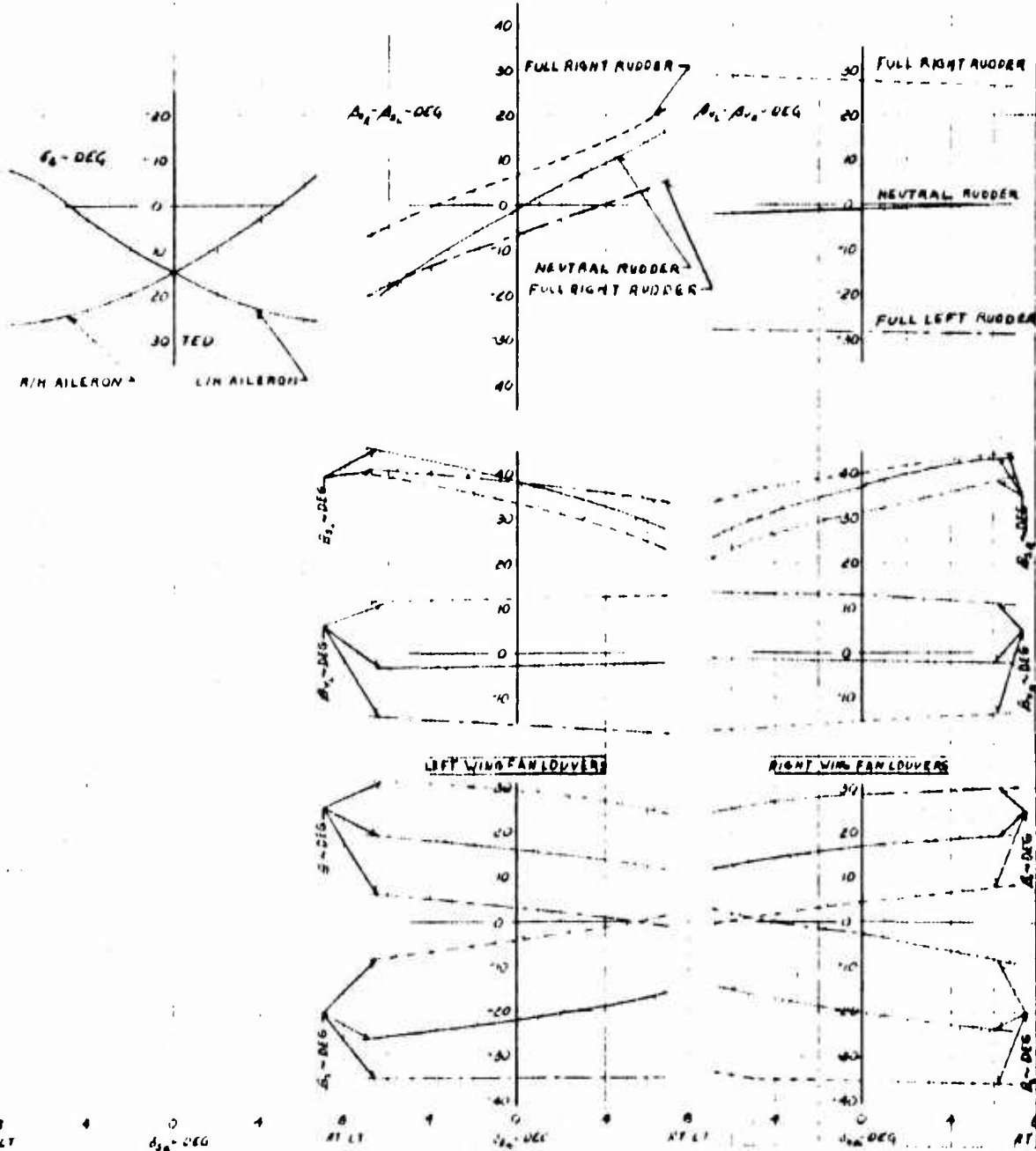


Figure 6.57 Static Wing Fan Louver Calibration - Lateral Stick Sweeps

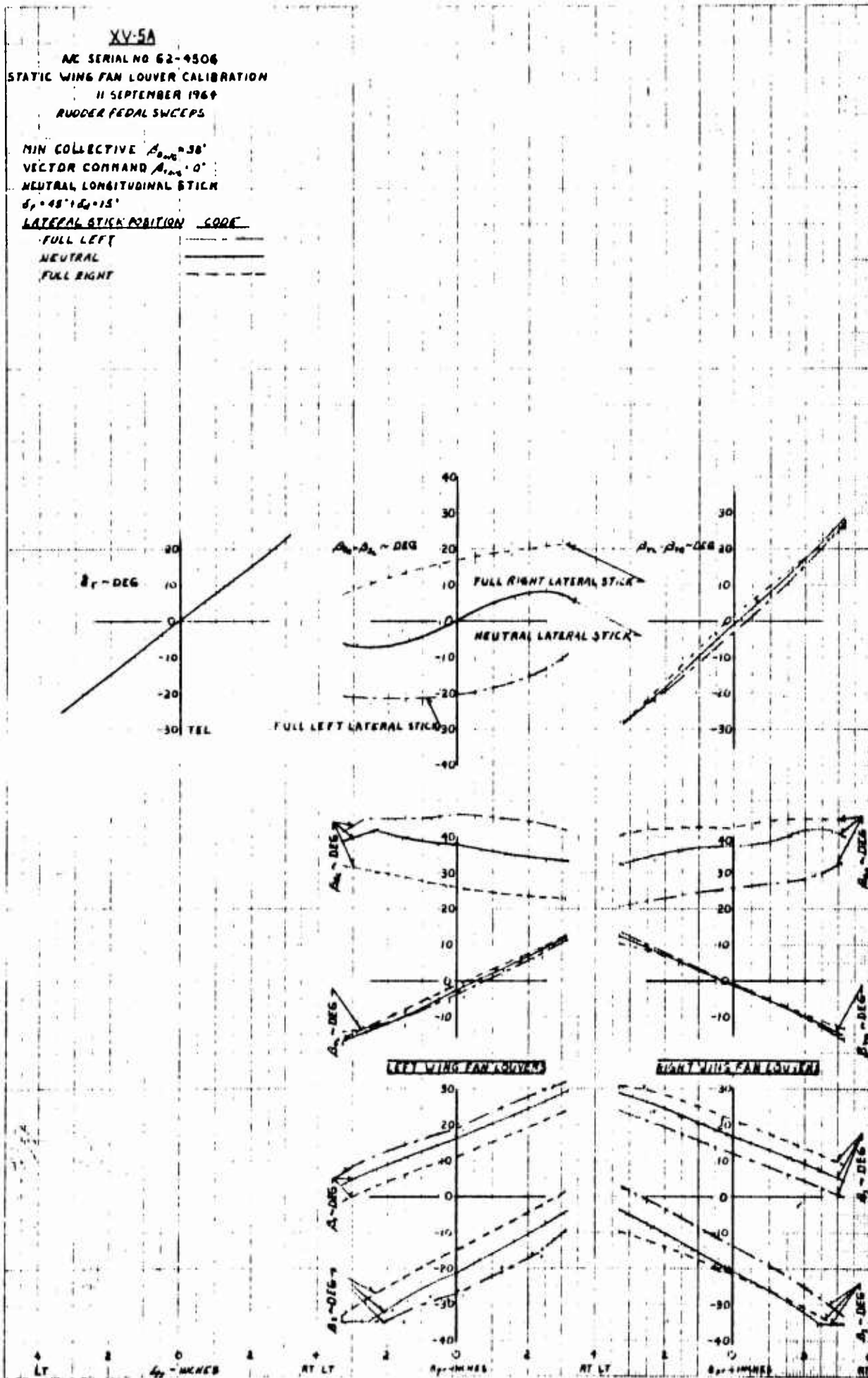


Figure 6.58 Static Wing Fan Louver Calibration - Rudder Pedal Sweeps

XV-5A

A/C SERIAL NO 62-4506

STATIC WING FAN LOUVER CALIBRATION

11 SEPTEMBER 1964

LATERAL STICK SWEEPS

MID COLLECTIVE $A_{y, \text{mid}} = 25^\circ$

VECTOR COMMAND $A_{y, \text{vec}} = 11^\circ$

NEUTRAL LONGITUDINAL STICK

$S_p = 46^\circ 18' 15''$

RUDDER POSITION	CODE
FULL RIGHT	---
NEUTRAL	—
FULL LEFT	---

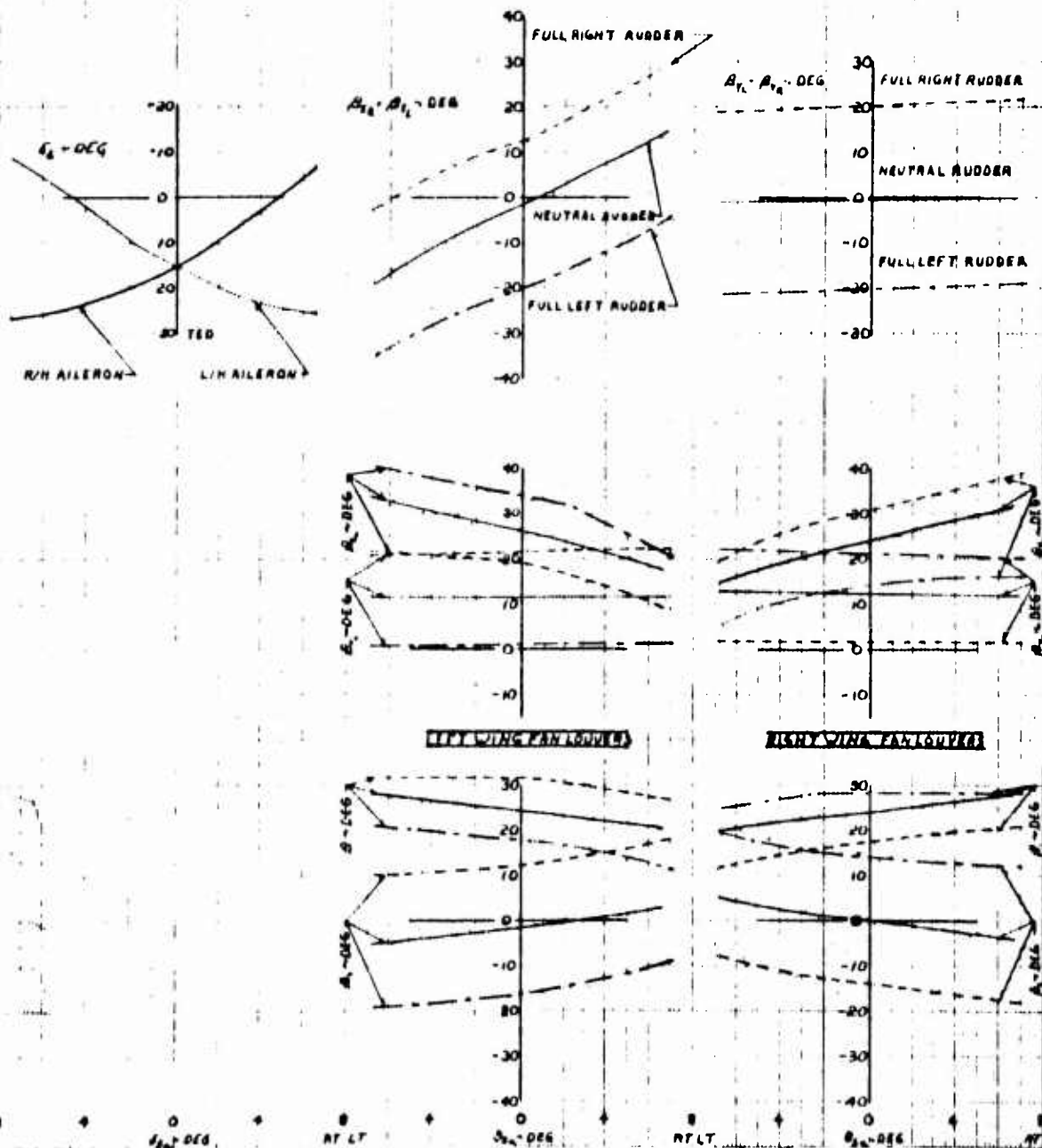


Figure 6.59 Static Wing Fan Louver Calibration - Lateral Stick Sweeps

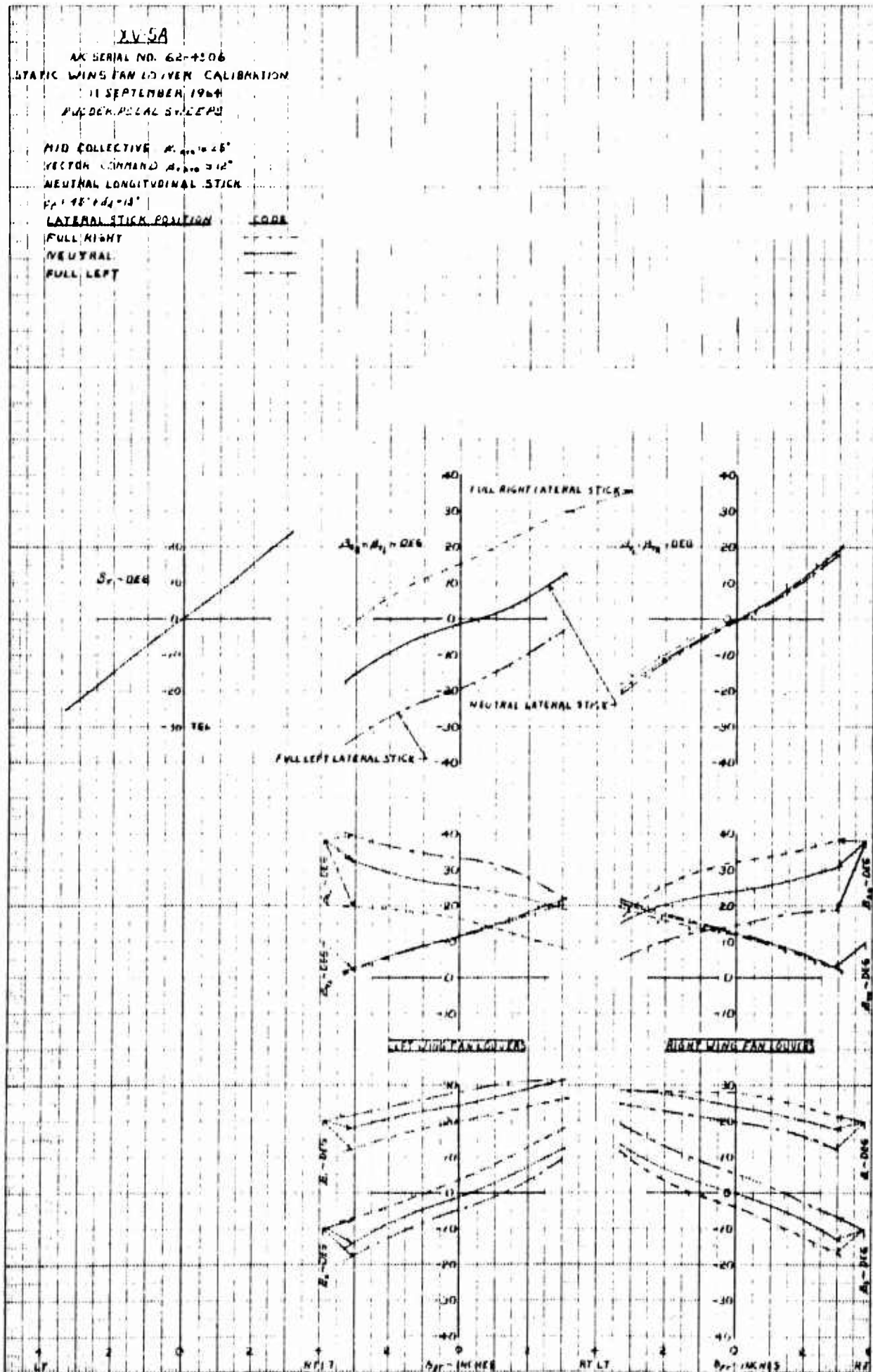


Figure 6.60 Static Wing Fan Louver Calibration - Rudder Pedal Sweeps

9 November 1964

A/C SERIAL NO. 62-4506

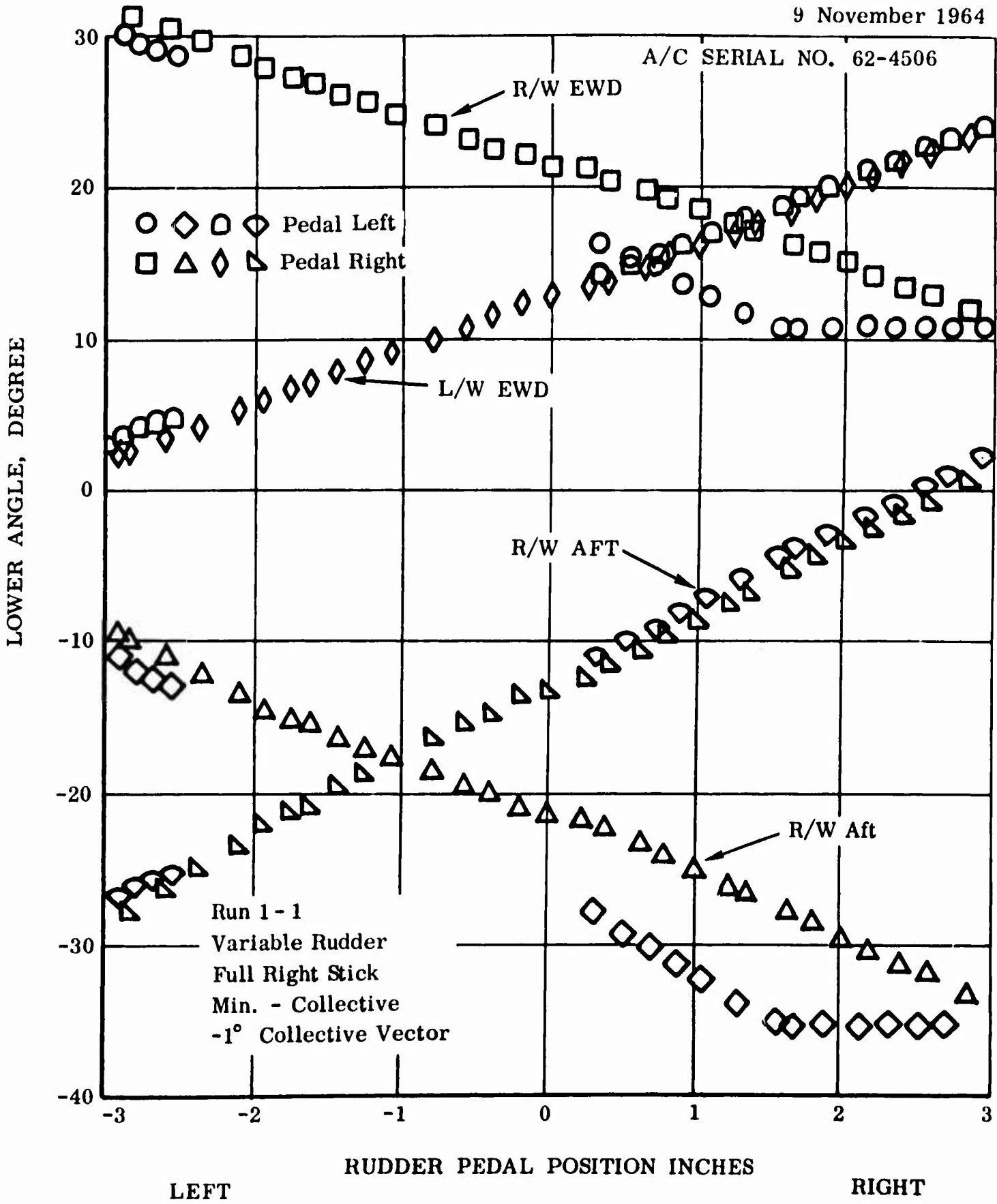
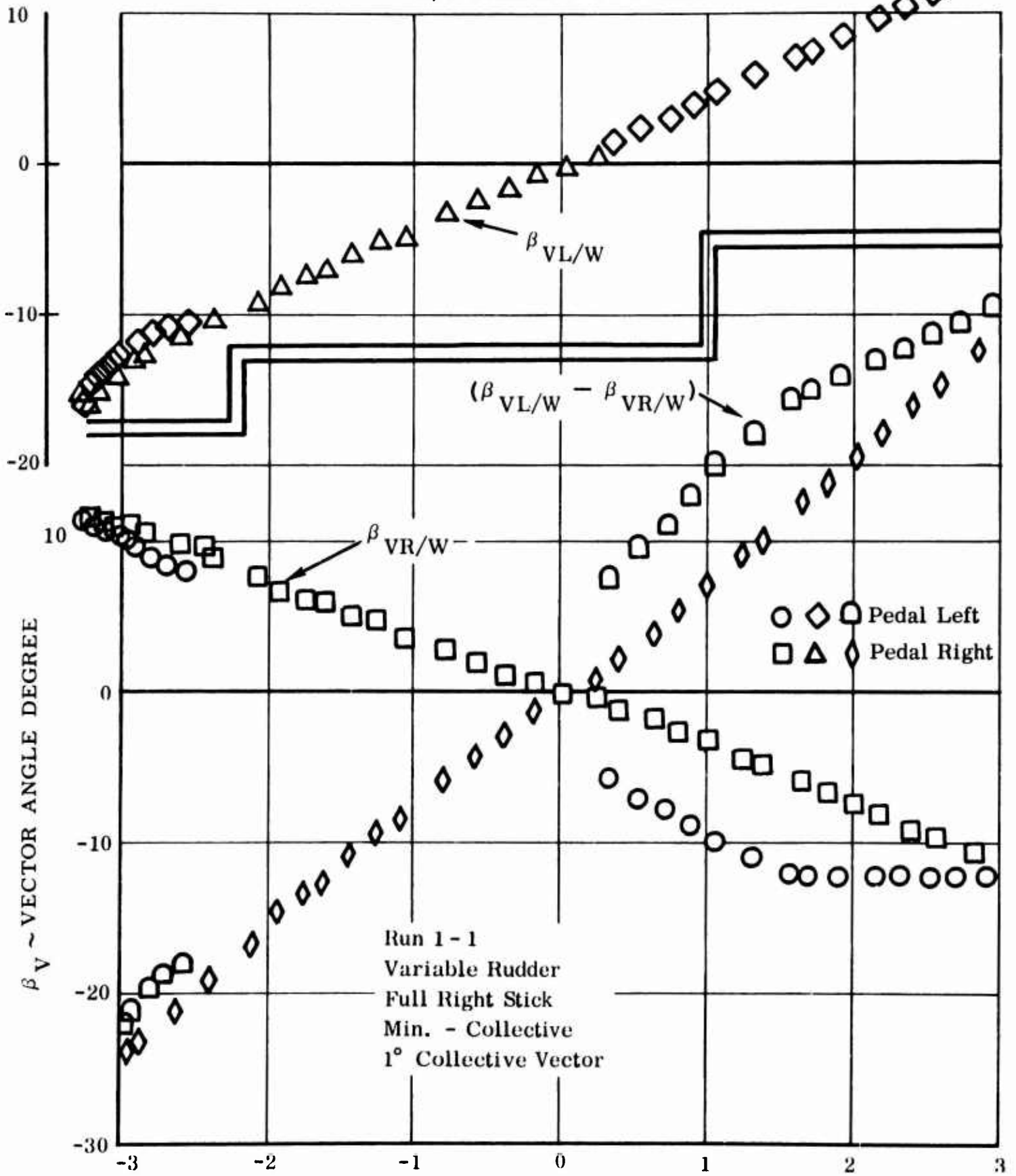


Figure 6.61 Rudder Pedal Position, Inches

9 November 1964

A/C SERIAL NO. 62-4506



LEFT

RIGHT

Figure 6.62 Static VTOL Control System Calibration

A/C SERIAL NO. 62-4506

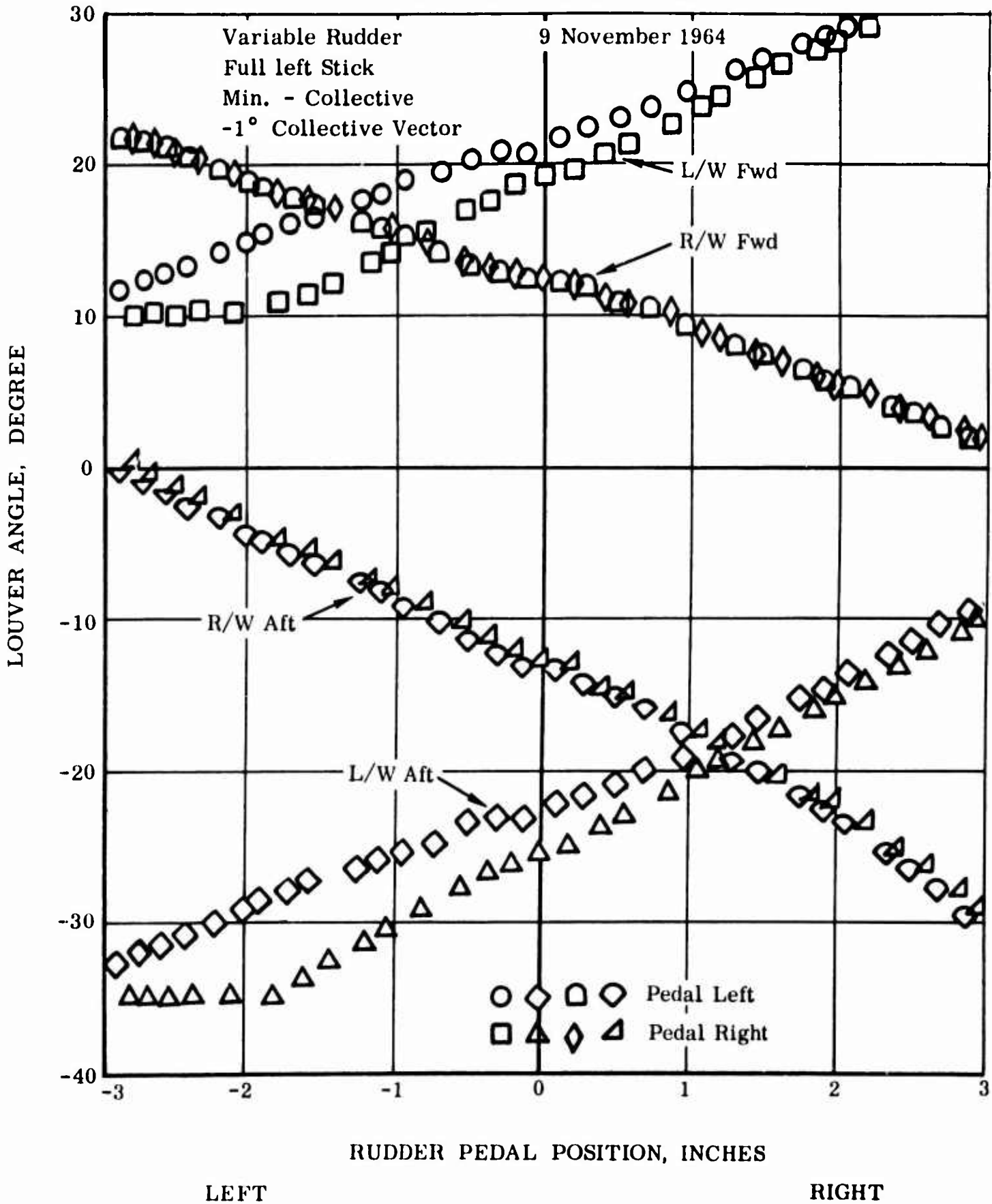


Figure 6.63 Static VTOL Control System Calibration

9 November 1964

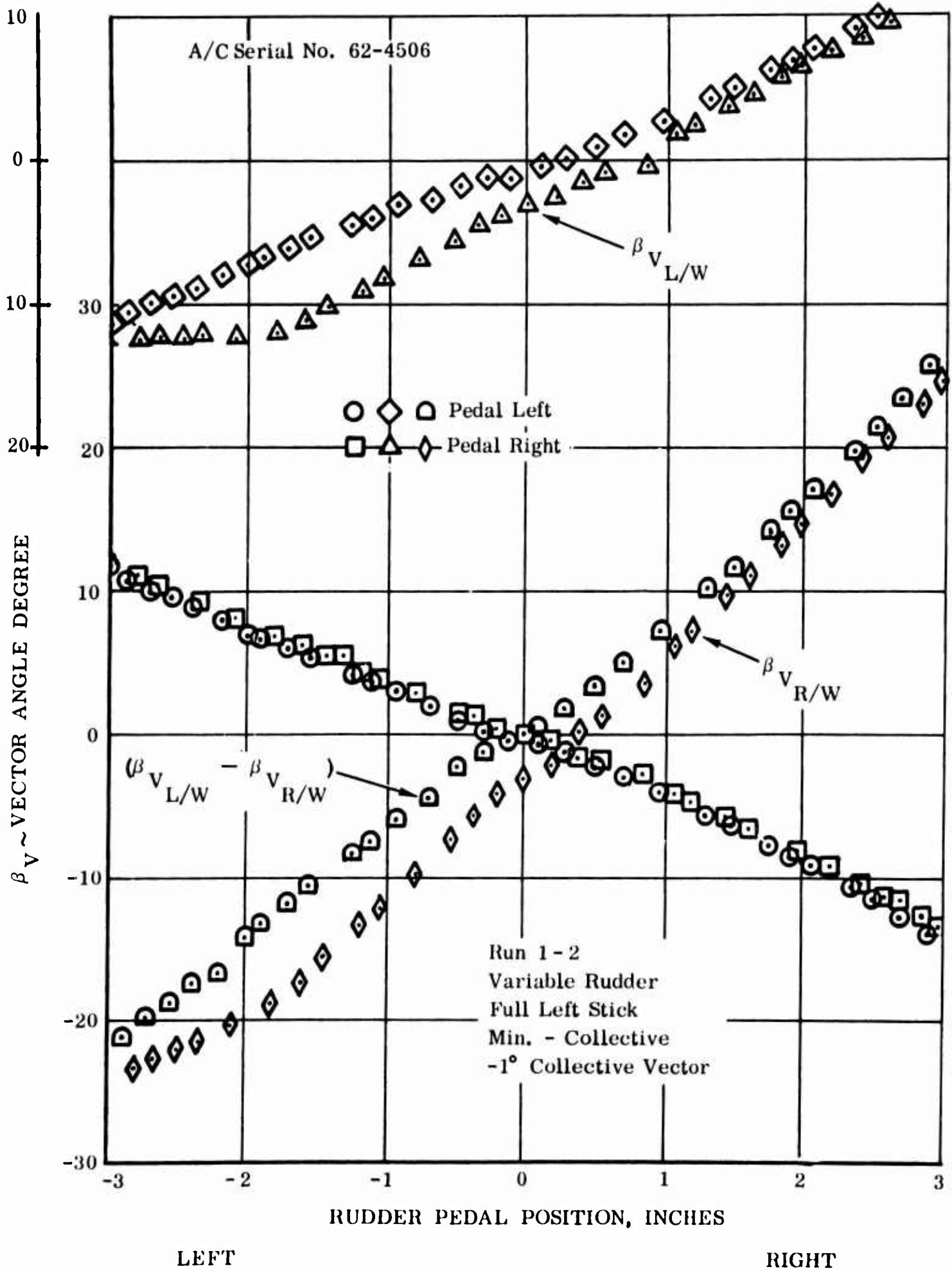


Figure 6.64 Static VTOL Control System Calibration

9 November 1964

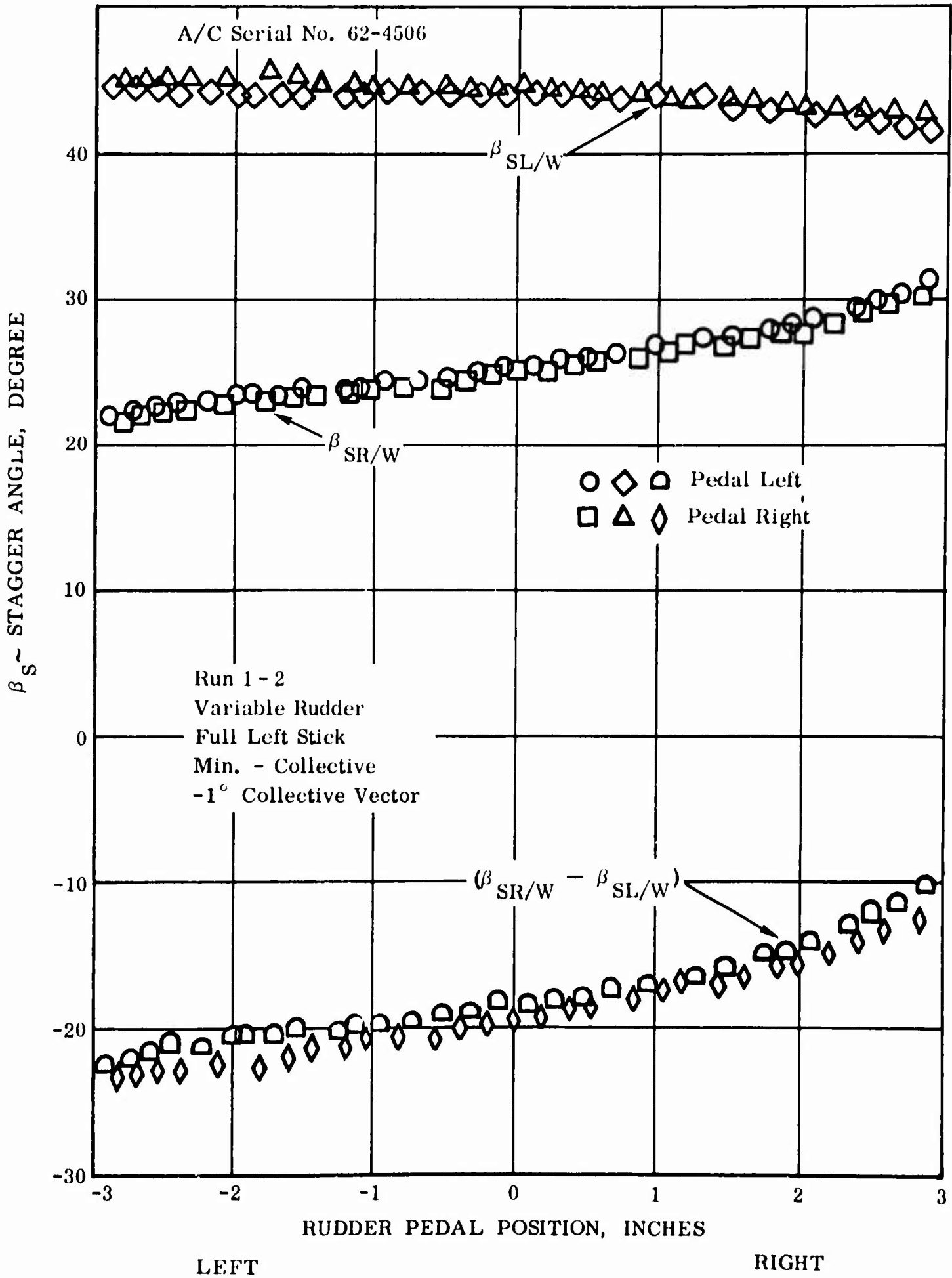


Figure 6.65 Static VTOL Control System Calibration

9 November 1964

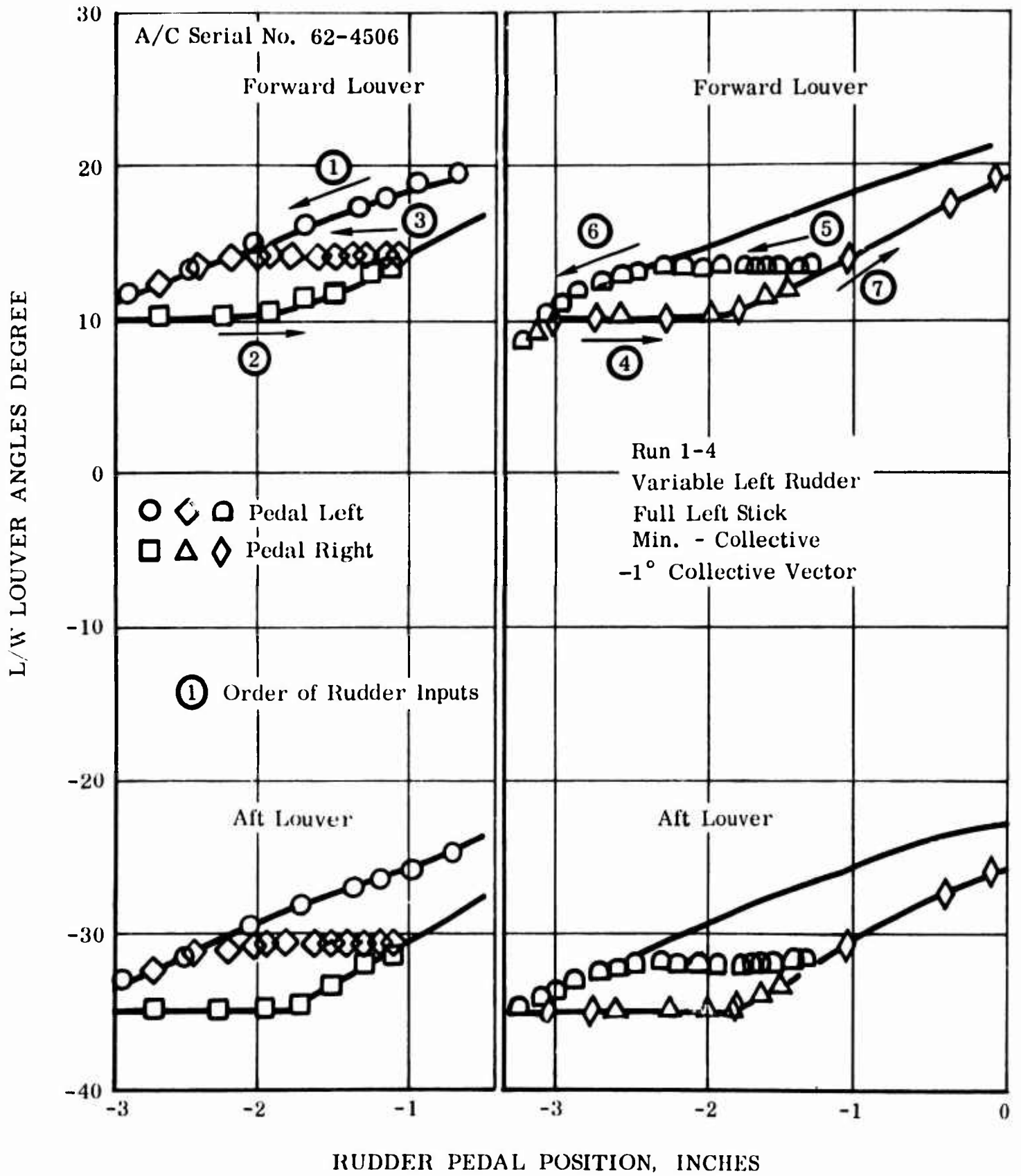


Figure 6.66 Static VTOL Control System Calibration

6.2.8 Horizontal Tail Downwash

6.2.8.1 Requirement for Additional Horizontal Tail Downwash Data

Disagreement between the estimated horizontal tail downwash derived from test data of a 1/6-scale, powered, wind tunnel model and a full-scale facsimile of the XV-5A aircraft with the results obtained on aircraft Serial Number 62-4505 in the NASA Ames 40 x 80-foot wind tunnel test, indicated a need for careful monitoring of tail angle of attack during initial transition flight development work. The NASA Ames test indicated that the downwash at the horizontal tail was substantially less than estimated for fan mode flight, and the possibility of tail stall during transition was therefore acute. Based upon recommendations received from NASA Ames personnel, a full-span leading edge slat was designed for the horizontal tail, and provisions for measuring horizontal tail angle of attack and dynamic pressure with a horizontal tail boom were initiated. Figure 6.67 illustrates the installation of the horizontal tail slat and boom as installed on aircraft serial number 62-4506. (Reference 6.9 and 6.10.)

6.2.8.2 Calibration of Horizontal Tail Angle-of-Attack Indicator

The horizontal tail angle-of-attack indicator was installed to measure the angle of attack at the span station corresponding approximately to the horizontal tail MAC. The horizontal tail boom was mounted at an angle of incidence of minus 7-1/2 degrees to the horizontal tail reference plane. This placed the tail angle-of-attack indicator ahead of and below the leading edge of the horizontal tail, as shown in Figure 6.67.

The proximity of the angle-of-attack indicator vane to the leading edge of the horizontal tail causes it to be influenced by the local induced upwash of the horizontal tail. Therefore, a correction between the indicated and the actual horizontal tail angle of attack had to be established in order to obtain accurate downwash data. The addition of the full-span leading edge horizontal tail slat further influenced the induced upwash and affected the calibration of the horizontal tail angle-of-attack indicator.

Experimental data were used to estimate the effect of induced upwash on the horizontal tail angle-of-attack vane and are presented in Figure 6.68. A test was conducted to obtain data on the induced upwash effect, using the airplane. The procedure involved several high-speed CTOL taxi runs with wing flaps retracted and with horizontal tail incid-

ence a variable.

Figure A-43A presents data from the vane calibration check from test 24.01G, with the horizontal tail slat installed. Figure A-43B presents calibration data from test 30.0F with the horizontal tail slat removed.

Figure 6.69 presents tail angle of attack calibrations for slat on and slat off and is based on the test data of Figures A-43A and A-43B and the estimated downwash for the XV-5A in ground effect with flaps retracted. The data agree reasonably well with the estimated data of Figure 6.68.

To simplify hangar calibration, the same protractor was used to calibrate the nose boom and the tail boom angle-of-attack indicator vanes. Since the centerline of the boom provides zero-degree reference for the protractor, a correction of + 7.5 degrees must be added to the PO-47 recorded tail angle-of-attack value to obtain uncorrected tail angle of attack to compensate for the angle at which the boom is mounted to the horizontal tail.

6.2.8.3 Presentation of Downwash Data

The majority of the data concerning horizontal tail downwash were obtained from tests with the horizontal tail full-span leading edge slat removed. All data were obtained from test of aircraft SN 62-4506.

High-speed fan mode taxi tests were conducted preceding investigation of high-speed transition flight. Taxi tests were followed by STOL operations and climb studies, which led to the first aircraft conversion (fan to conventional) at approximately 2,000 feet above the terrain.

The horizontal tail slat and the tail angle of attack and pitot static probes were installed prior to test 22.OF. This was followed by several hovering flights, and translation speeds to 20 knots were achieved. High-speed taxi tests and momentary STOL flights to an altitude of one to five feet above the runway were performed during tests 24.01G and 24.02G. The slat was removed prior to subsequent conventional flight test 25.OF.

The slat was nonretractable and was built as an expedient to permit investigation of horizontal tail downwash in the fan mode with the maximum possible safety in accordance with the findings of the NASA Ames wind tunnel tests. Stall of the tail at small negative angles of attack, as during trim in the conventional flight mode with flaps extended, was

considered a possibility and precluded the use of the slat in conventional flight. A retractable slat, with modification to the horizontal tail to accommodate, would have been required if a safe stall margin for fan flight had not been determined. Aerodynamic section characteristics typifying the effect of a leading-edge slat are presented in Figure 6.70.

Figures A-43C through A-43E present time histories from tests 24.01G and 24.02G of several parameters pertinent to the examination of horizontal tail downwash. Data from these early tests, along with data from test 58.OF, presented in Figures A-43F, A-44 and A-45, are plotted in Figure 6.71. Test 50.0F was previously conducted to investigate operation in proximity to the ground at various speeds and vector angles. The test also provided the opportunity of collecting data for evaluation of tail downwash characteristics in and out of ground effect.

Presented in Figure 6.71 is the calculated tail downwash as a function of airspeed and corresponding louver vector angle. Pitch attitude has been used for angle of attack for the aircraft in the calculations, as only horizontal flight path or taxi conditions are represented, eliminating the need for a position error correction for nose boom angle of attack. Corrections appropriate for slat-on or slat-off from Figure 6.69 were applied to obtain tail angle of attack.

The data shown in Figure 6.71 from test 24.01G were obtained while the aircraft was in contact with the ground. Data from 24.02G were obtained at altitudes up to 5 feet. Maximum flight altitudes attained during the momentary hops of flight 58.OF were observed as 15 to 30 feet. The data from 24.01G and 24.02G indicated a safe stall margin with tail incidence for trimmed flight at high vector angles in ground effect, and trends indicated increased downwash angle (i. e. reduced tail angle of attack) with increase in flight altitude. Based on the data, a tail angle of attack no greater than 10 degrees was expected during operation out of ground effect up to 5 degrees angle of attack.

This information closely matched estimates based on small-scale test data which showed a tail angle of attack for stall of 16 degrees, and provided a level of confidence sufficient to permit cautious expansion of the fan flight envelope without the tail slat. Tail angle-of-attack data were reviewed following each flight to ascertain continued conformance to expected levels until test 41.OF, when the indicated tail angle of attack was connected to telemetry and was monitored at the ground station during flight.

The data from test 58.0F, presented in Figure A-43F, substantiates the trends shown by the data of tests 24.01G and 24.02G. The data further indicate that the horizontal test downwash in ground effect is a function of vector angle and decreases at lower speeds for lower vector angles of 40 degrees.

Typical of all data of this section, the characteristics presented are approximate but are considered to be of sufficient value and accuracy to warrant inclusion herein. In some cases instrumentation biases have been applied, and establishment of level-flight conditions for selection of data was often difficult.

Figures 6.72 through 6.76 present the horizontal tail downwash calculated from flight test data using the curve of Figure 6.69 to obtain the horizontal tail angle of attack. These data are presented for several values of T^S and compared with the estimated downwash which was derived for the flight simulator program from small-scale powered model tests. Corrections were applied to the data for ambient conditions in the calculation of the T^S values; however, corrections were not applied for nose boom angle-of-attack position error. These data indicate that at around 30 knots the horizontal tail downwash is greater than estimated. In the 70-to-80-knot speed range, the horizontal tail downwash is somewhat less than estimated. The trend of $\partial \epsilon / \partial \alpha$ compares favorably in most cases when the downwash for a given horizontal tail incidence is considered separately. The horizontal tail angle-of-attack indicator vane does see a slightly different downwash distribution than that effective at the horizontal tail, due to the location of the probe approximately 30-1/2 inches ahead of the leading edge of the horizontal tail MAC. This effect, plus the possible position error of the nose probe angle-of-attack indicator, may account for the discrepancy between the data from the two sources.

6.2.8.4 Horizontal Tail Dynamic Pressure

The horizontal tail dynamic pressure was measured with a standard pitot probe mounted on the horizontal tail boom. It was connected to a ± 0.3 PSID Statham transducer and recorded by the PCM system. Originally, the transducer was mounted inside the aft end of the tail boom. This proved unsatisfactory due to the amount of noise introduced by the vibrations of the tail boom. Prior to test 41.0F, the horizontal tail dynamic pressure transducer was relocated and installed in the vertical tail. This reduced the noise level considerably. Sheets 2 of Figures A-46 through A-50 present time histories of the recorded nose boom and tail boom dynamic pressures. Although there is con-

siderable scatter in the data, faired comparisons between nose and test boom results show higher dynamic pressure measured at the tail boom (up to 2 PSF) in higher speed flight and slightly lower pressures (15 PSF) at speeds less than 35 knots.

Figures A-51 through A-53 present pertinent data time histories from some of the flights examined in study of the horizontal tail downwash and dynamic pressure out of ground effect.

6.2.9 Conversion Maneuver

A total of 72 in-flight conversions were made during the flight test program; five were accomplished using aircraft S/N 05, and 67 were accomplished using aircraft using aircraft S/N 06. During the program the maneuver was investigated to determine the effect of change in conversion initiation speed, and various piloting techniques; particularly, the use of longitudinal control and the application of power in conversion to the fan flight mode were evaluated. Conversions to the conventional flight mode were accomplished at representative single engine powers and in right and left banked turn conditions.

Conversion initiation points have been plotted in Figures 6.77 and 6.78 to show conversion experience envelopes for fan to turbojet and turbojet to fan conversions. Conversions from fan to turbojet mode were accomplished at airspeeds ranging from approximately 85 knots to 110 knots CAS and at altitudes between 500 ft. to 4,400 ft. above EAFB terrain. Conversions from turbojet to fan mode were recorded at airspeeds between approximately 90 knots and 114 knots CAS and at altitudes between 800 and 5,000 ft. above terrain.

6.2.9.1 Conversion From Fan to Conventional

Figure 6.79 is a block diagram of the mode change control system for the fan to conventional conversion. The following is a normal fan to conventional conversion sequence.

- A. With the vector setting at 43° to 45° , the flight mode selector switch is moved to the CTOL position.

Power to the horizontal stabilizer control solenoid comes through the horizontal stabilizer time delay interlock and the horizontal stabilizer program timer. When the horizontal stabilizer reaches operating speed, power goes through the hydraulic interlock switch and the sequencing time delay relay to the diverter valve control solenoid. If the diverter

moves from the VTOL position, the power to the horizontal stabilizer control solenoid is latched in; if, however, the diverter does not move from VTOL position after a specified length of time, the sequencing time delay relay and the horizontal stabilizer time delay interlock abort the conversion. Assuming the diverter valve moves to the CTOL position, then the wing fan door actuator's solenoid is energized through the diverter valve CTOL position interlock.

B. Louver Switch to Conventional or Flaps Switch to UP

The following will happen:

1. The pitch fan inlet louvers close
2. Wing fan inlet door latches lock doors closed
3. Wing fan louvers and vector actuator move to full closed
4. Flaps move up if flaps switch initiated action

Conversions from fan to conventional mode were normally performed at indicated airspeeds of 90 knots (96 knots CAS) or slightly higher speeds. Higher conversion speeds could only be obtained in descent due to limited speed performance capability. Fan speed, not power available, was the limiting factor in attaining a higher speed; however, removal of the wing fan overspeed restriction would not be expected to produce large increases in speed capability. Except for the rather careful monitoring of wing fan speeds required at the higher vector angles and flight speeds, the piloting procedure was regarded as a simple one.

The first fan to turbojet mode conversion accomplished during 34F was considered to be a very straightforward operation. According to the pilot no control corrections were necessary and only 20 ft. of altitude was lost. Although conversions from fan to conventional mode were considered essentially the same and were looked on as routine by the pilots after 34F, later comments and flight test data indicate that forward stick is usually applied to avoid overshooting the conventional flight trim angle of attack condition. Power reduction is normally made a few seconds following conversion.

A conversion vector angle of 50 degrees cockpit indicated (approximately 45 degrees actual) was selected from simulator studies for the first transition and conversion investigations. This vector angle with the stiffened louvers proved in flight test to be excessive based on flight performance and fan overspeed considerations, and vector actuator switch adjustments were made which moved the fan to conventional mode interlocks from 30 to 45 degrees indicated (40 degrees actual) vector angle.

Several time histories of conversion from fan to conventional mode are shown in Figures 6.80 through 6.85. Conversion from the fan mode flight where entry to fan flight was first made from conventional flight (38F) is shown in Figure 6.80. Other time histories of the fan to conventional conversion maneuver obtained in level flight during 39F, 72F, and 73F are shown in Figures 6.81 through 6.83. Figures 6.84 and 6.85 present time histories of selected parameters relating both longitudinal and lateral-directional characteristics recorded during conversions to conventional flight performed during 75F and 76F in approximately 30 degree banked turn conditions.

Pilot technique used during the conversions of Figures 6.80 through 6.83 do not differ to any degree. (Conversion from fan to conventional flight at half power and 90 knots IAS performed during 73F is shown in Figure 6.83.) Forward stick displacement equivalent to approximately 5 degrees of elevator was consistently used to arrest the pitch-up programmed into the maneuver by the horizontal tail. This action is evidently instinctive as it is coincident with automatic tail trim and pitch change of the aircraft. The control application is evidently excessive as the application of forward stick is compensated for by use of aft stick at the completion of the maneuver. Nevertheless some small loss in altitude is normally shown to occur.

Application of lateral or directional control was not required during conversions according to the pilots, except for 73F when a conversion from fan to conventional mode was made at 84 knots IAS. The pilot stated that the aircraft rolled to the right at conversion but was easily restored. Conversion at this low airspeed could place the aircraft in a near stalled condition and may account for the behavior. Pilots stated that the optimum speed for conversion was approximately 100 knots IAS which could only be achieved in a slight dive.

A small pitch fan control door transient appears in Figure 6.84B as the S.A. system is shut off at conversion. Both recorded maneuvers display damped pitch oscillations at approximately 1/2 CPS beginning at conversion which appear to be sustained by pilot control applications. Slight roll and yaw disturbances also appear to have occurred at conversion. These effects were evidently small as the pilot stated that banked conditions produced no changes in the behavior of the aircraft during conversion.

6.2.9.2 Conversion From Conventional to Fan Flight

The sequence for converting from conventional to fan modes of flight on the XV-5A is illustrated in Figure 6.86. The following is a normal conventional to fan conversion sequence:

- A. Flaps Commanded Down - Flaps move to full flaps-down position.
- B. Louver Switch Set to Fan
 - 1. Pitch Fan Inlet Louvers Open
 - 2. Wing Fan Door Lock Unlatches
 - 3. Vector Actuator Moved from Full Closed to 45°

The following interlocks will have closed after the specified periods:

- a. Flap Interlock
- b. Pitch Fan Inlet Louver Interlock
- c. Left and Right Wing Fan Inlet Latch Interlocks
- d. Vectoring Actuator, 47° β_v , Interlock

If all the interlocks function properly, the cockpit "NO-GO" indicator does not illuminate.

- C. Mode Selector Switch Set to VTOL - Wing fan inlet doors open; at 66% of full open, the interlocks close which connects power to the horizontal stabilizer control solenoid through the horizontal stabilizer time delay interlock and the horizontal stabilizer program timer. When the horizontal stabilizer reaches operating speed, power goes through the hydraulic interlock switch and the sequencing time delay relay to the diverter valve control solenoid, or through the horizontal stabilizer position override switch and the sequencing time delay relay to the diverter valve control solenoid. The horizontal stabilizer position override switch functions only if conversion is commanded when the horizontal stabilizer is at an angle greater than +8°.

If the diverter moves from the CTOL position, the power to the horizontal stabilizer control solenoid and the diverter valve control solenoid is

latched in; if, however, the diverter does not move from CTOL position after a specified length of time, the sequencing time delay relay and the horizontal stabilizer time delay interlock abort the conversion.

Conversions from conventional to fan mode were normally performed at approximately 100 knots IAS. Horizontal tail time sequencing and actuation rate used during these initial conversion maneuvers were developed on the flight simulator. The flight simulator was used to perform investigations of the conversion maneuver with and without use of the thrust spoiler system at various flight speeds. Horizontal tail trim rate and initiation time were selected during these studies. When the thrust spoiler, which permits operation in the jet mode at high power settings and low net thrust levels, is not used, power adjustments are normally made immediately prior to conversion command. A high power setting, but less than that which will produce fan overspeed and result in power cutback, is required in order to perform the maneuver smoothly and with a minimum altitude change. All conversions performed during the flight test program were accomplished without use of the thrust spoiler.

Several adjustments in the flight conversion control system were made affecting the conventional to fan maneuver. The changes included reduction of the diverter valve time delay from .3 to .15 seconds and adjustment in the preconversion position louver stops from an indicated 50 to 45 degrees (40 degrees actual) to provide a more open louver condition for conversion. The time delay change was made prior to test 39F to reduce the magnitude of the initial pitchover impulse applied to rotate the aircraft to the near level attitude for operation. The louver adjustment corresponded to a similar change made to reduce maximum vector louver limits for fan mode operation prior to 38F discussed in the previous section. Flight performance was considered improved and fan overspeed potential reduced at the lower louver angle.

Conversions from turbojet to fan were often performed smoothly and with little altitude change, i. e., less than 50 feet. However, the maneuver was considered to be more difficult than the fan to jet conversion due principally to the larger pitch trim transients - the character of which were significantly affected by power level.

Time histories of longitudinal data obtained during time histories of conversion maneuvers are shown in Figures 6.88 and 6.89. Data shown in Figure 6.88 were recorded during the first conversion from conventional to fan mode (38F). Power was advanced from 88 percent to

approximately 96 percent simultaneous with diverter valve cycling. The aircraft pitched from an attitude of positive 10 to a negative 11-1/2 degrees as the angle of attack was recorded to change from 13 to 2 degrees in the first 4.5 seconds following conversion command. Power was slowly advanced, following the pitchover to 100 percent rpm (102 percent maximum) as an angle of attack of 10 degrees was used to arrest a rate of sink of approximately 2,400 feet per minimum. A total of 480 feet of altitude was recorded as being lost in the maneuver. The pitchover was initiated by horizontal tail action and momentarily nearly full aft stick is shown as applied to oppose the pitchover.

The same maneuver was performed in the succeeding flight (39F) with power applied prior to diverter action. In general, the character of the maneuver was unchanged from that performed during 38F. After Flights 39 and 40, the pilot remarked that the aft stick movement was not due to pilot command but other factors. Although estimated to be small this effect may be produced or contributed to by the applied elevator hinge moment due to operation of the tail at positive angles of attack.

During 42F the technique of arresting the attitude change by applying aft stick as the angle of attack reached zero degrees was reported to result in little loss in altitude. The stability augmentation system was engaged for the conversion of 45F and the pilot remarked that the conversion transient was the mildest to date and that there was no loss in altitude. The conventional to fan conversion was performed as a "hands-off" maneuver during 47F. The pilot stated that no altitude was lost until the angle of attack became negative. Due to the negative speed stability of the aircraft, at this condition, it was noted that if allowed to accelerate in speed following a conversion, the aircraft will continue to nose over.

Test result from a jet to fan conversion during Flight 72 is shown in Figure 6.89. A negligible change in altitude is indicated by the data.

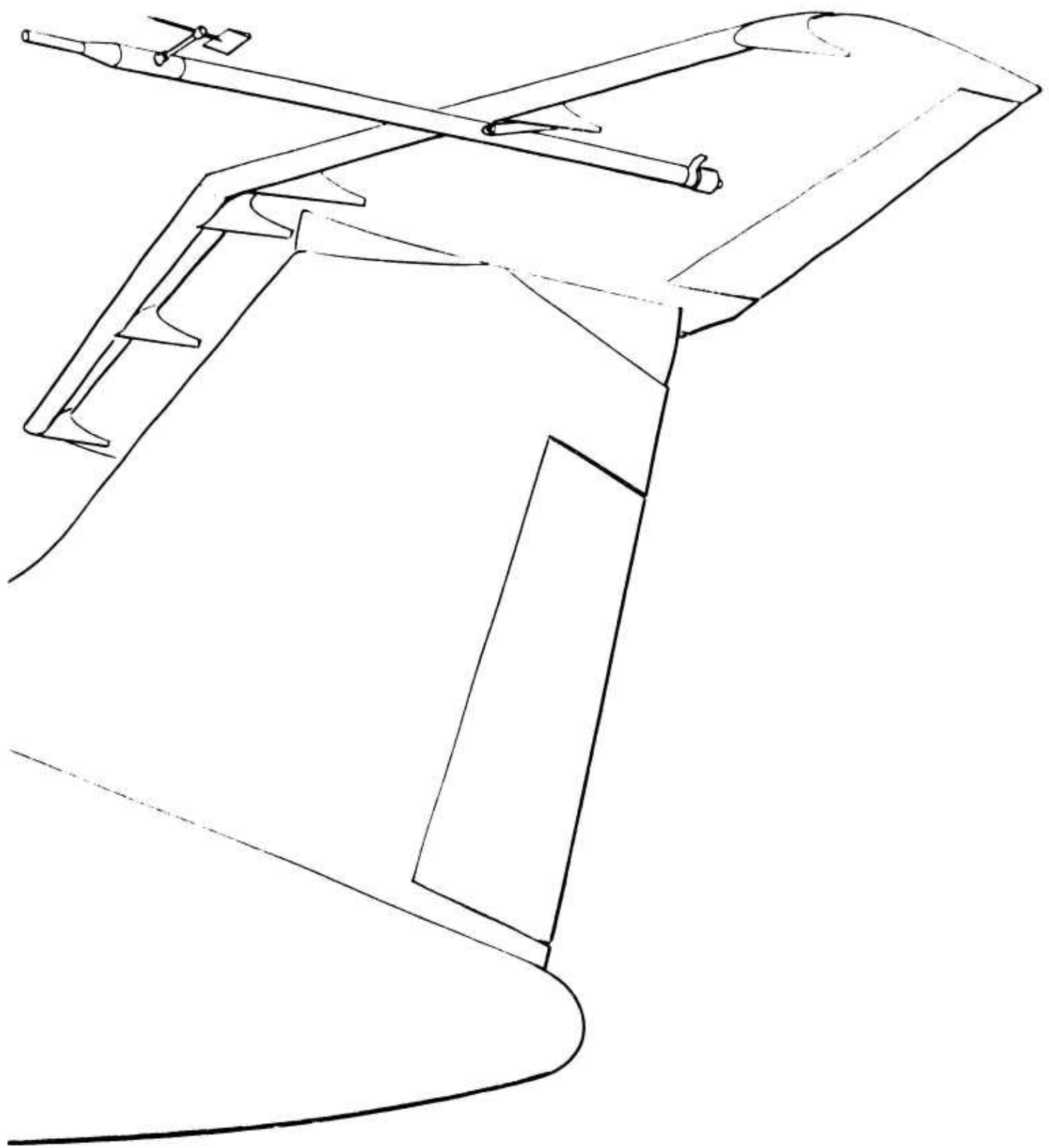


Figure 6.67 Location of Tail Angle of Attack Indicator

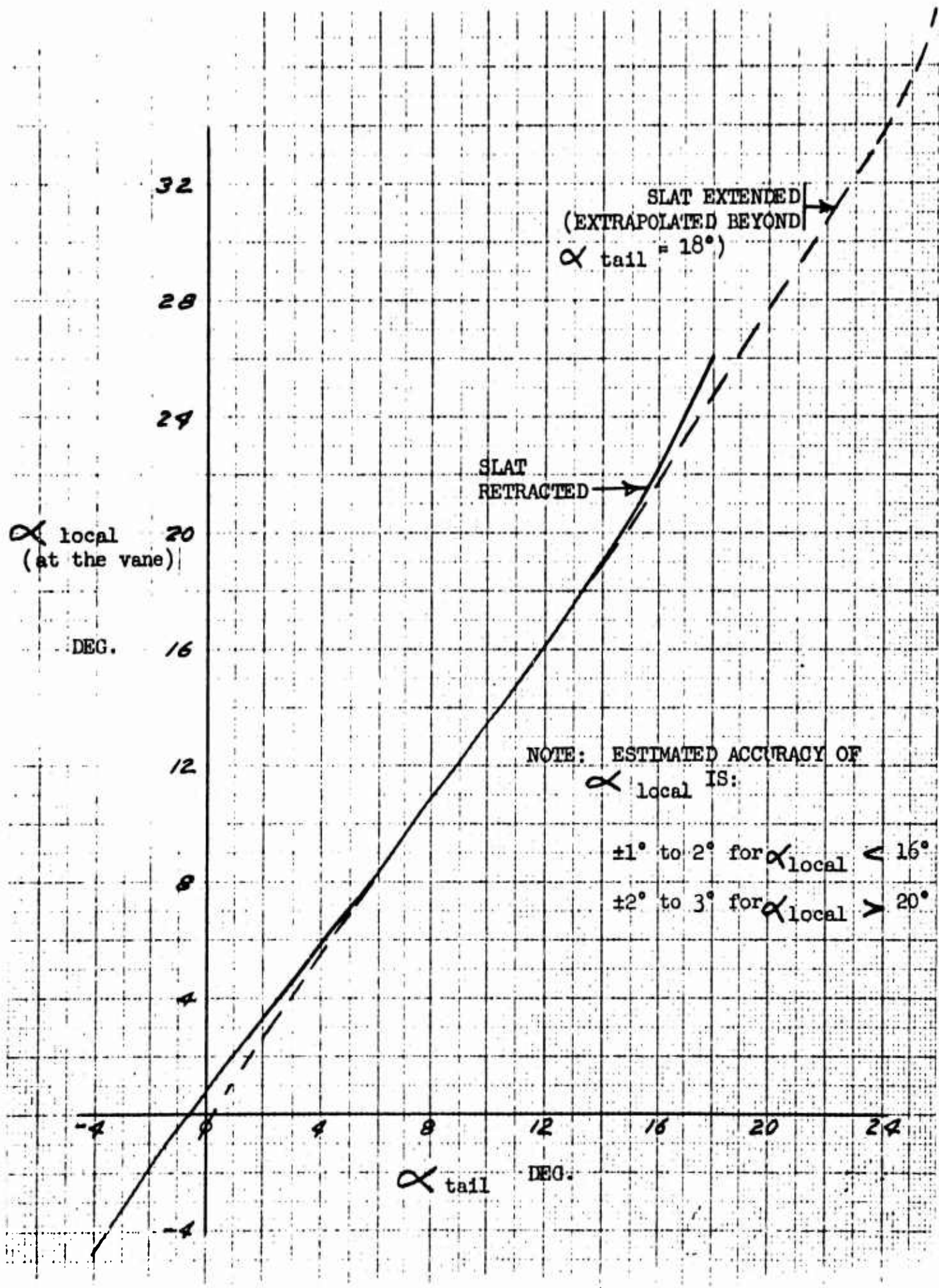


Figure 6.68 Estimated Effect of Upwash on Local Angle of Attack at Horizontal Tail Vane

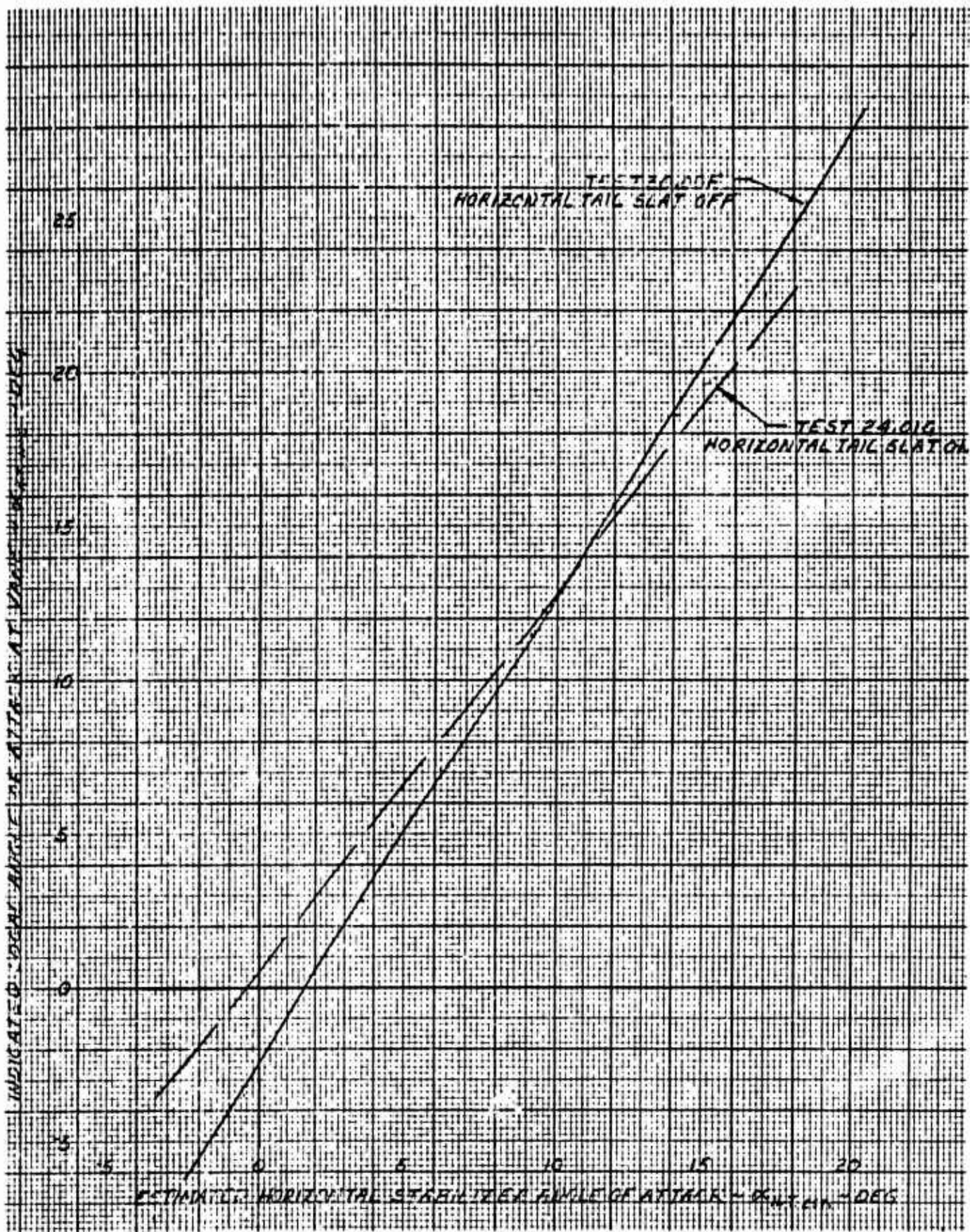


Figure 6.69 Indicated Local Angle of Attack at Vane vs Estimated Horizontal Stabilizer Angle of Attack

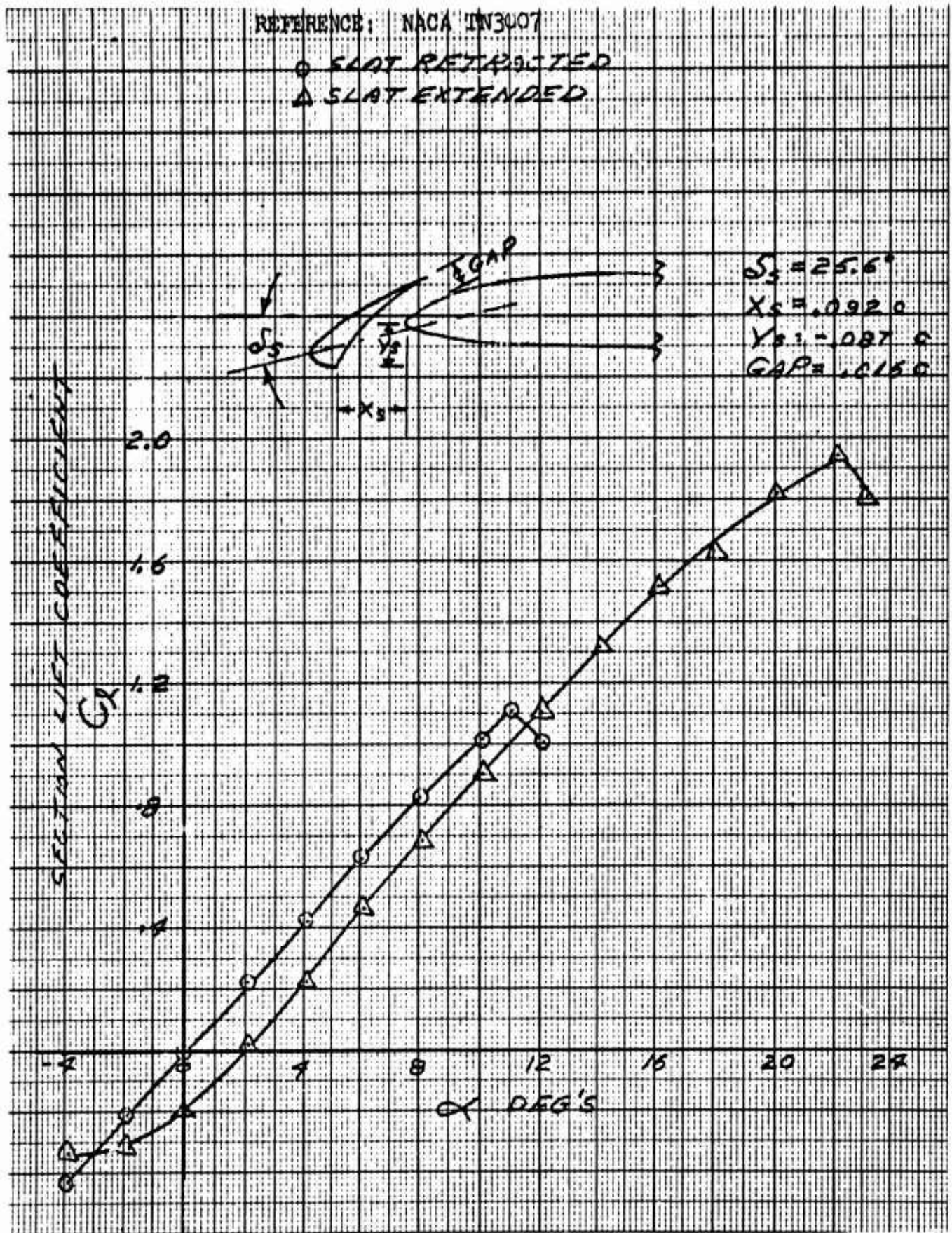


Figure 6.70 Typical Airfoil Section Characteristics Showing Effect of Leading Edge Slat

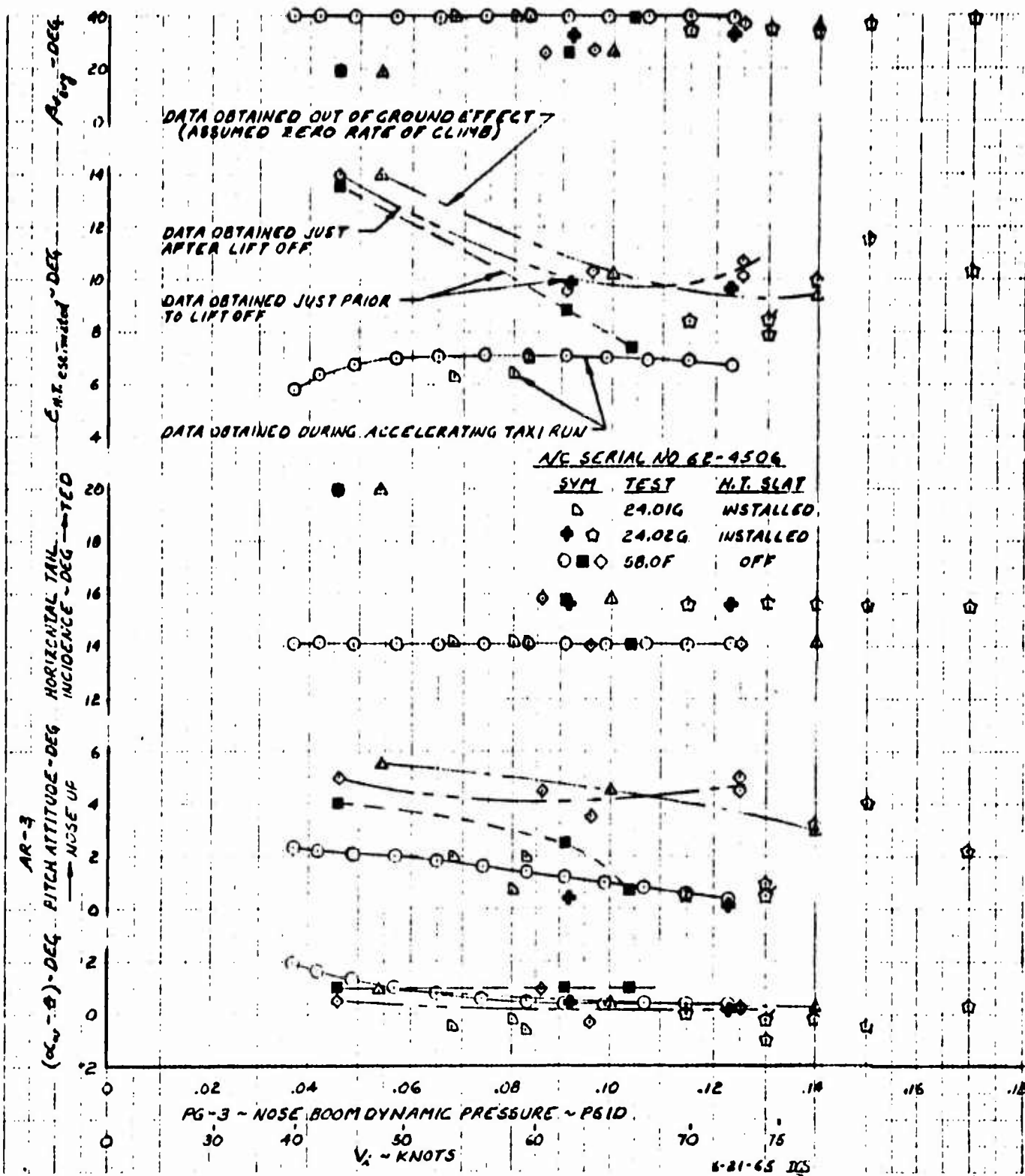


Figure 6.71 Ground Effect on Horizontal Tail Downwash

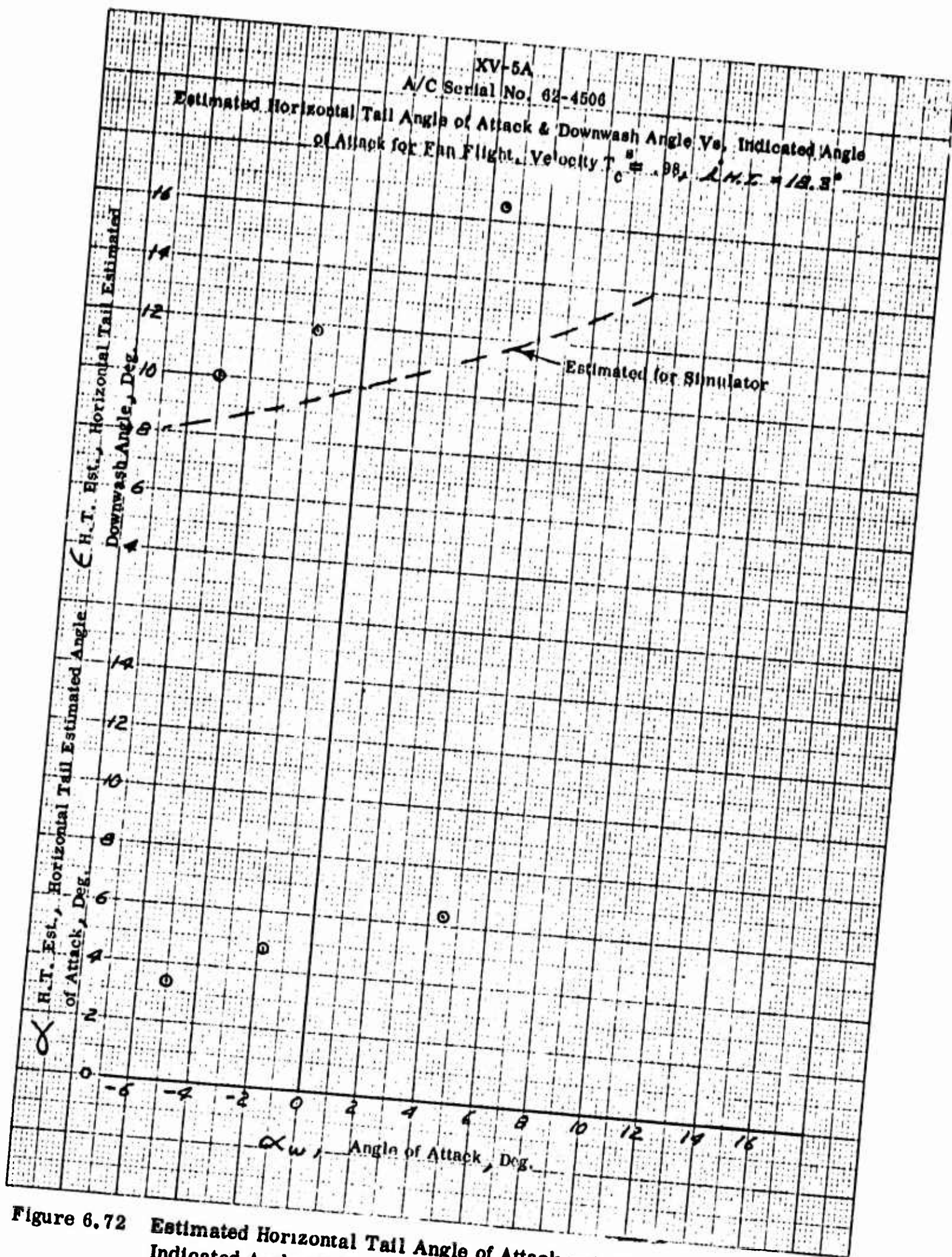


Figure 6.72 Estimated Horizontal Tail Angle of Attack and Downwash Angle vs Indicated Angle of Attack for Fan Flight

XV-5A

A/C Serial No, 62-4506

Estimated Horizontal Tail Angle of Attack & Downwash Angle vs. Indicated Angle of Attack for Fan Flight, Velocity $T_u^B = .96$

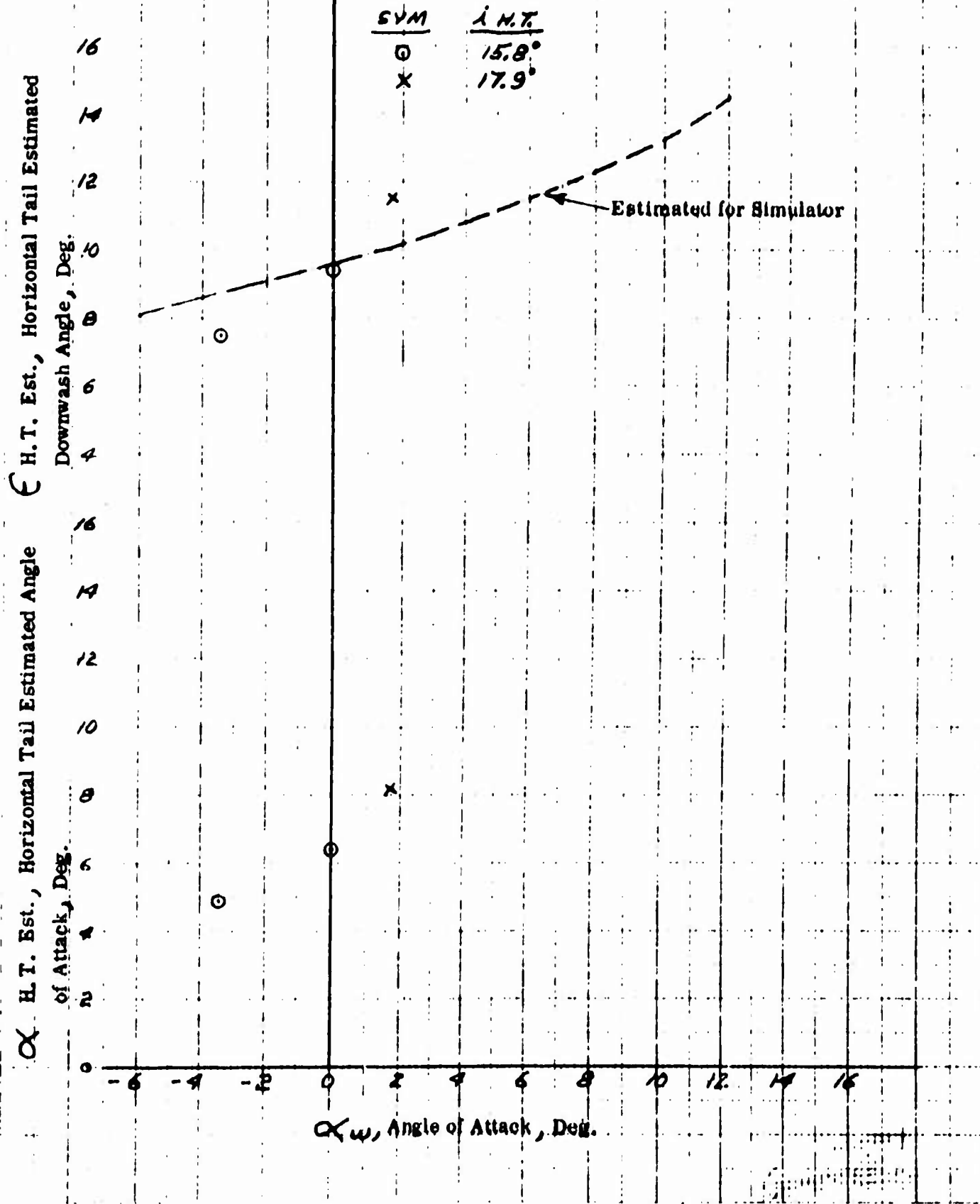


Figure 6.73 Estimated Horizontal Tail Angle of Attack and Downwash Angle vs Indicated Angle of Attack for Fan Flight

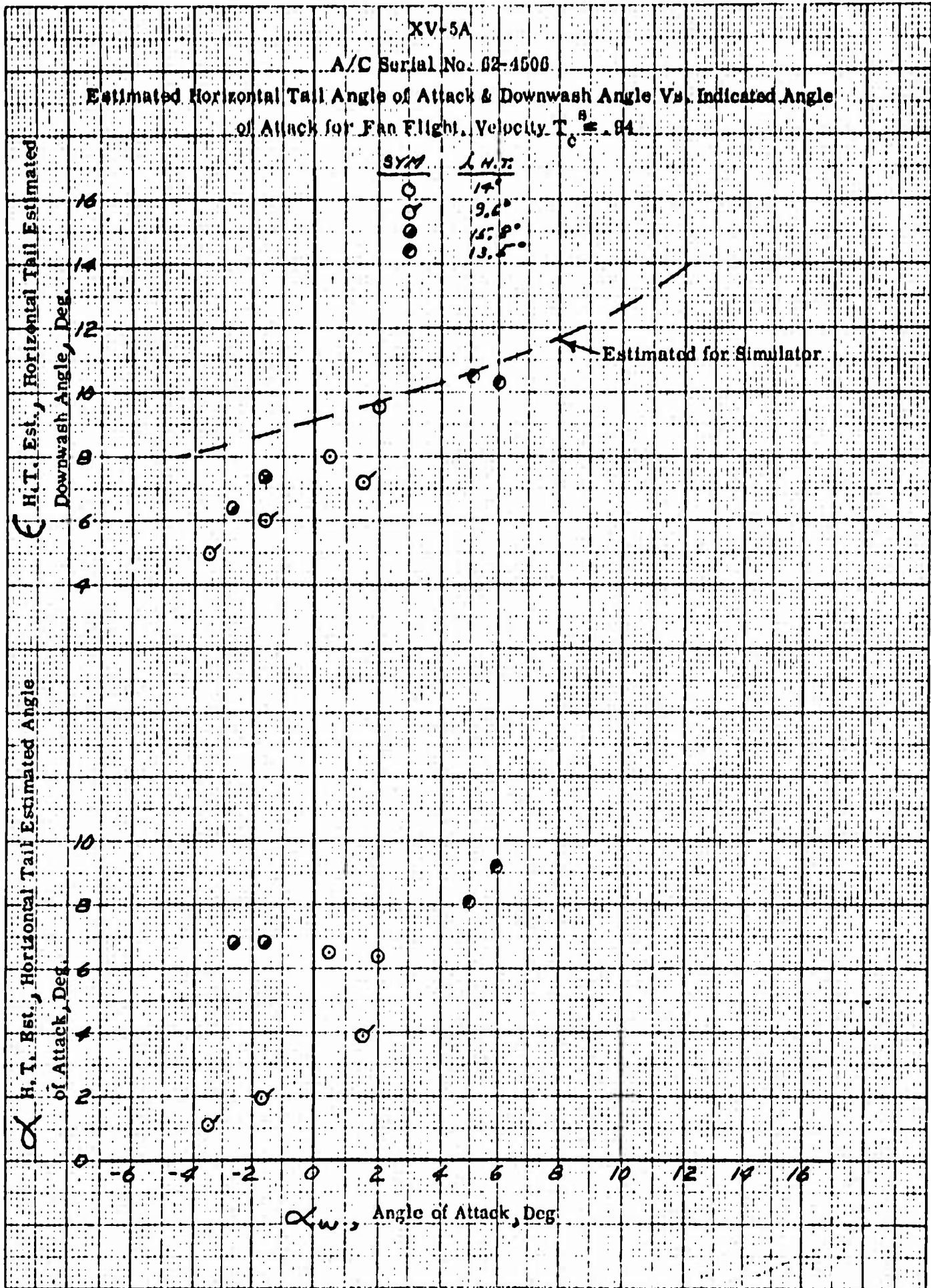


Figure 6.74 Estimated Horizontal Tail Angle of Attack and Downwash Angle vs Indicated Angle of Attack for Fan Flight

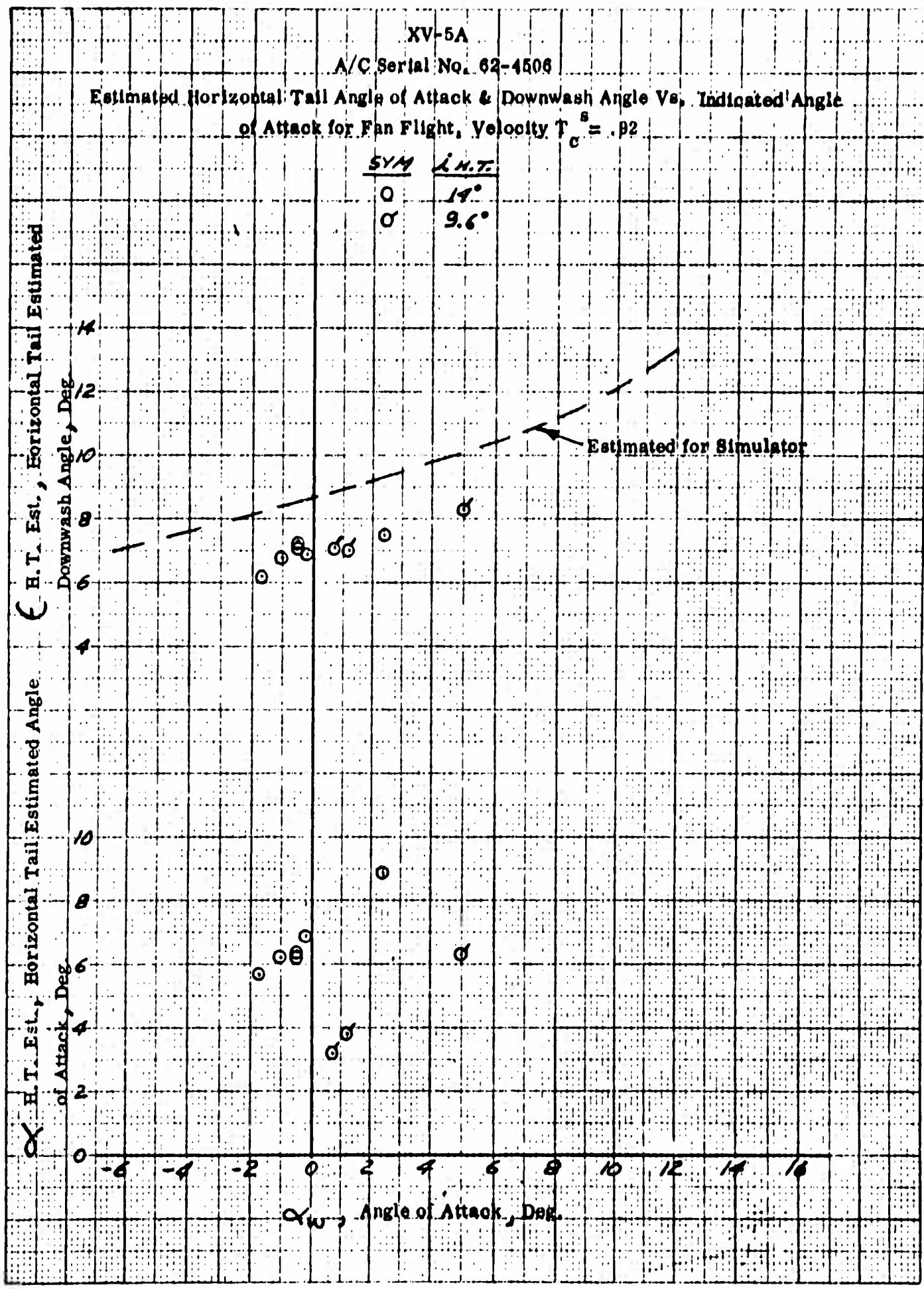


Figure 6.75 Estimated Horizontal Tail Angle of Attack and Downwash Angle vs Indicated Angle of Attack for Fan Flight

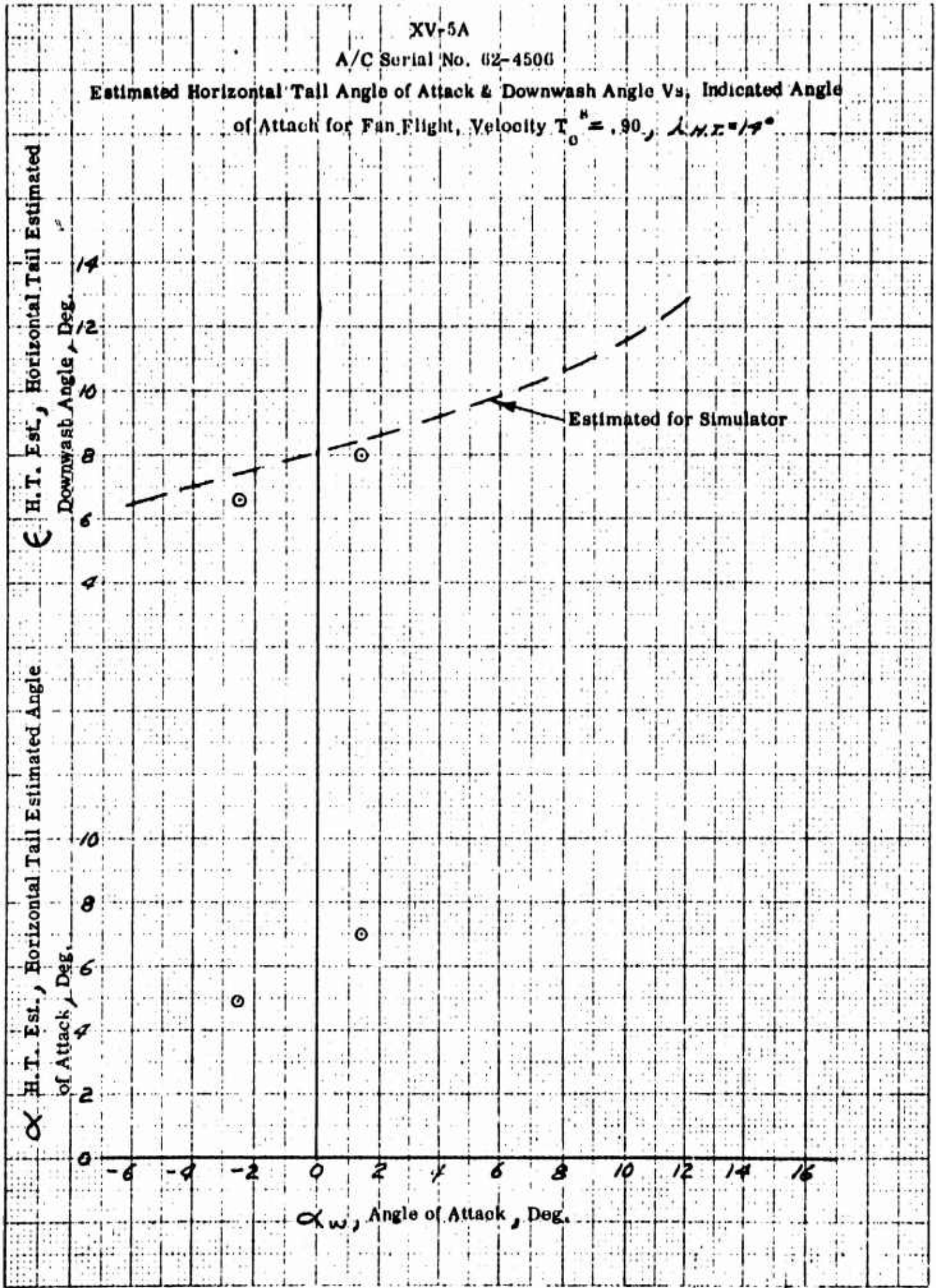


Figure 6.76 Estimated Horizontal Tail Angle of Attack and Downwash Angle vs Indicated Angle of Attack for Fan Flight

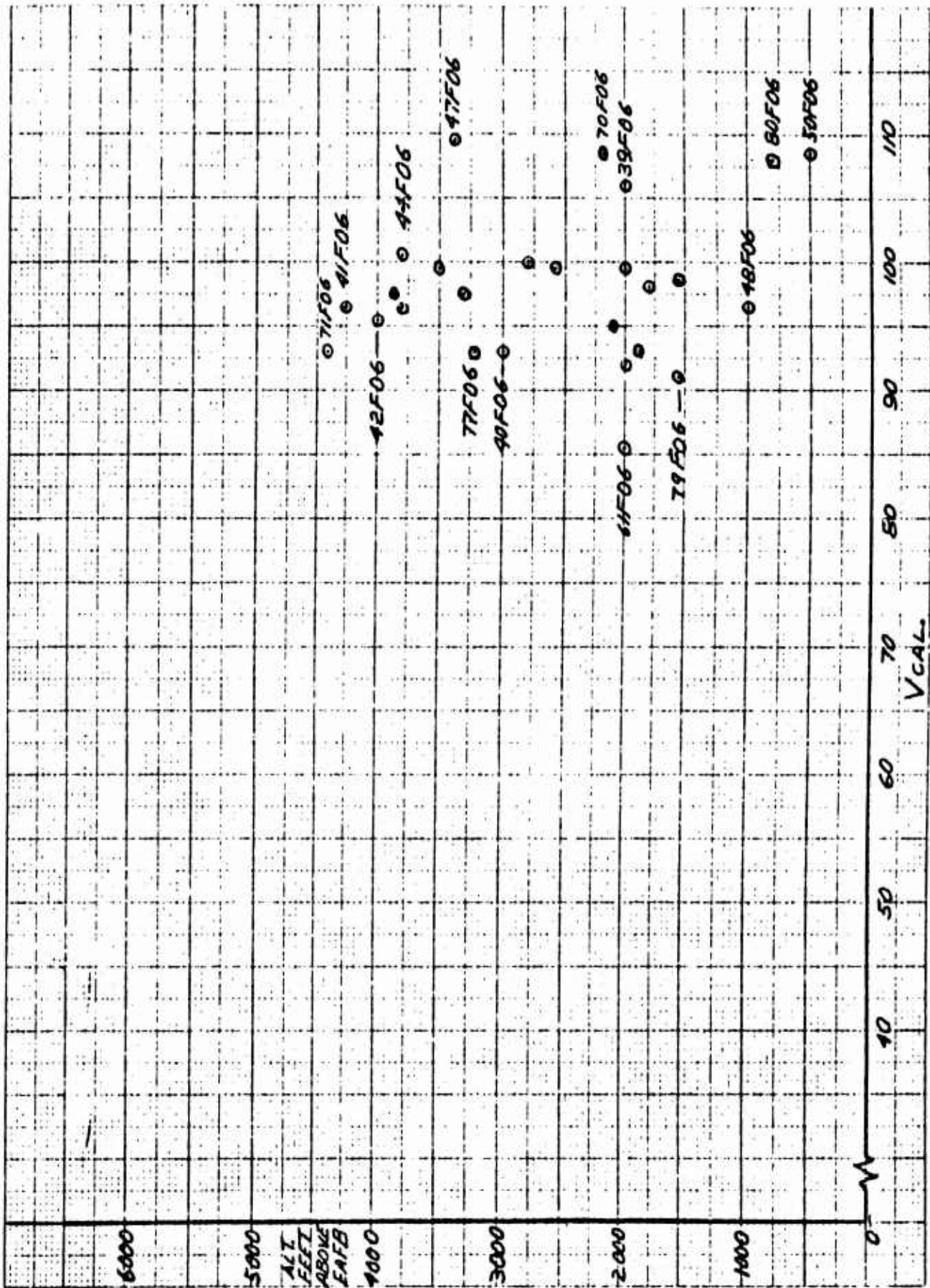


Figure 6.77 Fan to Turbojet Conversion Envelope

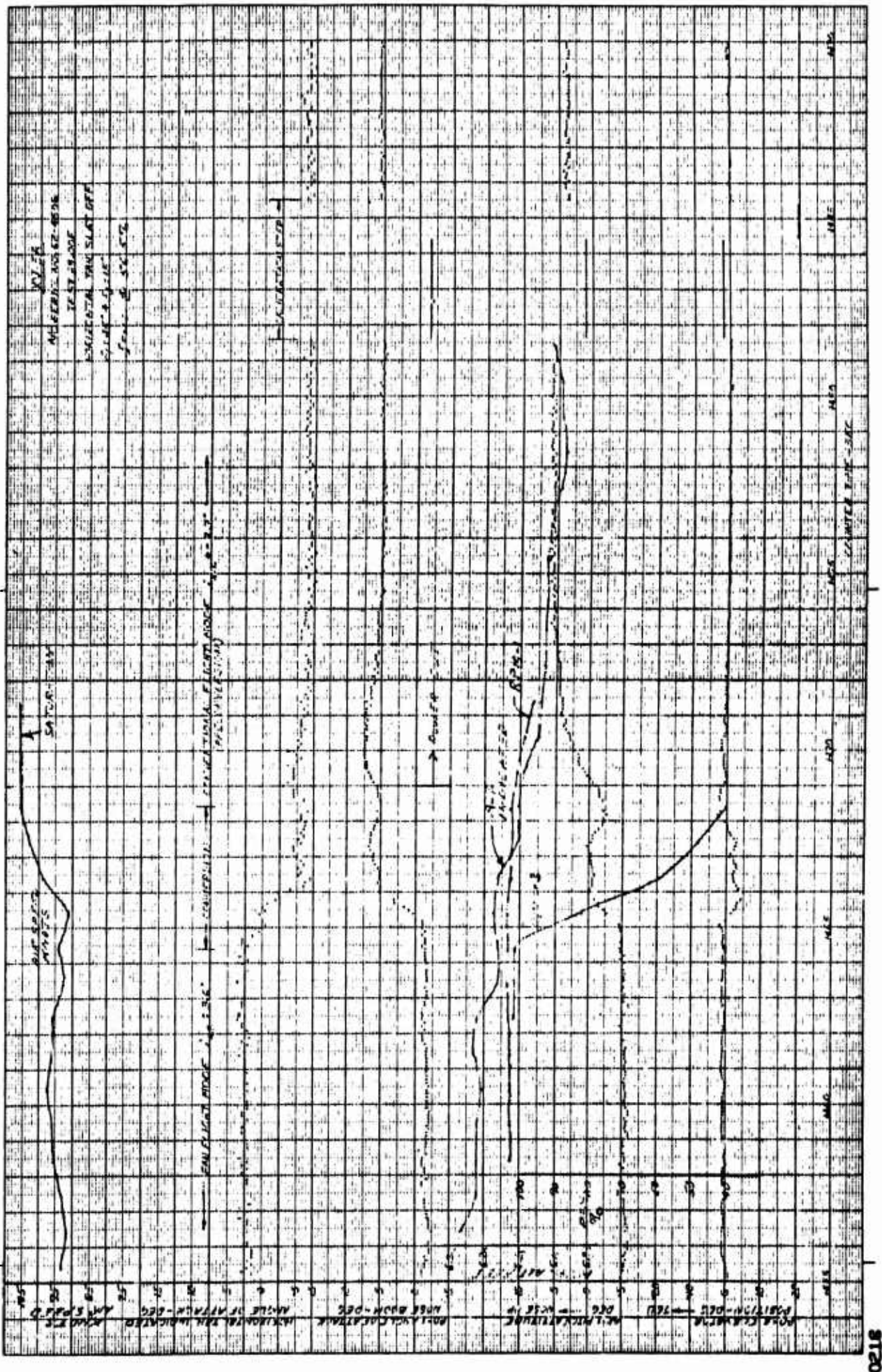


Figure 6.81 Flight Conversion Time Histories

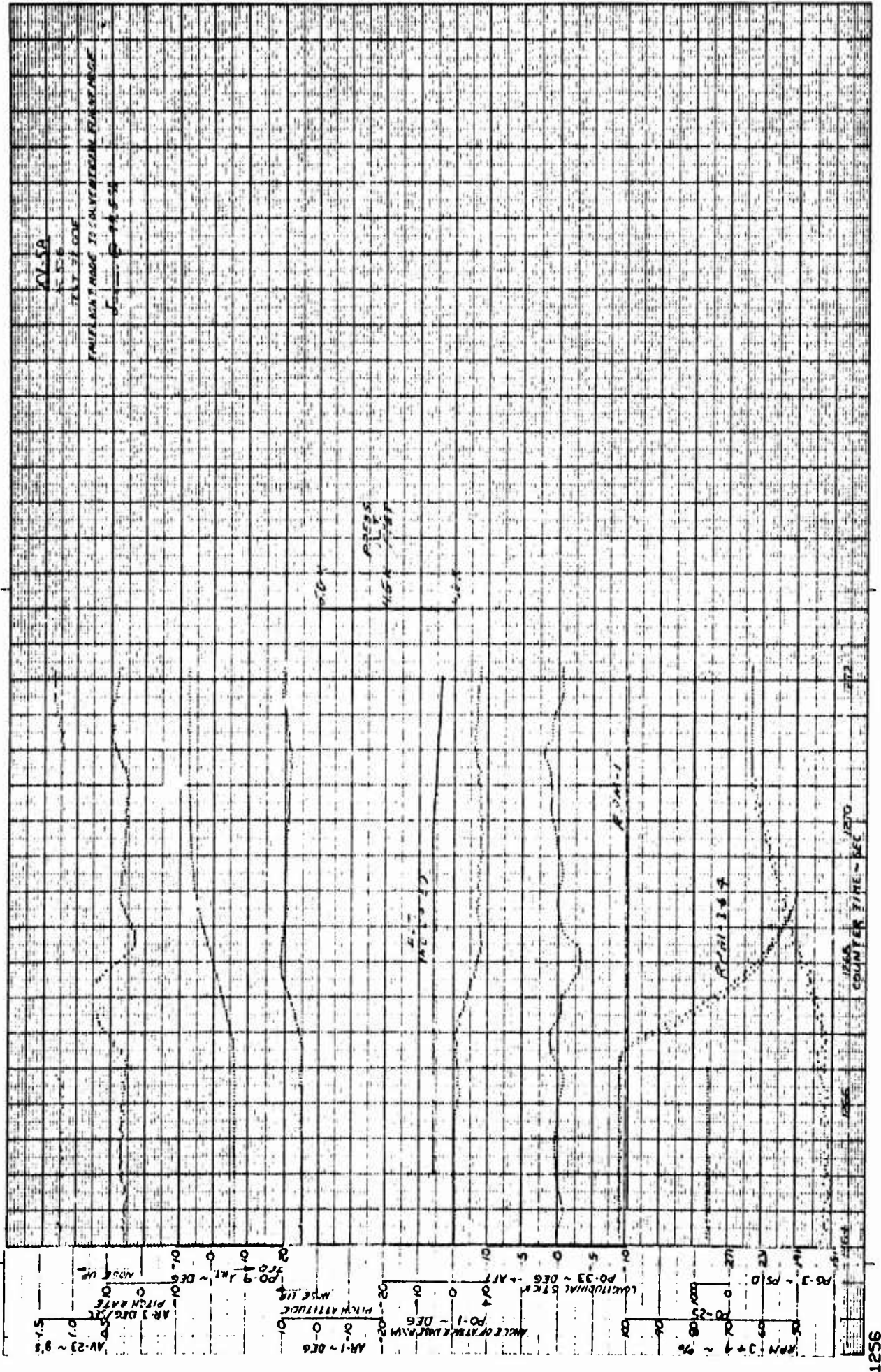


Figure 6.82 Flight Conversion Time Histories

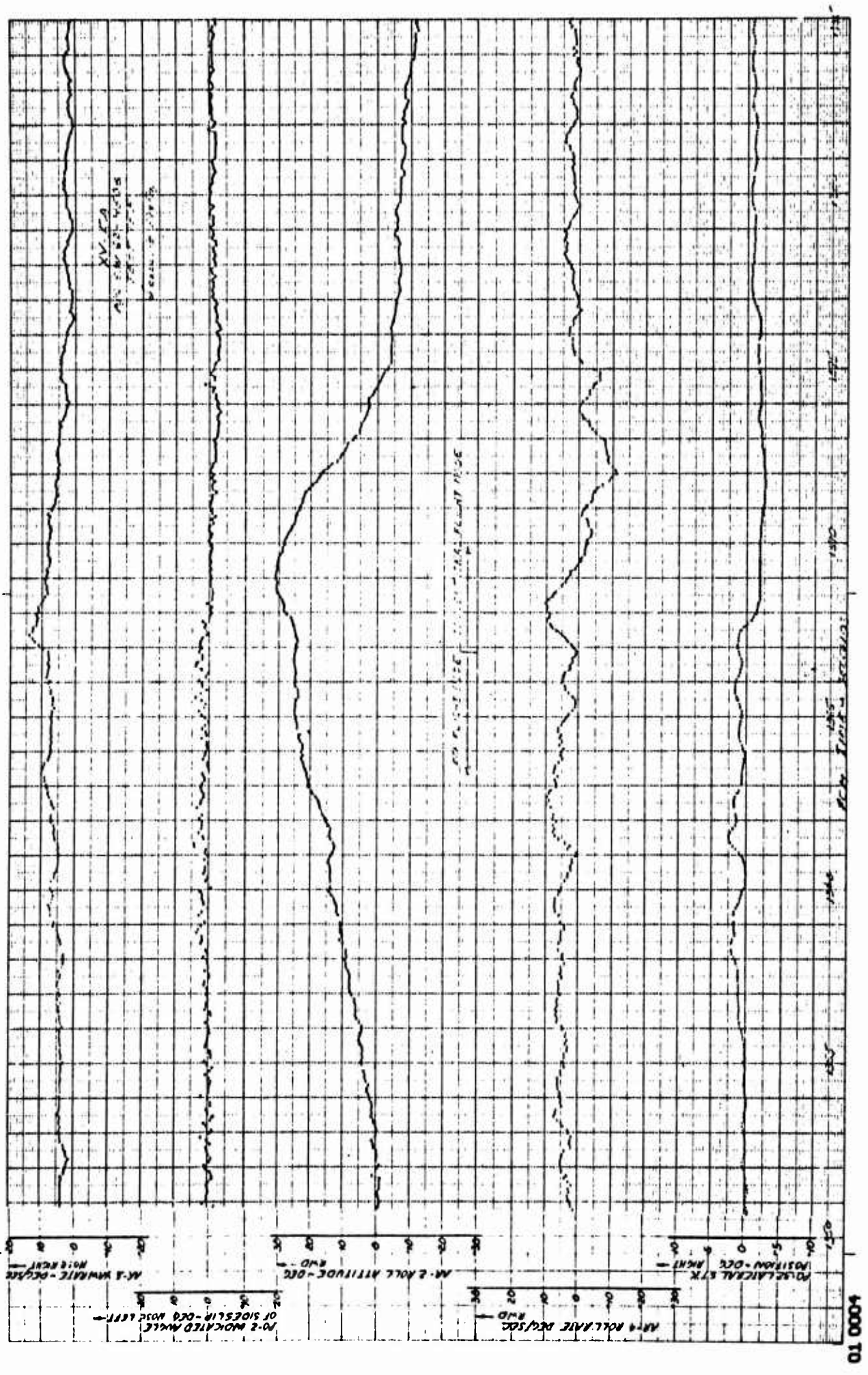


Figure 6.84A Flight Conversion Time Histories

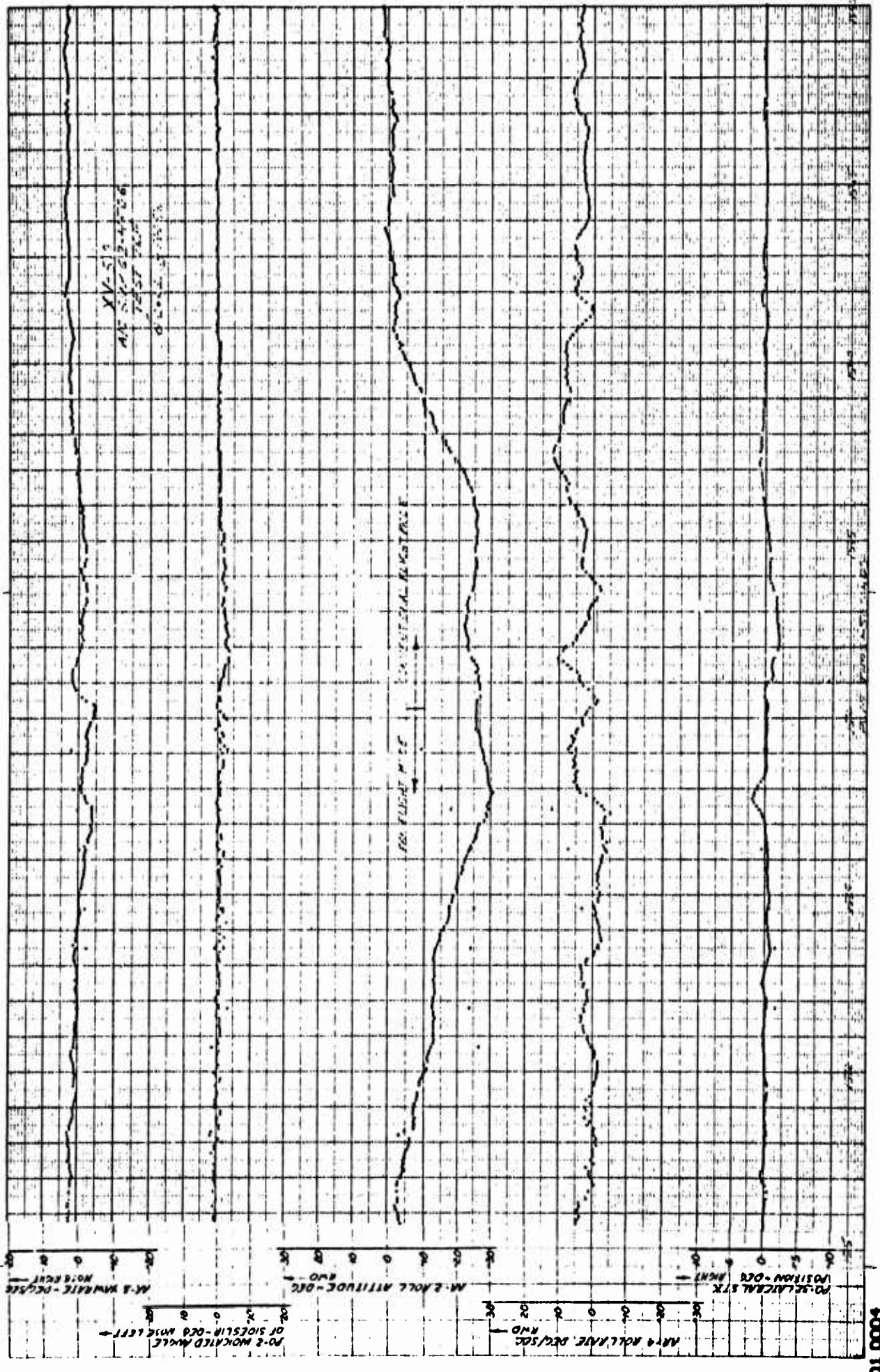


Figure 6.85A Flight Conversion Time Histories

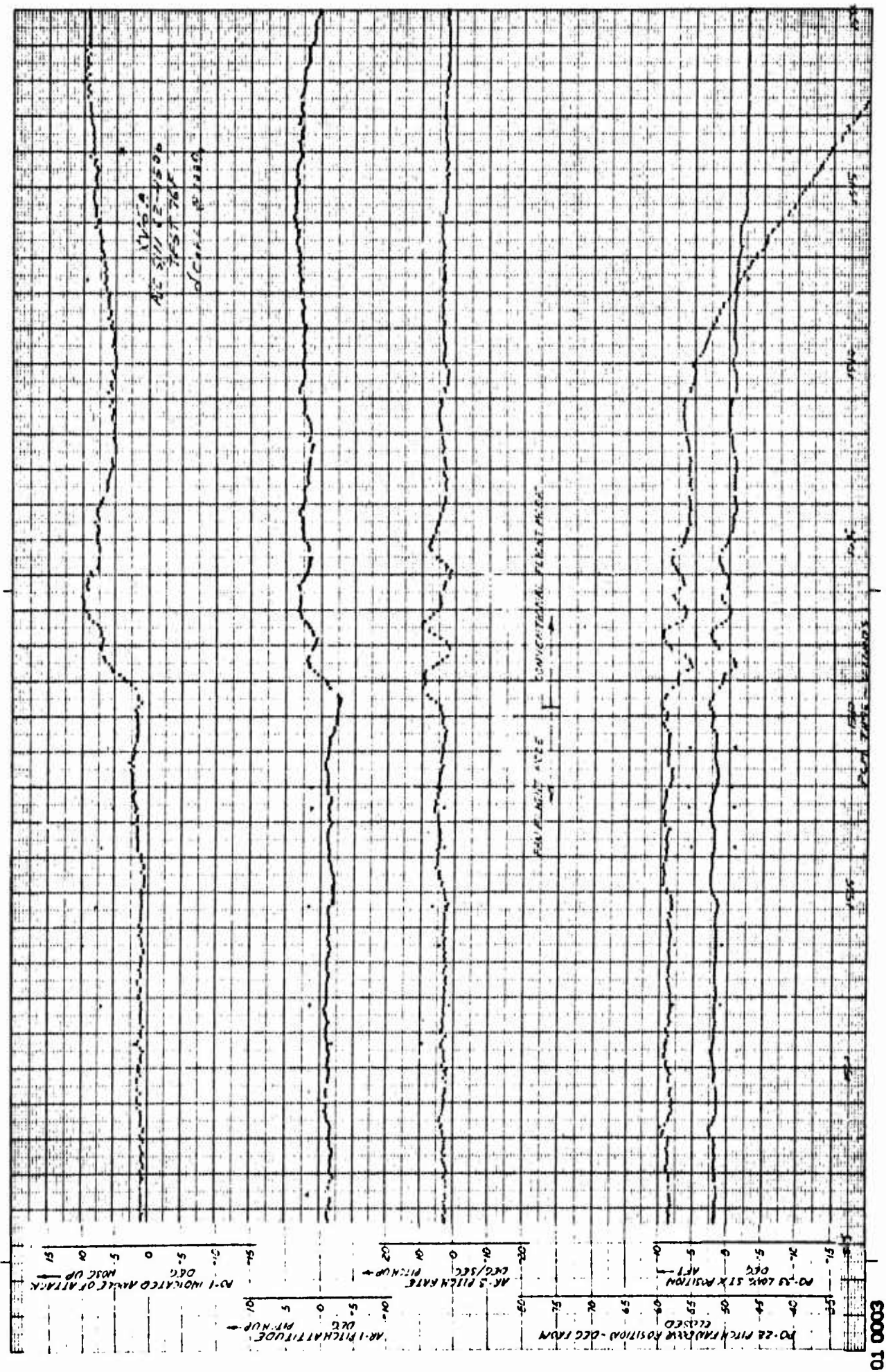


Figure 6.85B Flight Conversion Time Histories

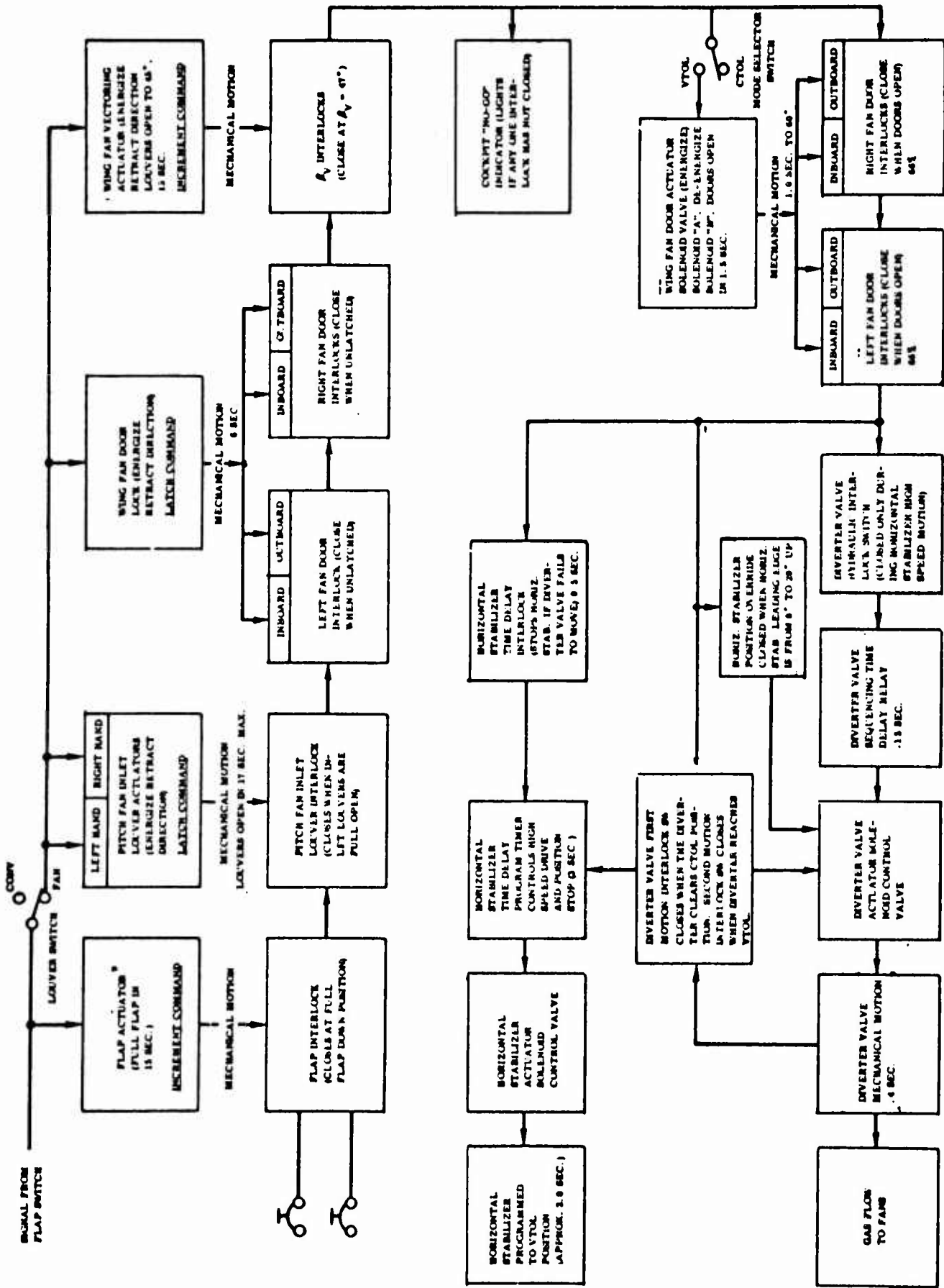


Figure 6.86 Flight Mode Conversion Control System Block Diagram - Conventional to Fan

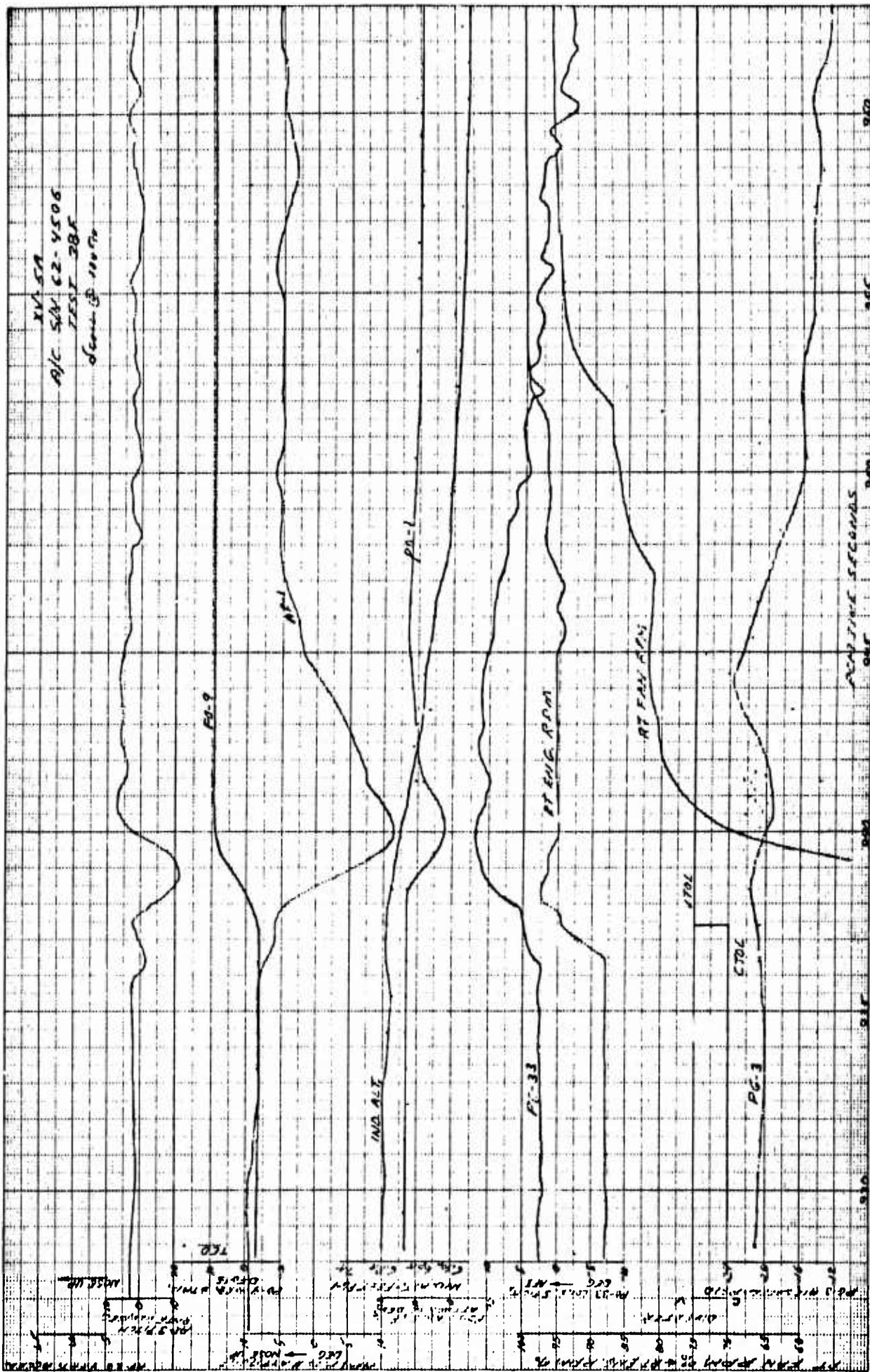
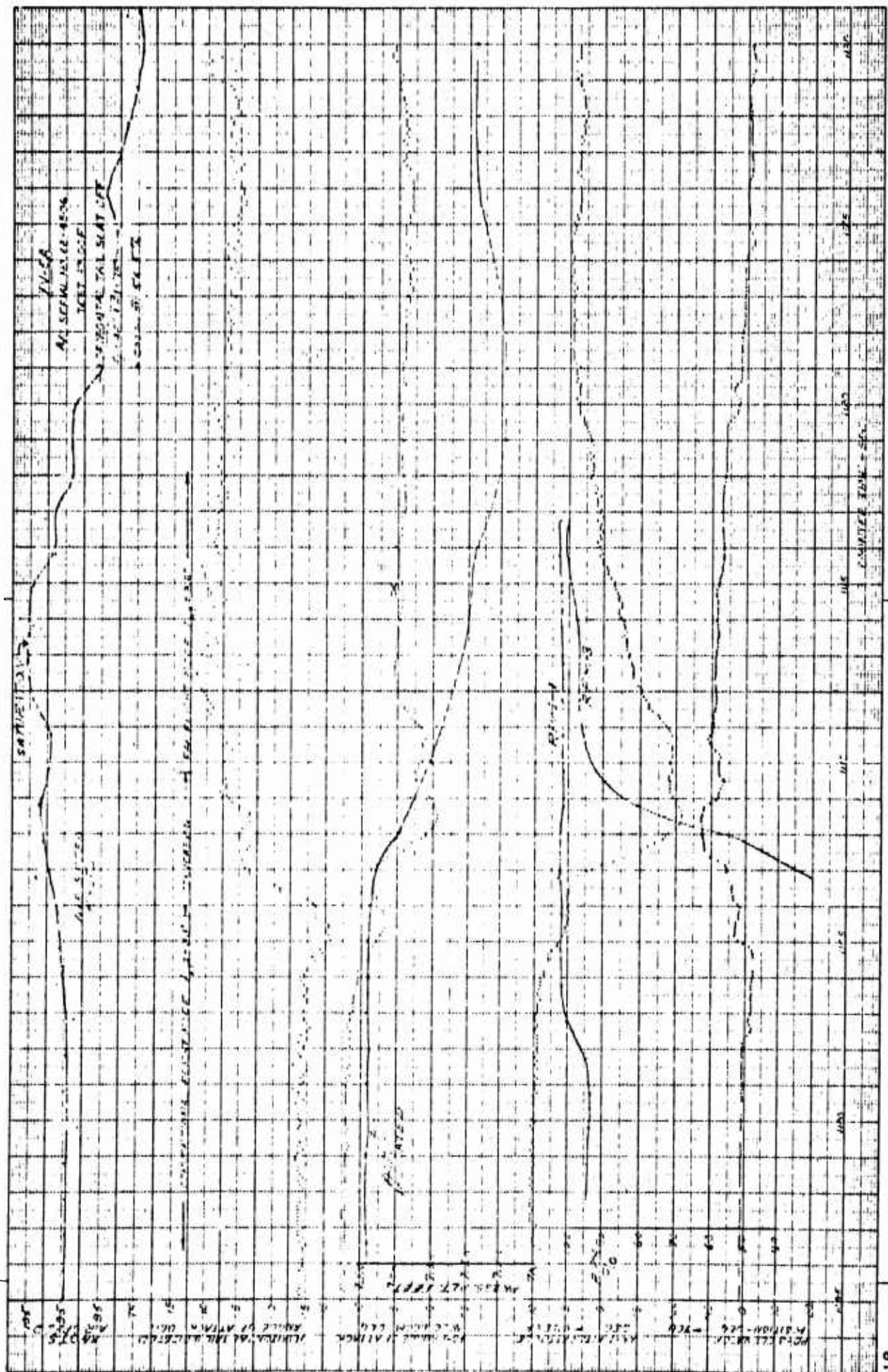


Figure 6.87 Flight Conversion Time Histories



0118

Figure 6.88 Flight Conversion Time Histories

